# A Novel Selection Technology for the Discovery of High-Affinity Human Proteins

By David A. Busha

B.A. Macalester College 2005

M.A. University of Colorado 2008

A Thesis submitted to the Faculty of the

Graduate School of the University of Colorado in partial fulfillment

of the requirement for the degree of

Doctor of Philosophy

Department of Molecular Cellular and Developmental Biology

2014

This thesis entitled:

A Novel Selection Technology for the Discovery of High-Affinity Human Proteins

Written by David A Busha

Has been approved for the Department of Molecular Cellular and Developmental Biology

_____

(Dr. Robert Garcea, Committee Chair)

_____

(Dr. Leslie Leinwand, Committee Member)

Date_____

The final copy of this thesis has been examined by the signatories, and we find that both the content and the form meet acceptable presentation standards of scholarly work in the above mentioned discipline.

Busha, David (Ph.D. Department of Molecular Cellular and Developmental Biology)

A Novel Selection Technology for the Discovery of High-Affinity Human Proteins

Thesis directed by Professor Dr. Leslie Leinwand

Proteins that bind with high-affinity to cellular targets can be useful therapeutic treatments. High-throughput affinity screening of large protein libraries is often more successful at discovering novel high-affinity proteins than rational-design approaches. Display techniques such and phage and yeast display are commonly used in this screening process. However, bacteria and yeast cells can misfold or otherwise inappropriately express mammalian and human proteins due to differences in codon usage, protein folding machinery and post-translational modifications. Therefore, a display system that is entirely based in human cells could aid in the discovery of novel, high-affinity proteins. No such system has been described to date without major limitations.

This thesis describes the development of a novel protein affinity selection system. This system entails the use of the human Herpes Simplex Virus 1 (HSV-1) as a particle for protein display. In this system, genes encoding proteins to be displayed are inserted into the HSV-1 chromosome via a novel recombination system. The viruses produced display the encoded proteins on their surface fused to the C-terminus of HSV-1 glycoprotein C. Large libraries of protein-displaying viruses are then subjected to a novel, competitive-infection selection procedure. Through Darwinian selection, viruses displaying proteins with high binding affinity for cell-surface targets are enriched over viruses displaying proteins with lower binding affinity. Proof-of-principle testing has shown this system can select for a gene encoding a high-affinity protein that is outnumbered $1:10^5$ by genes encoding lower-affinity proteins in a plasmid DNA library. Further testing of this system, using a mutant library of genes encoding the CX3CL1 chemokine, identified novel CX3CL1 mutants that may bind to the CX3CR1 receptor with higher affinity than wild-type CX3CL1. This system was also used to screen a B-cell antibody library from an HIV-

infected individual. This system identified several novel antibodies that are very similar to high-affinity antibodies previously discovered from the same library. The results of this work show that this novel selection system may be a widely-applicable tool for the discovery of high-affinity human and mammalian proteins.

Table of Contents


Pages:

**Chapter 1. Background and Significance**

**Part 1. Introduction**, The importance of discovering high-affinity proteins.

1.1.1 Background and Significance 1-2

1.1.2 Goal and purpose of this thesis 3

**Part 2. Display Techniques**

1.2.1 Bacteriophage Display 4

1.2.2 Complications with bacteriophage display and the development of new display techniques 4-5

1.2.3 Eukaryotic Display 5-8

1.2.3.1 Yeast Display 5-6

1.2.3.2 Baculovirus Display 6-7

1.2.3.3 Limitations to Yeast and Baculovirus Display 7-8

1.2.4 Mammalian cell display 9

1.2.5 In Vitro Display Techniques 9-10

**Part 3. The Importance of Post Translational Modifications**

1.3.1 Glycosylation 11-12

1.3.2 The Impact of Glycosylation on Therapeutic Proteins 13-14

1.3.3 Direct-effects of Glycosylation on Protein Binding Affinity. 15

1.3.4 Other Post Translational Modifications 15-16

**Part 4. Previous Reports of Mammalian Virus Systems for Protein Affinity Selection**

1.4.1 Murine Leukemia Virus Display, Lentivirus Display, Adenovirus Display 16-19

1.4.2 Advantages of HSV Display over Other Systems 20

**Part 5. Background on HSV-1**

1.5.1 HSV-1 Structure 20-24

1.5.2 HSV-1 Glycoproteins and Binding 24-34

1.5.3 Previous Reports of Redirected HSV-1 and their Relevance to this Novel System 34-38

**Part 6. Site Specific Recombination & its novel use to create HSV-1 libraries** 38-40

**Chapter 2. Development of a technique to create a library of HSV-1 virions with redirected Tropism**

**Part 1. Creation of a site-specific recombination system for the insertion of genes into the HSV-1chromosome**

2.1.1 Introduction 41-43

2.1.2 Methods 43-50

**Part 2. Creation of a protocol to efficiently create a library of recombinant viruses**

2.2.1 Introduction 50

2.2.2 General Methods 50-56

Experiment 1.1 RMCE via Co-transfection 56-59

Experiment 1.2 RMCE Exchange into Live Virus. 59-61

Experiment 1.3 Testing for the occurrence of unique recombination events. 62-64

Experiment 2.1 Improving live-virus RMCE. 65-67

Experiment 2.2 Improving live-virus RMCE BSS Protocol. 67-72

Experiment 2.3 Further improving the live-virus RMCE protocol. 72-78

Experiment 2.4 Addressing the results from experiment 2.3. Live-virus RMCE protocol optimization. 78-83

Experiment 2.5. Final Optimization to the Live-Virus RMCE Procedure 83-86

Experiment 2.6 Testing for the occurrence of unique recombinant viruses using

the optimized live-virus RMCE procedure from experiment 2.5 86-89

**Part 3. Creation of HSV-1 Viruses Displaying Fusion Proteins**

Experiment 2.7 Creation of HSV-1 Viruses Displaying Fusion Proteins 89-95

**Chapter 3. Testing for increased virus growth as a result of a high-affinity gC-fusion protein.**

Experiment 3.1. Creation of Cells Expressing the CX3CR1 receptor 96-102

Experiment 3.2. Growth Characterization of HSV-CX3CL1 in HeLa-CX3CR1 102-108

Experiment 3.3. Enrichment of High-affinity Viruses in Mixed-Population Infections 108-113

Experiment 3.4. Generation 2, a Second Round of Selection 114-117

Experiment 3.5.Testing for Enrichment Using Relaxed Selection Parameters 117-123

Experiment 3.6. Addressing Issues of Binding Avidity 123-128

Experiment 3.7. Expanding Enrichment in a Second Generation of Virus Competition 128-133

Experiment 3.8. Avoiding Viral Pseudotyping with Low MOI Virus Competitions. 133-136

Experiment 3.9. Rolling Dilutions Between Generations 136-141

**Chapter 4. Functional Testing of the HSV-1 selection system**

Experiment 4.1. Enrichment of Viruses with Genes from a Plasmid DNA Library 141-156

Experiment 4.2. Selection of Novel CX3CL1 Mutants from a Degenerate Library 156-175

Experiment 4.3. Using The Novel Virus Display System to Screen an Antibody Library 175-188

Final Conclusions 188

Bibliography 189-200

Appendix 1 201-205

Appendix 2 206-218

List of Figures


| Figure Name: | Page: |
|---|---|
| Figure 1. HSV-Structure and cell-entry process. | 21 |
| Figure 2. Schematics of the novel recombination system. | 42 |
| Figure 3. Exeriment 1.1. | 58 |
| Figure 4. Experiment 1.2. | 61 |
| Figure 5. Experiment 1.3. | 64 |
| Figure 6. Experiment 2.1. | 68 |
| Figure 7. Experiment 2.2. | 71 |
| Figure 8. Experiment 2.3. | 76 |
| Figure 9. Experiment 2.4. | 81 |
| Figure 10. Experiment 2.5. | 85 |
| Figure 11. Experiment 2.6. | 88 |
| Figure 12. Experiment 2.7. | 95 |
| Figure 13. Experiment 3.1. | 101 |
| Figure 14. Experiment 3.2. | 106 |
| Figure 15. Experiment 3.3. | 112 |
| Figure 16. Experiment 3.4. | 116 |
| Figure 17. Experiment 3.5. | 120 |
| Figure 18. Experiment 3.5. | 121 |
| Figure 19. Experiment 3.6. | 126 |
| Figure 20. Experiment 3.7. | 130 |
| Figure 21. Viral Pseudotyping. | 131 |
| Figure 22. Experiment 3.8. | 135 |
| Figure 23. Experiment 3.9. | 139 |

Figure 24. Experiment 3.9. 140

Figure 25. RMCE Viral Pseudotyping. 149

Figure 26. Experiment 4.1. 151

Figure 27. Experiment 4.1. 152

Figure 28. Experiment 4.1. 154

Figure 29. Experiment 4.2 mutant library design. 157

Figure 30. Experiment 4.2 mutant library construction. 161

Figure 31. Experiment 4.2. 166

Figure 32. Experiment 4.2. 167

Figure 33. Experiment 4.2 mutant recovery table. 169

Figure 34. Experiment 4.2 alignment and growth of novel mutants. 170

Figure 35. Experiment 4.3. 180

Figure 36. Experiment 4.3 mutant recovery table. 184

Figure 37. Experiment 4.3 mutant alignment. 185

Figure 38. Experiment 4.3 mutant growth. 186

# Chapter 1. Background and Significance

## Part 1. Introduction: The importance of discovering high affinity proteins.

### 1.1.1. Background and Significance

Proteins are one the four major classes of organic molecules produced by living organisms. The approximately 100,000 different types of proteins that make up the human body are involved in nearly every cellular function (Mattanovich et al., 2012). Proteins serve as effectors of cell growth, division, motility, maintenance and signaling. Due to their ubiquitous involvement in the functioning of biological systems, it is not surprising that a wide-array of human diseases are the result of the loss or the malfunction of a type or types of proteins. For this reason, modern medicine has often turned to the use of protein-based therapeutics for a large number of diseases including cancer, inflammation, degenerative diseases and autoimmune disorders(Kamionka, 2011). These protein-therapeutics are used to compensate for a loss of an endogenous protein or to correct the deleterious activities of malfunctioning proteins. To date there have been over 200 protein therapeutics approved for clinical use by the FDA such as Humira, Epogen and Herceptin (Carter, 2011).

Proteins carry out complex functions in biological systems and are therefore themselves complex molecules, by necessity. In many applications, protein-based therapeutics have been shown to be much more effective in the treatment of some diseases than small-molecule drugs (Leader et al., 2008). Therefore, the continual discovery and development of protein molecules for use as potential therapeutics and research tools is of great interest to the biomedical research community (Gerngross, 2004).

Protein therapeutics often carry-out their functions by binding to specific targets on the surface of cells. The therapeutic result of this binding is usually either to initiate some form of cell signaling or to block the binding of another molecule. Accordingly, the binding affinity and specificity of a protein

therapeutic for its cell-surface target is a major determinant of its therapeutic efficacy. Proteins with high binding affinity and specificity for their cell-surface target often have more potent therapeutic activity with fewer undesired side effects (Landon et al., 2004).

Many proteins are so structurally complex that they cannot be successfully synthesized and can only be produced by living cells (Gerngross, 2004). A result of this complexity is that it is often hard to predict or determine the functionality of a protein by examining its structure. This complexity makes the discovery of new proteins with high affinity to a therapeutic target quite difficult. High-throughput affinity screening of large protein libraries is often more successful than rational-design based approaches to find or create new high affinity proteins (Kamionka, 2011). Screening can involve the selection of high affinity proteins from naturally occurring protein repertories, such as antibody libraries, or can involve the creation of novel proteins using mutagenesis. The latter technique typically involves identifying a naturally occurring "parental" protein that exhibits some binding affinity to a binding target of interest. The gene encoding this protein is then subjected to mutagenesis, by techniques such as error prone PCR or DNA shuffling, in order to create a large diverse library of mutant genes (O'Neil and Hoess, 1995). The proteins encoded by these mutant genes are then screened to determine if the mutagenesis randomly produced a protein with higher affinity for the target than the parent. Iterative rounds of mutagenesis and selection are the basis of "Directed Evolution," "Affinity Maturation" and "Bio-panning" techniques.

A common requirement to nearly all protein affinity screening techniques is that a large library of many proteins must be screened. These can range in size from rather small libraries of $10^3$ to extremely large libraries of $>10^{10}$ different proteins (Levin and Weiss, 2006). Because of this, it is not feasible to test each library member individually for binding affinity. Instead large numbers of proteins must be screened "in batch." During this process it is necessary that each protein can be traced back to the gene that encoded it. As stated above, many proteins can only be produced from living cells,

therefore the encoding genetic sequence is absolutely required for any further production of a selected protein. For this reason, display techniques that physically link proteins with their genes have been developed (Levin and Weiss, 2006).

### 1.1.2. Goal and Purpose of this Thesis

This thesis describes the development and testing of a novel protein display and affinity selection system. The purpose of this work was to develop a scientific tool that can be applied to a wide-array of protein/target interactions for research and drug discovery applications. This work is specifically intended to advance the technique of screening human and mammalian proteins by creating a system based entirely in human cells. No such systems have yet been described without major limitations. This thesis describes the design, construction and proof-of-principal testing of this system.

The first portion of this thesis, chapter 1, will describe existing, well-established systems for protein display and selection. The limitations of these systems with regards to the specific requirements of human and mammalian proteins will be discussed as well as previous efforts to develop new systems to address these limitations. The advantages of the novel system, described in this thesis, over these previous attempts will then be discussed. This novel system will utilize human herpes simplex virus type 1 (HSV-1) as the basis for protein display. Therefore, relevant background information about HSV-1 structure and biology, as well as previous reports which have informed the design of this novel system, will be reviewed.

The second portion of this thesis, chapters 2-4, will describe the creation of a novel HSV-1 based display system for protein affinity screening. Incremental experiments that established important operational parameters for this system will be described. Finally, proof-of-concept experiments will be described that show the functionality of this system.

## Chapter 1. Part 2. Display Techniques

### 1.2.1. Bacteriophage Display

In order to accomplish phenotype-genotype linkage between proteins and gene, display techniques have been developed. The first such technique was phage display as reported by Smith in 1985 (Smith, 1985). Here, a gene for a protein was inserted into the genome of M13 bacteriophage as a fusion protein in frame with the phage pIII coat protein. When this genome was expressed it created a bacteriophage that displayed the fused protein on its surface. This system has become one of the most widely used techniques for protein affinity screening. For screening, large libraries of genes are inserted into phage genomes resulting in libraries of phage particles, each displaying a protein from the library on its surface and containing the gene within its genome. These phage particles are then applied to binding targets, lower affinity binders are washed away, the tightly-bound phage are eluted and the gene encoding the high-affinity protein is recovered from the genome. Many variations of phage display have been developed since its introduction (Irving et al., 2001; Kriplani and Kay, 2005; Osbourn et al., 1998).

Phage display has been successfully used to screen libraries as large as $10^{11}$ in size (Murase et al., 2003). Since its invention, phage display has been continually used and modified and has led to the discovery of numerous, useful high-affinity proteins such as antibodies (Jespers et al., 1994; McCafferty et al., 1990), immune signaling molecules (Renschler et al., 1994) and hormones (Wright et al., 1995). Many of which have been approved for therapeutic use by the FDA (Landon et al., 2004).

### 1.2.2. Complications with bacteriophage display and the development of new display techniques

Despite its success in identifying many useful high-affinity proteins, phage display does have limitations. One major limitation is that phage display requires the growth of the bacteriophage, and subsequently the protein being displayed, in bacteria. Bacteria can often misfold or otherwise inappropriately express mammalian and human proteins as a result in differences in codon usage,

protein folding machinery and post-translational modifications, which can lead to the unpredictable loss of library members (Alonso-Camino et al., 2009; Coia et al., 2001; Shusta et al., 1999). This loss is non-specific to binding affinity and can impair the potential discovery of high affinity mammalian and human proteins. It has been reported that changes as minor as single amino acid substitutions can completely eliminate the expression of some human proteins in bacteria (Ulrich et al., 1995). Furthermore, many attempts to produce phage expressing human single chain antibodies resulted in the aggregation of the antibodies within the bacterial cells and only a small proportion being functionally expressed on phage particles(Plückthun, 1991; Plückthun and Pfitzinger, 1991) .Since many proteins of therapeutic and research interest are human proteins, the inability of bacterial cells to appropriately express some mammalian and human proteins represents a major limitation to this system. For this reason, new display techniques based in eukaryotic cell systems have been developed.

### 1.2.3. Eukaryotic Display

#### 1.2.3.1. Yeast Display

First reported in 1997, the display of protein libraries on the surface of *Sacchromyces cerevisiae* as fusions with surface glycoproteins ag-alpha-1 and aga2 has become an attractive, eukaryotic alternative to bacteriophage display (Boder and Wittrup 1997). In this "yeast display" technique, the yeast cell serves as the means of genotype-phenotype linkage as the gene for the fusion protein being displayed is contained within the yeast cell. Due to the relatively large size of the yeast cell, the yeast cells are typically not applied to immobilized binding targets. Instead, soluble fluorescent binding targets are applied to the yeast library which is then subjected to Fluorescence Activated Cell Sorting (FACs) for selection (Boder and Wittrup, 1997; Wang and Shusta, 2005). While the average library size screened with this technique is approximately $10^6$, protein libraries as large as $10^{10}$ members have been screened (Gai and Wittrup, 2007). Yeast display has been shown to be highly effective and has allowed the discovery of many different types of high affinity proteins such as single chain antibodies (scFv)

(Boder and Wittrup, 1997; Gai and Wittrup, 2007; Lin et al., 2003) and cytokine receptors(Rao et al., 2003).

The display of human proteins in yeast as, as opposed to bacteria, benefits from eukaryotic protein expression pathways that are more similar to those found in human cells. An excellent example of this benefit was reported in 2007. Burton et al screened a B-cell derived human scFv library for high affinity antibodies to the HIV coat protein GP120 (Bowley et al., 2007). This library was screened using both phage and yeast display systems in a side by side comparison. The authors reported that phage display yielded the discovery of 6 high affinity (low nanomolar Kd) antibodies. They further reported that the same antibodies were discovered using yeast display as well as an additional 12 that were missed by phage display. To determine why these 12 antibodies were missed by the phage display selection, as they were not simply lower affinity, the authors attempted to individually express them on bacteriophage particles and as soluble fragments from E. coli. It was reported that these 12 antibodies had lower binding affinity when expressed in bacteria, probably due to misfolding or a lack of important post-translational modifications. Furthermore, these antibodies were expressed at very low abundance compared to the 6 antibodies found using phage display. This suggests these 12 antibodies were not selected by phage display because of bacterial expression biases; not because of affinity. This exemplifies the potential loss of discovery potential due to improper expression or handling of human proteins in bacterial cells.

#### **1.2.3.2. Baculovirus Display**

Another technique that has been developed to address the problems with the expression of human proteins in bacteria is baculovirus display. Here, proteins are displayed as fusions with the Gp64 coat protein of the *Autographa californica* multiple muclear polyhedrosis virus (AcMNPV) (Whitford 1989). This system, first reported in 1995, utilizes a virus that grows in insect cells to offer another eukaryotic platform for protein display (Boublik et al., 1995). Theoretically, a library of $10^6$ different

members can be anticipated based on average transfection efficiency of insect cells. However, libraries that have been successfully screened are more often much smaller (~$10^{3-4}$) (Ernst et al., 1998; Kitts and Possee, 1993). For selection, libraries of baculovirus genomes are engineered to contain fusions between library members and the Gp64 coat protein. These genomes are then transfected into insect cells to generate a library of baculoviruses displaying the fusion proteins. While these viruses can be panned for affinity to an immobilized target, a more commonly adopted strategy is to use the viruses to transduce expression of the transmembrane Gp64-fusion protein on insect or mammalian cells which are then FACs sorted for binding to a soluble, fluorescent target (Ernst et al., 1998)(Kitts and Possee, 1993). While much less widely used than bacterial display or yeast display, the baculovirus system has successfully been used to identify new high affinity HIV epitopes on GP120 (Ernst et al., 1998).

#### 1.2.3.3. Limitations to Yeast and Baculovirus Display

Both yeast and baculovirus display systems have some technical and practical limitations. The size of yeast cells largely restricts their use to FACs screening using soluble, fluorescent binding targets. This requirement can pose problems if a soluble binding target is difficult to produce. Reports of panning yeast-displayed libraries against cell-surface targets are infrequent and this technique is still being developed (Wang and Shusta, 2005). A major limitation of the baculovirus system is that they are sensitive to the size and copy number of the displayed proteins. Proteins larger than small peptide sequences have been reported to interfere with the growth and infectivity of these viruses as the Gp64 protein is required for cell entry (Oker-Blom et al., 2003).

There are also limitations with the use of yeast and baculovirus systems to display human proteins. One major limitation is that both of these systems lack human post-translational modifications. While both yeast and insect cells do perform post-translational modifications of proteins, the nature and pattern of these modifications can be quite different from those observed in human cells. Yeast hyper-mannosylate many N-glycosylation sites, a pattern which is not seen in human cells

(Gemmill and Trimble, 1999). This process produces proteins with long, simple carbohydrate molecules that are very different from the complex, branched molecules produced in human cells (Beck et al., 2010). Insect cells are also incapable of producing these types of complex glycosylation patterns (Bustos et al., 1988; Dee et al., 1997; Harrison and Jarvis, 2006). Furthermore, while the consensus sequence for the addition of N-linked glycosylation is the same in mammals, yeast and insects, it is unknown why the choice to fill or not fill some N-linked sites differs between mammals and these other species (Beck et al., 2010; Gerngross, 2004; Harrison and Jarvis, 2006). In addition, there is no known consensus sequence for O-linked glycosylation modifications and these types of modifications differ quite unpredictably between mammals and other eukaryotes (Harrison and Jarvis, 2006). Differences in glycosylation patterns can affect protein folding and activity (reviewed below). These differences can result in the loss of library proteins that require human glycosylation patters for proper folding or functionality. This could also cause these systems to potentially enrich for library members requiring glycosylation patterns that might not occur when the same protein is expressed in human cells. The extent of the importance of the differences in glycosylation between mammals and other eukaryotes is underscored by the ongoing efforts to create yeast and baculovirus protein production systems with humanized glycosylation pathways (Beck et al., 2010).

Lastly, non-glycosylation post translational modifications also differ between humans and other eukaryotic systems. Tyrosine sulfation has been shown to be important for antibody function, chemokine receptor binding and the binding interaction between many different proteins (Harrison and Jarvis, 2006). Yeast do not perform tyrosine sulfation and insect cells often do not modify the same sites as human cells(Moore, 2003; Schmidt et al., 2012). These differences could lead to unpredictable differences in the behavior of human proteins expressed in these systems.

### 1.2.4. Mammalian cell display

In response to the complications involved in expressing mammalian proteins in non-mammalian cells, a technique involving the display of protein libraries on the surface of cultured mammalian cells has recently emerged. In one of the first reports of this technique, Kitaguchi et al electroporated a plasmid library containing genes for membrane-bound antibodies against a hepatitis B protein into COS cells (Higuchi et al., 1997). These cells were screened using FACs to isolate those bound to a fluorescently labeled, soluble hepatitis B protein. The authors reported isolation of new antibodies that bound to the hepatitis B protein from a starting library of $10^6$ members. Since this initial report, there have been reports of mammalian display using many different mammalian cell types and different gene delivery systems such as plasmids, retroviral vectors and vaccinia virus (Ho et al., 2006; Wang and Shusta, 2005).

One major complication to this technique is the ability of cultured cells to take up multiple plasmids and viral vectors which can lead to the expression of multiple library members within a cell. For efficient screening of a library it is important that each cell only express one specific library member. Attempts to circumvent this problem have included the development of systems which require integration into the cellular genome using site-specific recombination (Zhou et al., 2010). While this technique did reduce the number of cells expressing multiple library members it also reduced the efficiency of library gene transfer into the cells. An additional complication with yeast display is that differences in levels of protein expression between library members can cause problems as this will result in variations in the amount of fluorescent targets bound to a cell unrelated to binding affinity.

### 1.2.5. *In vitro* display techniques

Several cell-free techniques have been developed which have allowed for the display of protein libraries of unprecedented size. These systems will only be reviewed briefly as they do not possess direct relevance to the cell-based HSV-1 display system described herein. Both ribosome display and

mRNA display techniques can reportedly routinely screen libraries containing >$10^{12}$ different members (Levin and Weiss, 2006; Schaffitzel et al., 1999). This impressive ability is due to these systems circumventing the limitations of producing libraries in living cell. The principle of these systems is that the proteins being screened are each directly linked to the RNA that encoded them. For ribosome display, this is accomplished by the use of an in vitro expression system in which DNA is reverse transcribed into mRNA. The mRNA is in turn translated but has been engineered to lack a stop codon which causes the ribosome to stall at the 3' end of the RNA with the nascent protein still attached and then the entire mRNA-ribosome-protein complex is stabilized by the addition of chlorampheincol (Schaffitzel et al., 1999). In mRNA display, a ssDNA linker is covalently added to the 3' end of mRNA molecules, this linker causes the ribosome to stall at this junction at which point a puromycin molecule can enter the ribosomal A-site and form a stable amide bond between the mRNA and the peptide (Wilson et al., 2001). These techniques are performed in completely cell-free reactions using either *E. coli* or rabbit reticulocyte cell extract systems for protein expression (Levin and Weiss, 2006). As a result, these systems are not limited by factors such as cell growth and transformation or transfection efficiencies. However, the cell-free protein expression systems used in these techniques lack the sophisticated protein folding and post-translational modification abilities of intact cells.

## **Chapter 1. Part 3. The importance of post translational modifications for protein expression and function**

As stated above one of the major disadvantages to display systems that are heterologous with respect to the expression of human proteins is a lack of appropriate human post-translational modifications. One of the potential advantages to the HSV-1 based protein affinity selection system described herein is that it allows for protein libraries to be completely produced in human and

mammalian cells and contain all naturally occurring post-translational modifications. Accordingly, the importance of these modifications on proteins and their functions will be briefly reviewed.

### 1.3.1. Glycosylation

Glycosylation, the addition of carbohydrate moieties, is one of the most common post-translational modifications of mammalian proteins. It is estimated that 2% of the entire human genome encodes proteins that contribute to the glycosylation process (Campbell and Yarema, 2005) and defects in glycosylation cause diseases with serious medical consequences (Freeze et al., 2014). However, despite estimates that 50% of all human proteins are glycosylated (Lis and Sharon, 1993)the effects of glycosylation on protein function are unpredictable and poorly understood. Approximately two thirds of all approved therapeutic proteins are glycosylated (Gerngross, 2004) and a substantial fraction of these require proper glycosylation for full therapeutic efficacy (Solá and Griebenow, 2010). These include proteins in the classes of: antibodies, erythropoietins, blood factors, thrombolytics, interferons, hormones and others (Beck et al., 2010). Glycosylation has been shown to influence protein-protein binding, protein stability and in vivo efficacy of many FDA approved protein therapeutics.

Patterns of glycosylation are believed to provide an additional layer of information at the molecular level beyond that of gene-derived primary sequences and the resulting secondary structure of a protein (Varki et al., 2009). The structures of these glycan moieties are highly complex and the result of a cascade of enzymatic steps. Intracellularly, glycan structures on newly synthesized proteins have been shown to be crucial for protein folding, trafficking, secretion and quality control (Encarnação et al., 2011; Kanno et al., 2010). Extracellular glycans are involved in cell-adhesion, signaling, lipid dynamics and endocytosis, immune surveillance, inflammation, cell growth signals and tumor metastasis(Varki, 1993).

The two main categories of glycosylation events are N-linked and O-linked. O-linked glycosylation, the lesser understood of the two processes, begins by the attachment of a

monosaccharide to either a serine or threonine residue (Beck et al., 2010). O-linked glycans are found on intracellular and extracellular proteins and are a major component of the extracellular matrix (Breloy et al., 2012). There is no recognized consensus sequence for O-glycosylation and this type of modification can compete with other enzymes such as kinases for the same amino acid sites (Van den Steen et al., 1998). It is believed that the decision by a glucotransferase enzyme to add an initial monosaccaride to a particular serine or threonine residue is heavily influenced by the surrounding secondary and tertiary structure of the protein (Hang and Bertozzi, 2005). O-linked glycans are classified by their initiating monosaccaride and include mucin glycans, mannose glycans and glycosoaminoglycans (Tian and Ten Hagen, 2009). Once added, the initiating monosaccaride is then elaborated by one or more of the 200 known glycosyltransferases, located primarily within the Golgi and endoplasmic reticulum (Beck et al., 2010). These enzymes are believed to compete with one another and their activity is influenced by many cellular factors (Unligil et al., 2000). Over 7000 glycan structures are estimated to result from different patterns of the ten basic monosaccaride units (Moremen et al., 2012; Varki et al., 2009).

N-linked glycosylation is a slightly better understood process and a consensus sequence, which is necessary but not sufficient for the initial attachment of carbohydrate, has been identified: Asn-X-Thr/Ser (Solá and Griebenow, 2010). It is estimated that the majority of human proteins that are glycosylated contain N-linked glycan structures (Lis and Sharon, 1993). Many of these structures are added to nascent polypeptides as they are being translated. These glycans are expanded and trimmed and eventually can form recognition sites for chaperones to assist in protein folding(Helenius and Aebi, 2004) .The continual trimming and re-addition of monosaccarides on glycans during protein folding help modulate chaperone interactions and can protect nascent proteins from hydrophobic aggregation and the formation of aberrant disulfide bonds (Ferris et al., 2014; Goder and Melero, 2011).

### 1.3.2. The impact of glycosylation on therapeutic proteins

To further illustrate the importance of glycosylation of mammalian proteins, the known effects of these modifications on therapeutic proteins will be briefly reviewed. The goal of this review is to emphasize the advantages of the human-cell based selection system described herein over non-mammalian cell based systems as it allows for the appropriate glycosylation of the proteins being screened. As stated above, approximately two thirds of all approved therapeutic proteins require glycosylation (Gerngross, 2004). This requirement is one of the main reasons that these proteins are produced in large bio-reactors of mammalian cells. Recombinant human erythropoietin, EPO (Epogen, Procrit) is widely used to treat anemia. Approximately 40% of its molecular mass comes from N- and O-linked glycans (Darling et al., 2002). Removal of any of the naturally occurring three N-linked glycans has little effect on the *in vitro* activity of the molecule, but dramatically reduces *in vivo* potency in mice by reducing the serum half-life of the molecule(Delorme et al., 1992). Furthermore the specific composition of these N-glycans has also been shown to be important. Removal of the highly branched, terminally sialyated carbohydrates, which occur in human cells, reduced the plasma half-life from ~6hr to <2 minutes (Elliott et al., 2004a).

Interferon β (IFN-β), produced from both mammalian cells and *E. coli* has been approved for the treatment of immune diseases such as multiple sclerosis. IFN-β has a naturally occurring N-linked glycosylation motif in mammalian cells and the absence of this carbohydrate has been shown to cause decreased *in vitro* activity and stability. While both glycosylated and non-glycosylated forms have been approved for use, the non-glycosylated form requires a bi-daily treatment regimen while the glycosylated form only needs only to be given weekly (Runkel et al., 1998).

Glycosylation has also been shown to play a major role in the activity of antibodies. The majority of approved therapeutic antibodies belong to the immunoglobulin G (IgG) family. Removal of glycosylation naturally found in the Fc region of IgG antibodies abolishes the complement-mediated

effector functions of these molecules (Jefferis, 2009; Nezlin and Ghetie, 2004). Furthermore, abnormally glycosylated human antibodies produced in CHO and mouse cells have been observed to have decreased potency. This decrease was corrected by the introduction of several human glycosylation enzymes into these cells (Davies et al., 2001; Patel et al., 1992).

While the effects of glycosylation on the therapeutic proteins reviewed above do not directly relate to the binding affinities of these proteins, a protein affinity selection system that would allow for the occurrence of these glycan modifications is still advantageous. During the creation of a mutant protein library it is possible that new glycosylation sites could be randomly (or by design) created in various positions on library members. This system would allow for the de-selection of proteins containing glycans in positions that have an adverse effect on binding ability. The addition of carbohydrate moieties in some positions can occlude binding pockets or otherwise adversely alter the final structure of the protein (Elliott et al., 2004b; Marinaro et al., 2000). By choosing selected library members with high affinity that also contain additional carbohydrate content it is possible that novel, high-affinity binders with increased stability could be discovered. For example, as previously stated, the amount of N-linked carbohydrates on recombinant human EPO was directly related to the serum half-life of the molecule as the removal of glycan sites decreased *in vivo* activity (Egrie and Browne, 2001). Subsequently Darbepoetin alfa (DA) was created, a hyperglycosylated form of human EPO with two additional N-linked glycosylation sites and a threefold increased serum half-life (Egrie et al., 2003). Similar hyperglycosylation strategies have been used to increase *in vivo* potency of Leptin, growth hormones, follicle stimulating hormone and cytokines (Egrie et al., 2003; Perlman et al., 2003; Ziltener et al., 1994). It has also been shown that increased glycosylation can protect against proteolysis, oxidation, crosslinking, precipitation, pH and thermal denaturation, aggregation and insolubility (Solá and Griebenow, 2009). Therefore, the selection of high-affinity, hyperglycosylation mutants may lead to the discovery of therapeutic molecules with increased potency past the effects of binding affinity.

### 1.3.3. Direct-effects of glycosylation on protein binding affinity

In addition to reports of the effects of glycosylation on protein stability and *in vivo* efficacy, there have been reports of the direct impact of glycosylation on protein binding affinity. It has been reported that some human antibodies have naturally occurring N-linked glycosylation sites within their variable regions at antigen-binding interfaces (Wawrzynczak et al., 1992; Wright et al., 1991). N-linked glycosylation within these regions has been reported to increase the antigen binding affinity of some antibodies by more than 10-fold (Wright and Morrison, 1998; Wright et al., 1991). The type of glycan chains produced by cell-lines from different species was shown to have a direct effect on the ability of αgp120 antibodies to bind to the HIV glycoprotein gp120(Raska et al., 2010). Here it was reported that gp120 produced in non-human cells contained glycan chains unlike those found on the same sites in gp120 produced in human cells. Human αgp120 antibodies showed reduced binding affinity for this non-human gp120. Ho et al showed that addition of N-linked glycans to the variable region of ibalizumab increased the ability of the antibody to interact with and neutralize some strains of HIV (Song et al., 2013). Lastly, glycosylation has been shown to directly affect the binding affinity of carbohydrate binding proteins such as enzymes, immunoglobulins and lectins (Fan et al., 1995).

### 1.3.4. Other Post Translational Modifications

Other types of protein post-translational modifications have also been shown to affect protein function. Tyrosine sulfation, the transfer of a sulfuryl group to certain tyrosine residues, is carried out by sulfotransferases found in the tran-Golgi network of mammalian cells. To date this process has not been observed in bacteria or yeast and only a loosely defined consensus sequence has been identified (Moore, 2003). The majority of the observed effects of tyrosine sulfation on proteins relate directly to protein binding and a general trend that removing tyrosine sulfation tends to decrease protein binding affinity has been observed (Bonomi et al., 2006; Costagliola et al., 2002; Farzan et al., 1999). Removal of tyrosine sulfation has been shown to decrease binding affinity of chemokine and hormone receptors for

their ligands (Costagliola et al., 2002), decrease the affinity of the anticoagulant peptide hirudin for thrombin (Stone and Hofsteenge, 1986) and decrease the affinity of HIV for the CCR5 receptor (Farzan et al., 1999). It was discovered that tyrosine sulfation naturally occurs in the variable region of some antibodies and that antibodies containing these modifications had increased binding to the CCR5 binding region of HIV GP120 (Farzan et al., 1999). While many other types of protein post-translational modifications occur such as phosphorylation, acetylation, ubiquitination, SUMO modification, the effects of the modifications reviewed above have been the most extensively investigated with regards to the binding and stability of proteins during display and affinity selection.

The reports summarized above underscore the importance of post-translational modifications on protein functions. This imporance includes the direct effects that these modifications have on binding affinity as well as the effects of these modifications on protein folding and stability. therefore, a protein affinity selection system that supports these modifications allows for the selection of native and novel modifications that can enhance protein binding. In addition such a system should allow for the selection of mutant proteins with new post translational modifications that do not impede binding and may confer increased protein stability.

## Chapter1 Part 4. Previous Reports of Mammalian Virus Systems for Protein Affinity Selection

### 1.4.1. Murine Leukemia Virus Display, Lentivirus Display, Adenovirus Display

There are many potential benefits to a protein affinity selection system based in human or mammalian cells as reviewed above. There have been several published reports of attempts to establish such a system. These reports have primarily focused on the use of mammalian and human viruses as direct protein display platforms or to transduce human cells which in turn display library proteins. Several such attempts are reviewed below.

Murine Leukemia Virus (MLV) has been shown to support fusions of growth factors (GFs), cytokines, and scFvs. In an attempt to create a protein-display system based in this mammalian virus,

Urban et al reported a MLV-based display system in which viruses were engineered to display human scFv against laminin (Urban et al., 2005). In this system, viruses were bound to immobilized laminin, non-specific binders were removed with washing, and the remaining viruses were overlaid with 3T3 cells, which allowed for non-scFv specific, MLV infection. Viruses displaying these fusions do not exhibit re-directed tropism. MLVs displaying a laminin-specific antibody were recovered when diluted with viruses displaying a non-specific antibody at a maximal dilution of $1:10^4$. However, it should be noted that this enrichment was only achieved when $10^3$ viruses expressing the laminin antibody where mixed with $10^7$ viruses expressing the non-specific antibody. These resuts suggests a relatively poor enrichment potential as this system requires a large amount of individual representation (N=1000) to allow for the enrichment of a library member. Furthermore, the sensitivity of this system is unclear as the competing virus used in this report was shown to exhibit essentially no binding ability to laminin. The authors further characterized the abilities of this system by cloning a synthetic αLaminin scFv library ($10^3$ diversity) into a retroviral plasmid library, which was then transfected into 293T cells to produce virus. In total, $10^5$ infectious units of virus were applied to immobilized laminin. Binding activity of the population pre and post-selection was compared. After the selection procedure, the laminin-binding activity of the population had increased only 10-fold and no successful iterative rounds of selection were reported. The authors acknowledge that the repertories that can be covered with retroviral libraries, at least in their current stage of development, are clearly below that of phage libraries.

In 2008, Taube et al reported “lentivirus display” in which a scFv targeting the Tat-recognition motif of cyclin T1 was engineered into the lentivirus genome so that it was expressed on the viral surface as a fusion with GP41 (Taube et al., 2008). Interestingly, while the functional display of the scFv on the surface of the virus particle was reported, no attempts were made to use the particle itself as the display vessel. Instead, the viruses were used to transduce expression of the fusion protein on the surface of human 293T cells. Selection was then carried out by applying fluorescently-labeled antigen to

the cells followed by FACs sorting, similar to yeast-display protocols. However, a major limitation to this system as reported is that the library test dilutions ultimately used in selection tests were created by mixing purified scFv-expressing 293T clones, not a lentivirus nor DNA library mixture. A universally necessary starting point for all display selection procedures is a DNA library. It is unclear whether the authors tried to create their test "library" by mixing plamids containing the two scFv genes (at decreasing ratios) which would then need to be converted into lentivirus in order to transduce cells. As no such attempt is reported this may be a potential pitfall of this technique or at least a parameter that has yet to be established.

A related technique was reported in 2009 (Alonso-Camino et al., 2009). Similar to the strategy of Marasco et al., here, lentivirus was used to transduce surface expression of an anti-carcinoembryonic antigen scFv on modified T cells. These cells were engineered to express a fluorescent reporter molecule upon antigen binding. The cells were treated with soluble antigen and sorted for binding using FACs. Cells expressing the scFv were mixed with non-scFv expressing cells at various dilutions. A maximal enrichment of $1{:}10^3$ , from $10^7$ total starting cells. Similar to the limitations in the reports reviewed above, this system required a large amount of individual member representation (N=1000) and the competing cells displayed virtually no antigen binding ability. Lastly, as was the case with the reports reviewed above, selection was performed using mixtures of individually produced scFv-expressing clones, not a mixture of plasmids containing scFv genes.

To date, the only known report of a mammalian virus-based protein affinity selection system to successfully screen genes starting from a DNA library was reported in 2007 (Lupold et al., 2007). This work, however, was done with the intention of creating a system to screen peptide libraries in order to identify novel adenoviral fiber-protein peptides that can successfully redirect adenovirus tropism for the purpose of discovering new tissue-specific adenoviral vectors. This work was not reported to be applicable to screening libraries of full-size proteins for protein affinity screening. The authors

acknowledge that one of the major limitations in creating retargeted adenoviral vectors is inserting new fiber-protein sequences that do not disrupt virus assembly. These are largely limited to small peptides no longer than 6 amino acids. The authors report a cre-lox based system to shuttle mutant fiber genes from a plasmid library into adenoviral chromosomes. Due to the direct relevance of this cre-lox technique to the novel system described in this thesis, this report is reviewed in detail below.

The cre-lox system in this report is based on the previously described concept of recombinase mediated cassette exchange (RMCE), which utilizes cre-recombinase and specially redesigned loxP sites (Langer et al., 2002). In the system reported by Rodriguez et al, plasmid shuttles, which contain the binding region of the adenovirus fiber gene flanked by lox sites, were constructed. The two lox sites in the shuttle plasmids corresponded to the two lox sites engineered into the adenovirus chromosome. The insertion of these lox sites resulted in the removal of the region chromosome that contains the fiber binding domain. The viruses encoded by these chromosomes lacked a functional fiber gene and could only grow in special, complementing cells. To transfer fiber genes from the shuttle plasmids into the viruses plasmids were transfected into cre-expressing cells infected with these viruses. When the shuttle plasmids came into contact with adenoviral genomes during viral replication within the infected cells, cre-lox recombination occurred between the plasmid and the viral chromosomes. This RMCE resulted in the insertion of the fiber C-terminus gene into the adenoviral chromosome and the incorporation of the fiber protein during virus assembly. When these viruses were then used to infect non-complementing cells, only viruses with the fiber gene could grow. The authors reported successfully recovering wild type (wt) fiber containing adenoviruses from transfected plasmid libraries containing a $1:10^5$ ratio of wt:binding null fiber genes. The authors further reported the successful recovery of novel peptide sequences from a plasmid library with six degenerate codons within the fiber binding domain. These novel fiber mutants supported adenoviral growth on cells which do not express the wt fiber receptor.

### 1.4.2. Advantages of the novel HSV-Display protein affinity selection system

To date there have been no known reports using human herpes simplex virus 1 (HSV-1) as a protein display and protein affinity selection system. The advantages to such a system, over established systems such as phage and yeast display, apply specifically to the screening of human and mammalian proteins. HSV-1 is a human virus that grows in human cells. Therefore this system would avoid the complications of heterologous expression and support human post-translational modifications (reviewed above). The HSV-1 glycoprotein C, used as the locus of display in this system, is processed through the protein secretory pathway and naturally contains many post-translational modifications. This glycoprotein, as reviewed below, is highly tolerant of modifications and protein fusions. As described in chapters 2-4, this system can be used to successfully screen a library of plasmid-based genes to enrich for viruses with genes encoding proteins with high affinity to cell-surface targets. This system can therefore both support the display of large, post-translationally modified human proteins and utilize plasmid DNA as the library source. This combination of achievements makes this system more successful than any mammalian-virus display system yet reported.

## Chapter 1. Part 5. Background on HSV-1

### 1.5.1. HSV-1 Structure

HSV-1 is a member of the alphaherpes subgroup of the herpesvirus family and is one of the most common pathogenic viruses infecting 40-80% of the population worldwide (Diefenbach et al., 2008). HSV-1 is commonly the cause of mucosal lesions known as “cold-sores.” The structure of HSV-1 consists of a viral envelope studded with glycoproteins, an amorphous protein layer called tegument, and an icosahedral capsid containing a double-stranded DNA genome (Fig. 1A) (Diefenbach et al., 2008). The mature assembled virus consists of a 162 capsomers composed of 6 different viral proteins, 22 tegument associated proteins and 16 membrane proteins including 12 known glycoproteins (Connolly et

Fig. 1

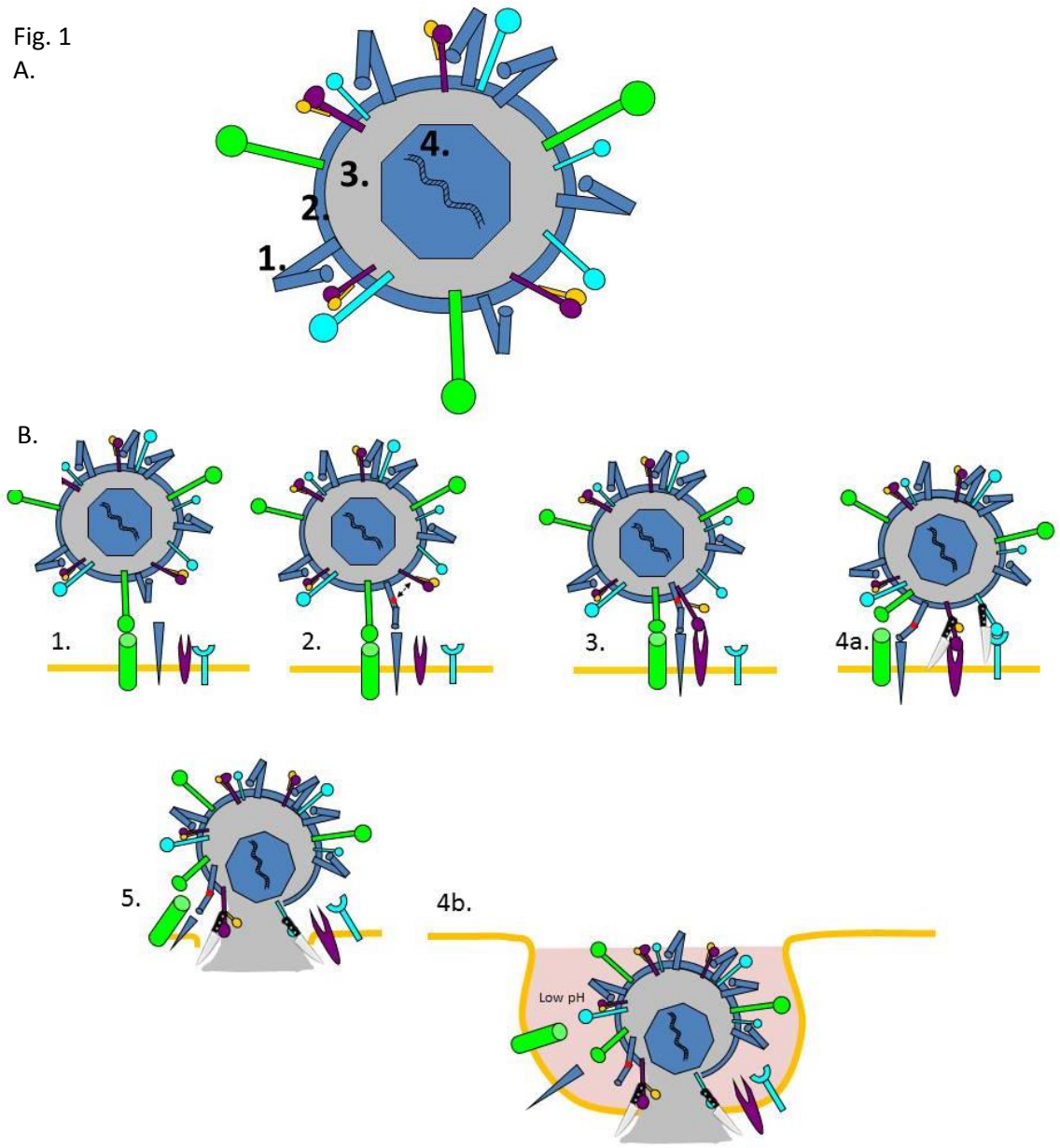


Fig. 1. **A.** A diagram of an HSV-1 virion. 1. Glycoproteins span the lipid envelope and project from the surface in functional clusters. 2. The lipid envelope. 3. A protein-rich amorphous "tegument" layer. 4. The icosahedral capsid containing the viral genome. **B.** The HSV-1 cell-entry process, the cell-surface is shown in gold. 1. Glycoprotein C (green) binds to cell-surface HSPG (green) and tethers the virus to the cell. 2. Glycoprotein D (dark blue) is brought into proximity to and binds with one of 3 possible receptors (dark blue), subsequently becoming unfolded and revealing an ecto-domain (red). 3. The glycoprotein H/L heterocomplex (purple and yellow) interacts with the ecto-domain and begins to disassociate and possibly bind an unknown cell-surface target (purple). 4a. Depending on cell-type, Glycoprotein B (light blue) binds to one of 3 possible receptors (light blue) and fusogenic domains on gB and possibly gH are exposed. 5. Direct fusion with the cell plasma membrane and delivery of the capsid to the cytoplasm. 4b. Depending on cell-type, gD binding triggers endocytosis of the gD receptor and the virus. The acidic environment of the endosome triggers fusogenic domains on gB and possibly gH to become exposed, fusion with the endosomal membrane occurs and the capsid is delivered to the cytoplasm.

al., 2011). Cryo-electron tomography has shown the structure of HSV-1 to be a bilayered membrane sphere averaging 170-200nm in diameter studded with membrane glycoproteins spikes projecting at various angles away from the surface making the full diameter of the particle approximately 225nm (Grünewald et al., 2003). The average number of glycoprotein spikes per virion is estimated to be 650 and they range in length from ~10-25nm. Some spikes appear to project away from the virus surface at dramatic angles while others are straight. These glycoproteins are involved in cellular attachment and entry, reviewed below. The viral capsid is ~125 nm in diameter, located within the envelope, and is surrounded by the tegument layer which occupies two thirds of the volume within the envelope (Grünewald et al., 2003). The tegument layer is believed to be composed of proteins including cellular actin and viral proteins responsible for navigating the capsid to the nucleus of a cell, anchoring the capsid to nuclear pores, host-cell subversion by mRNA degradation and initiation of viral gene transcription (Loret et al., 2008).

The double stranded DNA HSV-1 chromosome is linear and approximately 152kb in length. The chromosome consists of two large unique regions that are flanked on the ends by inverted terminal repeats (McGeoch et al., 1988). The genome contains at least 74 genes. Only a subset of these genes are required for growth in cultured cells while others have been shown to be involved in the processes of immune evasion, establishment of viral latency and reactivation(Batterson and Roizman, 1983) .

The infectious cycle of HSV-1 consists of cell binding and penetration, migration of the capsid to the nucleus, insertion of viral DNA into the nucleus, expression of viral genes, replication, and finally the assembly and egress of progeny virus. Depending on the cell type this cycle can take between 12 and 24 hours (Laquerre et al., 1998a; Tal-Singer et al., 1995). After cell entry, the delivery of viral capsid to the nucleus is a poorly understood process where viral tegument proteins hijack cellular dynein which is used for the retrograde transport of the capsid to the nucleus (Batterson and Roizman, 1983; Sodeik et

al., 1997). Upon the arrival of the capsid at the nucleus, capsid-associated viral tegument proteins are believed to facilitate a process of capsid uncoating and insertion of the viral chromosome into the nucleus(Ojala et al., 2000).

Once the viral chromosome is inserted into the cell nucleus, tegument proteins act to recruit cellular RNA polymerase II and initiate expression of viral genes (Grapes and O'Hare, 2000). Viral gene expression is divided into distinct phases. During immediate early (I.E.) expression, viral protein products that are essential to the transcription of other viral proteins are made and transported back into the nucleus (Dobrikova et al., 2010; Hayward et al., 1975). In addition, viral protein products are made which shut down cellular transcription, translation and DNA replication and make the cell refractory to infection by a subsequent virus (Stiles and Krummenacher, 2010; Stiles et al., 2010). After the I.E. phase the delayed early (D.E.) phase begins, this involves the initiation of viral DNA replication by the expression of virally-encoded DNA polymerase and replication machinery (Gac et al., 1996). Evidence also suggests that HSV-1 will subvert cellular DNA replication machinery in actively dividing cells to assist in viral replication (Boehmer and Nimonkar, 2003). The D.E. phase is also associated with the creation of discrete nuclear compartments which contain the replicating viral genomes (Lymberopoulos and Pearson, 2010; Monier et al., 2000). Synthesis of viral DNA then triggers the expression of Late (L) viral genes which include capsid proteins and envelope glycoproteins. New HSV-1 capsids are assembled within the nucleus and then exit through a highly contested process. Three competing models of HSV-1 nuclear egress have been proposed (Calistri et al., 2007; Diefenbach et al., 2008). In the most widely accepted model, fully-intact capsids exit through virally modified nuclear pores and are then enveloped into the trans Golgi network (TGN). During the expression of viral proteins, membrane-bound viral glycoproteins have been shown to cover endoplasmic reticulum and Golgi membranes (Handler et al., 1996; Miranda-Saksena et al., 2009). The progeny capsids therefore pick up their viral envelope and membrane bound glycoproteins during their envelopment into the TGN.

Enveloped viruses are then incorporated into transport vesicles which are transported to the cell surface.

HSV-1 has one of the widest ranges of different types of host cells of nearly any other mammalian virus and can infect both human and non-human cells (Karasneh and Shukla, 2011; Zago and Spear, 2003). One likely reason for this extensive tropism is the ability of the HSV-1 envelope glycoproteins to engage multiple, different cell-surface receptors to mediate virus binding and penetration. These glycoproteins and their contributions to HSV-1 cell binding and entry are reviewed below.

### 1.5.2. HSV-1 Glycoproteins and Binding

#### 1.5.2.1. Introduction to HSV-1 Glycoproteins

To date, the mature HSV-1 virus particle has been shown to contain 12 membrane-bound glycoproteins in its viral envelope (Karasneh and Shukla, 2011). Multiple copies of each of these 12 glycoproteins are distributed across the viral envelope. As previously stated, EM analysis has shown an average HSV-1 particle to contain approximately 600-700 total glycoprotein spikes (Steven 2003). These glycoproteins have been shown to be responsible for the binding and fusion of the HSV-1 particle to host cells (Fig. 1 B) (Karasneh and Shukla, 2011; Reske et al., 2007; Wittels and Spear, 1991). Of the 12 known glycoproteins, 4 are both necessary and sufficient to support HSV-1 infectivity in cultured cells, these are: glycoprotein B (gB), glycoprotein D (gD), glycoprotein H (gH) and glycoprotein L (gL) (Karasneh and Shukla, 2011; Milne et al., 2005). An additional glycoprotein, glycoprotein C (gC), while not absolutely necessary for viral growth, has been shown to greatly enhance infectivity in cultured cells (Laquerre et al., 1998a; Wittels and Spear, 1991). Glycoprotein molar ratios within purified virions have been calculated to be 1:1:14:9 for gB:gC:gD:gH (Handler et al., 1996).

Because of the integral role the HSV-1 glycoproteins play in cell-attachment, and subsequent infection, they are an attractive candidate to serve as a platform to display proteins in order to redirect viral tropism. However, care must be taken to not perturb glycoprotein functions that are essential and cannot be modified in order to maintain a viable virus. For the HSV-1 display system described in this thesis, the N-terminus of glycoprotein C was selected as the locus of protein display. This choice was based on the extensive body of research into the role of each glycoprotein in the infection process from the past 30 years. This research is summarized in the following section.

#### 1.5.2.2. Glycoprotein D

The most extensively investigated HSV-1 glycoprotein is glycoprotein D (gD). Glycoprotein D has been shown to be indispensable for HSV-1 infection (Johnson et al., 1990) and 4 gD receptors have been discovered that are naturally expressed on the surface of many different cell types (Karasneh and Shukla, 2011). Glycoprotein D is the shortest of the viral glycoproteins at 10nm in length and appears to be distributed across the viral envelope in a distinct and irregular pattern, possibly co-localizing with other glycoproteins in discrete functional units (Handler et al., 1996; Karasneh and Shukla, 2011). Glycoprotein D has been reported to potentially exist on the viral envelope as homo-dimers and trimers as well as in oligimeric complexes with other glycoproteins (Handler et al., 1996). The crystal structure of unbound gD shows an Ig-like folded core with N and C-terminal extensions (Cocchi et al., 2004). In the unbound state, the C-terminus appears to partially fold back onto the N-terminus. It is believed that during receptor binding this conformation becomes unfolded (Cocchi et al., 2004; Karasneh and Shukla, 2011).

Three separate classes of molecules that serve as gD receptors have been identified: Immunoglobulin, Tumor Necrosis Factor and Heparan Sulfate molecules. These three types of gD receptors were identified when they were each transiently expressed on CHO cells (naturally resistant to HSV-1 infection) which resulted in productive HSV-1 infections (Whitbeck et al., 1997). The two

members of the immunoglobulin superfamily are Nectin-1 and Nectin-2. These are ubiquitously expressed, cell-adhesion molecules present on many different types of epithelial and neuronal cells (O'Donnell et al., 2010; Stiles and Krummenacher, 2010). In the Tumor Necrosis Factor (TNF) superfamily, a molecule named Herpes Virus Entry Mediator (HVEM) has been identified as a gD receptor and is primarily found on lymphoid T and B cells and, to a lesser extent, on fibroblasts and endothelial cells (Stiles and Krummenacher, 2010). HVEM is believed to play a role in the activation and regulation of immune cells by responding to signaling by several different immune ligands (Stiles et al., 2010). Lastly, the least understood gD receptor class are the 3-O sulfated heparan sulfate (3-O-HS) proteoglycans (O'Donnell et al., 2010). The unique 3-O sulfation pattern of heparan sulfate modifications can be produced by any of the seven known isoforms of the 3-O sulfotransferase enzyme, six of which result in modifications that can serve as gD binding receptors (O'Donnell et al., 2010). 3-O-HS proteoglycans are expressed less ubiquitously across cell types than the gD immunoglobulin receptors but can be found on liver, kidney and endothelial cells (Karasneh and Shukla, 2011). 3-O sulfated heparan is unique as it is a polysaccharide while the other gD targets are protein receptors.

Glycoprotein D and at least one of its receptors must be present for HSV-1 infection (Cocchi et al., 2004; Johnson et al., 1990). While gD null viruses are not infectious they can still bind to the surface of cells, indicating that the role of gD is likely as a mediator of virus penetration and not cell-attachment (Johnson et al., 1990). However, in the absence of the other cell-binding glycoproteins,gC and gB, gD can mediate cell-attachment. Viruses lacking glycoprotein C and the glycoprotein B binding domains can still bind and infect cells, albeit with ~80% diminished efficiency (Laquerre et al., 1998a; Wittels and Spear, 1991). The lower affinity of gD for its receptors, $Kd=2x10^{-6}$ M, (Stiles et al., 2010) compared to the affinity of gB and gC to their targets, $Kd=1x10^{-7}$M (Rux et al., 2002), and a low abundance of gD receptors likely result in inefficient cell-attachment of these mutants. Unlike the gC and gB HS-binding targets, it has been shown that, on some cultured cells, the number of glycoprotein D receptors is quite

limited. On Vero cells, soluble gD molecules can completely block HSV-1 infectivity indicating a saturatable number of cell-surface receptors (Johnson et al., 1990). However, it should be noted that this type of testing has only been performed on Vero cells which predominantly express only Nectin-1 and have been shown to express the lowest levels of 3-O sulfated heparan of nearly all other cultured cell types that support HSV-1 infection. This level is important because HS proteoglycans, including those with 3-O modifications, are highly expressed on the surface HeLa and 293 cultured cells (O'Donnell et al., 2010)making 3-O HS moieties an efficient and abundant binding target.

It is believed that gD serves as an activator of the HSV-1 fusiogenic machinery. Antibody mapping and mutational analysis has shown that gD contains two discrete functional domains, a receptor binding N-terminal domain and a "pro-fusion" ecto-domain immediately adjacent to the viral surface (Cocchi et al., 2004). Mutant viruses lacking this ecto-domain can still bind to gD receptors, but these viruses cannot initiate fusion and infect cells (Cocchi et al., 2004; Johnson et al., 1990). Interestingly, when soluble gD containing the pro-fusion ecto-domain was added to cultured cells along with a gD null virus it rescued infectivity (Cocchi et al., 2004). This rescue was only seen when this soluble gD was added to the cells along with the virus, as the protein did not appear to bind significantly to either the virus or the cells separately. Conversely, when full length gD is expressed on the surface of cells it makes the cells refractory to infection (Johnson et al., 1990; Stiles et al., 2010). Lastly, when a gD mutant only containing the ectodomain was incorporated along with wt gD into viruses it acted as a dominant negative and inhibited infection (Cocchi et al., 2004). These results together suggest that gD forms a tripirtate complex between cell-surface gD receptors, gD itself, and other viral glycoproteins needed for virus penetration. A proposed model is that upon gD receptor binding, the C-terminus becomes unfolded. This in turn stabilizes gD receptor binding and allows the now exposed pro-fusion domain to interact with other viral glycoproteins which initiates HSV-1 fusion.

Due to the important and intricate role of gD in the process of HSV-1 cell entry, as well as its apparent interactions with other glycoproteins in multimeric complexes, gD was excluded as a possible locus for protein display in the system described in this thesis.

#### 1.5.2.3. Glycoprotein gH/gL

While shown to be necessary for HSV-1 infectivity (Reske et al., 2007) glycoproteins H and L are the least understood HSV-1 glycoproteins. These two glycoproteins are seen to heterodimerize shorty after expression. Deletion of either glycoprotein results in the loss of incorporation of the other into the viral envelope (Peng et al., 1998). Some believe the structure of gH resembles fusion proteins seen on other viruses however the extent of this resemblance remains controversial (Gianni et al., 2005). Evidence for gH's role as the primary HSV-1 fusion protein comes from mutant viruses lacking a gH αhelix domain. These viruses cannot penetrate cells but penetration can be restored by the insertion of fusion domains from the fusion proteins of other viruses (Gianni et al., 2005). Opponents to the model of gH as the HSV-1 fusion protein site a greater resemblance of the gB to other known viral fusion proteins and that gD and gH/gL alone are not sufficient to induce virus-free cell-cell fusion without gB (Karasneh and Shukla, 2011). Some propose that both gB and gH work in concert as co-fusion proteins each initiating hemi-fusion (Subramanian and Geraghty, 2007).

The structure of gL is unique among the HSV-1 membrane glycoproteins in that it lacks a transmembrane domain (Peng et al., 1998). However, gL is always found on the HSV-1 surface as it associates as a heterodimer with gH shortly after expression (Hutchinson et al., 1992; Peng et al., 1998). It is believed that gL may function as a chaperone protein for gH, allowing the appropriate incorporation of the hydrophobic protein into the viral envelope. Furthermore, it is possible that the association of gL with gH on mature virus particles acts to prevent pre-mature and inappropriate fusion of gH with non-target lipid membranes. It has been proposed that upon binding to the gD receptor, the gD profusion

domain becomes exposed and interacts with gL, resulting in the exposure of the fusion domain and insertion of the gH fusion domain with the cell membrane (Karasneh and Shukla, 2011).

The identity and existence of gH/gL cell surface receptors remains unknown. A report that the expression of gH/gL on the surface of cells confers resistance to HSV-1 infection suggests the existence of a required receptor which can become sequestered (Scanlan et al., 2003). Reports of soluble gH/gL binding to αvβ3 integrin indicate its possible role as a gH/gL receptor (Parry et al., 2005). However, this is contradicted by a report that the removal of an RGD motif in gH had no effect on infectivity (Galdiero et al., 1997) and that soluble gH/gL can bind to cells lacking αvβ3 integrin (Gianni et al., 2010). It is quite possible that gH/gL target multiple cell surface molecules.

As is the case with gD, gH/gL appear to be indispensable for virus infectivity. Furthermore, it is possible that modification of gH/gL by incorporation of foreign fusion proteins may disrupt the proposed fusiogenic activity of this protein and disrupt viral infectivity. For these reasons, gH and gL were also ruled out as possible locus for protein display.

#### 1.5.3.4. Glycoprotein B

The most widely accepted candidate as the HSV-1 fusion protein is gB, one of the 4 viral glycoproteins that are indispensable for HSV-1 infectivity. Glycoprotein B is found to protrude from the virus surface as 14nm spikes that are invariably clustered, possibly suggesting functional distribution (Claesson-Welsh and Spear, 1987; Karasneh and Shukla, 2011). The crystal structure of gB shows a trimer with five distinct structural domains including a fusion loop and αhelical colid coil that could be responsible for membrane-insertion (Heldwein et al., 2006). Glycoprotein B contains both α-helicies and β-sheets as major elements in its secondary structure. These elements are found in class I and class II viral fusion proteins respectively and therefore gB is categorized as a class III viral fusion protein (Dollery et al., 2011).

There appear to be several cell-surface gB receptors. Unlike the other HSV-1 glycoproteins that are essential for infection, gB actually has a measurable contribution to normal cell-attachment. Glycoprotein B binds to cell-surface heparin sulfate proteoglycans (HSPG) through a discrete N-terminal, poly-lysine binding domain. Removal of this domain results in a 20% decrease in virus binding to Vero cells but had no effect on cell-penetration (Laquerre et al., 1998b). Furthermore, the removal of this poly-lysine domain had no effect on the binding of soluble gB to HSPG deficient cells and soluble heparin only partially inhibited binding of gB to HSPG expressing cells (Bender et al., 2005). These reports led to the discovery of additional gB cell-surface receptors. Paired immunoglobulin-like type 2 receptor-α (PILRα), primarily expressed on immune cells, myelin-associated glycoprotein (MAG), found on glial cells, and non-muscle myosin heavy chain IIA (NMHC-IIA), involved in the reshaping and movement of cells, have all been identified as gB binding targets (Arii et al., 2010; Satoh and Arase, 2008). Given the evidence that gB null viruses are not infectious (Pertel et al., 2001), the removal of the gB HSPG-binding domain only causes a slight reduction in infectivity (Laquerre et al., 1998b) and treating cells with a PILRα blocking antibody can block HSV-1 infection (Satoh and Arase, 2008), it is likely that gB binding to one of its non-HSPG receptors is both crucial to infectivity and controlled by a separate domain(s) in the protein. It has been proposed that gB HSPG binding serves as an initial tethering of the HSV-1 particle to the cell surface, increasing the likelihood of interaction between gB and its other protein receptors (Bender et al., 2005; Laquerre et al., 1998b). While the binding affinity of HSV-1 gB to either HSPG or the other gB receptors has not yet been determined, it has been shown that heparin can only inhibit the binding of soluble gB to vero cells by 50% (Bender et al., 2005). These results suggests that the binding affinity of gB to other cell surface receptors is comparable to its affinity to HSPG, especially since vero cells have a reportedly high level of HSPG expression (Laquerre et al., 1998b; O'Donnell et al., 2010).

The crystal structure of unbound gB show a high degree of similarity between HSV-1 gB and the prebound structure of the vesicular stomatitis virus (VSV) fusion protein glycoprotein G which

undergoes extensive refolding during the fusion process (Heldwein et al., 2006). Similar to VSV gG, HSV-1 gB has been shown to undergo conformational changes upon exposure to low pH (Dollery et al., 2011). On many cell-types, HSV-1 penetrates the cell surface by triggering endocytosis and subsequently escapes the endosome in a pH-dependent process of fusion with the endosomal membrane that requires gD, gB and gH/gL (Karasneh and Shukla, 2011; Reske et al., 2007).

It has been reported that HSV-1 does not undergo cell-penetration in Vero cells lacking PILRα (Satoh and Arase, 2008) and BHK cells treated with BFLA, which blocks endosomal acidification (Dollery et al., 2011). This evidence suggests that gB may undergo conformational changes allowing membrane fusion after either binding to gB receptors found on cells in which the virus infects via plasma membrane fusion, or after exposure to endosomal low pH. Reports with gD mutants suggest that neither of these processes can be triggered in the absence of gD binding. It is tempting to speculate that gD-receptor binding serves as a necessary regulatory checkpoint. Once gD binds to a gD-receptor, indicating contact with an suitable host-cell membrane, it interacts with gB and frees it to undergo a pro-fusion conformational change in response to either of two additional criteria: gB-receptor binding or pH acidification.

Glycoprotein B does appear to have a discrete binding domain that is only involved in mediating viral-attachment to cells. Furthermore, as this is a potential high-affinity interaction gB, the gB HSPG-binding domain was an initial candidate as a locus for protein display for affinity selection. However, due to the apparent involvement of gB with membrane fusion, gB was ruled out in favor of the other HSV high-affinity binding protein, gC.

#### 1.5.4.5. Glycoprotein C

The final HSV-1 glycoprotein involved in cell-binding and entry to be reviewed here is the non-essential glycoprotein C. Glycoprotein C is a heavily glycosylated, 511 amino acid, monomeric protein. It contains a single transmembrane domain, a short “cytoplasmic” C-terminal domain and an N-terminus

that projects away from the viral surface at a length of 24nm (Handler et al., 1996; Rux et al., 2002). Glycoprotein C has been observed to be distributed across the viral surface as a monomer and fewer copies of gC are present on the viral surface than any other glycoprotein (Handler et al., 1996). Unlike the other glycoproteins reviewed above, gC is completely dispensable in that glycoprotein C null mutants are still completely infectious (Laquerre et al., 1998b; Tal-Singer et al., 1995). However, these mutants exhibited nearly tenfold less infectivity (virus particle input to PFU production) compared to wildtype (wt) KOS strain HSV-1(Herold et al., 1991). This loss in infectivity was found to be entirely attributable to a reduction in binding of the gC null viruses to the surface of cells. Virus adsorption kinetic assays showed that 30% of wt virus binds to cells within 3 hours. At this same time point, only 3% of the gC null viruses had bound (Herold et al., 1991). Similar results were found by several different groups using various binding assays and cell types (Laquerre et al., 1998b). The loss of infectivity of these gC null viruses was found to be specific to cell-adsorption and that, once bound to cells, these viruses exhibited the same rate of cell-penetration and replication as wt HSV (Herold et al., 1991; Laquerre et al., 1998b). It is now widely accepted that gC plays no role in the mechanics of cell-entry and membrane fusion other than to tether the HSV-1 particle to the surface of the cell and increase the efficiency and likelihood of interaction between the next viral glycoprotein, believed to be gD, and its cell-surface targets (Herold et al., 1991). A survey of the binding affinities of various HSV-1 glycoproteins to their cell-surface targets shows that the binding affinity of gC for its target, HSPG, is the highest of the glycoproteins tested thus far (Rux et al., 2002).

Cell-surface HSPG have been identified as the sole binding target of gC and the major initial attachment target for the entire HSV-1 particle (Laquerre et al., 1998a; Reske et al., 2007; Rux et al., 2002). Cells lacking cell-surface HSPG show markedly reduced binding to wt HSV-1 and no significant binding by soluble gC (Herold et al., 1991; Laquerre et al., 1998a). While no single HSPG binding domain has been discovered on gC, removal of a lysine-rich region between a.a. 33-123 results in a 75 fold

reduction in binding to HSPG (Laquerre et al., 1998a; Rux et al., 2002). Heparin, which is structurally similar and commonly used as a surrogate for cell-surface HSPGs has been shown to tightly bind soluble gC (gC-HSPG Kd=$1x10^{-7}$M, gC-heparin Kd=$1x10^{-8}$M (Rux et al., 2002)) and can inhibit HSV-1 infectivity on vero cells by nearly 50 fold (Laquerre et al., 1998b). Since gB has also been shown to also have HSPG binding properties, the effect of heparin on HSV-1 attachment cannot be entirely attributed to inhibition of gC binding. Therefore, a panel of HSV-1 mutants were tested for their sensitivity to heparin inhibition. Viruses lacking the gB HSPG binding mutant exhibited 20% less binding, gC null virus exhibited 60% less and a double mutant exhibited 80% less binding compared to wt HSV-1 (Laquerre et al., 1998b). The remaining 20% binding ability of the double mutant is likely the result of glycoprotein D binding (Laquerre et al., 1998a). It is important to note here that, while much less dramatic, heparin does have some measurable inhibition on the double mutant. It is possible this is a result of inhibition of gD binding to 3-O sulfated HSPGs which are known to be one of the gD binding targets expressed on vero cells.

The reports summarized above show that HSV-1 glycoprotein C is an important element of efficient HSV-1 infectivity, yet not absolutely required as gC null viruses are still viable but greatly impaired. Glycoprotein C acts only to tether viruses to cells, and has no role in the HSV-1 fusogenic machinery. These attibutes make glycoprotein C a logical choice as the platform on which to display protein candidates in the protein affinity selection system described herein. By replacing wt gC with a different protein, expressed as an N-terminal fusion with the gC transmembrane domain, the resulting viral particle would be redirected to no longer bind to cells expressing HSPG but rather cells expressing the binding partner of the new protein. Since glycoprotein C does not play a role in the fusogenic actions of HSV-1, this alteration should not impair the ability of the virus to enter the cell. Furthermore, since gC appears to be the naturally-occurring mediator of high-affinity cell-attachment, it is likely this is the most appropriate locus to introduce fusion proteins for affinity selection.

This strategy has in fact been employed by several groups to create HSV-1 particles with redirected tropism for use as gene therapy and anti-cancer treatments. These reports are summarized below.

### 1.5.2. Previous reports of redirected HSV-1 and their relevance to this novel system

The first published report of an HSV-1 particle with redirected tropism was over twenty years ago from the laboratory of Dr. Joseph Glorioso (Laquerre et al., 1998a). This report was a proof of concept work that proved the possibility of creating HSV-1 particles with redirected tropism for the intended purpose of tissue-specific therapeutic gene delivery. It was the work of Dr. Glorioso's research team that lead to the construction of the first HSPG-binding null HSV-1 mutant, reviewed in the previous section. In order to redirect viral tropism, the HSPG binding domain of gB was deleted, and the gC HSPG binding domain, between a.a. 83 and 161, was replaced by the gene encoding human erythropoietin (EPO). The resulting gC-fusion protein, pgCEPO1, featured the gC signal peptide, the full length EPO molecule, and the gC C-terminus including the transmembrane domain. In addition, a second fusion protein, pgCEPO2, was also tested. This second protein was identical to pgCEPO1 except that the gC signal peptide was replaced by the natural EPO signal peptide. Lastly a third fusion protein, an extreme truncation mutant, was created. This final protein pgCEPO3 was designed in order to test the minimal amount of gC protein required to still obtain successful incorporation into the viral envelope. For pgCEPO3, the gC N-terminal residues a.a. 1-376 were replaced with the EPO protein and signal peptide. First, cells were transfected with plasmids encoding the gCEPO fusion constructs and reactivity of cell lysates with αgC and αEPO antibodies was seen. Then, immunohistochemical analysis of fixed monolayers of transfected cells showed all three protein constructs were expressed on the surface of transfected Vero cells, suggesting efficient membrane incorporation. Soluble versions of all three fusion proteins were able to bind the soluble EPO receptor (ERE x). HSPG-binding null HSV-1

viruses expressing the gCEPO fusions were then created by inserting the genes encoding the fusion proteins into the gC locus of the HSV-1 chromosome by homologous recombination. These mutant viruses were shown to successfully express the gCEPO fusion proteins and incorporate them into their viral envelopes by immunoprecipitation of purified virions using αEPO antibodies. The amount of viral envelope-incorporation for gcEPO1 and gcEPO2 was the same as gC into wt HSV-1, however, the extreme truncation mutant gcEPO3 had 80% reduced incorporation. Viruses displaying the gCEPO fusions were shown to efficiently bind to EREx columns. Lastly, wt and gCEPO viruses were applied to EPO-receptor expressing FD-EPO cells. These cells do not support HSV-1 infectivity as they don't express any gD receptor and gD-receptor binding is required for HSV-1 penetration. When treated with 100 pfu/ml of the gCEPO virus these cells showed growth stimulation equal to that of 1 unit/ml of EPO. EM analysis showed that only gCEPO2 and not wt HSV-1 were bound to the surface and endocytosed into the FD-EPO cells. This EPO-induced receptor endocytosis did not result in infection as these viruses were unable to escape the endosome without the presence of a gD receptor.

The results of this work demonstrated the first successful account of redirecting HSV-1 binding, albeit not infectivity, by displaying a gC-fusion protein. Several important aspects of this work helped direct subsequent attempts to create HSV-1 viruses with altered tropism by additional groups. Importantly, this work showed a specific gC domain which can, once removed, abolish HSPG binding and can support the incorporation of a fully-functional exogenous protein incorporated into a HSV-1 particle.

The next step in the development of HSV-1 particles with redirected tropism from gC-fusion proteins was reported by the research group of Dr. Xandra Breakefield. This group reported the creation of an HSV-1 amplicon peptide display vector for the purposes of creating "gutless" HSV-1 particles with redirected tropism for tissue-specific gene delivery (Spear et al., 2003). Here they created an HSV-1 amplicon plasmid, that was engineered to contain a gene encoding gC with the HSPG binding domain removed (a.a. 33-174) and replaced with unique restriction sites which allow for the insertion of

genes encoding exogenous protein to create gC-fusion proteins (USPTO 09/592,537,2000). This construct could then be transfected into cells infected with helper HSV-1, to create HSV-1 particles that display the gC-fusion proteins. These particles are not infectious viruses as they lack an intact viral genome. This group then reported successfully creating modified HSV-1 particles, using this amplicon system, which had redirected binding (Grandi et al., 2004). Here, a peptide encoding a hexahistidine tag was cloned into the gC-binding domain restriction sites within the amplicon vector. These HSV-His6 particles, as well as wt gC and gC null virus particles, were then applied to HEK293 cells and 293 cells stably expressing a scFv that binds to His6 (293-6H). Since these viruses were replication defective, virus-encoded β-galactosidase expression was then used to measure levels of infectivity. Cells were incubated with the viruses (MOI 0.1) at 4$^{o}$C for various amounts of time over a 30-120 minute time course. Unbound viruses were then washed away, the temperature was raised to 37$^{o}$C and 24hr later cells were stained for β-galactosidase expression. After 30 minutes of binding, the HSV-His6 particles applied to the 293-6H cells had induced over twice the amount βgalactosidase expression than when applied to 293 cells and over twice the amount of expression induced by the gC-containing particles applied to either cell type. After 120 minutes of binding this difference increased to nearly four times the amount. This increased amount of β-galactosidase expression was shown to be specific to His6 binding to the αHis6 scFv as competition with a soluble His6-protein abolished this increase and had no effect on the binding of gC-expressing particles nor any effect on the gC-His6 particles applied to 293 cells lacking the 6H receptor.

Unlike in the report by Glorioso , this report shows that this redirected gC binding resulted in successful penetration of the virus into the cell and delivery of genetic cargo. Presumably if these would have been replication competent viruses this would have resulted in viral replication and production of progeny virus also displaying the gC-His6 fusion protein. Another factor highlighted by this report is perhaps the most important in regards to using gC-fusions to create redirected HSV-1 for the purposes

of selecting for high-affinity protein binding. It was obsered that the virus particles displaying the gC-His6 fusion, when applied to 293-6H cells, produced nearly 4 fold more βgalactosidase expression than particles displaying wt-gC applied to HSPG expressing cells. This increased expression is likely the result of more efficient viral binding, and subsequently entry and transgene delivery, due to the higher affinity of gC-His6 for the αHis6 scFv than gC for HSPG (Grandi et al., 2004). This importantly demonstrates that increased cell-binding affinity correlates to increased levels of infection and likely to increased viral growth. This increase in infection would then make high-affinity binding a selectable trait by selecting for increased viral growth.

Following these reports, several groups reported success in the next step in the progression of this technology. In 2005 and again in 2008, Geller et al reported creating HSV-1 particles displaying a full-length, complex protein. Viruses were created that expressed prepro glial-cell-derived neurotropic factor (GDNF) and prepro brain-derived neurotropic factor (BDNF) as a fusion to truncated gC at a.a. 153 for the purposes of targeting nigrostriatal neurons for gene-delivery (Cao et al., 2008; Wang et al., 2005). While the genes for the prepro version of each protein, 211 and 247 a.a. in length for GDNF and BDNF respectively, were inserted next to truncated gC, the mature form of each protein (134 and 199 a.a.) were displayed on the virus (Wang et al., 2005). These results demonstrated that a complex exogenous protein could be correctly processed and efficiently displayed on HSV-1 particles. When injected into the midbrain of rats, these particles were shown to bind GDNF receptor α1 and the BDNF receptor TrkB on nigrostriatal neurons and efficiently deliver a LacZ transgene resulting in β-galactosidase expression. While these viruses were not replication competent, the delivery of the LacZ transgene shows successful cell penetration and delivery of genetic cargo. When compared to both gC containing and gC null virus particles, the gC-BDNF and gC-GDNF particles resulted in 5-fold more β-galactosidase expressing nigrostriatal neurons. This difference in expression was abolished by pretreating the virus particles with αBDNF and αGDNF antibodies. These particles did still contain the gB

HSPG binding domain which would support some amount of non-target cell binding. The authors speculate that removal of this domain could potentially reduce non-target cell binding even further.

This and several additional reports (Cao et al., 2008; Kouvatsis et al., 2007) show that HSV-1 can display many different types of full-length exogenous proteins fused to truncated gC. They also show that these fusion proteins result in redirected virus binding and entry into cells bearing target receptors. These reports suggest that the HSV-1 protein affinity selection system, describe herein, can be successfully applied to a wide number of different types and sizes of proteins. The ability of HSV-1 to tolerate the modification to gC is one of the major reasons behind the selection of HSV-1, over other mammalian viruses, for this system. An additional advantage to using HSV-1 gC as the locus for protein display is that these previous reports have shown that proteins displayed here are correctly folded and completely post-translationally modified. The importance of such post-translational modifications for a protein affinity selection system was reviewed in section 3.

**Chapter 1 Part 6. Site Specific Recombination & its novel use to create HSV-1 libraries**

As discussed briefly in chapter 1 section 4, HSV-1 viruses containing modified genetic sequences are typically created using traditional cloning techniques. These techniques involve genetically altering cloned viral DNA segments. Once altered, the modified DNA segment is introduced back into the HSV-1 chromosome either through homologous recombination with purified viral DNA, or the use of large cosmid DNA vectors. These cosmid vectors contain separate regions of the viral chromosome as well as regions of homology to allow reassembly of the intact chromosome (Spear et al., 2003)(Breakefield 2002). For homologous recombination, the DNA segments are transfected into mammalian cells so that cellular DNA repair machinery can facilitate recombination. The cells will then begin to express the viral chromosome, initiating production of viral proteins and the assembly of virions. These techniques are typically quite slow and inefficient as homologous recombination between the desired molecules is a

relatively rare occurrence (Glorioso 1992). Selectable markers are required for the recovery of recombinant viruses from the large background of non-recombinant viruses. Because of these inefficiencies, systems involving the use of site-specific recombination of the HSV-1 genome have been developed (Conner et al., 2008; Gage et al., 1992). Enzyme mediated site-specific recombination is both highly specific and very efficient. While these systems do require the insertion of recombination sites, typically done via homologous recombination, they capitalize on the efficiency of recombinase enzymes such as cre and λ integrase (Hartley et al., 2000; Sheren et al., 2007). Once recombination sites have been introduced into the viral chromosome, new DNA sequences can be inserted relatively easily using *in vitro* recombination reactions. These recombination reactions are highly efficient, resulting in as much as 90-100% of the chromosomes in the reaction being successfully recombined (Conner et al., 2008; Hartley et al., 2000; Lupold et al., 2007). The resulting recombinant viral chromosome can then be transfected into mammalian cells in order to produce the recombinant virus. While these systems are more efficient at creating recombinant viral chromosomes, the end result is the same as traditional cloning techniques: viral DNA that must be transfected into mammalian cells to produce virus. As previously stated, inefficiencies in the conversion of transfected viral DNA into infectious virus are well documented. It is estimated that 1 in $10^6$ transfected chromosomes are converted into a live virus (Lupold et al., 2007; Werstuck et al., 1990). This level of inefficiency is acceptable when only a single recombinant clone is required. For this, many micrograms of the same recombinant chromosome can be transfected and only one resulting virus is necessary as it can then be grown and expanded. However, if a library many recombinant viruses is desired, then a library of the different viral chromosomes would need to be transfected. If $10^4$-$10^6$ copies of each library member are required the total library diversity will be quite limited.

A solution to this problem is to perform DNA recombination in live, actively replicating viruses. As stated above, it is estimated that only 1 in $10^6$ transfected chromosomes are converted into a live

virus, however it is not uncommon to achieve efficient viral replication from as little as 1 plaque forming unit (PFU). During the process of viral replication the viral genome is expressed, copied and packaged into virus particles assembled from the proteins encoded within the genome. Therefore, if the viral chromosome is modified during an active infection, the modified sequence will be expressed and the gene products will be incorporated into virions along with the modified chromosome. Such a system does not require production of virus from transfected viral DNA. Therefore, the rate of successfully producing recombinant virions would be much higher. An attempt to create such a system was reported by Rodriguez et al in 2007 and was extensively reviewed in chapter 1 section 4. This system utilized live adenoviruses containing lox sites within their viral chromosomes to insert library genes from transfected shuttle plasmids using cre-mediated recombination during viral replication in HEK293 cells. This system appeared to allow the successful screening of a library consisting of $10^5$ different members. This system was however quite limited by the biological constraints of adenovirus assembly which does not support the insertion of exogenous peptide sequences bigger than ~6 amino acids(Lupold et al., 2007) .No known reports of such a system have ever been described for HSV-1 or any other large enveloped DNA virus. Therefore, the novel HSV-1 based protein affinity selection system described herein is the first known report of such a system.

## Chapter 2. Creation of a novel HSV-1 system for the display of proteins

## Chapter 2 Part 1. Creation of a site-specific recombination system for the insertion of genes into the HSV-1 chromosome

### 2.1.1. Introduction

In order to create large, diverse libraries of viruses displaying protein candidates, a system to efficiently shuttle genes into HSV-1 chromosomes was developed. Due to the large size of the HSV-1 genome, ~152kb, and the potential number of unique recombinants required to encompass an average-size protein library, $10^{3-6}$, traditional cloning methods would not be sufficient (reviewed in Chapter 1 Part 6).

Recombinase Mediated Cassette Exchange (RMCE) is a technique involving the exchange of a region of DNA that is flanked by two lox sites (Fig. 2C) (Langer et al., 2002). Lox sites (Locus Of eXchange) are naturally occurring bacteriophage P1 DNA elements that serve as binding sites for the recombinase enzyme cre (Causes recombination). This bacteriophage recombination system has been used for a wide variety of genetic engineering applications. While classically the cre/lox recombination system has been used as a means to delete regions of DNA, the system can also be used for the reverse reaction; site-specific insertion of DNA sequences. However, due to the reciprocal nature of Cre/lox recombination events, insertion reactions between wild type lox sites are largely unstable. The discovery and characterization of lox sites with mutant arm and spacer sequences allows irreversible, unidirectional cre-mediated site-specific DNA insertion reactions (Albert et al., 1995; Hoess et al., 1986; Langer et al., 2002).

Within is the first known report of Cre/lox RMCE being used to shuttle genes into a herpesvirus chromosome which allows the efficient insertion of plasmid-encoded genes into the HSV-1 chromosome. This process was designed to support the insertion of a library of protein candidate genes

Fig. 2

A.

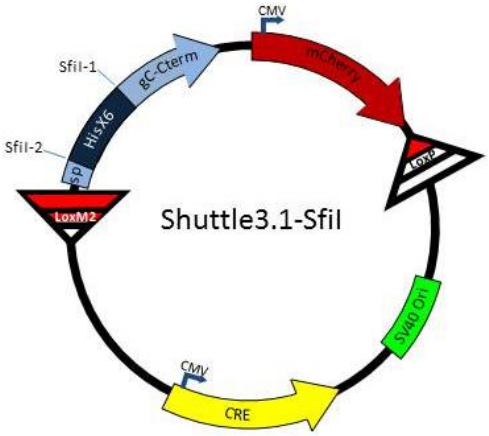


B.

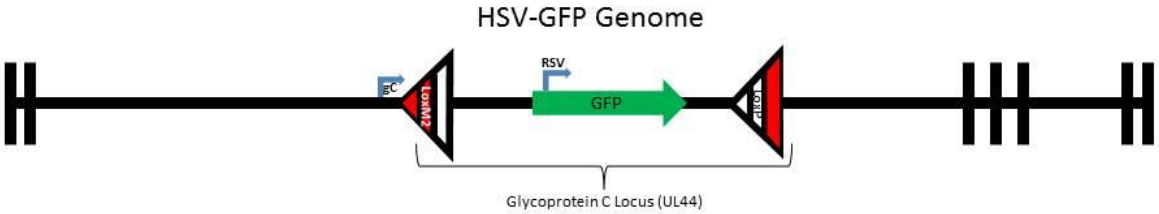


C.

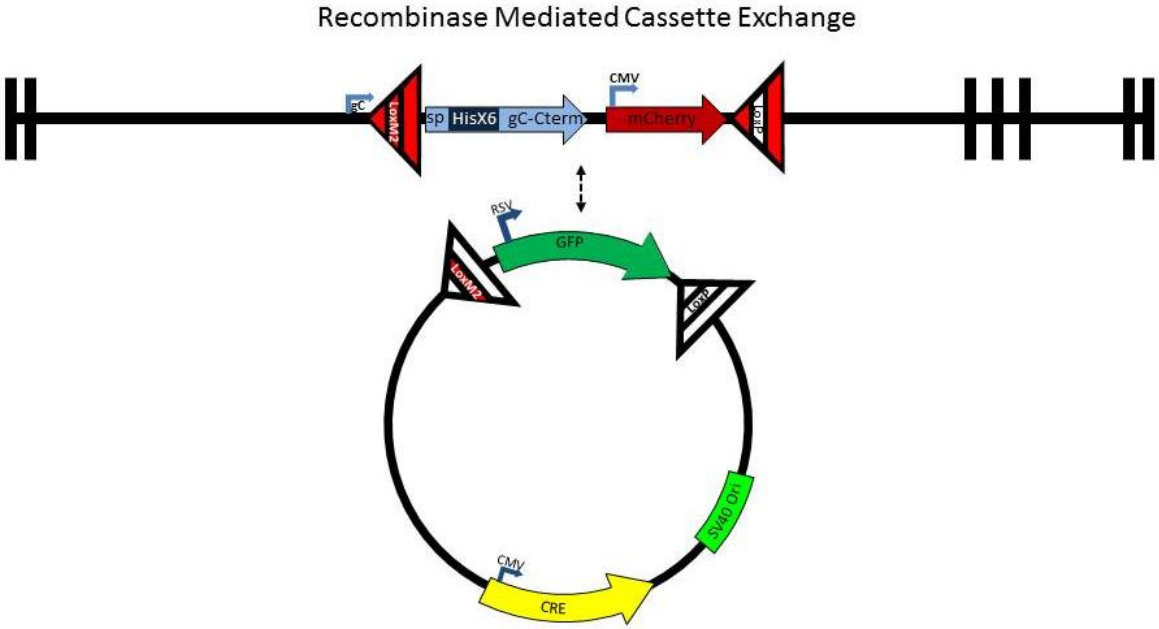


Fig. 2. **A.** A diagram of plasmid "Shuttle3.1-SfiI" which is capable of Recombinase Mediated Cassette Exchage (RMCE) with the HSV-GFP recipient genome. **B.** A diagram of the linear dsDNA HSV-GFP genome. **C.** The resulting products from a RMCE reaction between Shuttle3.1-Sfi1 and the HSV-GFP genome.

into HSV-1 chromosomes in such a manner that the encoded proteins are displayed on the surfaces of HSV-1 virions.

### 2.1.2. Methods

#### Shuttle Plasmid Construction

The half-mutant semi-compatible lox site M2-66 features a 5' wild type LoxP 13bp arm, the M2 mutant sequence for the 8bp spacer and a 3' mutant arm (Langer 2002). This site was created by annealing the oligos 5-M2-66-HindIII top; 5-AGCTTATAACTTCGTATATGGTTTCTTATACGAACGGTAC-3 and 5-M2-66-HindIII-bottom; 5-AGCTGTACCGTTCGTATAAGAAACCATATACGAAGTTATA-3. The half-mutant semi-compatible lox site LoxP-71 contains a 5' mutant 13bp arm, the wild type LoxP 8bp spacer and a 3' wild type LoxP arm. This site was created by annealing the oligos 3-LoxP-71-SacI-top 5-TACCGTTCGTATAGCATACATTATACGAAGTTATGAGCT-3 and 3-LoxP-71-SacI-Bottom 5-CATAACTTCGTATAATGTATGCTATACGAACGGTAAGCT-3. For the creation of each dsDNA lox site, the top and bottom primers were mixed at a concentration of 100pg/ul in 50mM NaCl. The solutions were heated in a 70$^{o}$C heat-block for 10 minutes and then removed and allowed to slowly cool to room temperature. The resulting two dsDNA fragments contained the M2-66 and LoxP-71 sites as well as 5' and 3' overhangs complementary to those created by the HindIII and SacI restriction endonucleases respectively. These overhangs were used to facilitate a two-step cloning procedure. The plasmid pGem3 was digested with the restriction enzyme HindIII and the M2-66 dsDNA fragment containing HindIII overhangs was ligated into the linearized plasmid using T4 DNA ligase (NEB) following the manufacturer's protocol. The ligation reaction was then used to transform chemically competent *E. coli* DH5α cells which were then plated onto Luria-Broth-Agar Ampicillin (LB-Amp) plates. Bacterial clones were picked from these plates, grown in Lura-Broth containing ampicillin, and plasmid DNA was extracted using Zippy Plasmid MiniPrep Kits (Zymo Research) following the manufacturer's protocol. Plasmids from these clones were screened to confirm the insertion and correct orientation of the insert

via DNA sequencing. DNA sequence was performed by ACGT inc. These processes were used for all other cloning steps unless otherwise specific. Plasmid DNA from a clone containing the correct insert was selected and used in the next step where the dsDNA fragment containing the LoxP-71 site was inserted into the SacI site. A bacterial clone containing the resulting plasmid, "Shuttle13" was confirmed via sequencing and plasmid DNA was isolated as before.

The plasmid pgC1 (obtained from Dr. Joseph Glorioso, University of Pittsburg) contains a portion of the HSV-1 genome that includes the glycoprotein C gene (UL44) as well as ~2kb of homology with the HSV-1 genome on either side (5' and 3') . The DNA sequence encoding the binding domain of glycoprotein C (a.a. 33-174, reviewed in Chapter 1, 1.5.2.5 & 1.5.3.1) was removed and replaced with a 6-histidine tag via an inverse PCR reaction using forward primer gC-AA33; 5-GTGCGACCCGCGCCCGGTGGAGGCAGTT-3 and reverse primer gC-AA174; 5-CACCACCACCACCACCTAGAGGAGGTCCTGA-3. This PCR reaction, and unless specific all others, was performed using iProof DNA polymerase (BioRad) following the manufacturer's protocol. The PCR product was gel purified and then phosphorylated with T4 poly-nucleotide kinase (NEB), following manufacturer's instructions, and subsequently re-circularized using T4 DNA ligase. The resulting plasmid was cloned and verified, as described above, to create the plasmid "pGC1-gC-Hisx6." The entire open reading frame for this gC-Hisx6 gene was amplified from plasmid pGC1-gC-Hisx6 using the PCR primers gC-Sph1; 5-TATAGCATGCTAGGAGGCGTCGGGCA-3 and gC-Kpn1; 5-ATATGGTACCAATTACCGCCGATGACGCT-3. These primers add a 5' Sph1 site and a 3'Kpn1 site to facilitate cloning of the gC-Hisx6 ORF into the Sph1 and Kpn1 sites in Shuttle13. In order to also add a fluorescent marker to the floxed cassette within Shuttle13, CMV-mCherry was amplified from plasmid pmCherry-C1 using PCR with forward primer mCh-5'-Kpn-pA-Nhe1; 5-GCAAGTACCAATAAAGCTAGCAATAGTTAATTAATAGTAATCAATTACGGGGTCA-3 and reverse primer mCh-3'-Stop-pA-Kpn1; 5-TTAAGGTACCTTTATTGAAAATATATTACTTGTACAGCTCGTCCATGC-3. These primers

add both 5' and 3' Kpn1 sites for cloning into Shuttle13, downstream of the gC-Hisx6 ORF, a Nhe1 site for directional screening as well as a poly-adenylation consensus sequence following the mCherry stop codon. This PCR fragment was cloned into the Kpn1 site of Shuttle13. Clones were selected and verified as before. The resulting plasmid, named "Shuttle5," contains the gC-Hisx6 open reading frame (ORF), followed by the CMV-mCherry cassette, all contained between the M2-66 and LoxP-71 lox sites.

In order to add a cassette for the expression of cre recombinase in mammalian-cells, the entire M2-66 LoxP-71 floxed region of Shuttle5, including the lox sites, was removed by digestion with HindIII and EcoRI restriction endonucleases and was cloned into the HindIII and EcoRI sites of the plasmid pEPI-cre-Zeo. pEPI-cre-Zeo contains a CMV-cre expression cassette. The resulting plasmid was named "pEPI-Shuttle5." To add an SV40 origin of replication, in order to support episomal replication of the plasmid in cells expressing SV40 Large T-Antigen, the entire region of pEPI-Shuttle5 containing the CMV-cre cassette and the entire floxed RMCE cassette was amplified by PCR and inserted into the plasmid pcDNA3.1+. The PCR primers pepi-5'-Xho1; 5-AATTCTCGAGGTATTACCGCCATGCATTAG-3 and pepi-3'-Spe1; 5-GTAGACTAGTCGTCGACTGCAGAATTCG-3 were used to amplify the region of pEPI-Shuttle5 containing CMV-cre and the floxed RMCE cassette. These primers also add a 5' Xho1 and 3' Spe1 restriction endonuclease sites onto the outside of the amplified region. The PCR primers pc3.1-5'-Xho1; 5-AATTCTCGAGGATCTCCCGATCCGTC-3 and pc3.1-3'-Spe1; 5-GTAGACTAGTTAGAGGGCCCGTTTAAAC-3 were used in an inverse PCR reaction with the plasmid pcDNA3.1+ to add Xho1 and Spe1 restriction endonuclease sites to the plasmid. The two PCR products were then digested with Xho1 and Spe1 restriction endonucleases, ligated together to create plasmid "pcDNA3.1-CMV-cre-Shuttle5." A bacterial clone containing this plasmid were created and verified and plasmid DNA was isolated as previously described.

The restriction endonuclease Sfi1 is commonly used for the cloning of plasmid libraries. The middle 5 nucleotides of the 13bp Sfi1 recognition sequence are degenerate; GGCCNNNNNGGCC. This

site allows for the ability to design sites with unique overhangs that allow for directional cloning, while only requiring the use of one restriction endonuclease. Furthermore, the large size of the Sfi recognition sequence reduces the possibility of this sequence being present inside the open reading frame of library members. Two unique Sfi1 sites were sequentially placed in frame with the Hisx6-glycoproteinC fusion within pcDNA3.1-CMV-cre-Shuttle5. These sites will facilitate the cloning of genes encoding library proteins so that they are expressed on the surface of the virus as N-terminal fusions with the glycoprotein C (gC) C-terminus. A naturally occurring Sfi1 recognition site naturally present within the wildtype glycoprotein C gene was removed by the introduction of a single nucleotide change; GGC to AGC. This alteration did not change the translated sequence. To produce this point mutation, two sets of PCR primers were used in a 2-step manipulation. First the PCR primers Sfi-KO-anti; 5-CGTAACGGCtGACTTAGC-3 and Sfi-KO-H3; 5-ATACAAGCTTATAACTTCGTATATG-3 were used to amplify the region spanning from the Sfi1 site to an upstream HindIII site and the primers Sfi-KO-sense; 5-GCTAAGTCaGCCGTTACG-3 and Sfi-KO-Sac1-3; 5-TGGCTGGCAACTAGAAGG-3 were used to amplify a region spanning from the Sfi1 site to a downstream Sac1 site. The primers Sfi-KO-anti and Sfi-KO-sense introduce the point mutation in the Sfi1 site and the PCR products from both reactions share 18bp of overlapping sequence identity. In the second step, these two PCR products were combined in a PCR reaction using primers Sfi1-KO-H3 and Sfi1-KO-Sac1-3. The resulting PCR product was then cut with HindIII and SacI restriction endonucleases and was inserted between the HindIII and SacI sites in the plasmid pcDNA3.1-CMV-cre-Shuttle5. The resulting plasmid was identical to pcDNA3.1-CMV-cre-Shuttle5 except that now the naturally occurring SfiI site had been removed. A bacterial clone containing this plasmid was isolated and verified as before.

Next, two unique Sfi1 restriction sites were added into plasmid pcDNA3.1-CMV-cre-Shuttle5 to allow insertion of library member genes in-frame with the glycoprotein C C-terminus. The PCR primers gC-Sfi1-5'; 5-TCCGGCCGCCTGGGCCTAGCATGCAAGCTGTACC-3 and gC-Sfi1-3'; 5-

TCCGGCCAGGCCGGCCTAGAGGAGGTCCTGAC-3 were used in an inverse PCR reaction using pcDNA3.1-CMV-cre-Shuttle5 as the template. The resulting PCR product was gel purified, phosphorylated and ligated together as before. The resulting plasmid now contains two unique sfi1 sites, one immediately downstream of the 5' Lox site and the other immediately upstream of amino acid 174 in the gC C-terminus. The resulting plasmid was named "Shuttle3.1-Sfi1" (Fig. 2A). A bacterial clone containing the plasmid was verified as before.

Shuttle3.1-Sfi1 encodes for a fusion between a gene cloned into the Sfi1 sites and the gC C-terminus. These gene can then be inserted via RMCE into a recipient HSV-1 chromosome (Fig. 2 B & C) (see below), along with the CMV-mCherry cassette. This chromosome will then encode for a virus which will display the gC-fusion protein.

**Recipient HSV-1 Chromosome Construction**

The parental virus chromosome HSV KgPk-gC- was obtained from Dr. Joseph Glorioso (University of Pittsburg). This chromosome encodes a virus where the entire glycoprotein-C coding sequence has been removed and replaced by the LacZ gene. Furthermore the glycoprotein-B coding sequence of this virus has been altered so that the lysine-rich region (residues 68-76) is not present. These modifications result in a HSV-1 that is significantly impaired for its ability to bind cells and almost devoid of HSPG binding ability (Glorioso 1998).

The plasmid pgC1 (above) contains a region of the HSV-1 genome including the glycoprotein C gene (UL44) as well as approximately 1kb of upstream and downstream genomic sequence. This plasmid was used to create a homologous recombination vector for the insertion of acceptor lox sites (corresponding with the sites inside Shuttle plasmid) as well as a fluorescent GFP marker. The PCR primers pgC1-5'-END-Bstb1-Hpa1; 5-AGTTAACATTCGAAGCCCGACGCCTCCCCCTCGCA-3 and pgC1-3'-End-Spe1-Stu1; 5-TAGGCCTAACTAGTCGCGAGACCCCCCCGTTACCTTT-3 were used in an inverse PCR reaction with pgC1 to remove the UL44 open reading frame as well as to introduce restriction sites for

subsequent cloning steps. The PCR product was phosphorylated, recircularized and cloned into bacteria as before. This plasmid was named "pgC1ΔgC." In the first of two subsequent cloning steps, the 5' acceptor lox site Lox-71-M2 (corresponding with the 5' Lox-66-M2 site in Shuttle3.1-Sfi1) was created via annealing the single-stranded oligonucleotides 1-Bstb1-71-M2-Pme1-Hpa1; 5-CGAATACCGTTCGTATATGGTTTCTTATACGAAGTTATGTTTAAACATGTT-3 and 2-Bstb1-71-M2-Pme1-Hpa1; 5-AACATGTTTAAACATAACTTCGTATAAGAAACCATATACGAACGGTATT-3 as described before. The resulting dsDNA product contains a BstB1 overhang and Hpa1 blunt end and was inserted into the BstB1 and Hpa1 sites within pgC1ΔgC. In the second step, the 3' acceptor lox site LoxP-66 (corresponding with the 3' LoxP-71 site in Shuttle) was created via annealing the single-stranded oligonucleotides 1-Stu1-Pac1-Loxp-66-Spe1; 5-CCTACTTAATTAAATAACTTCGTATAGCATACATTATACGAACGGTAA-3 and 2-Stu1-Pac1-Loxp-66-Spe1; 5-CTAGTTACCGTTCGTATAATGTATGCTATACGAAGTTATTTAATTAAGTAGG-3. The resulting double stranded product contains a SpeI overhang and Stu1 blunt end and was inserted into the SpeI and StuI sites in pgC1ΔgC. The resulting plasmid, named "pgC1-Lox2," was cloned into bacteria and verified as before. Of note, the 5' lox site is positioned immediately downstream of the glycoprotein C endogenous promoter which will therefore control the expression of any gene inserted between the lox sites.

The gene encoding RSV-eGFP was added between the lox sites to serve the dual purposes of 1. A selectable marker for the homologous recombination insertion 2. An outgoing fluorescent marker for RMCE exchange. The RSV-eGFP cassette was amplified from plasmid pRC/RSV-eGFP with the PCR primers RSV-eGFP-Pme1; 5-ATCCGTTTAAACGCTGCTTCGCGATGTACG-3 and RSV-eGFP-Pac1; 5-GCTGTTAATTAAGCCTCAGAAGCCATAGAGC-3. The resulting PCR product had Pme1 and Pac1 sites added to the ends of the RSV-eGFP gene and was inserted into the Pme1 and Pac1 sites in pgC1-Lox2. The resulting plasmid, named "pgC1-Lox2-eGFP," was cloned into bacteria, screened, and plasmid DNA was isolated as before.

**Homologous Recombination into the HSV-1 Chromosome**

In order to insert the floxed GFP cassette into the HSV-1 chromosome via homologous recombination, the plasmid pgC1-Lox2-eGFP was first linearized by cutting with the restriction endonuclease Xmn1. One microgram of this linear product and was co-transfected into HEK293 cells plated on a 10cm dish, using a $CaCl_2$ transfection procedure, with 9 micrograms of the HSV-1 viral chromosome HSV KgPk-gC-. Detailed general cell-culture and transfection methods can be found below.

Fourteen days after the transfection, cells showed significant signs of viral infection (CPE) as well as patches of green fluorescence. Several GFP positive cell clusters were manually harvested with a P100 pipette, and placed into Eppendorf tubes containing DMEM. These tubes were freeze-thawed three times to lyse the cells and release intracellular virus. This lysate was then used to infect a new 10cm dish of 50% confluent HEK293 cells in order to amplify the virus. Seven days following infection, cells and media were harvested, freeze-thawed three times in liquid nitrogen, lysed cell debris was pelleted via centrifugation for 5min at 3000xg and the virus-containing cell-free supernatant (referred to as clarified lysate) was collected.

**Plaque Purification and Titer of Recombinant Virus**

Confluent HEK293 cells were infected with serial dilutions of the recombinant virus-containing clarified lysate (from above). Two hours following infection, the liquid media was removed from the dishes and cells were overlaid with a warm mixture of 1.6% molten noble agar, 1XDMEM, 1%FBS, Pen-Strep (100 I.U./ml) and $NaHCO_3$ (3.7g/L) buffer. This mixture hardens upon cooling and is conducive to cell growth but inhibits viral spread via diffusion. Three days after the first overlay, cells were overlaid again with the same mixture as before plus the addition of 0.01% Neutral Red vital stain. Twenty four hours after this second overlay, viral plaques become visible. Virus clones were isolated by manually picking individual plaques using a sterile glass pipette inserted completely through the hard agar to the

bottom of the dish. Several plaques were picked, placed in separate Eppendorf tubes containing ~200ul DMEM and freeze-thawed three times to release virus. These virus clones were then applied to fresh plates of HEK293 cells and a GFP expressing clone, named "HSV-GFP," (Fig. 2B) was selected and amplified via infection of additional HEK293 cells and a stock of HSV-GFP clarified lysate was generated (see 2.1.2.1). Viral DNA was extracted from a sample of the HSV-GFP and PCR primers were used to amplify and verify the portion of the HSV-1 chromosome containing the floxed GFP cassette via DNA sequencing as described below. This viral plaque procedure was also used to establish titer (plaque forming units/ml) of the HSV-GFP virus stock by counting plaques produced by a series of dilutions of this stock.

## Chapter 2. Part 2. Creation of a protocol to efficiently create a library of recombinant viruses

### 2.2.1. Introduction

It was necessary to determine the optimal procedure for efficient RMCE (reviewed in 2.1.1) between the plasmid Shuttle and the recipient HSV-GFP viral chromosome. For the purposes of screening a large library of protein-encoding genes, the transfer of plasmid-based library genes into viral chromosomes must be efficient. Two protocols for this exchange were developed and tested. 1: RMCE between co-transfected shuttles and viral chromosomes and 2: RMCE exchange into live virus (Fig. 2C).

### 2.2.2. General Methods

*Purification of HSV Viral DNA For Transfection & Standardization*

HSV-GFP (from 2.1.2.4) was used to infect 30 dishes of HEK293 cells at 80% confluency, MOI=1. Seven days after infection these cells showed significant CPE. Cells and viruses were harvested and into sterile 50ml conical tubes, 45ml per tube. 500ul of sterile 2M Tris pH 9.0 was added to each tube to act as a pH buffer and prevent acidification during freeze-thaw. Tubes were subjected to 3 freeze-thaw cycles of liquid nitrogen followed by a 37$^{o}$C water bath to release intracellular virus. Cell debris was

pelleted by 5 minute centrifugation at 3000xg. The supernantant was removed and placed in new 50ml conicals. This "clarified lysate" was then loaded into UltraClear SW28 ultracentrifuge tubes (Beckman) on top of a 2ml 5% wt/vol sterile sucrose cushion. Tubes were centrifuged in a SW28 rotor on a Model L-70 Ultracentrifuge (Beckman) for 1hr at 4$^{o}$C at 22,500xg. Supernatant was removed by aspiration and the visible viral pellets were resuspended in a total of 500ml of TE buffer pH8 (10mM Tris-HCl, 1mM EDTA). 20ml of 10mg/ml proteinase-K solution was added as well as SDS for a final SDS concentration of 0.1%. The proteinase-K digestion was allowed to proceed overnight in a 50$^{o}$C water-bath. DNA was extracted from the digestion once using a phenol-chloroform isoamyl-alcohol (PCI) extraction and once using a chloroform isoamyl-alcohol (CI) extraction. DNA was then precipitated using 1/20$^{th}$ volume 6M sodium acetate pH 5.2 and 2 volumes of 100% Ethanol and was shaken gently as to not shear the viral DNA. DNA was pelleted by centrifugation at 10,000xg for 10minutes and resuspended in sterile water at a concentration of 1ug/ul.

HSV-Lox-mC-KO and HSV-Lox-mCherry virues was created using the co-transfection procedure as described in experiment 1.1 (below) using plasmids Shuttle3.1-Sfi1Δcre-mC-KO and Shuttle3.1-Sfi1Δcre respectively. The resulting virus was plaque purified (as described in Chapter2, 2.1.2.4), expanded, and viral DNA was prepared as described for HSV-GFP.

*Purification of HSV Viral DNA For qPCR analysis*

For all qPCR analysis, viral DNA was extracted from 200ul of clarified lysates using NucleoSpin Blood DNA-extraction kits (Clontech) according to manufacturers' instructions except that 10ul of 10ug/ul sheared salmon sperm DNA was added as carrier prior to the DNA precipitation step. Following elution of DNA from the columns, samples were briefly spun at 1000K for 5mins at 50$^{o}$C under vacuum pressure in a table-top SpeedVac (Eppendorf) to remove any residual ethanol. Samples were diluted 50% with milli-Q water and loaded onto clear-bottomed qPCR plates (Bio-Rad).

*Quantitative PCR*

All quantitative PCR was run on a CFX96 Real-Time Quantitative PCR Cycler (Bio-Rad). 4ul of the 50% diluted samples were mixed with 5ul of SYBR Green PCR Master Mix (Bio-Rad) and 1ul of forward and reverse primer (12.5uM). All samples were loaded in triplicate wells. For all primers except for MCKO primers the cycling protocol was 50$^{o}$C for 2mins, 95$^{o}$C for 10mins followed by 39 cycles of 95$^{o}$C for 15sec and 60$^{o}$C for 1min. For MCKO primers the 60$^{o}$C elongation step was only 11sec. For detection of HSV-GFP the forward primer GFP ORF1 Sense 5'-CTGGAGTACAACTACAACAGC-3' and the reverse primer GFP ORF1 Anti 5'-GCGAGCTGCACGCTGC-3' was used. For detection of all recombinant, RMCE produced viruses the forward primer RT RMCE 5' Sense2 5'-GGGAACGCTAGCCGATCC-3' and the reverse primer RT RMCE 5' Anti2 5'-gctgtgagggagccatgg-3' was used. For detection of HSV-Lox-mC-KO the forward primer RT MCKO SENSE1 5'-CGCTTCAAGGTGCACATGG-3' and reverse primer RT MCKO ANTI1 5'-CTTGTACAGCTCGTCCATGC-3' was used. For some experiments, were indicated, detection of recombinant, RMCE-produced viruses used the forward primer Red ORF1 Sense 5'-CGGCGAGTTCATCTACAAGG-3' and the reverse primer Red ORF1 Anti 5'-GGGGTACATCCGCTCGG-3'. All primers were extensively screened for target specificity and efficiency.

*Data Analysis of qPCR for Titering*

To generate a qPCR-based system for the quantification of viral titers serial dilutions of plaque-titered clarified lysate stocks (as described in Chapter2 2.1.2.4.) of each virus clone HSV-GFP and HSV-Lox-mCherry were analyzed. Viral DNA was extracted from these serial dilutions which were then analyzed via qPCR with their corresponding primers. The CT value from each dilution was then plotted against the titer (pfu/ml) of the sample that produced the value. From this regression equations were generated that were used to make titer predictions based off CT values from unknown samples. These equations and qPCR procedure were verified across many different plaque-titered samples and were found to be highly accurate. The equation for the HSV-GFP primers generated was Y=32.048ln(x)+1.272

where Y=CT value obtained and X=pfu/ml. The equation for HSV-Lox-mCherry primers generated was RMCE2 Primers Y=39.483ln(x)+1.564. The stock of HSV-Lox-mC-KO was not titered and therefore a regression equation was generated by plotting the CT values obtained from known dilutions of purified HSV-Lox-mC-KO DNA against the concentration of viral DNA. The equation for HSV-Lox-mC-KO primers generated was Y=5.46358ln(x)+1.6028 where Y=CT value obtained and X=ng/ul viral DNA. A similar approach was also used for some experiments using the GFP primers and RED primers listed above. For these using the GFP primers the equation generated was GFP Primers ng/ul DNA Y=4.3698ln(x)+1.534 where Y=CT value obtained and X=ng/ul viral DNA. For these using RED primers the equation generated was RED Primers ng/ul DNA Y=5.6884ln(x)+1.488.

*Statistical Analysis*

Statistical analysis was performed using *KaleidaGraph* statistical software. Raw data obtained from quantitative PCR analysis of samples was used to extrapolate viral titers and viral DNA concentrations as described above. For each experiment, viral concentration readings, including all replicates, from each experimental condition and controls were analyzed as a group using a one way ANOVA. If a mean main effect for the entire group was seen to be statistically significant ($P<.05$) then Post-hoc analysis was performed using Turkey's HSD test. This single step, multiple comparison procedure compares all possible pairs of means based on a studentized range distribution. For data reporting, individual biological samples have a mean computed from triplicate readings. These means are then averaged between biological replicates for the same condition and this mean is displayed on graphs. Standard error is shown on all graphs for each condition and is computed by the standard deviation of all replicates divided by the square root of the number of replicates (N) for that condition.

*PCR of Recombinant HSV-Viral DNA for sequencing*

In order to verify the recombinant viruses produced by the RMCE procedures were the result of site-specific exchange between Lox sites, regions of the recombinant chromosomes were amplified by

PCR and these PCR products were then sequenced. The primers #2 Seq 5' pgC1 5'-TCACTACCGAGGGCGCTT-3' and Sfi ORF Anti1 5'-GCGGTGATGTTCGTCAGG-3' amplify a ~1kb region spanning from upstream of the 5' lox site to the middle of Shuttle3.1-Sfi1 cassette. These primers span a unique junction created as a result of RMCE and were screened in order to endure they are specific to only recombinant viruses containing a Shuttle3.1-Sfi1Δcre cassette. These primers were used in a 50ul reaction using iProof DNA polymerase (Bio-Rad) according to the manufacturer's protocol. For these reactions 5ul of plaque purified clarified viral lysate was used as template. The sequencing primer Sfi ORF Sense1 5'-GAGGCGTCGGGCTTCG-3' was used and sequencing was performed by ACGT DNA Sequencing Services. Unique sequence alterations that occur in the lox site after RMCE was used to verify RMCE products.

*Viruses*

All virus stocks were prepared according to the "clarified lysate" production protocol as described above. 293T cells were used to grow all viruses unless otherwise indicated. Aliquots of clarified lysates were flash frozen in liquid nitrogen and stored at -80$^{o}$C. Aliquots were not used if they had been thawed and re-frozen more than 3 times. All stocks were derived from plaque purified virus clones and titered according to the plaque titering procedure described in section 2.1.2.4. All viral stocks were sequenced to verify recombinant sequences using the procedure described above. HSV-GFP virus was generated via homologous recombination as described in section 2.1.2.3. HSV-Lox-mCherry virus was generated using the $CaCl_2$ co-transfection RMCE procedure with shuttle plasmid Shuttle3.1-Sfi1 as described in section 2.1.3 Experiment 1.1. HSV-Lox-mC-KO virus was generated using the $CaCl_2$ co-transfection RMCE procedure with shuttle plasmid Shuttle3.1-Sfi1-mc-KO.

*Plasmids*

To generate Shuttle3.1-Sfi1-mc-KO a 591 b.p. region of the mCherry gene (bp 2804-3375) within the plasmid Shuttle3.1-Sfi1 was removed using an inverse-PCR reaction. Forward primer shut-mCher-

KO-INV-sense1 5'-atgattaattaaATCGTGGAACAGTACGAACG-3' and reverse primer Shut-mCher-KO-INV-Anti1 5'-gtcattaattaaCTCCATGTGCACCTTGAAGC-3' were used in a PCR reaction using iProof DNA polymerase (Bio-Rad) according to manufacturer's protocol. These primers introduce a Pac1 restriction endonuclease recognition sequence and create a PCR product that contains the entire Shuttle3.1-Sfi1 sequence except the 591bp region of the mCherry gene. The linear PCR product was gel purified, digested with Pac1 endonuclease, and then recircularized via ligation with T4 DNA ligase (NEB). Bacterial clones were created and screened as described above.

Plasmids Shuttle3.1Δcre-Sfi1-mc-KO and Shuttle3.1Δcre-Sfi1 were used for all cre-negative control conditions in experiments described below. The 910bp region between a unique Cla1 restriction endonuclease recognition sequence and a unique Xho1 recognition sequence in Shuttle3.1-Sfi1 which contains the CMV-cre expression cassette was removed via restriction digest. The plasmid backbone was gel purified and re-circularized by first blunting the ends of the linear DNA fragment using the Klenow fragment of DNA polymerase (Invitrogen) then by ligation and cloning as described above.

For transfections, large quantities of plasmid DNA were prepared from 100ml liquid Luria-Broth (with ampicillin) cultures of bacterial DH5α E. coli using a Plasmid Maxi-Prep Kit (Quiagen) following manufacturer's instructions. Purified plasmid DNA was sterilized via ethanol precipitation, pelleted by spinning for 10min at 14,000xg in a table top microcentrifuge, and resuspended in a small volume of 0.22um filtered Mili-Q water. Plasmid DNA concentrations were measured using a NanoDrop U.V. spectrophotometer (Thermo Scientific). Additional sterile water was added to bring the final DNA concentration to 1ug/ul.

*Cell Culture*

All cells were grown on 10cm sterile tissue-culture dishes unless otherwise indicated in specific experiments. HEK293 cells and HEK293cre cells were obtained from Dr. Steven Langer (described Langer 2002). HEK293T cells were obtained from ATCC. Cells were maintained in humidified, water-

jacketed incubators at 37$^{o}$C and 5% $CO_2$ unless otherwise indicated in specific experiments. Cells were grown in Dulbecco's Modified Eagle Medium (DMEM) containing 10% fetal bovine serum (FBS). Media was supplemented with penicillin-streptomycin, L-glutamine and fungiozone all at 1X concentration according to manufacturer's suggestion (Gibco). For passaging, media was aspirated, cells were washed once with PBS containing EDTA and then detached with Trypsin-EDTA. All tissue culture manipulations were performed inside a BSL2-certified BioSafety Cabinet.

**Experiment 1.1 RMCE via Co-transfection**

The principle behind the RMCE via Co-transfection protocol is that when HSV-GFP chromosomes and Shuttle plasmids are simultaneously transfected onto cells, the two DNA molecules will have a high likelihood of encountering one another. In the presence of cre, this will result in a RMCE reaction between the two DNA molecules and subsequently the insertion of the floxed, mCherry-containing cassette into the HSV genome. This will ultimately result in the conversion of the virus HSV-GFP into the virus HSV-Lox-mCherry. Experiment1.1 will test if the cre-Lox-based insertion of genes into the viral chromosome can be used to create a large library of many different recombinant viruses. This transfection-based site-specific recombination technique is being used because bacterial cloning techniques and homologous recombination have been reported to be inefficient in creating recombinant HSV-1 (reviewed chapter 1 Part 6).

In this experiment, cells were co-transfected with HSV-GFP viral DNA and Shuttle3.1-Sfi1. The insertion of the mCherry-containing lox-cassette from the plasmid into the viral chromosome was detected by the creation of mCherry-containing viral chromosomes and the loss of GFP-containing viral chromosomes. Quantitative PCR primers specific to each viral chromosome were used for detection as described above.

Seven identical 10cm dishes of 293cre cells were transfected using the $CaCl_2$ transfection procedure as described by (Graham and van der Eb, 1973). Briefly, 9ug of purified HSV-GFP (1ug/ul) and 1ug of Shuttle3.1-Sfi1Δcre (1ug/ul) was mixed with 500ml of 2M $CaCl_2$. This mixture was then added drop-wise to a solution of 50mM HEPES, 280mM NaCl, 1.5mM $NaH_2PO_4$ at pH 7. The resulting DNA-Calcium Phosphate precipitate was added onto a dish of 80% confluent 293cre cells. For controls, two additional dishes were transfected only with HSV-GFP DNA, two dishes were transfected with only plasmid Shuttle3.1-Sfi1 and two dishes of HEK293 cells (non cre-expressing) were transfected the same as the co-transfection conditions except that the plasmid Shuttle3.1-Sfi1Δcre was used. 5 hours after the transfection, media was aspirated from the cells, cells were washed once with 5ml of PBS, and fresh media was applied. Cells were then placed in a tissue culture incubator for 14 days at which point visible cytopathic effect (CPE) indicated successful creation of virus. The cells and media were then harvested and a clarified lysate was prepared to separate the cells from the virus-containing media. 1ml of this clarified lysate from each dish was used to infect a fresh dish of HEK293 cells at 80% confluency. Seven days after infection, cells showed significant CPE, cells and media were harvested and a clarified lysate was prepared as before. Viral DNA was then extracted from a sample of this media. This DNA was then analyzed for the presence of GFP and mCherry containing viral DNA using quantitative PCR as described above.

**Results. Experiment 1.1 RMCE via Co-transfection**

Quantitative PCR analysis showed that ~91% of the virus population in the clarified lysate from the RMCE via Co-transfection procedure contained the plasmid-derived mCherry cassette. Only non-significant background levels of HSV-Lox-mCherry were detected in any of the three control conditions: no viral DNA, no shuttle plasmid, no cre (Fig. 3).

Fig. 3A

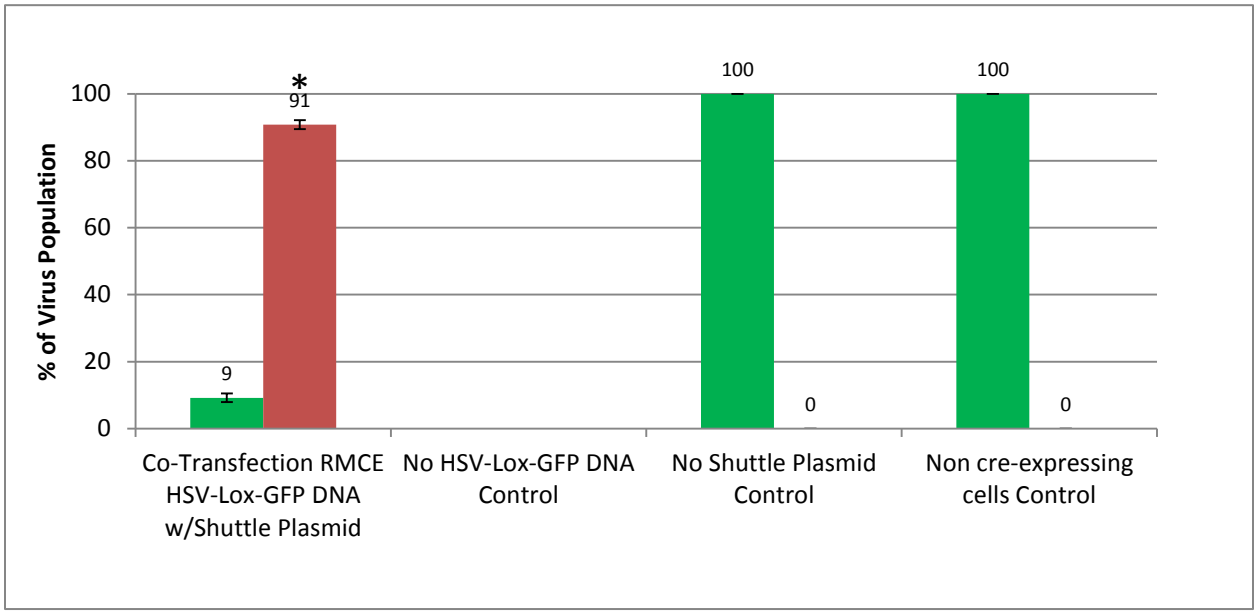


Fig. 3B

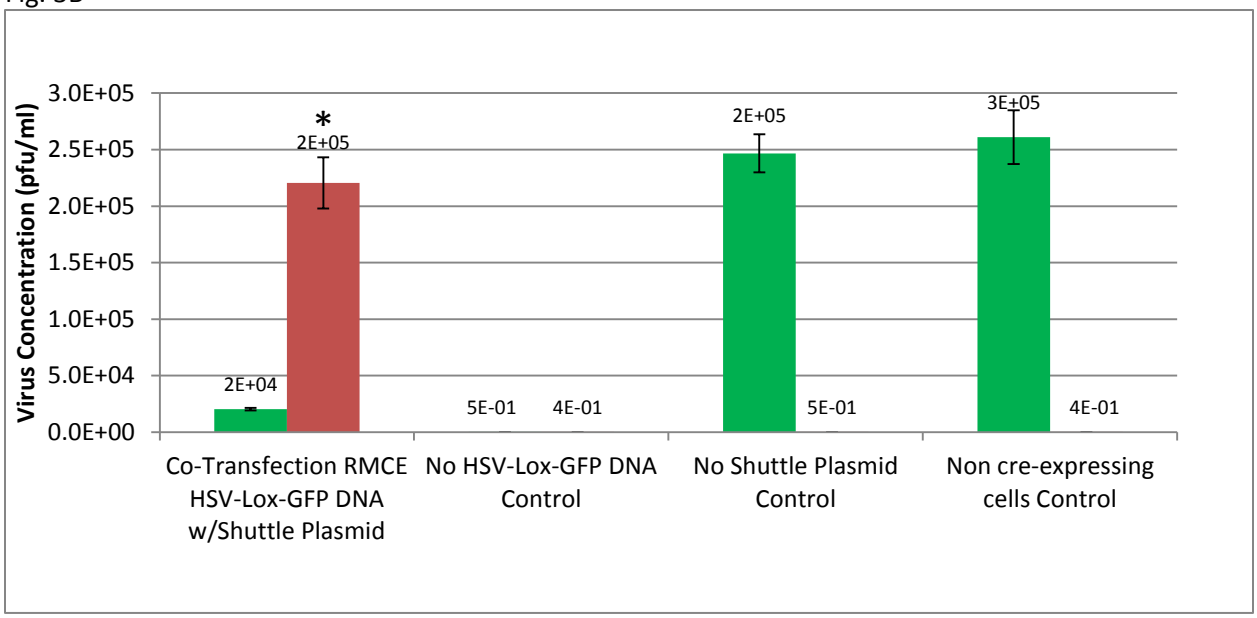


Fig. 3. Experiment 1.1. Quantitaive PCR analysis of cells infected with clarified lysates from 293cre cells co-transfected with HSV-Lox-GFP recipient viral DNA and a mCherry shuttle plasmid. Control cells were transfected with only one of the two DNAs and non-cre expresing cells were co-transfected with both. Cells were transfected using a $CaPO_4$ transfection protocol and harvested 14 days later once showing significant CPE. Signal from primers specific to the parental HSV-Lox-GFP viral chromosome are shown in green and signal from primers specific to the RMCE-produced recombinant HSV-Lox-mCherry viral chromosome are shown in red. Each primer pair has been standardized to plaque titered viral stocks of the corresponding target virus. **A.** The percentage of each virus in the total virus population from each clarified lysate sample derived from the viral concentrations shown in B. **B.** The calculated total concentration of each virus. * Indicates significantly diffent from control (P<.01) Bars represent S.E.M.

**Conclusions. Experiment 1.1 RMCE via Co-transfection**

The percentage and total amount of HSV-Lox-mCherry viruses were both very consistent across all replicate plates tested. Results from control transfections lacking either HSV-GFP viral DNA or the Plasmid shuttle DNA, as well as control transfections with both DNAs on non-cre expressing cells, show that these HSV-Lox-mCherry viruses are the result of cre-mediated RMCE. The average total amount of HSV-Lox-mCherry virus in the samples was $2.2x10^5$ pfu/ml. Therefore, if each HSV-Lox-mCherry virus was the result of a unique RMCE reaction (Tested in Experiment 1.3 below) and not simply the replication of a small number of HSV-Lox-mCherry viruses, then this technique can be used to make a viral library of ~$10^5$ different library members. This procedure was much more efficient at creating recombinant HSV-1 than the homologous recombination procedure used to make the HSV-GFP chromosome (section 2.1.2.3.) where less than 1% CPE expressing cells appeared to express GFP (data not shown). DNA sequencing results confirmed this viral chromosome to be the result of site-specific recombination between the Lox sites.

**Experiment 1.2 RMCE Exchange into Live Virus. Experimental Design.**

The principle behind Live-Virus RMCE exchange reaction is that exchange will occur once cells containing the Shuttle plasmid are infected with the recipient virus. During the infection cycle, in the presence of cre, site-specific recombination will occur between the HSV-1 chromosomes and the shuttle plasmids. As in experiment 1.1, a HSV-Lox-mCherry viral chromosome will be the result. The purpose of this procedure was to determine if site-specific recombination into viral chromosomes engaged in an active infection is more efficient at creating recombinant viruses than methods involving transfection of viral DNA. As previously discussed (Chapter1 Part6), creating viruses via transfection of viral DNA is quite inefficient and could limit the possible library size.

For the Live-virus RMCE procedure, 8 replicate dishes of 293cre cells were transfected with 10ug (1ug/ul) Shuttle3.1-Sfi1 using the $CaCl_2$ transfection procedure as described above. Control dishes were identical to those in experiment 1.1 except that the no HSV-GFP DNA condition was replaced with a no HSV-GFP virus condition. HSV-GFP from the stock described in section 2.1.2.4 was applied to the cells 48hrs after the transfection procedure at MOI=1. Five days after the infection, the cells were completely detached and showed robust viral CPE. As in experiment 1, a clarified lysate was prepared and 1ml was used to infect fresh HEK293 cells. As in experiment 1 clarified lysates were generated from these cells and viral DNA was extracted and analyzed via qPCR.

**Results. Experiment 1.2 RMCE Exchange into Live Virus.**

Quantitative PCR analysis showed that ~1.1% of the virus population in the clarified lysate from the live-virus RMCE procedure contained the plasmid-derived mCherry cassette (Fig. 4A). Only non-significant background levels of HSV-Lox-mCherry was seen in any of the 3 control conditions: no shuttle plasmid, non-cre expressing cells, no recipient virus (Fig. 4B). The average total amount of HSV-Lox-mCherry virus in the samples was $1.0x10^4$.

**Conclusions. Experiment 1.2 RMCE Exchange into Live Virus.**

The live-virus RMCE procedure appeared to be much less efficient at creating recombinant viruses than the RMCE via co-transfection procedure. The average percentage of HSV-Lox-mCherry virus created by these procedures were 1.1% and 91% respectively. Furthermore there was less total amount of HSV-Lox-mCherry virus created by the live-virus RMCE, $1.0x10^4$ pfu/ml compared to $2.2x10^5$ pfu/ml for the co-transfection procedure. If each HSV-Lox-mCherry virus was the result of a unique RMCE reaction (Tested in Experiment 1.3 below) then this technique can be used to make a viral library of ~$10^4$ different library members. As above, DNA sequencing results confirmed this viral chromosome to be the result of site-specific recombination between the Lox sites.

Fig. 4A

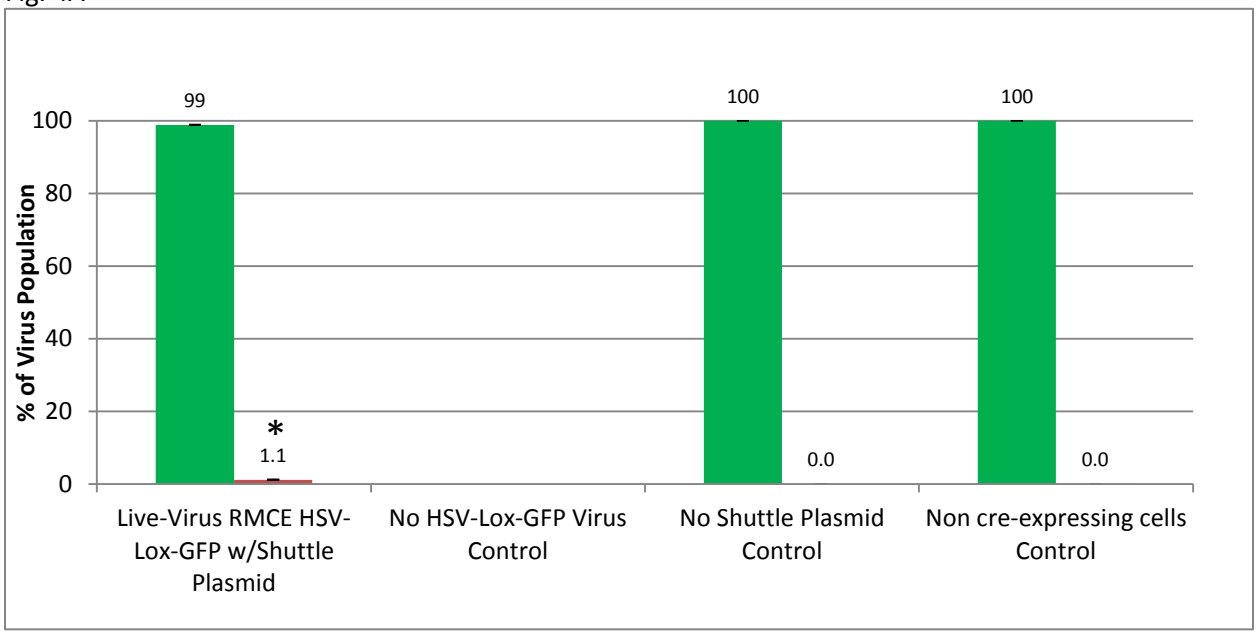


Fig. 4B

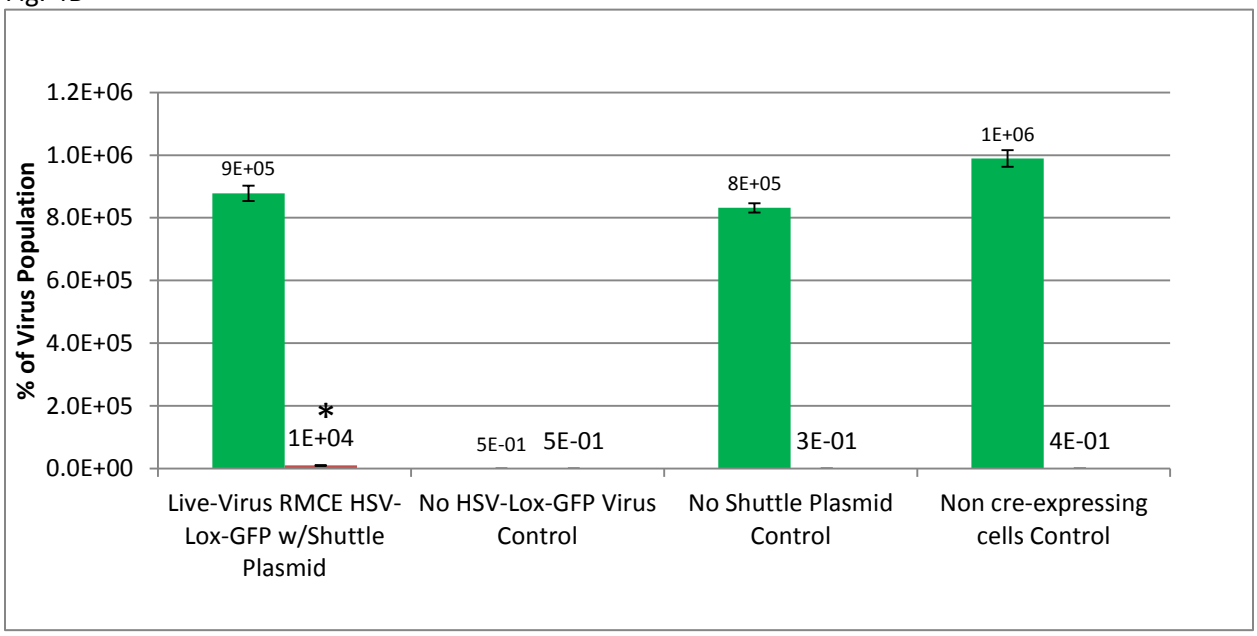


Fig. 4. Experiment 1.2. Quantitaive PCR analysis of cells infected with clarified lysates from 293cre cells co-transfected with a mCherry shuttle plasmid and infected with the recipient virus HSV-Lox-GFP (MOI=1) 48hrs later. Control cells were transfected and not infected, infected and not transfected, and non-cre expresing cells that were transfected and infected. Cells were transfected using a $CaPO_4$ transfection protocol and harvested 5 days after infection when showing significant CPE. Signal from primers specific to the parental HSV-Lox-GFP viral chromosome is shown in green and signal from primers specific to the RMCE-produced recombinant HSV-Lox-mCherry viral chromosome is shown in red. Each primer pair has been standardized to plaque titered viral stocks of the corresponding target virus. **A.** The percentage of each virus in the total virus population from each clarified lysate sample, derived from B. **B.** The calculated total concentration of each virus. * indicates significantly different from control (P<.01) Bars represent S.E.M.

**Experiment 1.3 Testing for the occurrence of unique recombination events.**

The results from experiment 1.1 and 1.2 suggest that the RMCE via-cotransfection procedure is more efficient at inserting genes from shuttle plasmids into the HSV-GFP chromosome than the live-virus RMCE procedure. This is indicated by the greater percentage and total amount of HSV-Lox-mCherry virus created by the cotransfection procedure (Fig. 3 & 4, A & B respectively). However, in order to determine if this is actually the case, the number of unique recombination events occurring during this procedure must be measured. The viruses created in these experiments can grow and replicate within the cells. Therefore it is possible that the large amount of HSV-Lox-mCherry virus seen in the co-transfection procedure is the result of a single (or few) recombinant virus that replicated many times. If this is the case, then the procedure would not be able to efficiently produce a large library of different viruses.

To test for the frequency of unique recombination events a two-plasmid experiment was performed. 293cre cells were treated with the RMCE protocols as described in experiments 1.1 and 1.2. However, the plasmid DNA used in the transfections contained a mixture of plasmid Shuttle3.1-Sfi1, and Shuttle3.1-Sfi1-mC-KO. Shuttle3.1-Sfi1-mC-KO lacks a large region of the mCherry gene (Described in Chapter 2, section 2.1.2.1). Viral chromosomes created by RMCE with this plasmid can be distinguished with qPCR primers specific to the unique sequence junction created by this removal. Eight different mixtures of these two plasmids were made and transfected onto separate dishes. The total amount of plasmid DNA in the transfections was always constant. Ratios of the two plasmids in the mixtures were: 1:1, 1:10, $1:10^2$, $1:10^3$, $1:10^4$, $1:10^5$, $1:10^6$, 0:1, (Shuttle3.1-Sfi1-mC-KO : Shuttle3.1-Sfi1). Duplicate dishes were transfected with each plasmid mixture for each of the RMCE protocols. For co-transfection RMCE, controls were two additional dishes transfected with only the 1:1 plasmid mixture and two dishes of 293HEK cells (non cre-expressing) transfected with the 1:1 mixture plus HSV-GFP-DNA. For Live-Virus RMCE controls, two additional dishes were transfected with only 1:1 plasmid mixture and left uninfected

two dishes of HEK293 cells (not expressing cre) were treated with the full RMCE procedure using a 1:1 mixture of shuttle plasmids lacking the cre expression cassette.

**Results. Experiment 1.3. Testing for the occurrence of unique recombination events.**

Quantitative PCR analysis of the viral populations generated using the co-transfection RMCE procedure showed that only when plasmid Shuttle3.1-Sfi1-mC-KO was present at a ratio of 1:1 and 1:10 with plasmid Shuttle3.1-Sfi1 was any significant amount of HSV-Lox-mC-KO detected (Fig. 5 A). At all lower dilutions, the amount of HSV-Lox-mc-KO detected was not significantly above the amount detected in the negative control where no Shuttle3.1-Sfi1-mC-KO was added. Interestingly, the results from the live-virus RMCE procedure show that HSV-Lox-mc-KO was detected as far out as the $1:10^3$ dilution of Shuttle3.1-Sfi1-mC-KO (Fig. 5 B). The level detected at this dilution was significantly higher ($P<.01$) than control conditions. As the primers used for this analysis have not been standardized to titered virus, only to dilutions of viral DNA, these numbers cannot be used to interpret total amount of HSV-Lox-mc-KO in the population.

**Conclusions. Experiments 1.1-3.**

The results from experiments 1.1 and 1.2 suggest that the co-transfection procedure is more efficient at creating a population of recombinant viruses. However, the results from experiment 1.3 show that this is not because this procedure is more efficient at creating many recombinant viruses (Fig. 5 A). The co-transfection procedure leads to the very efficient insertion of genes from the shuttle plasmid into the recipient HSV-GFP chromosome. However, it is likely that a very small number of these recombinant HSV-Lox-mCherry chromosomes are expressed and converted into viruses. This is consistent with the reported inefficiencies of creating infectious virus from transfected viral DNA (reviewed in chapter1 part6). It is possible that 95% of all viral chromosomes in this cotransfection procedure undergo RMCE with the shuttle plasmids, however only ~1- 10 of these chromosomes actually go on to become live viruses.

Fig. 5A

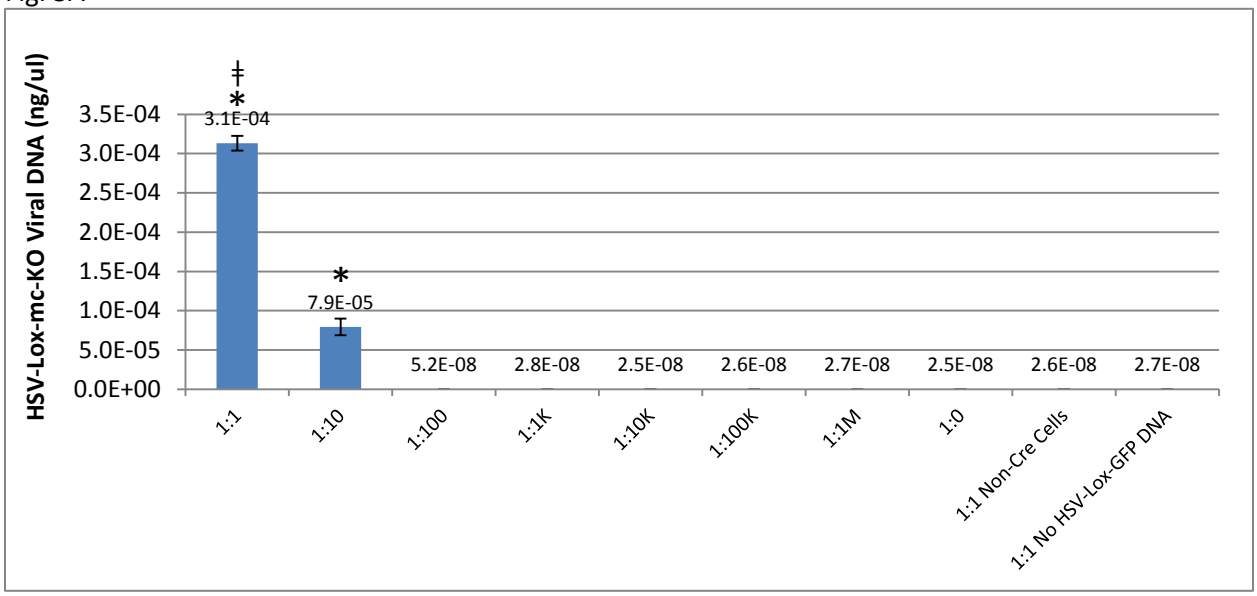


Fig. 5B

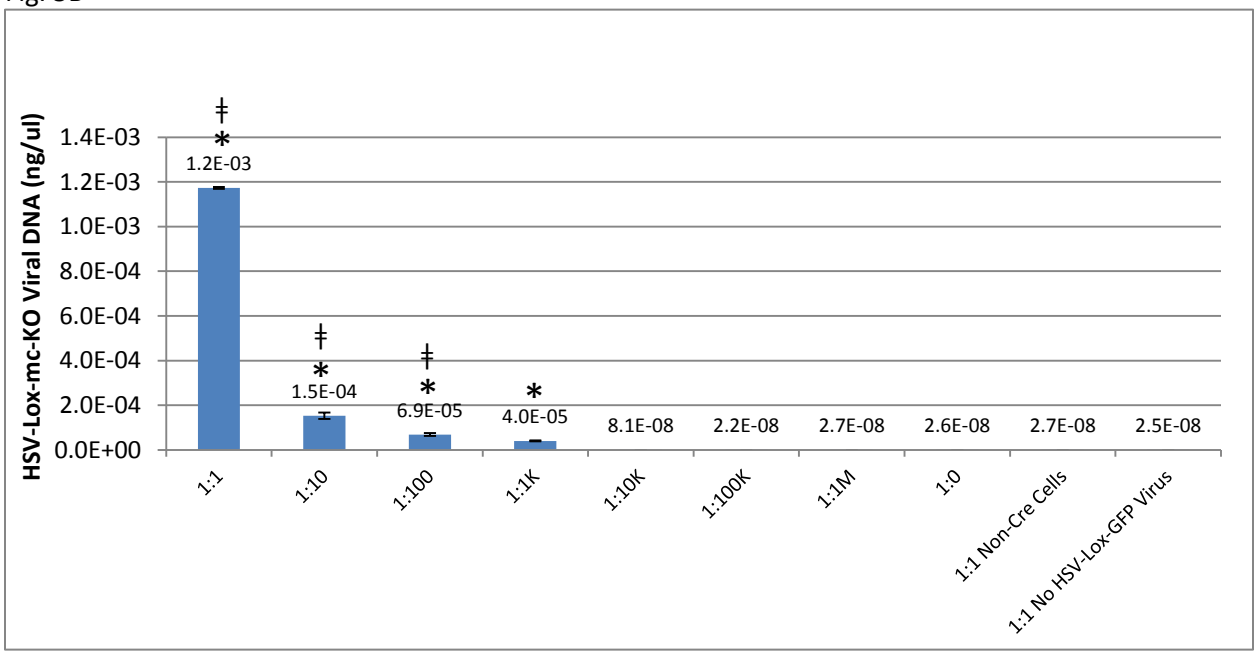


Fig. 5. Experiment 1.3. Quantitaive PCR analysis of clarified lysates from cells infected with clarified lysates from cells treated with an RMCE procedure containing two different shuttle plasmids. Cells were transfected with shuttle at different ratios of plasmid Shuttle3.1-Sfi1-mc-KO : Shuttle3.1-Sfi. Ratios of the two plamids are shown on the X-axis. Control cells lacking cre and control cells without recipient virus or viral DNA were transfected with a 1:1 ratio. Signal from primers specific to the RMCE produced HSV-Lox-mC-KO viral chromosome is shown. Primers are standardized to a standard curve of purified HSV-Lox-mC-KO DNA. **A.** Cells treated with the co-transfection RMCE procedure as in experiment 1.1. **B.** Cells treated with the live-virus RMCE procedure as in experiment 1.2. * indicates significantly different from control (P<.01) ‡ indicates significant different from the next higher dilution sample which is significantly different from control. Bars represent S.E.M.

The results from experiment 1.2 suggested that the live-virus RMCE procedure is much less efficient at creating recombinant HSV-Lox-mCherry chromosomes than the co-transfection RMCE procedure. However, while results from experiment 1.2 show that this procedure created ~$10^4$ recombinant viruses (Fig. 4B), results from experiment 3 show that HSV-Lox-mc-KO was detected when shuttle Shuttle3.1-Sfi1-mC-KO was diluted $10^3$-fold with the other plasmid (Fig. 5B). These results could be extrapolated to mean that nearly every recombinant virus produced by live-virus RMCE is the result of a unique recombination event.

The results from experiments 1.1-3 show that the live-virus RMCE procedure is better suited than co-transfection RMCE to create a diverse library of different recombinant viruses. Additional experimentation (described below) will be performed to further improve this procedure and the size of the viral library that can be generated.

**Experiment 2.1. Improving live-virus RMCE. Experimental Design.**

The results obtained from experiments 1.1-3 above show that a live-virus RMCE reaction may be able to support the creation of a diverse virus library. These results also show that in its current form, the live-virus RMCE procedure is not particularly efficient. Therefore, the purpose of this experiment is to explore many different procedural modifications to the live-virus RMCE reaction to increase the efficiency over that seen in experiment 1.2 above. The modified parameters tested and the results are discussed below. Many different parameters were first tested in order to increase the total percentage of recombinant virus created by the RMCE reaction. In order to streamline this process, only when a final set of parameters had been determined to be optimal it was the protocol then tested for the ability to create many unique recombinants as described in experiment 1.3 above.

***Parameter 1. Transfection reagent.*** The calcium phosphate transfection protocol as described by was used to transfect shuttle plasmids into cells in experiment 1.2 above. While this is one of the

most widely used transfection protocols, many other transfection protocols exist. The BES transfection protocol as described by (Chen and Okayama, 1987) modifies the original calcium phosphate protocol and reportedly results in increased rates of transfection over the standard $CaCl_2$ method. The Okayama transfection procedure (abbreviated BES) was used to replace the calcium phosphate procedure used in the live-virus RMCE protocol. All other experimental parameters remained the same as experiment 1.2 (above).

**Experiment 2.1. Detailed Methods. Improving live-virus RMCE.**

Cells were grown as described in experiment 1.2. In addition all other parameters including the qPCR analysis were also identical. As above, cells were infected with HSV-GFP 48hrs after transfection. Cells were harvested and a clarified lysate was prepared 5 days after infection.

***BES Modified Calcium Phosphate Transfection Procedure***

The transfection protocol described by Okayama is able to support greater amounts of plasmid DNA without adversely affecting the quality of the precipitate as can occur in the procedure described by Graham (Graham and van der Eb, 1973). The optimal amount of DNA in this BES modified procedure was reported to be 20ug of DNA. In this experiment, both 10ug (as used in experiment 1.2 above) and 20ug of plasmid DNA were tested. In the precipitation reactions either 10ug (1ug/ul) or 20ug 1(ug/ul) Shuttle3.1-Sfi1 were mixed in a 1.5ml Eppendorf tube with 50ul 2.5M $CaCl_2$ and sterile water to bring the final volume to 500ul. 500ul of 2XBES-buffered-saline (BES reagent: 50nM BES, 280mM NaCl, 1.5mM $Na_2HPO_4$, pH 6.95) was added drop-wise to this tube with brief agitation between drops to mix. This solution was then allowed to sit at room temperature for 20minutes while precipitate formed. The solution containing the DNA precipitate was then added to the cells which were mixed by gently rocking and placed back into an incubator. 24hr after transfection the media was aspirated, cells were washed once with 5ml of media, and then 10ml of new media was applied. As in experiment 1.2, 2 control dishes of HEK293 cells not expressing cre was transfected with 20ug of the plasmid Shuttle3.1-Sfi1ΔCre.

**Experiment 2.1. Results. Improving live-virus RMCE.**

Quantitative PCR analysis showed that live-virus RMCE with the modified BES transfection procedure using 10ug and 20ug shuttle plasmid produced ~1% and 3% recombinant viruses respectively (Fig.6A). This corresponded to concentrations of recombinant viruses of ~$1.2x10^4$pfu/ml and ~$3x10^4$ pfu/ml respectively (Fig. 6B). Significantly more HSV-Lox-mCherry was produced by the BES transfection protocol using 20ug shuttle plasmid than with 10ug of shuttle plasmid. As previously observed, the production of recombinant virus was dependent on the presence of the shuttle plasmid and cre recombinase. Therefore these controls will be omitted from future experiments. Lastly, very similar percentage and concentrations were obtained when clarified lysate from the RMCE cells was tested directly as when fresh cells infected with 1ml of this lysate were tested (data not shown). Therefore to streamline the processes, clarified lysates directly from the RMCE cells were tested for all following experiments.

**Experiment 2.1. Conclusions. Improving live-virus RMCE.**

The results from experiment 2.1 show that the modified BES transfection procedure using 20ug of shuttle plasmid produced a 2-fold improvement in the total percentage of the virus population containing the RMCE cassette over using 10ug with either transfection procedure (Fig. 6 A). Furthermore, this amount of shuttle plasmid produced 3-fold more total recombinant virus ($3x10^4$ pfu/ml ) than either transfection procedure using 10ug of plasmid DNA (Fig. 6B). Therefore additional parameters will be tested using this new BES procedure in order to further improve the live-virus RMCE reaction

**2.2.7 Experiment 2.2 Improving live-virus RMCE BES Protocol. Experimental Design.**

The results from experiment 2.1 show that the modified BES transfection procedure using 20ug of shuttle plasmid was the best live-virus RMCE procedure tested thus far. Therefore, this procedure

Fig. 6A

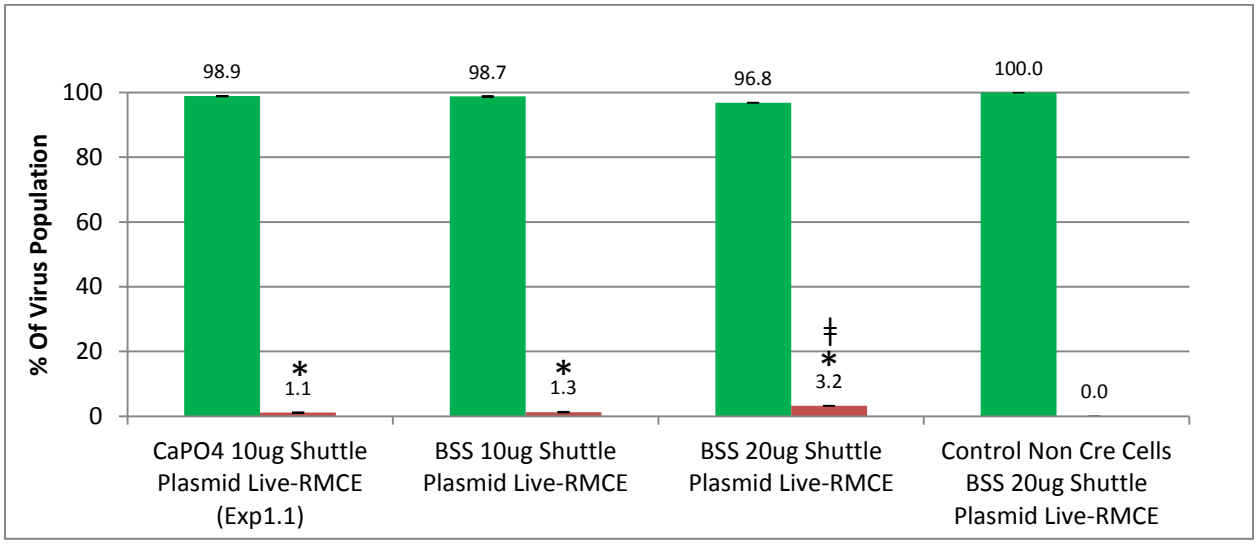


Fig. 6B

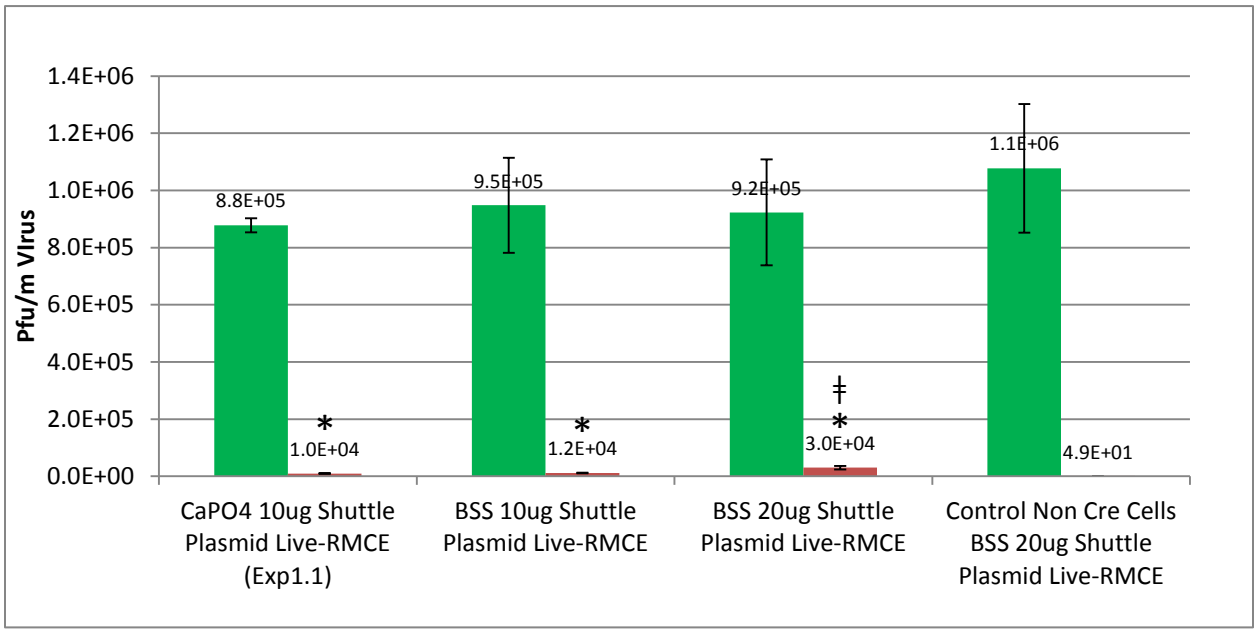


Fig. 6 Experiment 2.1. Quantitaive PCR analysis of clarified lysates from cells treated with different live-virus RMCE procedures. Cells were transfected with mCherry shuttle plasmid using a $CaPO_4$ (10ug) or modified BSS (10 & 20ug) transfection protocol. For RMCE, cells were infected (MOI=1) with recipient virus HSV-Lox-GFP 48hrs after transfection. Signal from primers specific to the parental HSV-Lox-GFP viral chromosome are shown in green and signal from primers specific to the RMCE-produced recombinant HSV-Lox-mCherry viral chromosome are shown in red. Each primer pair has been standardized to plaque titered viral stocks of the corresponding target virus. **A.** The percentage of each virus in the total virus population from each clarified lysate sample, derived from B. **B.** The calculated total concentration of each virus. * indicates significantly different from control (P<.01) ǂ indicates significant different frm all other samples in addition to control. Bars represent S.E.M.

was further tested using a large panel of different parameters to determine additional alterations that can increase the efficiency of recombinant virus production. These parameters are reviewed below.

*Parameter 1. Timing between transfection and infection with recipient virus*

Cells were infected with the recipient virus at different times following the transfection of shuttle plasmids. It is possible that the addition of virus too early after the transfection might lead to the death of cells before taking-in sufficient amount of plasmid. It is also possible that addition of virus too late after the transfection could result in a low-efficiency infection caused by the cells reaching confluency. Furthermore it is known that upon the initiation of viral DNA replication, discrete nuclear compartments are formed around the replicating viral DNA (reviewed in Chapter 1). It is therefore possible that there is a small window that HSV-1 chromosomes may be accessible for RMCE with the shuttle plasmid. This may be the time between insertion of viral DNA into the nucleus and the formation of these replication compartments. This time-course was designed to help determine if there is an optimal time of infection with the recipient virus relative to the time of transfection to achieve the most efficient interaction between the shuttle plasmids and the HSV chromosome. In this experiment, the HSV-GFP virus (MOI=1 as before) was be added to cells simultaneously with the transfection (0hr) as well as 24hr, 48hr, 72hr and 144hr after transfection.

*Parameter 2. Quantity of plasmid DNA in the transfection*

While the results of experiment 2.1 showed that 20ug of plasmid DNA produced more recombinant virus than 10ug, it was decided once again to test transfections using both 10ug and 20ug over the time-course listed in parameter 1. The reason for this is that at the 0hr infection time-point, the DNA precipitate cannot be washed from the cells (previously done 24hrs after transfection) as this would wash away the virus which had just been applied. It has been observed that not washing the precipitate from the cells appears to inhibit the infection probably by inhibiting charge-dependent binding of the virus to the cells (personal observation data not shown). Using less DNA may produce

less precipitate that can impede the virus. This is likely the most relevant to the 0hr infection time-point but will be tested across all 4 time-points.

*Parameter 3. Viral DNA in the transfection*

The results from experiments 1.3 show that co-transfection of HSV-GFP viral DNA with the shuttle plasmid does not result in the production of a large number of different viruses. However the results from experiment 1.1 suggest that this procedure is quite efficient at creating recombinant viral chromosomes. It is has been reported that proteins contained within the viral tegument are delivered to cells upon infection (Reviewed in Chapter 1). These proteins assist in infection by helping to shut down expression of cellular genes and to promote the production of viral gene products. Some of these proteins have also been shown to act as transcription factors for genes within the viral chromosome. Therefore, it is possible that the presence of a live virus may help initiate the expression of the recombinant viral chromosomes produced by co-transfection RMCE. Therefore, for all time-points and amounts of DNA listed above, a condition was tested where half of the total amount of DNA in the transfection was purified HSV-GFP viral DNA. This viral DNA was prepared as described in Chapter 2 (2.1.2.1).

**Experiment 2.2. Results. Improving the live-virus RMCE BES Protocol.**

Quantitative PCR analysis of the 16 different combinations of parameters tested showed several trends (Fig. 7). For all infection time-points tested, 20ug of shuttle plasmid produced a greater percentage and total amount of recombinant virus than 10ug of shuttle plasmid. There appeared to be no increase in percentage or total amount of recombinant virus as a result of adding HSV-GFP viral DNA to the transfection. Lastly, the greatest amount of total virus, recombinant and non-recombinant, was produced by the 24hr infection time-point (Fig. 7A&B).

Fig. 7A

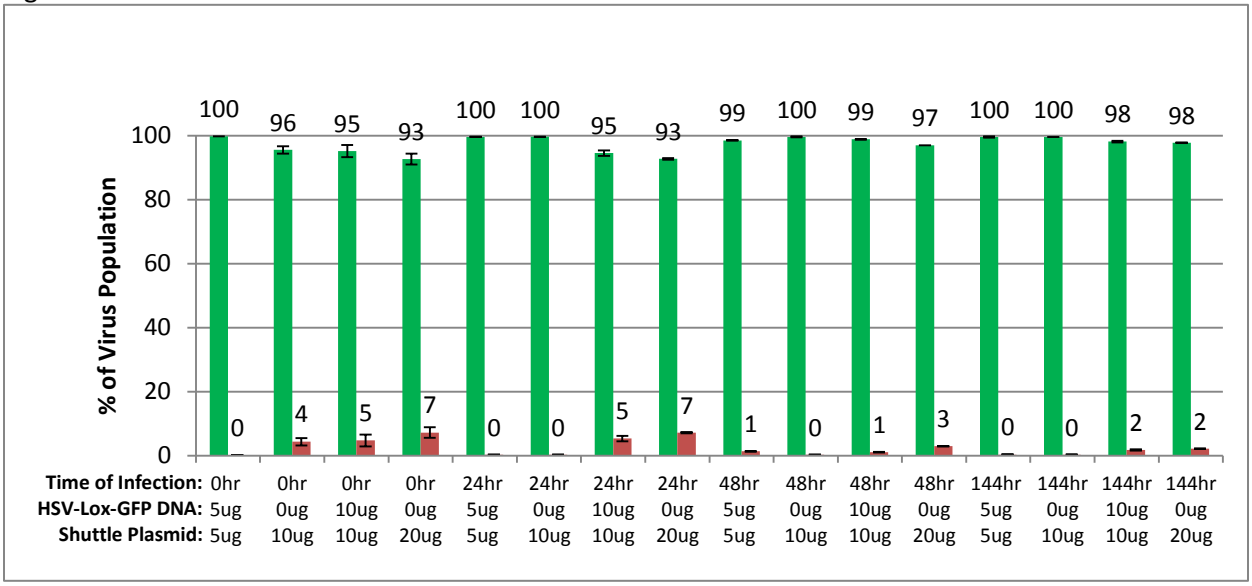


Fig. 7B

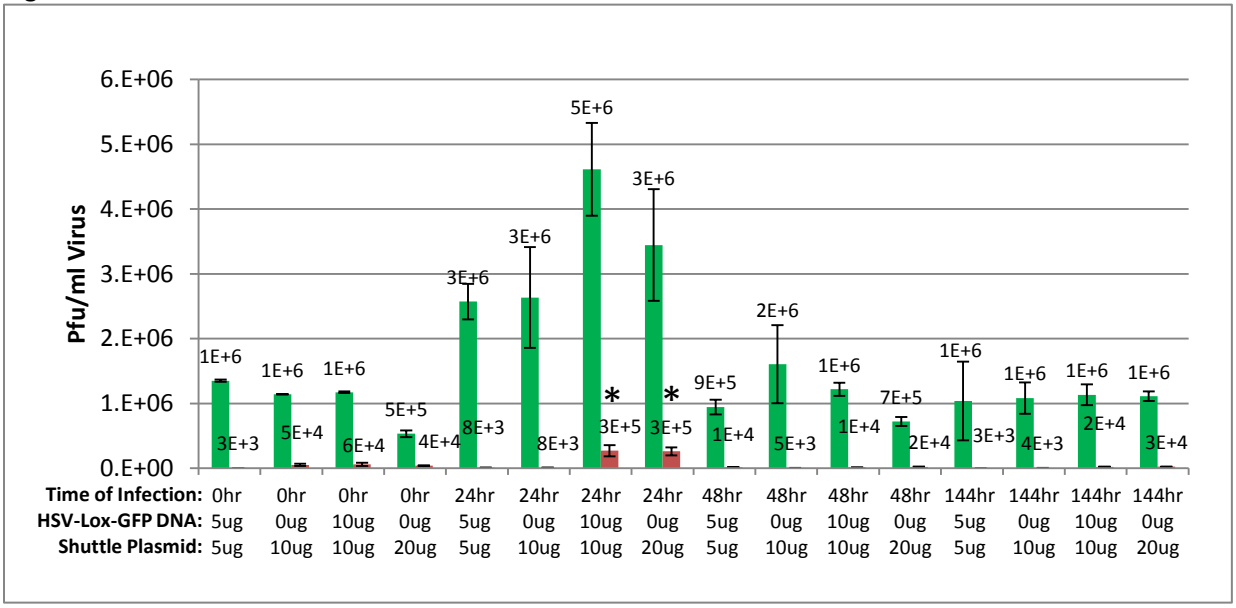


Fig. 7 Experiment 2.2. Quantitaive PCR analysis of clarified lysates from cells treated with different live-virus RMCE procedures. Cells were transfected using the modified BSS transfection protocol as in experiment 2.1. Cells were transfected with 20ug and 10ug total DNA consisting of different combinations of mCherry shuttle plasmid and HSV-Lox-GFP viral DNA. Cells were infected (MOI=1) with recipient virus HSV-Lox-GFP immediately (0hr), 24hr, 48hr or 144hr after transfection. Signal from primers specific to the parental HSV-Lox-GFP viral chromosome are shown in green and signal from primers specific to the RMCE-produced recombinant HSV-Lox-mCherry viral chromosome are shown in red. Each primer pair has been standardized to plaque titered viral stocks of the corresponding target virus. **A.** The percentage of each virus in the total virus population from each clarified lysate sample, derived from B. **B**. The calculated total concentration of each virus. * indicates significantly different (P<.01) amount of recombinant HSV-Lox-mCherry virus detected compared to the other conditions tested. Bars represent S.E.M.

**Experiment 2.2. Conclusions. Improving the live-virus RMCE BES Protocol.**

The results from experiment 2.2 show that new parameters were discovered which increased the percentage and total amount of recombinant virus produced by the live-virus RMCE procedure over experiment 2.1. Both the 0hr and 24hr post-transfection infection time-point appeared to produce the greatest percentage of recombinant virus in the total population, 9% and 7% respectively (Fig. 7A). This is almost a 10-fold increase from experiment 2.1. For both time-points the greatest percentage of recombinant virus was produced using 20ug of shuttle plasmid. Furthermore, the greatest total amount of recombinant virus was produced from the 24hr infection time-point (Fig. 7B). Here, almost 10-fold more recombinant virus was produced than from the 0hr time-point. As an increase in the production of non-recombined HSV-GFP is also seen at this 24hr time-point. It is likely this increase is the result of overall increased infection efficiency at this time-point compared to the 0hr time-point. As mentioned above, this is possibly the result of the DNA precipitate not being washed off the cells at the 0hr time-point allowing it to either inhibit infection or impair overall cell-health. It is also possible that reduced amounts of total virus seen at the 48hr and 144hr time-points are also a result of reduced infection efficiency. It has been widely reported that actively growing cultured-cells infect more efficiently and produce more virus than confluent monolayers. At these later time-points the cells were almost 100% confluent by the time virus was added. It is also possible at these later time-points that cells containing plasmids had become less abundant due to either active plasmid clearance from cells or simply from cell division.

**2.2.8. Experiment 2.3. Further improving the live-virus RMCE protocol.**

The results from experiment 2.2 show that the greatest percentage and total amount of recombinant virus is produced using a live-virus RMCE protocol with the modified BES reagent, using 20ug of shuttle plasmid, when cells are infected 24hrs after transfection. As discussed above, these results also suggest that an increased efficiency of infection could result in an increased production of

recombinant virus. Therefore, additional parameters designed to increase infection efficiency were tested in an attempt to further increase the production of RMCE-produced recombinant virus. Unless otherwise noted, all parameters and data analysis was identical to experiment 2.2. As before, all parameter combinations were tested in duplicate dishes.

*Parameter 1. High MOI infections using concentrated virus*

The results from experiment 2.2 showed that the DNA precipitate present at the 0hr infection time-point may have caused a decrease in the total amount of recombinant virus produced. This suggests that the amount of recombinant virus produced could be directly related to the amount of HSV-GFP that infects the cells. To test if increasing the amount of virus in the infection can further increase the production of recombinant virus a higher MOI of HSV-GFP was used. An MOI of 1 was used for all experiments thus far. This has largely been determined by the concentration of virus obtained in the clarified lysates ~$1x10^6$ pfu/ml and the number of cells present at the time of infection (~$1x10^6$ cells). It is not feasible to increase the MOI an additional order of magnitude using the clarified lysate stocks as this would require using 10ml of clarified lysate to infect a 10cm dish. Therefore a concentrated stock of HSV-GFP was produced. As described in detail in Chapter 2 (2.1.2.1) HSV-GFP was concentrated by ultracentrifugation onto a sucrose cushion. The resulting virus pellet was gently resuspended in PBS. In total, virus from 230ml of clarified lysate was resuspended in 500ul of PBS. This concentrated viral slurry was allowed to gently mix over-night in a rotating mixer at $4^oC$. This solution was then brought up to a total volume of 1ml with DMEM. This concentrated stock of HSV-GFP had a concentration of ~$9x10^7$ pfu/ml according to qPCR and plaque assay analysis. This is nearly 100-fold more concentrated then the clarified lysate stock. 100ul of this concentrated virus stock was used per dish containing ~$1x10^6$ cells for a total MOI of ~10.

*Parameter 2. Increased multiplicity of infection by using centrifugal infection*

There are numerous reports of successfully increasing viral infectivity by forcing virions onto cells by centrifugation. Increases in infectivity with retroviruses have been reported by the centrifugation of cells at speeds ranging from 800xg to 10,000xg (Barranger 1995) for 1 hour. While it is unlikely that centrifugation at 800xg for 1hr sediments virus in suspension, reports speculate that the increases in infectivity at these speeds likely results simply from stabilizing virus attachment to cell membranes. Therefore a protocol was developed, based on published reports and the capabilities of available equipment, where cells were spun for 1hr at 3000xg in a table-top swinging-arm GS-6R centrifuge (Beckman) at 4$^{o}$C. Preliminary testing showed that both the cell culture dishes and cells themselves were unaffected by this procedure. Control testing showed that spun cells had the same growth profile apparent vitality as non-spun parallel dishes (data not shown).

*Parameter 3. Neutralization and Removal of Excess Extracellular Virus*

It is possible that adding 10-fold more virus to the infection may result in increased viral entry into cells and subsequently increased incidents of RMCE between viral chromosomes and plasmids. However, it also possible that a large percentage of the virus in these high MOI infections is simply excess and does not enter a cell. This increased extracellular virus would not serve as a possible target for RMCE and would increase the non-recombinant population when the dish is harvested. To prevent this, a protocol to remove excess extracellular virus was developed. As reviewed in Chapter 1, penetration of HSV-1 occurs within 20min after cell binding. Furthermore no increases in cell binding by WT HSV-1 are seen after 3hrs at 4$^{o}$C and the reported infectious cycle of HSV-1, and first instances of progeny virions emerging from infected cells is, is ~12hr. Therefore, 10hr after infection, media was removed and cells were washed once with 5ml PBS. 2ml of 0.1M glycine pH 3 was added to cells for 1.5mins. The glycine was then removed, cells were washed once more with 5ml PBS, 10ml fresh media was added and cells were placed back into the incubator. Low pH treatment of cells with acidic glycine

has been shown to very efficiently and permanently neutralize extracellular virus while having no adverse effects on the cells or the production of intracellular virus(Laquerre et al., 1998b).

*Parameter 4: Cells*

In addition to the 293cre cells used previously, 293T cells were also used in this experiment. 293T cells constitutively express Simian Virus 40 (SV40) large T antigen (Durocher et al., 2002). This protein can recognize and bind to the SV40 origin of DNA replication, resulting in replication and episomal maintenance of transfected plasmids containing this sequence. The plasmid Shuttle3.1-Sfi1 contains this sequence and will therefore be replicated and present in high copy number within these cells. Using these cells will help to determine if increasing the copy number of shuttle plasmids within the cells helps facilitate the incidence of interaction, and subsequently RMCE, between plasmids and viral chromosomes. One potential complication is that the 293T cells have not been engineered to express cre. However the shuttle plasmid does contain a functional mammalian expression cassette for cre.

*Parameter 5: Cell Confluency at Transfection*

The results from experiment 2.2 suggest that greater amounts of virus are produced from cells that are less dense at the time of infection. To test the extent of this effect, cells were transfected at 40% as well as at 80% confluency (as in experiment 2.2). These resulted in ~70% and 90% confluency at the time of infection, 24hrs later.

**Experiment 2.3. Results. Further improving the live-virus RMCE protocol.**

The results from experiment 2.3 show several trends (Fig. 8). In both cell lines tested, cells at a lower density at the time of transfection produced significantly higher percentages of recombinant viruses than cells at a higher density. 293T cells transfected at 40% and not spun also produced a significantly higher total amount of recombinant HSV-Lox-mCherry than all other conditions (Fig. 8B). Another apparent trend was that 293T cells produced more overall virus than 293cre cells. This

Fig. 8A

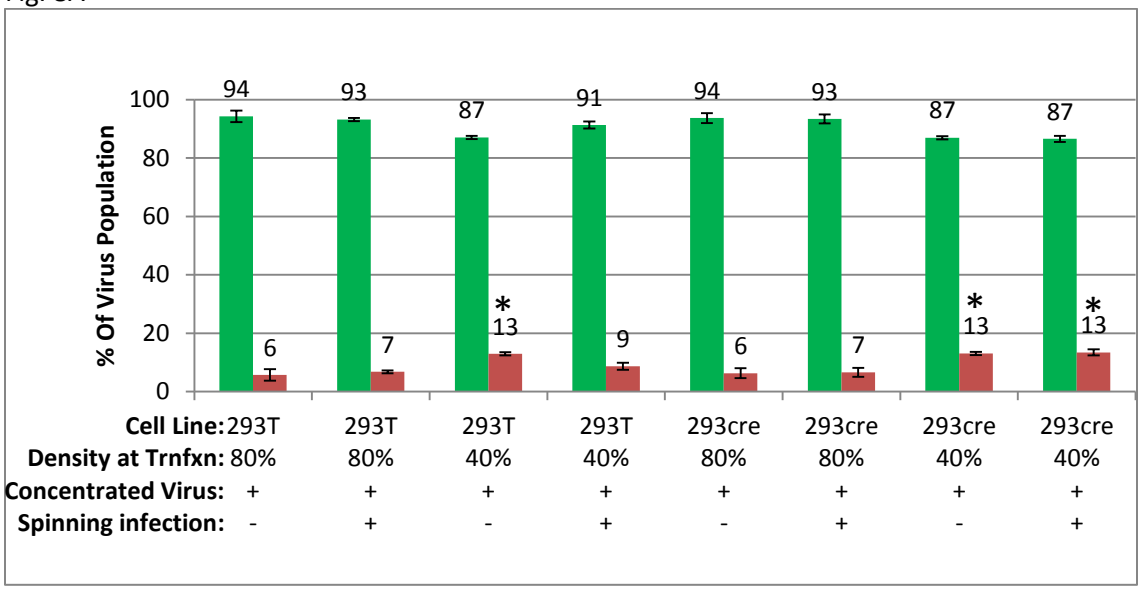


Fig. 8B

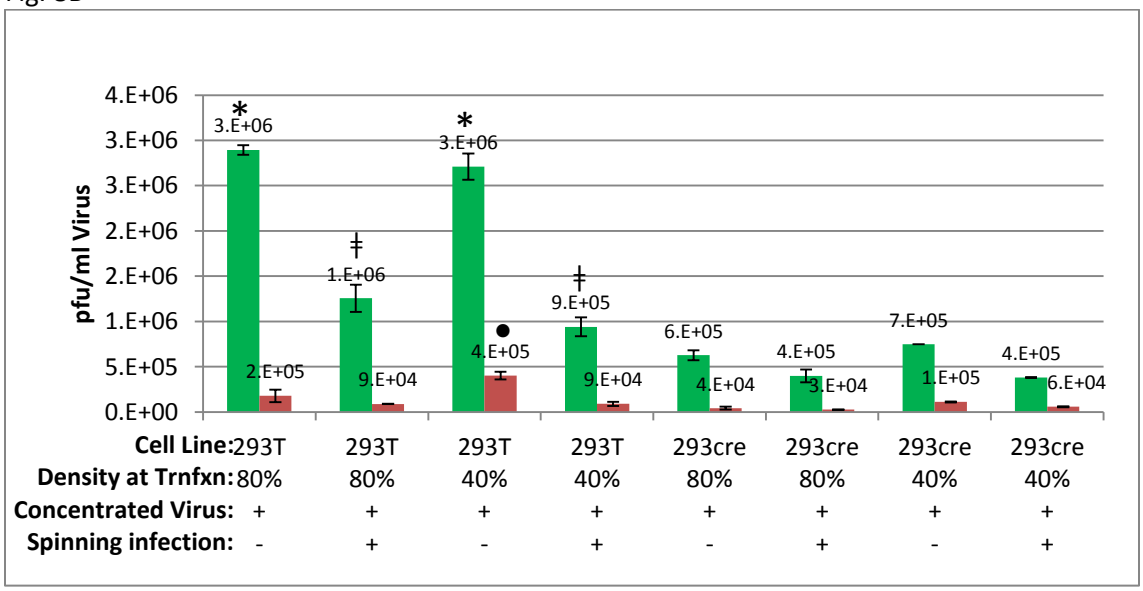


Fig. 8 Experiment 2.3. Quantitaive PCR analysis of clarified lysates from cells treated with different live-virus RMCE procedures. Cells were transfected with 20ug mCherry shuttle plasmid using the modified BSS transfection protocol. 293T and 293cre cell lines were transfected at either 80% or 40% confluency. 24hr after transfection all cells were infected with concentrated HSV-Lox-GFP recipient virus (MOI=10). Cells were spun for 1hr 3000xg at 4°C or placed at 4°C 1hr 1xg immediately following infection. Media was removed 10hr following infection and extracellular virus was neutralized using acidic glycine. **A.** The percentage of each virus in the sample derived from B. * indicates significantly higher (P<.01) percentage of HSV-Lox-mCherry than conditions without symbol. **B.** The calculated total concentration of each virus. * indicates significantly more (P<.01) HSV-Lox-GFP than all other conditions, ‡ indicates significantly more HSV-Lox-GFP than all conditions without symbol, • indicates significantly more HSV-Lox-mCherry than all conditions without symbol. Bars represent S.E.M. Detection of HSV-Lox-GFP is shown in green and detection of HSV-Lox-mCherry is shown in red. Each primer pair has been standardized to plaque titered viral stocks of the corresponding target virus.

difference was significant for the amount of HSV-GFP produced in all 4 conditions using 293T cells and for the amount of HSV-Lox-mCherry produced for one condition while the other 3 were trending but not significant. For both cell types at both densities, spinning appeared to decrease the overall amount of virus produced. This difference was significant in all 4 conditions using 293T cells and trending in conditions using 293cre cells. Lastly, individual samples from the supernatant removed at 10hr post infection showed nearly twice the amount of HSV-GFP in the supernatant from cells that were spun than from those that were not, $1.1x10^6$ pfu/ml vs $4.5x10^5$ pfu/ml (N=1, data not shown).

**Experiment 2.3. Conclusions. Further improving the live-virus RMCE protocol.**

The results from experiment 2.3 show several definitive trends (Fig. 8). Cells transfected at a lower density appeared to produce a greater percentage and overall amount of the recombinant HSV-Lox-mCherry virus. This same trend is not seen in the amount of non-recombined HSV-GFP produced. It is therefore unlikely that the increased amount of recombinant virus production in this condition is a result of an overall increase in virus production. One explanation is that cells at a lower density are more actively growing than cells near confluency and this active growth state may lead to a higher rate of plasmid uptake and subsequently more targets for RMCE. An additional trend observed was that 293T cells produced more overall virus than 293cre cells. This trend remained constant over all experimental conditions. This is unlikely due to cell density as the two cell lines were transfected and infected at the same cell densities. One possible explanation is that fewer 293T cells were seen to become unattached during the various washes steps.

Additionally, two unexpected results were observed. The first is that spinning-infections, a procedure that reportedly increases infectivity, appeared to reduce the overall amount of virus produced. This was seen in both cell lines and at both densities tested. The second was the observation that more extracellular HSV-GFP was seen in the media 10hrs after infection (removed before the washing procedure) from spun cells compared to not spun cells. These two results suggest that the

spinning process actually reduced the amount of virus that entered the cells. After the experiment was performed, it was discovered that this was possibly the result of microbial contamination in the cells. When samples of each clarified lysate were passaged onto fresh cells, a high level of microbial contamination was observed after 7 days of incubation. This suggests that the RMCE cells had a low-level contamination during the infection process which could have affected cell health and subsequently virus production. It is possible that the additional stress of the spinning procedure exacerbated this. It was determined that the source of contamination was the concentrated virus stock. Contamination likely occurred during one of the many manipulations required to concentrate the virus. Experiment 2.4 below will address this issue.

### 2.2.9 Experiment 2.4 Addressing the results from experiment 2.3. Live-virus RMCE protocol optimization.

Experiment 2.3 showed definitively that the use of 293T cells at a density of 40% at the time of transfection yielded the highest percentage and total amount of recombinant virus of any procedure tested thus far. Therefore, in order to further focus the process of protocol optimization, this cell type and density was used for all further experiments. The results from the use of concentrated viruses were inconclusive due to the possibility of contamination. Experiment 2.4 addresses this issue as well as additional issues identified in experiment 2.3 Unless otherwise noted all methods used were identical to those used in experiment 2.3.

*Parameter 1: Removal of Microbial Contamination in the Concentrated Virus Stock*

It was determined that the concentrated virus stock used in experiment 2.3 contained a microbial contamination. Additional steps were taken to ensure this contamination was eliminated in experiment 2.4. Here, polyallomer ultracentrifuge SW28 tubes (Beckman) were used. These tubes can be sterilized via autoclave not just via ethanol as was the case with the UltraClear tubes used in experiment 2.3. Concentrated virus was prepared as in experiment 2.3 with the exception that the final

concentrated stock was filtered using a 0.4um filter. This filtration did not significantly reduce the titer of this concentrated stock. Lastly, unlike experiment 2.3, infections using concentrated and non-concentrated virus were both tested.

*Parameter 2: Spinning*

Cells were spun for 1hr after virus was applied in an attempt to increase the rate of infection using the same procedure as in experiment 2.3. Unlike experiment 2.3, both spun and not-spun cells were tested.

*Parameter 3: Glycine Wash*

Samples from the virus-containing media removed 10hrs after infection from experiment 2.3 suggested that the possible contribution of this extracellular virus to the final overall virus population may be insignificant (50% at most). Interestingly, the cells in experiment 2.3 produced as much or more virus than previous experiments where no wash step was used. To verify and further explore this counterintuitive result both glycine washed and unwashed cells were tested.

*Parameter 4: Optimized BES Protocol Using Cells Maintained at 3% $CO_2$*

The results from experiment 2.3 showed that cells transfected at a lower density resulted in greater production of recombinant virus. It is likely that this is the result of increased transfection efficiency of these cells resulting in an increased absorbance of shuttle plasmid. Therefore an additional modification was made to the BES transfection protocol. During published optimization of the BES transfection protocol, transfection of cells maintained in a 3% $CO_2$ incubator, beginning 24hrs prior to transfection, reportedly contained up to 40% more stable transformants then cells maintained at 5% $CO_2$(Tognon et al., 1996) . It was reported that the decreased level of $CO_2$ slightly increased the pH of the media which improved the quality of the precipitate forming on the cells. Initially this parameter was not used due to equipment constraints. This procedure was employed in experiment 2.4. Flow cytometery was used to measure transfection efficiency of cells maintained at 3% and at 5%.

*Detailed Methods: Flow Cytometery*

Cells were transfected as described in experiment 2.4. 293T cells seeded in a 10cm tissue culture petri dish were maintained in a 5% $CO_2$ incubator. Twenty four hours before transfection, the fully confluent cells were detached using trypsin EDTA and cells from one confluent dish were used to seed 6 new 10cm dishes (10ml media per dish). At this time two dishes was placed into a 5% $CO_2$ incubator and two dishes were placed into a 3% $CO_2$ incubator. One dish in each incubator was transfected with the mCherry-expressing shuttle plasmid as described in experiment 2.4. 24hrs after transfection cells were washed 1x with PBS, detached using trypsin EDTA, placed into 15ml conical tubes containing 10ml of fresh media and spun at 1000xg for 5 min to gently pellet the cells. 9ml of supernatant was removed and the cell pellet was gently resuspended in the remaining 1ml of media using a P1000 pipette. Cells were strained through a 70um sterile mesh cell-strainer into a new 15ml conical tube and placed on ice. For flow cytometery analysis cells were loaded into a FACSAria III workstation (BD Biosciences). Control cells were first analyzed in order to set detection gate parameters for mCherry fluorescence (FL5) as well as forward scattering and side scattering gates to eliminate detection of dead cells and cell debris. mCherry fluorescence was excited using a 562 nm laser.

**Experiment 2.4 Results. Addressing the results from experiment 2.3. Live-virus RMCE protocol optimization.**

The results from experiment 2.4 (Fig. 9) showed similar overall levels of total virus production as seen in experiment 2.3. However, higher percentages of recombinant virus were produced than in any previous experiment (Fig. 9A). This increase was seen across all conditions tested. Flow cytometry analysis of transfected control cells showed a higher transfection efficiency 72% (compared to untransfected controls) in cells maintained at 3% $CO_2$ compared to 31% (compared to untransfected controls) for cells at 5%. There was a trend of higher levels of virus production in samples that were both not-spun and treated with non-concentrated virus (Fig. 9B). Between cells that were not treated

Fig. 9A

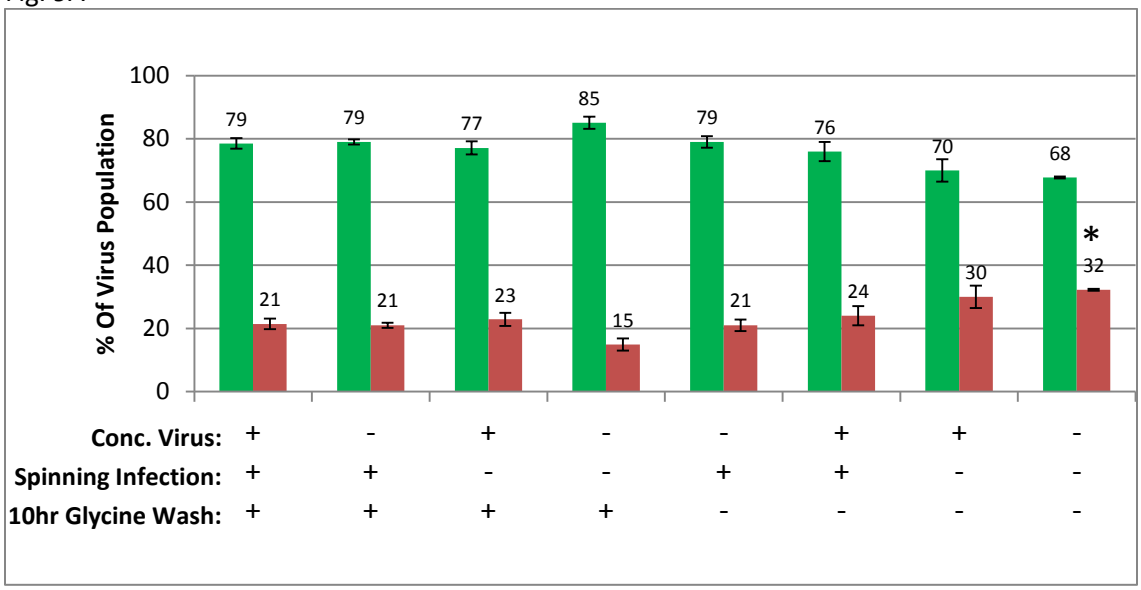


Fig. 9B

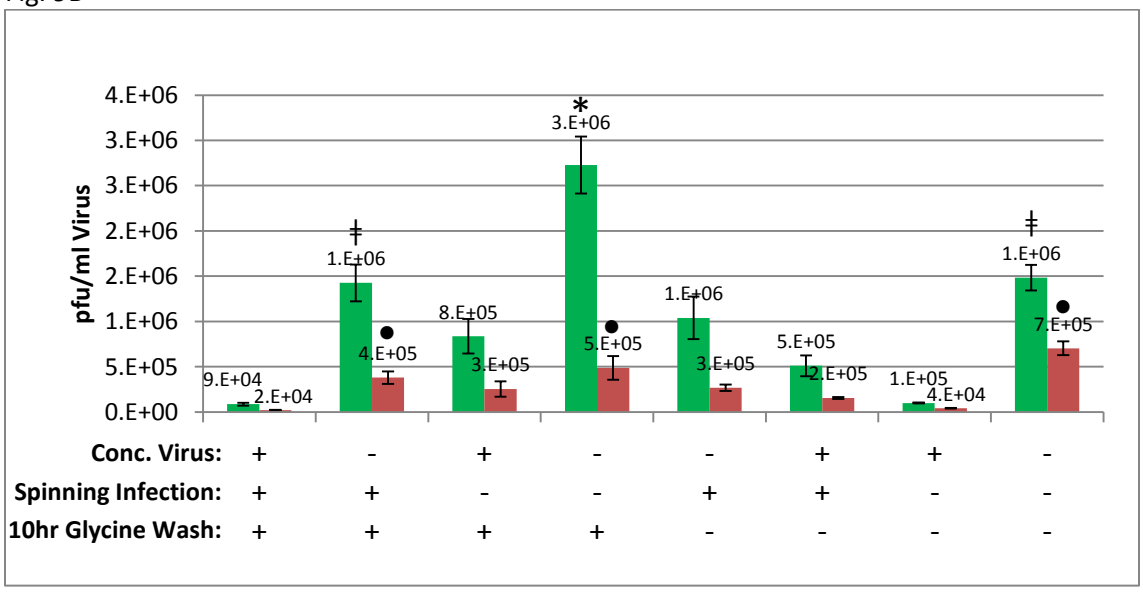


Fig. 9 Experiment 2.4. Quantitaive PCR analysis of clarified lysates from cells treated with different live-virus RMCE procedures. 293T cells at 40% confluency were transfected with 20ug mCherry shuttle plasmid using the modified 3% CO2 BSS transfection protocol. 24hr after transfection all cells were infected with concentrated (MOI=10) or non-concentrated (MOI=1) HSV-Lox-GFP recipient virus . Cells were spun for 1hr 3000xg at 4°C or placed at 4°C 1hr 1xg immediately following infection. Media was removed 10hr following infection and extracellular virus was neutralized using acidic glycine (+ 10hr glycine) or no treatment (- 10hr glycine). **A.** The percentage of each virus in the sample derived from B. * indicates significantly higher (P<.01) percentage of HSV-Lox-mCherry than the lowest condition (- - +). **B.** Total concentration of each virus. * indicates significantly more (P<.01) HSV-Lox-GFP than all other conditions, ‡ indicates significantly more HSV-Lox-GFP than the two lowest conditions (+++ & +- -), • indicates significantly more HSV-Lox-mCherry than the lowest conditions (+++ & + - -). Bars represent S.E.M. Detection of HSV-Lox-GFP is shown in green and detection of HSV-Lox-mCherry is shown in red. Each primer pair has been standardized to plaque titered viral stocks of the corresponding target virus.

with spinning nor glycine wash, those infected with non-concentrated virus had significantly higher levels of HSV-GFP and HSV-Lox-mCherry than those infected with concentrated virus (- - - vs + - - Fig. 9A). Cells treated with non-concentrated virus that were not spun and received the 10hr glycine wash had significantly higher levels of HSV-GFP than all other samples and significantly higher levels of HSV-Lox-mCherry than the two lowest conditions (+ + + & + - - Fig. 9A). Overall, glycine washing at 10hrs significantly increased total virus production, with the one exception of cells that were treated with concentrated virus and spun (+++ Fig. 9A) which had the lowest overall virus production of all conditions tested.

**Experiment 2.4 Conclusions. Addressing the results from experiment 2.3. Live-virus RMCE protocol optimization.**

More recombinant HSV-Lox-mCherry virus was produced in experiment 2.4 than in any previous experiment. This increase may have largely been due to the increased transfection efficiency as a result of maintaining the BES transfected cells at 3% $CO_2$ as opposed to 5% $CO_2$ levels used in all previous experiments. In addition, as observed in experiment 2.3, spinning significantly reduced the amount of virus production across nearly all other parameters. The one exception to this was seen between spun and un-spun cells treated with concentrated virus and not washed with glycine at 10hrs (+ + - vs + - -). However these were two of the lowest producing conditions tested. It therefore appears that spinning infections do not increase the infectivity of HSV-1 in transfected 293T cells. This contradicts results published for other viruses but no such reports have ever been made for HSV-1. All samples were negative for any microbial contamination therefore the observed results can be interpreted to be specific to the parameters tested.

Cells treated with concentrated virus produced significantly lower overall levels of virus than cells treated with non-concentrated clarified lysates. This result is unexpected as this concentrated stock of virus contained ~10-fold more pfu/ml than the un-concentrated stocks used. One possible

explanation for this is that the concentrated stock has increased toxicity when applied to cells in the format of this experiment that is not apparent in the format of the plaque assay. For the plaque assay, (Chapter 2, 2.1.2.1), 2hrs after infection the media is removed and cells are overlaid with Nobel Agar. The infection then persists over several days in this non-liquid, diffusion-free format. Therefore it is possible that the concentrated virus stock contains some factor that is inhibitory to infection in a long-term liquid media format that is not apparent in the plaque overlaid cells. Toxicity could result from the virus-containing pellet from ultracentrifugation also having concentrated amounts of other media-born particulates that could inhibit infection.

Lastly, the use of a glycine wash at 10hr significantly increased the overall amount of virus produced across nearly all parameters tested. While increases in both recombinant and non-recombinant viruses were seen, the glycine washes caused a greater increase in the production of non-recombinant HSV-GFP virus production. This ultimately had the effect of slightly reducing the total percentage of recombinant virus produced.

The overall conclusion that can be drawn from the results obtained in experiment 2.4 is that doing less to the cells appears to result in the highest percentage of recombinant virus in the final population. The non-washed, non-spun cells treated with non-concentrated virus (- - -) produced a significantly higher percentage of recombinant viruses than all other conditions tested (Fig. 9A). The one exception to this was the non-washed, non-spun cells treated with concentrated virus (+ - -) which produced a similar percentage of recombinant virus, but significantly less overall virus. Therefore, for all further experimentation this protocol (- - -) will be used.

### 2.2.10. Experiment 2.5. Final Optimization to the Live-Virus RMCE Procedure

The results from experiment 2.1-2.4 showed that the best production of recombinant virus comes from a modified BES transfection protocol using 20ug of shuttle plasmid onto 293T cells kept at

3% $CO_2$ that are 40% confluent and infected with HSV-GFP (MOI=1) 24hrs after transfection. These parameters were used and further improved upon in the final optimization experiment 2.5. Unless otherwise noted all experimental procedures used in experiment 2.5 were identical to those used above.

*Parameter 1: The use of 0.22um Filtered Clarified Viral Lysates*

The results from experiment 2.4 suggested the presence of a substance in the concentrated virus samples that was inhibitory to infection. These samples were filtered with a 0.4um filter but overall lower levels of infection, despite a higher pfu/ml content, were observed. This suggests that this filtration step was ineffective at removing the inhibitory factor. It was hypothesized that a lower level of the same inhibitory substance could be present in the non-concentrated clarified lysates. To test this, the clarified lysate stocks of HSV-GFP were filtered using a 0.22um filter. The reported average diameter of a HSV-1 particle is ~180-200nm. This 0.22um filtration step appeared to only reduce the qPCR-determined titer of the clarified lysate stocks by ~<10% (data not shown).

**Experiment 2.5. Results. Final Optimization to the Live-Virus RMCE Procedure**

The results from experiment 2.5 show that cells infected with a 0.22um-filtered HSV-GFP viral stock had a significantly higher ($P<.05$) level of HSV-Lox-mCherry virus production than cells infected with unfiltered viral stocks (Fig. 10B). These cells also had trending ($P = .07$) increases in HSV-GFP production compared to cells treated with the unfiltered virus stock. These cells produced recombinant virus at a concentration of ~$6.3x10^5$ and ~$1.7x10^6$ pfu/ml respectively (Fig. 10B). Although the cells treated with filtered virus appeared to produce higher percentages of HSV-Lox-mCherry than cells treated with unfiltered virus this difference was not significant (Fig. 10A).

**Experiment 2.5. Conclusions. Final Optimization to the Live-Virus RMCE Procedure**

The results from experiment 2.5 show that cells infected with a HSV-GFP clarified lysate that was 0.22um filtered produced significantly more virus than cells infected with non-filtered virus. These

Fig. 10A

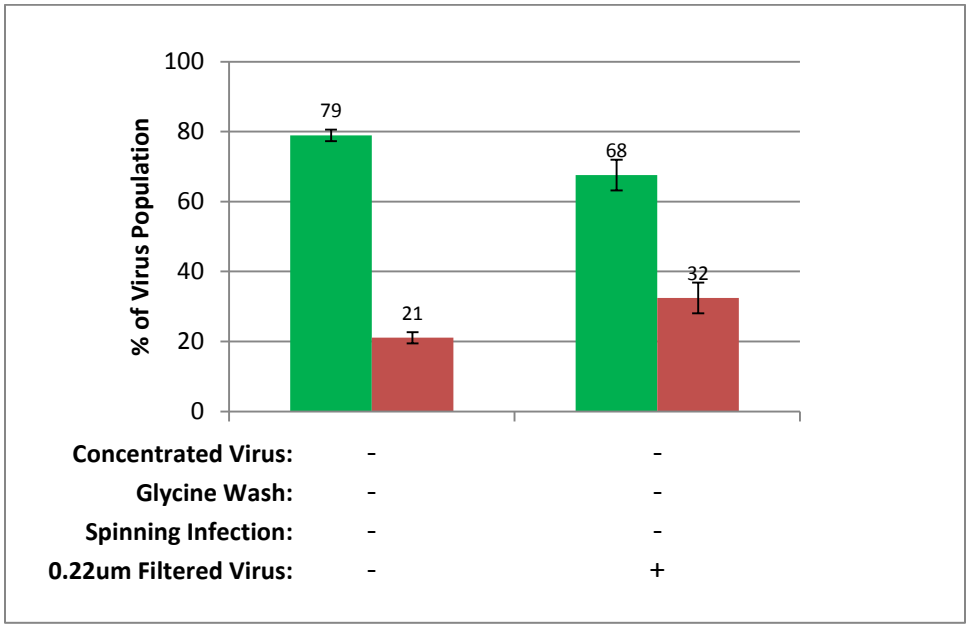


Fig. 10B

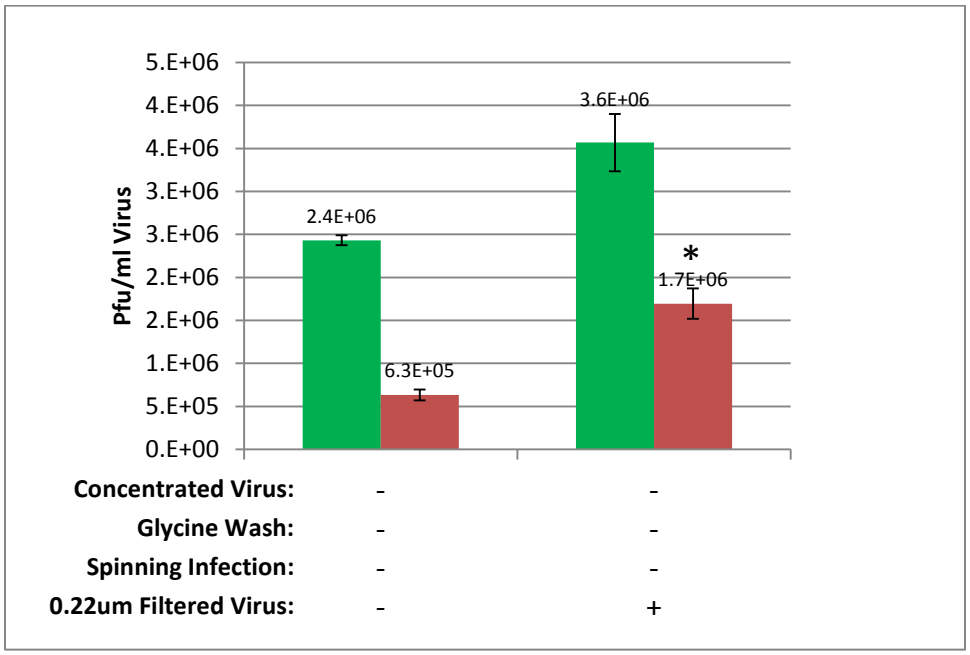


Fig. 10 Experiment 2.5. Quantitaive PCR analysis of clarified lysates from cells treated with the most succesful live-virus RMCE procedure from experiment 2.4. 293T cells at 40% confluency were transfected with 20ug mCherry shuttle plasmid using the modified 3% $CO_2$ BSS transfection protocol. 24hr after transfection all cells were infected with 0.22um filtered or non-filtered (+ & -) non-concentrated (-)HSV-Lox-GFP recipient virus (MOI=1) . Cells were not spun (-) and no glycine wash was used (-). **A.** The percentage of each virus in the sample derived from B. **B.** Total concentration of each virus. * indicates significantly more (P<.01) HSV-Lox-mCherry. No other differences are significant. Bars represent S.E.M. Detection of HSV-Lox-GFP is shown in green and detection of HSV-Lox-mCherry is shown in red. Each primer pair has been standardized to plaque titered viral stocks of the corresponding target virus.

results suggest that a substance that is inhibitory to infection is removed by filtration with a 0.22um filter. It is very possible that the inhibitory substance is incomplete or otherwise immature virus particles which have been reported to aggregate within cells and are toxic to cells. This observation was reported in 1978 in a paper titled "Excess of Interfering over Infectious Particles in Herpes Simplex Virus Passaged at High MOI and their Effect on Single-Cell Survival" (Schröder and Urbaczka, 1978). No reports were made of removing these particles via filtration. The parameters used in experiment 2.5 resulted in the combination of the highest percentage and total amount of recombinant virus produced from any protocol tested. Nearly 30% of the virus population, at a concentration of $1.5x10^6$pfu/ml, was the recombinant product of the live-virus RMCE reaction.

**Experiment 2.1-2.5 Overall Conclusions.**

Through the stepwise optimization approach outlined in experiment 2, the efficiency of the live-virus RMCE reaction was increased several orders of magnitude from levels seen in experiment 1.2. The production of recombinant viruses was increased from an average of 1.1% ($1.0x10^4$ viruses per ml) to an average of 30% ($1.5x10^6$ viruses per ml). If each virus represents a unique recombination event then this technique can be used to create a viral library of $10^6 – 10^7$ different members in the total 10ml collected. The basic principal of the live-virus RMCE reaction was not changed during the optimization process. Therefore it is likely that, as seen in experiment 1.3, the majority of these viruses each represent unique recombination events. This is tested in experiment 2.6

**Experiment 2.6 Testing for the occurrence of unique recombinant viruses using the optimized live-virus RMCE procedure from experiment 2.5.**

The optimized live-virus RMCE procedure as described in experiment 2.5 produced two orders of magnitude more recombinant virus than the original live-virus RMCE procedure as described in

experiment 1.2. As shown in experiment 1.3, the recombinant viruses produced in the original live-virus RMCE procedure appeared to be the result of at least $1x10^3$ unique recombination events. In experiment 1.3, two different plasmids were used in the RMCE reaction over a series of dilutions ranging from 1:1 to $1:1x10^6$. Viruses containing the RMCE cassette from the minority plasmid were detected via qPCR primers specific for a unique sequence contained within this cassette. The same procedure was used to test if the increased amount of recombinant virus produced in the optimized RMCE protocol (experiment 2.5) results from an increased number of unique RMCE events.

**Experiment 2.6. Results. Testing for the occurrence of unique recombinant viruses using the optimized live-virus RMCE procedure from experiment 2.5.**

The results of experiment 2.6 (Fig. 11) show that qPCR primers specific to viruses containing the unique RMCE cassette from shuttle plasmid Shuttle3.1-Sfi1-mc-KO (HSV-Lox-mc-KO) were able to detect significant levels of virus when this shuttle plasmid was diluted as much as 1 in 10,000 with the other shuttle plasmid in the transfection mixture. The level of HSV-Lox-mc-KO DNA detected in this dilution was significantly higher ($P<.01$) than all three negative controls. The amount of HSV-Lox-mc-KO DNA detected in 1 in 100,000 dilution was on the edge ($P= .059$) of being significantly higher than the negative controls. The overall amount recombinant HSV-Lox-mc-KO DNA detected in the less diluted samples was higher than the same dilutions tested using the RMCE procedure from experiment 1.3.

**Experiment 2.6 Conclusions. Testing for the occurrence of unique recombinant viruses using the optimized live-virus RMCE procedure from experiment 2.5**

The results from experiment 2.6 show that the optimized live-virus RMCE procedure produced significantly more unique recombinant viruses than the original procedure in experiment 1.3. When the unique mc-KO shuttle plasmid was diluted as much as 1 in 100,000 with the other shuttle plasmid, levels of HSV-Lox-mc-KO were just barely not significantly higher than negative controls ($P=.059$). The levels of

Fig. 11

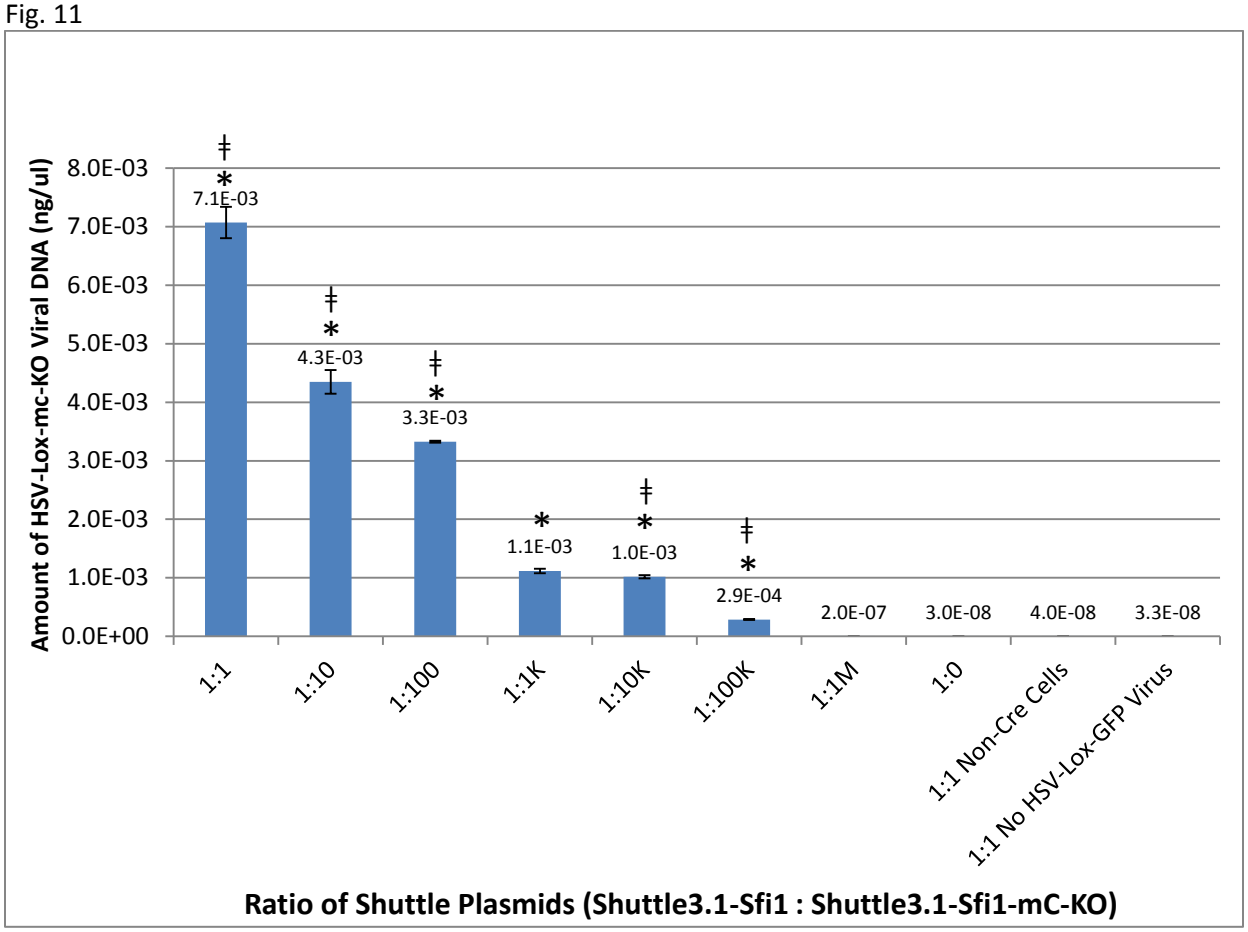


Fig. 11 Experiment 2.6. Quantitaive PCR analysis of clarified lysates from cells infected with clarified lysates from cells treated with the final optimized (experiment 2.5) RMCE procedure containing two different shuttle plasmids. Cells were transfected with different ratios of the plasmid Shuttle3.1-Sfi1-mc-KO : Shuttle3.1-Sfi. Ratios of the two plamids used in each condition are shown on the X-axis. Control cells lacking cre and control cells without recipient virus or viral DNA were transfected with the 1:1 mixture. Signal from primers specific to the RMCE produced HSV-Lox-mC-KO viral chromosome is shown. Primers are standardized to a standard curve of purified HSV-Lox-mC-KO DNA. * indicates significantly different from control (P<.01), ǂ indicates significant different from the next higher dilution sample. Bars represent S.E.M.

HSV-Lox-mc-KO detected in the 1 in 10,000 dilution were easily significantly (P<.01) higher than negative controls. This was not the case with live-virus RMCE protocol from experiment 1.3. Furthermore, the overall levels of HSV-Lox-mc-KO DNA detected in the lower dilutions, (1:1 and 1:10), were nearly an order of magnitude higher than the levels seen from the same dilutions in experiment 1.3. These results all show that the increased amount of recombinant virus produced in the optimized live-virus RMCE procedure is the result of an increased number of unique recombination events and not simply a higher rate of recombinant virus growth. As there is no selective advantage for recombinant viruses in this assay this would not be expected anyway. It appears that the novel live-virus RMCE procedure optimized in these experiments is capable of creating a virus library containing as many as $1x10^5$ unique viruses containing plasmid-derived library genes. This is the highest known efficiency of such a procedure using any large, enveloped DNA virus.

## Chapter 2. Part 3. Creation of HSV-1 Viruses Displaying Fusion Proteins

Two proof of concept glycoprotein-C fusion proteins were designed in order to test the ability of the RMCE system to generate recombinant HSV-1 viruses displaying proteins fused to the C-terminal region of gC. The first fusion protein created was a gC-6-histidine tag fusion and the second was a fusion of gC with the extracellular domain of the chemokine protein fractalkine (CX3CL1).

### Experiment 2.7. Methods-1. Creation of HSV-His6.

The HSV-His6 virus is engineered to display a glycoprotein C hexa-histidine (6His) tag fusion protein. This protein, (gene manipulation described in detail in Chapter2 section 2.1.2.1) includes a region of the glycoprotein C C-terminus containing the transmembrane domain, a hexa-histidine tag, and a small portion of the normal glycoprotein C N-terminus containing the signal peptide. In this protein, amino acids 33-174, which are reported to contain the glycoprotein C HSPG binding domain (Tal-Singer et al., 1995), have been replaced by six codons encoding the amino acid histidine. This

glycoprotein-C 6-histidine fusion protein (gC-His6) was initially reported by Breakefield et al in 2004 (Grandi et al., 2004). Because of its simplicity, as well previous reports of its successful expression, it was selected as the first proof of concept protein to test the ability of the RMCE system to produce viruses displaying a foreign protein sequence.

The shuttle plasmid Shuttle3.1-Sfi1 was co-transfected along with HSV-GFP viral DNA into 293cre cells according to the RMCE co-transfection protocol as described in chapter 2 experiment 1.1. The co-transfection RMCE procedure was used instead of the optimized live-virus RMCE procedure because only a single virus clone was being created, not a diverse library. This procedure was more efficient at producing a virus population containing very little non-recombined parent and would therefore lead to easier isolation of a recombinant virus clone. 15 days following transfection cells showed significant CPE. A virus-containing clarified lysate was generated from these cells. This lysate was used in a plaque assay (described above) in order to isolate individual recombinant virus clones. Plaques were manually picked and placed in Eppendorf tubes containing ~200ul of DMEM. Intracellular virus was released via freeze-thaw, and the solution was then applied to fresh 6cm dishes of HEK293 cells (~10% confluency). Dishes were monitored for fluorescence using an epi-fluorescent microscope. In total 38 of the 40 plaques isolated contained mCherry expressing virus, while 2 contained GFP expressing virus. These numbers are within the expected range of recombination efficiency of the co-transfection RMCE reaction. One of the mCherry expressing virus clones was randomly selected and amplified for further characterization. Clarified lysate from the 6cmm dish was used to infect 4 10cm dishes of 50% confluent HEK293 cells. Six days later, clarified lysate from these 4 dishes was used to infect 36 10cm dishes. The resulting 360ml of clarified lysate was loaded into Beckman SW28 ultra-centrifuge tubes (25x89 mm) and virus was pelleted by centrifugation through a 5% sucrose cushion at 100,000 x g for 1 hour. The resulting virus pellets were then resuspended in PBS and loaded into Beckman SW40 ultra-centrifuge tubes on top of a stepwise sucrose gradient of 10%, 30% and 60% and

centrifuged at 30,000 x g for 5 hours. The visible band of purified virus particles at the 30%/60% interface was then collected (Tal-Singer et al., 1995). These purified particles were then mixed with Laemlli sample lysis buffer, boiled for 2 minutes and loaded onto SDS-PAGE gels for western blot analysis (described below).

**Experiment 2.7. Methods-2. Creation of HSV-CX3CL1.**

To generate a virus displaying a full-sized, complex, mammalian protein, a shuttle plasmid was engineered to create a fusion between the gC-C-terminus and the chemokine protein fractalkine. Fractalkine, also annotated CX3CL1, is a member of the chemokine superfamily that is involved in immune cell trafficking. This protein was chosen to serve as proof-of-principal protein to demonstrate the ability of the live-virus RMCE procedure to generate HSV-1 particles displaying a large, complex mammalian protein. CX3CL1 was selected for several reasons including availability of reagents, a complex structure containing disulfide bridges and glycosylation and an extensive body of literature surrounding the functional and structural characterization of the protein (Harrison et al., 2001). The binding interactions of CX3CL1 with its receptor, CX3CR1, are also well characterized. The structural domains within the protein important for receptor binding have been extensively investigated and the binding affinity of CX3CL1 for CX3CR1 has been determined ($1x10^{-10}$ M Kd) (Harrison et al., 2001; Streit et al., 2005).

The HSV-CX3CL1 virus generated displays a fusion between a large portion of the N-terminus of the rat chemokine fractalkine (CX3CL1) and the glycoprotein C C-terminus. A plasmid containing the gene for CX3CL1 was a generous gift from Dr. Jeffry Harrison (University of Florida). The N-terminus of CX3CL1 (amino acids 1-337) was amplified using forward primer Fract-Sfi1-Sense; 5-TACTGGCCCAGGCGGCCATGGCTCCCTCACAGC-3 and reverse primer Fract-Sfi1-Anti2; -5TTAAGGCCGGCCTGGCCCTGCCTCCGGGTGG-3 from in a PCR reaction using iProof DNA polymerase (Bio Rad) according to manufacturer's protocol. These primers amplify a region of the CX3CL1 gene including

the entire extracellular cheomokine domain and mucin-like stalk (Harrison et al., 2001). The chemokine domain reportedly contains all receptor-binding activity and the region of the C-terminus that was omitted (a.a. 338-393) only serves to anchor the protein within cell membranes (Streit et al., 2005). This transmembrane region was omitted because the gC C-terminus already contains a transmembrane domain. The PCR primers also add 5' and 3' Sfi1 restriction sites which correspond with the Sfi1 restriction sites in the Shuttle3.1-Sfi1 plasmid and allowed for the CX3CL1 N-terminus to be inserted in-frame with the glycoprotein-C C terminus resulting in a CX3CL1-gC fusion protein. The PCR product and the Shuttle plasmid were digested with Sfi1 endonuclease and ligated together using T4 DNA ligase. The resulting plasmid, named "FKN-Shuttle," was transformed into e. coli DH5α cells and clones were selected and verified by DNA sequencing. Plasmids were then prepared as previously described.

In order to create a HSV-1 virus displaying the CX3CL1-gC fusion, co-transfection RMCE with the HSV-GFP protocol was performed. Plaque purified HSV-CX3CL1 was expanded and virus particles were purified on sucrose gradients in the same manner as HSV-His6. A sample of these purified particles were then mixed with Laemlli sample lysis buffer, boiled for 2 minutes and loaded onto SDS-PAGE gels for western blot analysis (described below).

**Experiment 2.7. Methods-3. Plasmid Controls for gC-fusion protein Expression.**

As a positive control for expression of the gC fusion proteins, the gC-His6 containing shuttle, Shuttle3.1-Sfi1, and gC-CX3CL1 shuttle, FKN-Shuttle, were separately co-transfected with the plasmid pCDNA3.1-Hygro+m2-LacZ-66 (pCMV-Lox) into 293cre cells. Plasmid pCMV-Lox, provided by Dr. Steve Langer, contains the lox sites Lox71M2 and Lox66LoxP which are the same sites present in the recipient viral chromosome. This plasmid will therefore act as a plasmid-surrogate for the HSV-GFP chromosome and will support RMCE with both shuttle plasmids in the presence of cre. This plasmid was used because it contains a CMV promoter immediately upstream of the 5' lox site which will result in high levels of expression of genes inserted into the RMCE locus. This control was used due to concern of the

naturally occurring small amount of gC present in intact viruses being insufficient for western blot detection. 5ug of each shuttle plasmid was co-transfected along with 5ug of pCMV-Lox onto 293cre cells using the $CaCl_2$ transfection procedure (as described in chapter 2 Experiment 1.1). Two days after transfection, cells were harvested in lysis buffer (1M Hepes 5M NaCL, .5M EGTA, 50% Glycerol, 5% Triton X-100). Lysates were then mixed with Laemlli sample buffer, boiled for 2 minutes and loaded onto SDS-PAGE gels for western blot analysis.

To control for any non-RMCE mediated expression of the gC-fusion proteins, the FKN-shuttle and Shuttle3.1-Sfi1 (10ug each) were separately transfected into 293cre cells without the presence of recipient virus nor recipient plasmid. Since the shuttle plasmids contain no promoter of their own, these cells should show no expression of the gC fusion proteins. Cells were transfected, harvested and prepared as described above.

**Experiment 2.7. Methods-4. Western Blot Analysis of Purified Virus Particles and Control Cells.**

All samples were resolved on 12% SDS-PAGE gels, transferred to nitrocellulose and then probed with antibodies. For loading, lanes were loaded with 100ug total protein from transfected cells or with 20ul (from 100ul total harvested) of lysed purified virus. All blotting was performed according to antibody manufacturer's specifications. For detection of CX3CL1 the antibody AF537 (R&D Systems) was used. For detection of the His6 tag the Penta-His antibody (Qiagen, 34660) was used. For detection of the glycoprotein C C-terminus the anti-gC1 serum R46 (kindly provided by Dr. Roselyn Eisenberg, University of Pennsylvania) was used. Blots were developed with ECL Plus reagent (Amersham) and exposed onto Kodak X-ray film.

**Experiment 2.7. Results. Creation of HSV-1 Viruses Displaying Fusion Proteins.**

In total, 10 different samples were run on 4 different blots treated with one of the 3 aforementioned antibodies. A ~50kda band corresponding with the predicted size of the gC-Hisx6 fusion protein was present in both blots treated with the His6 antibody as well as the anti-gC serum (Fig. 12

A&B Lanes 2 and 10). A ~120kDa band corresponding with the predicted size of the gC-CX3CL1 fusions protein was seen in both blots treated with the anti-gC serum and CX3CL1 antibody (Fig. 12 A & C Lanes 4 and 9). Very robust immunoreactivity was seen in samples from cells co-transfected with either shuttle plasmid or the pCMV recipient plasmid. Slightly less robust bands of identical sizes were seen in lanes loaded with sucrose purified HSV-His6 and HSV-CX3CL1 virus particles.

**Experiment 2.7. Conclusions. Creation of HSV-1 Viruses Displaying Fusion Proteins**

The results of experiment 2.7 show immunoreactivity with bands of the predicted sizes for both gC fusion proteins created. The size of the gC-His6 fusion was consistent with published reports (Breakefield 2004). The heavy 110kDa band corresponding to the gC-CX3CL1 fusion protein was expected and this corresponds with a high degree of glycosylation that is known to occur in the chemokine domain and mucin-like stalk of the CX3CL1 protein (Harrison et al., 2001). Expression of the fusion proteins appears to be dependent on successful RMCE as no bands were observed in samples from cells transfected with the shuttle plasmids or pCMV alone. Differences in band intensity between blots using anti-His6 and anti-CX3CL1 antibodies are likely the result of differences in antibody quality. The differences in band intensity between transfected cells and purified viral particles are likely the result of much higher levels of expression from the CMV promoter within plasmid pCMV compared to amount of gC that is normally incorporated into virus particles.

Both gC fusion proteins appeared to be incorporated into mature HSV-1 virions. Lanes containing sucrose purified virions (Fig. 12, lanes 2 and 4) showed bands of expected size and of relativity similar levels of expression for both fusion proteins. These results show that the RMCE between the shuttle plasmid and virus chromosomes results in the expression and incorporation of gC fusion proteins into mature virus particles.

Fig. 12

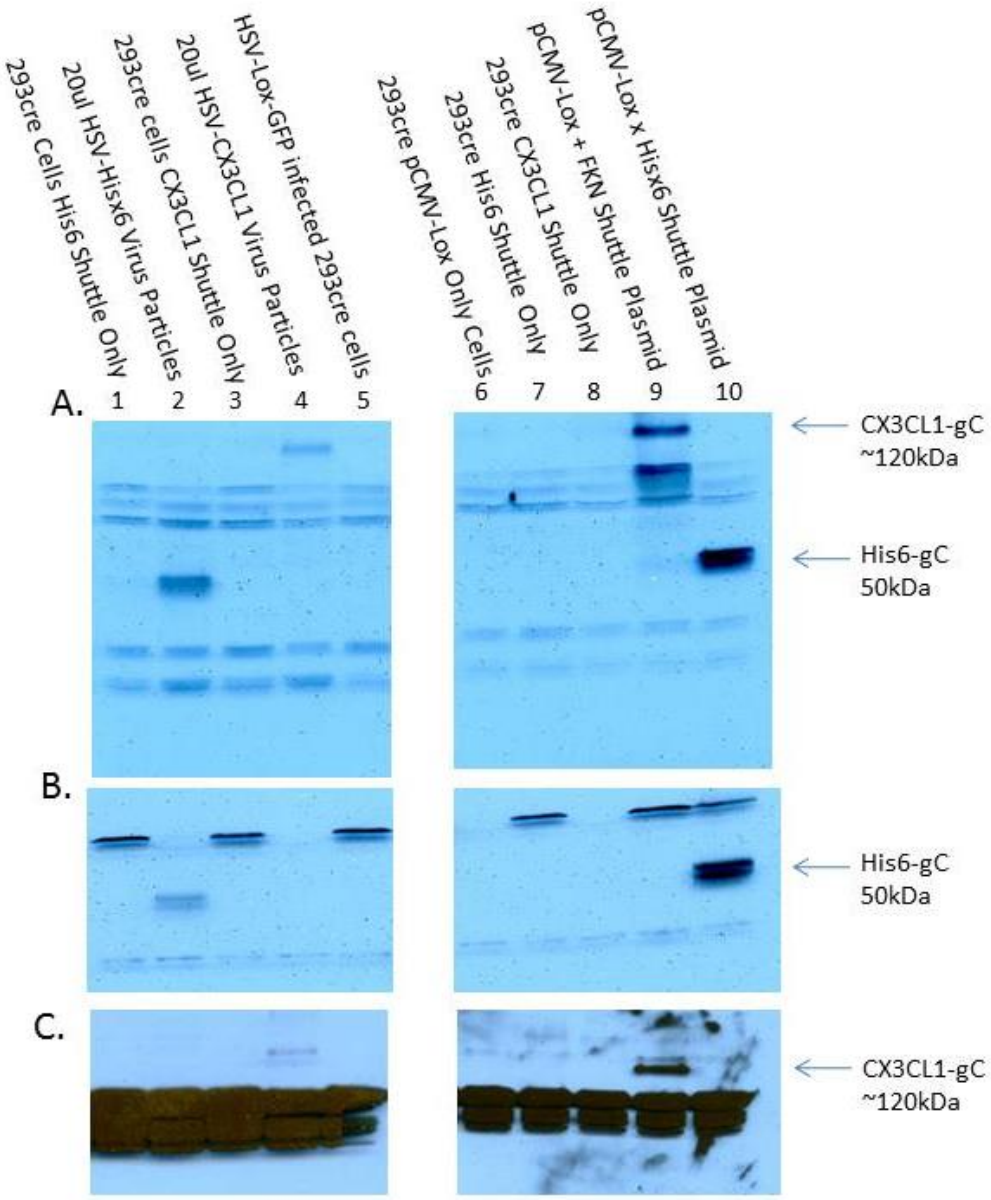


Fig. 12 Experiment 2.7. Western blot analysis of transfected cells and sucrose purified viruses to detect expression of gC-Hisx6 and gC-CX3CL1 fusions proteins using: **A.** A αGlycoproteinC anti-gC1 serum R46 which is reactive to an epitope in the gC C-terminus present in both fusion proteins. **B.** A αHis6 antibody. **C.** A αCX3CL1 antibody. Control lanes 1, 3, 6, 7, 8 contain cell lysates from 293cre cells transfected with only a shuttle plasmid or only the RMCE control CMV expression plasmid pCMV. Shuttle plasmids contain no promoter therefore protein expression will only occur as a result of RMCE with the pCMV plasmid or with a viral chromosome. This is seen in lanes 9 & 10. In lanes 2 & 4 immunoreactivity is seen with sucrose purified virions only by the corresponding antibody. Lanes 1 & 3 are redundant controls with lanes 7 & 8.

## Chapter 3. Testing for increased virus growth as a result of a high-affinity gC-fusion protein.

### Experiment 3.1. Introduction. Creation of Cells Expressing the CX3CR1 receptor

The ultimate goal of the work described within this thesis was to create a human-virus-based system for the affinity screening of human and mammalian proteins. The selection premise of this technology is based on the theory that viruses displaying proteins with high-affinity for cell-surface receptors will bind, enter, and infect cells more efficiently than viruses displaying low-affinity proteins. Upon infection by a virus, a cell soon becomes refractory to subsequent infection by other viruses (reviewed in chapter 1) and will eventually die after the replication of progeny virions. The progeny of high-affinity viruses will, through natural selection, eventually dominate a mixed virus population as they are able to out-compete other viruses for the limited number of cells in the dish.

For this system to be successful, four goals must be achieved. The first is to establish a method to create a diverse library of viruses that contain genes from a DNA library. The second is that the viruses created using this method must display protein ligands encoded by the DNA that was inserted. The third is that a displayed protein ligand which has high binding affinity for a cell-surface target must convey a growth advantage over other viruses that display lower affinity proteins. The final goal is that this growth advantage must allow for the enrichment of a very small number of high-affinity viruses over a large number of lower affinity viruses in a large virus library.

The first two goals were accomplished and described in chapter 2 of this thesis. The third and fourth goal are addressed in this chapter. The virus created in chapter 2, HSV-CX3C1, displays the chemokine protein CX3CL1. CX3CL1 binds to the chemokine receptor CX3CR1 with $1x10^{-10}$ M Kd (Harrison et al., 2001; Mizoue et al., 2001). Therefore, in order to determine if the binding of HSV-displayed CX3CL1 to the CX3CR1 receptor imparts a selectable growth advantage, a cell-line that expresses the CX3CR1 receptor was created.

**Experiment 3.1. Methods. Creation of Cells Expressing the CX3CR1 receptor**

Immortalized human cervical cancer cells (HeLa) were used to create a CX3CR1-expressing cell-line. HeLa cells, like many other cells, are permissive to HSV-1 infection and replication. The HeLa cell-line HELA-TK-FRT, provided by Dr. Ina Weidenfeld, was used as the progenitor cell-line from which the CX3CR1-expressing cell-line was created. Genome of the HeLa-TK-FRT cells has been engineered to contain two Flippase Recognition Target (FRT) sites which support efficient insertion of exogenous genes. These FRT sites allow site-specific recombination into a highly transcptionally active locus of the cellular genome. For gene insertion, shuttle plasmids containing corresponding FRT sites are transfected into HeLa-TK-FRT and, in the presence of Flippase (Flp) recombinase, an exchange between the plasmid and cellular genome occurs. This exchange ultimately results in the insertion of the shuttle plasmid genes contained between the FRT sites into the cellular genome, and the removal of a thymidine kinase selectable marker that was contained within the FRT sites in the cellular genome. This system is similar to the cre-recombinase mediated RMCE reaction (described Chapter 2).

The CX3CR1 gene was amplified from the plasmid pFKN-R1 using PCR primers CX3CR1-EcoR1; 5-GCTGGAATTCACCATGCCTACCTCCTTCCCG-3 and CX3CR1-Not1-pA; 5-TAATGCGGCCGCTTTATTGCTCAGAGCAGGAGAGATCC-3. These primers amplify the entire CX3CR1 open reading frame and add a polyadenylation signal after the stop codon as well as 5' and 3' EcoR1 and Not1 restriction sites. This PCR product and the plasmid pSIN.Bi-F3-Ig-F were digested using EcoR1 and Not1 restriction endonucleases. Plasmid pSIN.Bi-F3-Ig-F contains FRT recombination sites which correspond with the recombination sites within the genome of HeLa-TK-FRT cells. The digested products were gel purified, ligated together and clones into *E. coli* DH5α cells as described above. The resulting plasmid was named pINA-CX3CR1. Plasmid DNA was isolated from a verified bacterial clone as described in chapter 2.

The plasmid pINA-CX3CR1 contains the CX3CR1 open reading frame under the control of a doxycycline-inducible (tet-on) promoter. This promoter is bi-directional and also controls the expression of the Firefly Luciferase gene. This feature allows for analysis of doxycycline (Dox) -induced gene expression using a commercially available luciferase assay kit (Promega). Plasmid pINA-CX3CR1 (1.25ug) was co-transfected with the plasmid pFLP (1.25ug) into the Hela-TK-FRT cells (~80% confluency in a single 6-well well) using the TransIT transfection (Mirus Bio) reagent according to the manufacturer's instructions. Cells were grown and maintained according to the cell culture methods described in chapter 2. The plasmid pFLP, which encodes for the expression of the Flp recombinase, was also provided by Dr Ina Weidenfeld. Along with the recombinase, this plasmid contains an expression cassette for the puromycin resistance gene which serves as a selectable marker for transfected cells. Approximately 16hrs after transfection, these cells were detached with trypsin/EDTA and transferred into a 100cm cell-culture dish. Puromycin (5ug/ml) was added to the media in order to select against cells not containing the pFLP plasmid. Cells were incubated for 36 hours and then the puromycin-containing media was removed and replaced with fresh media containing 80uM ganciclovir. Ganciclovir is toxic to HeLa-TK-FRT cells which have not undergone RMCE, as they will still contain the HSV thymidine kinase cassette. This cassette is engineered into the cells to serve as a selectable marker for recombinants as it will be removed in cells that have undergone RMCE . Cells were grown for 10 days and the ganciclovir-containing media was refreshed every 3$^{rd}$ day until resistant colonies became visible. Individual colonies were manually picked using a P200 pipette and were placed into separate, 24-well plate wells containing 1ml of regular DMEM media. Clones were expanded into 60mm dishes, at which point they were tested for Dox-inducible luciferase expression. For this, clones were treated with 500ng/ml of Dox, harvested, and analyzed for luciferase expression using the Dual-Luciferase Reporter Assay System (Promega) according to the manufacturer's instructions. Luciferase expression was

measured using a TD 20/20 Luminometer (Turner Designs). The clone showing the highest amount of Dox-induced luciferase expression (named Clone15) was selected for propagation and further use.

**Experiment 3.1 Methods**. **Clone15 HeLa cell mRNA Expression of CX3CR1 Transcript**

The HeLa cell-line Clone15 was tested for Dox-induced expression of the CX3CR1 mRNA transcript. A confluent 10cm dish of Clone15 cells was split into 6 10cm dishes, three of which were treated with 500ng/ml Dox. Cells were then harvested for RNA extraction 24hrs later. RNA was extracted using an RNAeasy kit (Qiagen) following manufacturer's instructions. Total cDNA was synthesized using the First Strand cDNA Synthesis Kit (Roche) according to manufacturer's instructions.

Quantitative PCR for the detection of CX3CR1 cDNA was performed on a CFX96 Real Time System C1000 Thermal Cycler (BioRad) using SYBR Green RT-PCR Master Mix (Applied Biosystems) following the manufacturer's instructions and as described in detail in chapter 2. The PCR primers CX3CR1 RT1; 5-CTCCTTCCCGGAATTGGATC-3 and CX3CR1-RT2; 5-GGGAGTAGAAAATAGATAGGAAG-3 were used for the detection of CX3CR1 cDNA. The PCR primers 18S-RT-Forward 5'-GTAACCCGTTGAACCCCATT-3' and 18S-RT-Reverse 5'-CCATCCAATCGGTAGTAGCG-3' were used for the detection of 18S ribosomal RNA cDNA for normalization of gene expression. For data analysis, the levels of CX3CR1 measured in each sample were normalized to the amount of 18S detected in that sample. For this, signal from 18S and CX3CR1 specific primers were measured across a dilution series of eight 10-fold total cDNA serial dilutions. Regression equations were then generated from this series of dilutions where total amount of cDNA, from 6.25ng/ul to 0ng/ul, was plotted against CT values obtained from each primer pair for that dilution. This generated the equations $Y=-1.369\ln(x)+20.685$ ($R^2 = .9885$) and $Y=-1.458\ln(x)+11.101$($R^2 = .9997$) where Y=CT and X=cDNA concentration (ng/ul) for the CX3CR1 and 18S primers respectively. These equations were then used to calculate cDNA concentrations for CX3CR1 and 18S in +Dox and -Dox treated Clone15 cells. For normalization of gene expression, the calculated cDNA concentrations across triplicate samples were averaged and these averages were divided by the

average amount of 18S cDNA for each sample. To calculate levels of Dox-induced gene expression, the normalized CX3CR1 value from +Dox treated cells was divided by the normalized CX3CR1 value from -Dox treated cells. The normalized values from triplicate readings were analyzed by one way ANOVA and Turkey's HSD post-hoc comparison between means as described in chapter 2.

**Experiment 3.1 Methods. Clone15 Hela Cell Expression of CX3CR1 Protein**

The Clone15 cell-line was tested for Dox-induced expression of CX3CR1 protein. For this, a confluent 10cm dish of Clone15 cells was split into 6 10cm dishes. Two dishes were treated with 500ng/ml Dox, two with 1000ng/ml Dox and two were left untreated. Cells from each dose were collected using the lysis protocol described in the section "Plasmid-Plasmid RMCE Controls" (chapter 2) at 24 and 48 hours following Dox treatment. Cell lysates were blotted for CX3CR1 protein expression (also as described in chapter 2) using the anti-CX3CR1 antibody TP501 (Torrey Pines Biolabs) following manufacturer's instructions.

**Experiment 3.1 Results. Clone15 Hela Cell Expression of CX3CR1.**

Robust CX3CR1 transcript expression was seen in Clone15 cells 24hrs after 500ng/ml Dox treatment (Fig. 13 A & B). Dox treatment resulted in ~20,000-fold higher levels of CX3CR1 transcript expression compared to untreated cells. CX3CR1 protein expression was seen as indicated by the presence of a robust 41 kDa band corresponding with the correct size of the CX3CR1 protein (Miller, PNAS, 2000) (Fig. 13 C, lanes 1,2,4,5). A slight increase in CX3CR1 protein expression is observed at 24hrs as a result of the 1000ng/ml dose of Dox compared to the 500ng/ml dose (Fig. 13 C lanes 1&2). Slightly higher levels of CX3CR1 protein expression were seen 48hrs after doxycycline treatment compared to 24hrs after treatment with no appreciable differences between doxycycline doses (Fig. 13 C, lanes 1&2 vs 4&5). No expression of CX3CR1 protein was seen at either 24 or 48hrs in the -Dox cells (Fig. 13 C, lanes 3&6).

Fig. 13 A

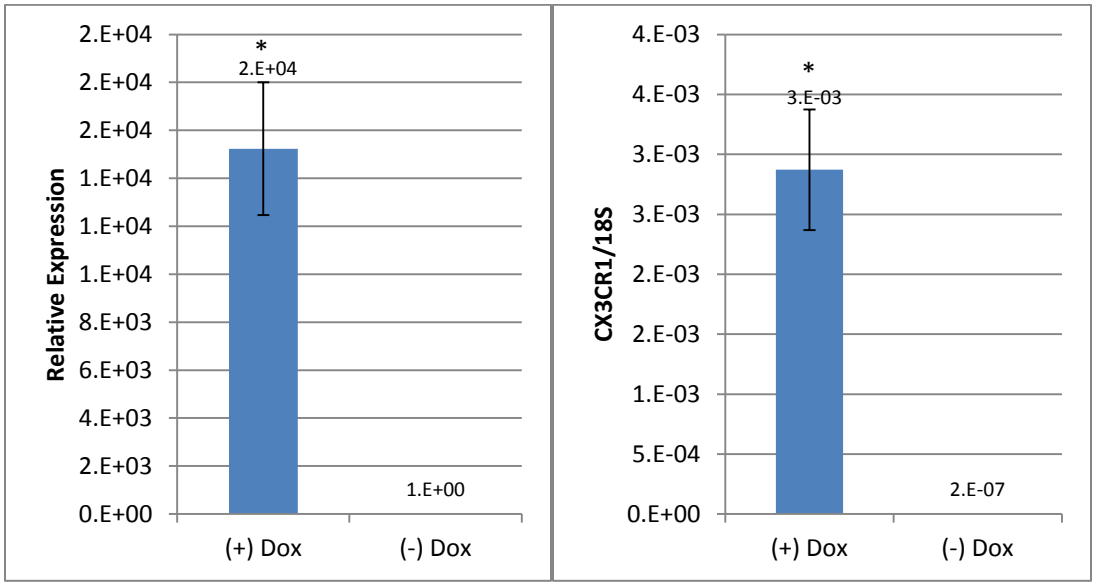


13 B




13 C

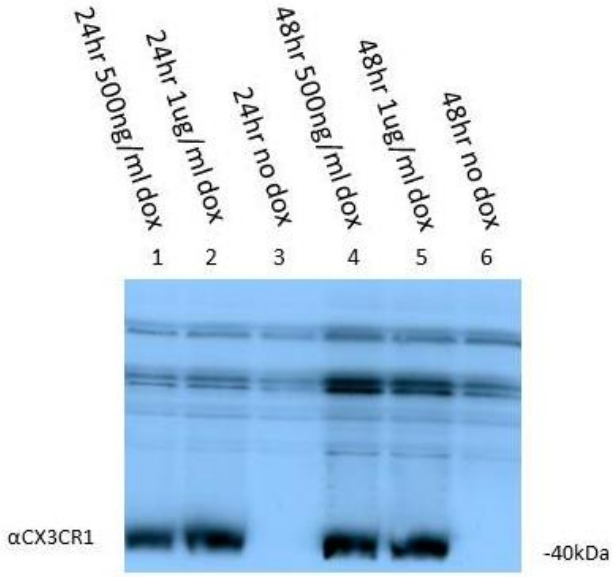


Fig. 13. Experiment 3.1. Dox Inducible Expression of CX3CR1 in the Clone15 HeLa cell line. **A&B.** Quantitative PCR analysis of CX3CR1 transcript expression 24hrs after 500ng/ml Dox treatment. Relative levels of Dox-induced expression (average of +Dox cells/-Dox cells) are shown in **A.** Raw levels of expression normalized to 18s ribosomal RNA expression are shown in **B.** * indicates significantly higher (P<.01) levels of expression compared to -Dox treated control cells. Bars represent SEM. **C.** Western blot analysis of lysates from Clone15 cells treated with 500ng/ul (lanes 1&4) and 1ug/ul (lanes 2&5) Dox at 24hrs (lanes 1-3) and 48hrs (lanes 4-6) after treatment. Control -Dox cells from both time-points are also shown (lanes 3&6). A 40kDa band of the expected molecular weight for CX3CR1 is indicated.

**Experiment 3.1 Conclusions. Clone15 Hela Cell Expression of CX3CR1.**

The results shown in Fig. 13 indicate that the Clone15 cell-line engineered as described in experiment 3.1 expresses robust levels of the CX3CR1 receptor in response to Dox treatment. Furthermore, these results show a very tight level of expression control as no significant levels of mRNA or protein are seen in cells not treated with Dox. The results also suggest that the levels of protein expression 48hrs after Dox treatment are only marginally higher than levels seen after 24hrs. There also appeared to be only a slight increase in CX3CR1 protein expression using 1ug/ml Dox compared to 500ng/ml. This indicates saturated levels of expression have possibly been reached. For all further experiments employing the use of this cell-line, the 1ug/ml dose and 24hr post-Dox time-point will be used. For the purpose of simplifying nomenclature Clone15 will be referred to as HeLa-CX3CR1.

**Experiment 3.2. Growth Characterization of HSV-CX3CL1 in HeLa-CX3CR1.**

As previously stated, the protein affinity selection technology described in this thesis is based on the theory that viruses displaying proteins with high binding-affinity for cell-surface receptors will infect and a replicate more efficiently than viruses displaying proteins with lower binding-affinity. Furthermore, in a mixed population of high-affinity and low-affinity viruses, the high-affinity viruses will have a selectable growth advantage over the low-affinity viruses. This advantage will then allow for a small number of high-affinity viruses to be enriched from a large population of lower-affinity viruses. To test this, the virus HSV-CX3CL1 and the cell-line HeLa-CX3CR1, as described above, were used. HSV-CX3CL1 was engineered to display the protein CX3CL1, which binds to the receptor CX3CR1 with a reported binding affinity of $1x10^{-10}$ M Kd (Harrison 2001). The growth rate of this virus in the presence and absence of the CX3CR1 receptor was compared to that of a non-CX3CL1 displaying virus.

The growth rate of HSV-CX3CL1 on HeLa-CX3CR1 +/- Dox was compared to the growth rate of the progenitor, unrecombined HSV-GFP virus. HSV-GFP, described in chapter 2, was used as a model

low-affinity virus. HSV-GFP lacks the wild-type HSV-1 high-affinity heparan sulfate-binding capabilities, as it lacks gC and the gB HSPG binding domain. It must, therefore, rely on the lower affinity binding of gD for cell attachment. Glycoprotein D binds to several cell-surface targets: nectin-1/2, HVEM, and 3-O sulfated heparan sulfate moieties all with similar affinity ~$1x10^{-6}$M Kd (reviewed in chapter 1). It has been shown that HSV-1 mutants relying solely on gD binding for cell attachment are still fully infectious and can bind and penetrate cells, but with ~80% reduced binding ability compared to wt HSV-1.

**Experiment. 3.2. Experimental Design. Growth Characterization of HSV-CX3CL1 in HeLa-CX3CR1.**

The growth rates of HSV-CX3CL1 and HSV-GFP on HeLa-CX3CR1 cells +/- Dox were analyzed by measuring viral growth every 24hours across a 6 day time-course. Eight different starting amounts of virus, multiplicity of infection (MOIs), were tested. These ranged from high to extremely low MOIs. HeLa-CX3CR1 cells were plated on 6-well sterile tissue culture dishes and treated with 500ng/ml dox (or PBS) 24 hours prior to infection. At the time of infection, cells were approximately ~50% confluent (~500,000 cells).

An infection protocol to favor high-affinity viral binding was created. Some of the elements in this protocol were tested in chapter 2 and shown to not enhance infectivity. However, the experiments in chapter 2 were performed on HEK293 cells as opposed to HeLa cells used in the procedure described below. Parameters in this protocol were based on those used to examine binding differences between HSV-1 mutants described by (Glorioso 1998). Cells were placed at 4$^{o}$C for 20 minutes, then 1ml of 4$^{o}$C virus-containing clarified lysate was added to the cells. Cells were infected at 8 different MOIs ranging from 10 to $1x10^{-6}$ PFU/cell. The plates were loaded into a Beckman GS-6R swing bucket centrifuge, pre-chilled at 4$^{o}$C, and spun for 1hr at 3,000xg. This “spinfect” procedure was used to enhance contact between virus and cells as described above. Following the spin, cells were immediately washed three times with ice-cold PBS to remove unbound or weakly bound virus. Up to this point the cells had been

kept at 4°C to reduce membrane motility to allow viral binding but not penetration into the cells. Warm media (37°C) was then added and the plates were placed in a tissue culture incubator (37°C 5% CO2) for 10 minutes to allow penetration of bound virus to occur. In studies of wild-type HSV-1, ~50% of bound virus was able to penetrate into cells within 10 minutes at 37°C (reviewed in chapter 1). In order to neutralize and remove any remaining extracellular virus, the media was aspirated, cells were washed once with room temperature PBS then treated with 0.1M glycine pH3 for 90 seconds. This acidic treatment is effective at neutralizing nearly all extracellular virus while not harming intracellular virus or the cells themselves (Glorioso, 1998). The glycine was then removed, cells were washed once more with room temperature PBS and 3ml of 37°C media was added. Plates were then placed back into the incubator until the time of collection. For collection, cells were detached via scraping, and cells and media were transferred into a sterile 15ml Falcon Centrifuge tube. Cells were pelleted by spinning at 2000xg for 5 minutes, the supernatants were discarded and total DNA (virus and cellular) was extracted from the cell pellet using a "DNeasy Blood and Tissue Kit" (Qiagen) according to manufacturer's instructions.

*Quantitative PCR Analysis of Viral DNA*

In order to quantify the relative viral titer in the cells at the time of collection, quantitative PCR was used to measure the content of viral DNA in the total DNA extracted from the cells. This procedure, and the viral DNA extraction procedure, differs from that used in chapter 2 as the experiment described here was performed first. The more efficient protocol which uses clarified viral lysates and not cell pellets, as described in chapter 2, was adopted later. The DNA content of each sample was measured using a Thermoscientific Nanodrop 2000C spectrophotometer and then diluted to a concentration of 40ng/ul. Quantitative PCR for the detection of viral DNA was performed on a CFX96 Real Time System C1000 Thermal Cycler (BioRad) using SYBR Green RT-PCR Master Mix (Applied Biosystems) following the manufacturer's instructions. A total of 160ng (4ul) of each diluted DNA sample was mixed with 5ul of

SYBR green master mix and 1ul of 12.5nM primers. For the detection of HSV-CX3CL1 DNA, the primers Red-ORF1-Sense; 5-CGGCGAGTTCATCTACAAGG-3 and Red-ORF1-Anti; 5-GGGGTACATCCGCTCGG-3, were used and for the detection of HSV-GFP DNA the primers GFP-ORF1-Sense; 5-CTGGAGTACAACTACAACAGC-3 and GFP-ORF1-Anti; 5-GCGAGCTGCACGCTGC-3 were used. The specificity and efficiency of these primer pairs was examined prior to their use. Each primer pair showed excellent specificity, failing to give a significant signal with DNA from uninfected cells as well as DNA from cells infected with the non-target virus. Furthermore, these primers showed identical efficiency across a standard curve of plasmid templates ranging from 40ng/ul to $4x10^{-5}$ng/ul. Samples were loaded onto clear, 96-well quantitative PCR plates (BioRad) along with standards in triplicate replicate wells. CT measurements from the standard curve dilutions were plotted against the known DNA concentrations and a logarithmic regression equation was generated. This equation was then used to convert the raw qPCR data, CTs, into concentrations of viral DNA (described in detail in chapter 2). Viral DNA concentrations for all eight starting MOIs were plotted across the six day time-course. Statistical analysis was performed using a one-way ANOVA against all 4 virus and Dox treatment combinations. After a main effect of means collapsed across the time-course for Dox treatment was observed ($P<.05$), individual comparisons were performed between MOI, day and Dox conditions, using Turkey's HSD post-hoc test as described in chapter 2. Statistical comparisons were also made between Dox and virus conditions at the same MOI with readings collapsed across all six days of time course.

**Experiment 3.2. Results. Growth Characterization of HSV-CX3CL1 in HeLa-CX3CR1.**

The high affinity (HSV-CX3CL1) and low affinity (HSV-GFP) had nearly identical growth curves on the HeLa-CX3CR1 cells in the absence of the CX3CR1 receptor (-Dox) (Fig. 14 A & B). There were no significant differences in the amount of viral DNA detected for these two viruses between the same MOIs at the six day growth curves. For both viruses, there was a MOI-dependent and day-dependent increase in viral DNA indicating normal virus growth. A dramatic difference was seen between the two

Fig. 14A 14B

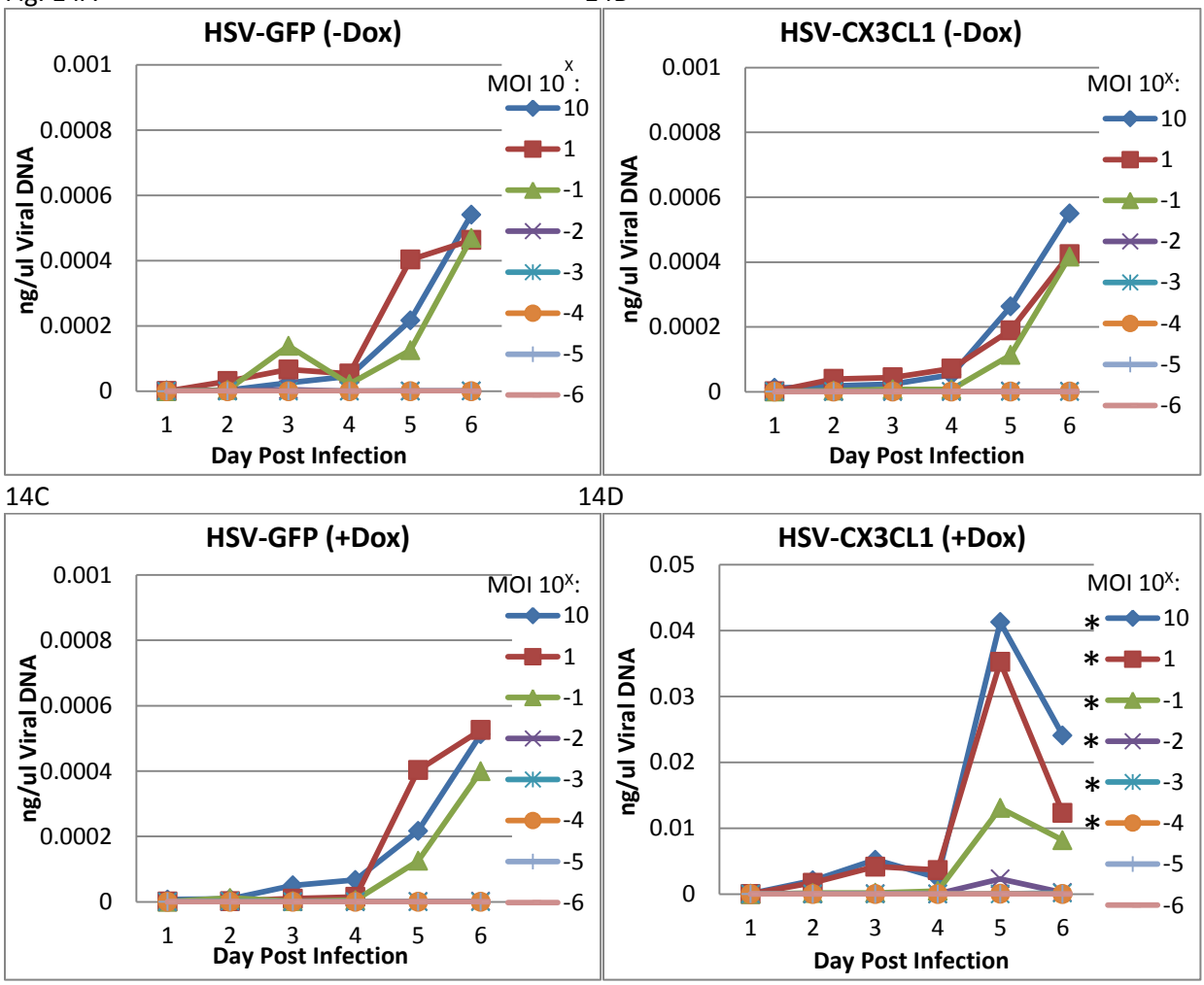


14C 14D

Fig. 14. Experiment 3.2. Quantitative PCR analysis of intracellular viral DNA across a 6-day timecourse at eight different multiplicities of infection (MOI) for two different viruses. HSV-GFP and HSV-CX3CL1 viruses were independently applied to HeLa-CX3CR1 cells in the absence or presence of doxycycline (-Dox/+Dox). Dox treatment induces the expression of the CX3CR1 receptor. The concentration of intracellular viral DNA detected is shown for each MOI tested at each day post infection (PI). Viral DNA was extracted from cell pellets harvested at the day indicated. Each sample was analyzed in triplicate using qPCR primers specific for the virus being tested. Primers were standardized using dilutions of known concentrations of purified target DNA. Regression equations from this standardization were used to calculate the amount of viral DNA from qPCR readings. * indicates a significantly higher ($P<.05$) level of viral DNA for a MOI collapsed across the 6 day time course compared to the same collapsed MOI for HSV-GFP +/-Dox and HSV-CX3CL1 –Dox. Note the different Y-axis scale for HSV-CX3CL1 +Dox.

viruses on cells that had been treated with Dox to induce expression of the CX3CR1 receptor (Fig. 14 C & D). No increase in viral DNA was detected for HSV-GFP infected +Dox treated cells compared to HSV-GFP infected -Dox cells (Fig. 14 A vs C). However, there was as significant ($P<.01$) increase in the amount of HSV-CX3C1 viral DNA detected in HSV-CX3C1 infected +Dox treated cells compared to -Dox cells (Fig. 14 B vs D). Significantly higher ($P<.05$) amounts of HSV-CX3CL1 viral DNA were also seen in +Dox cells infected with HSV-CX3CL1 at MOI 10, 1, $1^{-1}$, $1^{-2}$, $1^{-3}$, $1^{-4}$ when compared to all other combinations (HSV-GFP +/- Dox and HSV-CX3CL1 –Dox) collapsed across the six day time course. No significant differences in the amount of viral DNA detected in -Dox infected cells were seen between the two viruses. On average 100-fold more HSV-CX3CL1 viral DNA was detected in HSV-CX3CL1 infected +Dox cells compared to HSV-CX3CL1 infected -Dox cells.

**Experiment 3.2 Conclusions. Growth Characterization of HSV-CX3CL1 in HeLa-CX3CR1.**

The results from experiment 3.2 showed that the presence of a high-affinity CX3CL1 protein ligand displayed on HSV-CX3CL1 allowed for a faster rate of viral growth on cells expressing the CX3CR1 receptor than a virus not displaying the high-affinity protein. This increased rate of growth appears to be specific to CX3CL1 binding to the CX3CR1 receptor since HSV-CX3CL1 had a growth rate nearly identical to that of the low affinity HSV-GFP virus on cells not expressing the receptor (-Dox). The lowest two MOIs tested ($1x10^{-5}$ and $1x10^{-6}$) showed no difference between the growth rate of HSV-CX3CL1 and HSV-GFP on +Dox or -Dox treated cells. In fact many of these MOI/day combinations failed to even give a significant quantitative PCR signal. These MOIs correspond to initial virus concentrations of 5 and 0.5 total viruses per well. It is possible that some of these starting amounts of virus are simply too low to result in a productive infection even for the high-affinity virus. It is possible that the binding selection washes used in this experiment were too harsh to allow growth from these small initial amounts of viruses.

The highest concentration of viral DNA was detected at day 5 post infection indicating the highest concentration of virus occurred at this time-point. On day 6, this value actually dropped by ~50% (Fig. 14D). It is possible that this is a result of only analyzing cellular viral DNA content. As described above (methods 3.2), cells were harvested, pelleted by centrifugation and this pellet was then lysed to extract viral DNA to serve as a measure of virus growth. The method was used as it was thought that pelleting of infected cells could serve as a means to easily concentrate virus and viral DNA and subsequently increase detection sensitivity of the PCR assay. It is possible that by day 6 the infection had uniformly reached completion and, at this point, all cells in the dish had lysed as a result of infection, subsequently releasing the majority of intracellular virus. This was not seen in the other virus and Dox treatment conditions as these infections were not nearly at as high of a rate of virus growth.

The results from experiment 3.2 demonstrated that the CX3CL1 protein displayed on the virus and the CX3CR1 receptor expressed on the cells facilitated a functional binding interaction. In addition, these results confirm the hypothesis that a virus displaying a protein ligand that binds with high-affinity to a cell-surface target will infect more efficiently, and produce progeny virions more rapidly, than a virus that does not have a high-affinity protein. Lastly, these results show that the current selection parameters and/or analysis procedure cannot detect a significant amount of viral DNA from the high affinity HSV-CX3CL1 virus in +Dox treated cells at the two lowest MOIs tested. This suggests a minimum amount of individual representation that is required to recover a high affinity virus

.

**Experiment 3.3. Enrichment of High-affinity Viruses in Mixed-Population Infections**

In order to demonstrate the practicality of a viral competition system for protein affinity screening, two requirements must be met in proof-of-principal experiments. The first is that a virus displaying a high affinity protein must be able to be enriched from a population of mixed viruses to the point of easy detection. A virus displaying a protein with significantly higher affinity than proteins

displayed by other viruses must eventually represent the majority of the virus population. Once this level of enrichment is achieved, this final "winning" virus would be recovered multiple times from a small sampling of virus plaques from a virus library that has undergone selection. In a real-world application of this system, libraries consisting of unknown proteins will be screened. Therefore, this over-representation is the only way to definitively indicate that a virus displaying a protein with significantly higher binding affinity than all other library members has emerged and the selection process is complete. The second requirement is that the system must be able to screen a large library of many different viruses. Currently established display techniques frequently screen libraries containing $10^4$-$10^7$ unique members. Therefore, the goal of experiment 3.3 is to establish procedural parameters that enrich for the high affinity HSV-CX3CL1 virus from a large library of lower affinity viruses. For enrichment to be deemed successful, the HSV-CX3CL1 virus must represent the majority, >50%, of the final virus population.

The results from experiment 3.2 show that a virus displaying a protein ligand with high binding-affinity ($1x10^{-10}$ M Kd) for a cell surface target had an accelerated rate of growth compared to a virus that doesn't display such a ligand, the HSV-GFP virus. Experiment 3.3 will attempt to determine the ability of the binding selection procedure as described in experiment 3.2 (PBS and acidic glycine washing) to enrich for the HSV-CX3CL1 virus when diluted in a large amount of HSV-GFP virus. These mixed populations will serve to simulate a virus library where a rare, high-affinity virus is greatly outnumbered by lower affinity viruses. In these proof-of-principle experiments, HSV-GFP is being used as a model low-affinity virus. HSV-GFP lacks all normal HSV-1 binding glycoproteins and therefore must rely on the binding of glycoprotein D to its cellular targets found on HeLa cells: Nectin-1 and 3-O HSPG (~$1x10^{-6}$M Kd).

**Experiment 3.3. Experimental design. Generation 1.**

The results from experiment 3.2 showed that both maximal virus growth and maximal levels of Dox-dependent increases in viral growth of HSV-CX3CL1 occurred between days 5 and 6 post-infection. However, the results showed a decrease in intracellular virus concentration at day 6 compared to day 5. This was attributed to final viral exodus from the cells at this time. Despite this observed decrease, intracellular viral DNA content was still measured at day 6 post infection. It was hypothesized that the presence of a competing virus may slow the rate of growth of the high affinity virus. Therefore the infection was allowed to proceed the entire duration of the 6 day time course. No significant increases in virus growth are typically seen after 6 days; by this point the cells are either quite over-crowded or completely dead. 24 hours prior to infection, HeLa-CX3CR1 cells were plated onto 10cm tissue culture dishes at a density of 20% in +/-Dox containing media. For infection, six different mixtures of HSV-GFP and HSV-CX3CL1 virus (total MOI=10) were used. At the time of infection, ~$1x10^6$ cells were present on the dish. HSV-CX3CL1 was mixed with HSV-GFP at ratios of 1:1, $1:10^{-1}$, $1:10^{-2}$,1:10-$^3$,$1:10^{-4}$, $1:10^{-5}$ (PFUs of HSV-GFP : PFUs of HSV-CX3CL1). For each of these dilutions, in the total 10,000,000 viruses added to the cells, there were 5,000,000, 1,000,000, 100,000, 10,000, 1,000 and 100 HSV-CX3CL1 viruses respectively. To determine the effect that the presence of the competing lower-affinity virus has on HSV-CX3CL1 growth, cells were also infected with the same amounts of HSV-CX3CL1 contained in each mixture described above but in the absence of HSV-GFP: 0:1, $0:10^{-1}$, $0:10^{-2}$,0:10-$^3$,$0:10^{-4}$, $0:10^{-5}$. The infection parameters described in experiment 3.2 were used in experiment 3.3. These parameters were designed to enrich for viruses with high binding affinity to cell surface targets and select against lower affinity viruses. Six days after infection, cells and media were harvested and briefly centrifuged to pellet the cells, and viral DNA was extracted from half of the cell pellet using the DNeasy Blood and Tissue Kit (Qiagen) as described above. The other half of the cell pellet was resuspended in 1ml of fresh media and then freeze-thawed three times with liquid nitrogen to release intracellular viruses. The cell debris was then removed from the virus-containing media by brief centrifugation for 5 min at 1000xg. This

cell-pellet clarified lysate was then used to infect fresh cells in a second round of selection. This "generation 2" infection was performed using the same procedure as described above and is discussed in section 3.4.

Four replicate wells (6-well plate) of cells were infected with each condition. Viral DNA from each replicate was measured in triplicate qPCR readings. Quantitative PCR detection of viral DNA was performed as described in experiment 3.2. For statistical analysis, averages of the triplicates for each biological replicate were computed. For each parameter measured, HSV-GFP viral DNA concentration, HSV-CX3CL1 viral DNA concentration and percent of HSV-CX3CL1 in the final population, averages from +Dox treated cells were compared to averages from -Dox treated cells using a one way ANOVA. If a main effect of means ($P<.05$) was observed when comparing between +Dox and -Dox averages collapsed across all conditions, then individual averages between +Dox and -Dox replicates infected with the same virus mixture were compared using a one-way ANOVA and Turkey's HSD post-hoc comparison of means.

**Experiment 3.3. Results. Generation 1.**

A significantly greater amount of HSV-CX3CL1 enrichment was seen in +Dox treated HeLa-CX3CR1 cells compared to -Dox treated cells (Fig. 15). Significantly higher amounts ($P<.05$) of HSV-CX3CL1 viral DNA was detected in +Dox than in -Dox treated cells infected with virus mixtures containing 1:1, $1:10^{-1}$, $1:10^{-2}$ ratios of HSV-GFP to HSV-CX3CL1 (Fig. 15 A & C). These same mixtures also contained a greater percentage of HSV-CX3CL1 viral DNA in +Dox treated cells compared to -Dox cells (Fig. 15 B & D). No significant differences in the total amount of HSV-GFP viral DNA were seen between any conditions. Higher amounts of HSV-CX3CL1 viral DNA were detected in +Dox cells compared to -Dox cells infected with HSV-CX3CL1 virus alone, $0:10^{-1}$, $0:10^{-2}$ (Fig. 15 E & F). While the average amount of HSV-CX3CL1 viral DNA detected in +Dox cells infected with the highest concentration of HSV-CX3CL1 alone (0:1) appeared much higher than that detected in all other conditions, a high degree of variation between replicates within this condition rendered this difference not statistically significant ($P=0.11$).

Fig. 15

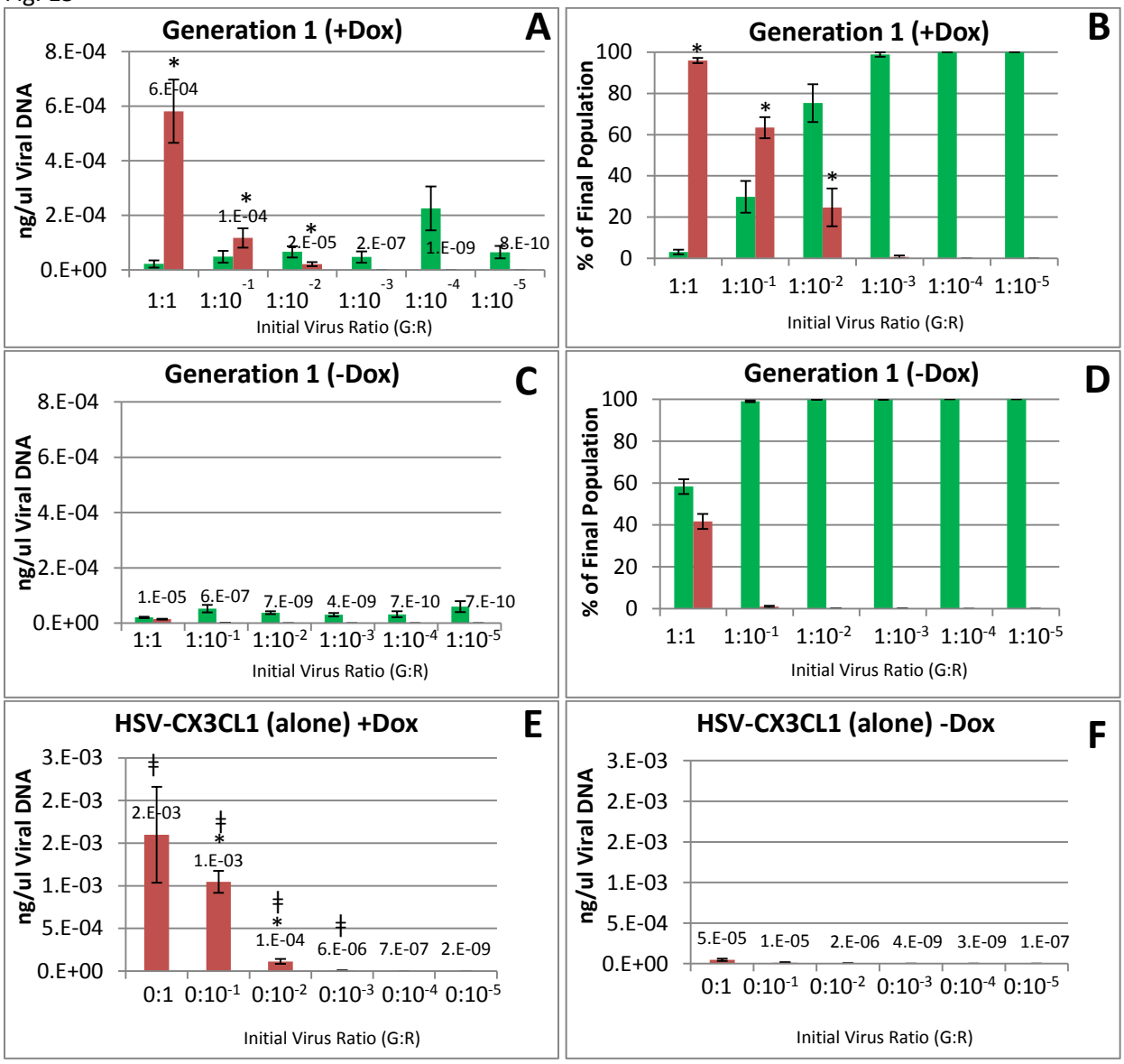


Fig. 15. Experiment 3.3. Quantitative PCR analysis of viral DNA isolated from HeLa-CX3CR1 cells infected with 6 different mixtures of low-affinity HSV-GFP virus and high-affinity HSV-CX3CL1 virus at a total MOI of 10. The ratios of input virus HSV-GFP:HSV-CX3CL1 (G:R) are indicated across horizontal axis of each graph. Cells were treated (+Dox A, B, E) or not treated (-Dox C, D, F) with doxycycline to induce the expression of the CX3CR1 receptor 24 hrs prior to infection. Cells were harvested 6 days after infection. Primers specific to each virus were used for detection, viral DNA detected with primers specific to HSV-CX3CL1 is shown in red (values shown) and HSV-GFP in green. The percentage of each virus in the final population (B & D) was calculated from the concentration of each viral DNA detected (A & C). E and F show the amount of HSV-CX3CL1 viral DNA detected in +Dox and -Dox treated cells infected with the same amount of CX3CL1 contained in the mixed virus infections but without any competing HSV-GFP virus present. * indicates a significantly ($P<.05$) higher value (ng/ul viral DNA or percentage) than the same virus mixture on -Dox treated cells. ‡ indicates a significantly ($P<.01$) higher value of HSV-CX3CL1 viral DNA from +Dox cells infected with HSV-CX3CL1 alone (E) compared to +Dox cells infected with the same amount of HSV-CX3CL1 in the presence of the competing HSV-GFP virus. Bars represent SEM.

Lastly, significantly higher amounts of HSV-CX3CL1 viral DNA were detected in +Dox treated cells infected with HSV-CX3CL1 alone compared to +Dox cells infected with the same amount of HSV-CX3CL1 in the presence of the competing HSV-GFP virus (Fig. 15 E vs A). These differences were significant for the 4 conditions containing the highest amount of HSV-CX3CL1 (1, $10^{-1}$,$10^{-2}$,$10^{-3}$).

**Experiment 3.3. Conclusions. Generation 1.**

The results from experiment 3.3 showed a high degree of enrichment for the HSV-CX3CL1 virus over the competing HSV-GFP virus across several of the virus ratios tested. The HSV-CX3CL1 virus was enriched to more than 50% of the final virus population when it was present as low as 10% in the initial virus population (1:$10^{-1}$) representing 5-fold enrichment. Furthermore, 20-fold and 100-fold enrichment was seen in +Dox cells infected with virus mixtures initially containing 1% and 0.1% HSV-CX3CL1 virus (1:$10^{-2}$ and 1:$10^{-3}$ respectively) respectively. However, the 100-fold enrichment was only trending and not significant as the average amount of HSV-CX3CL1 viral DNA detected in +Dox cells infected with the 1:$10^{-3}$ mixture of virus was not found to be significantly higher than the average amount detected in -Dox cells infected with the same mixture (($1.8X10^{-7}$ng/ul and $4.12X10^{-9}$ ng/ul respectively)( P=0.36). It is possible that these levels of viral DNA are at the edge of detection sensitivity of the DNA extraction or qPCR analysis. Collectively, these results confirm the hypothesis that a virus displaying a ligand with higher binding affinity to a cell-surface target than that of ligands displayed by other viruses will have a selectable growth advantage. Furthermore, this advantage appears to be specific to binding to the cell-surface target, as no enrichment for HSV-CX3CL1 was seen on -Dox treated cells which do not express the CX3CR1 receptor.

Lastly, the results from this experiment also reveal several things about the nature of these competitive infections. The observation that the HSV-CX3CL1 virus grew to significantly higher levels when not challenged with a competing virus shows that a true competition is taking place and that the results do not simply reflect two viruses growing independently of each other in the same dish. This is

likely the result of competition for the limited number of cells in the dish. After a virus completes its infection cycle, the cell will die or otherwise becomes incapable of supporting the growth of other viruses. Furthermore, a "founder-effect" has been observed for HSV-1 (reviewed in chapter 1) where, after the entry of an initial virus, a cell becomes refractory to infection by subsequent viruses in less than 1 hour. An additional interesting observation was that there was no significant increase in the total amount of HSV-GFP produced in -Dox treated cells compared to +Dox treated cells. As there was a massive decrease in the amount of HSV-CX3CL1 produced in these -Dox treated cells there would presumably be less to compete with the HSV-GFP viruses. The cells are clearly able to support higher levels of virus growth as seen in the high amounts of HSV-CX3CL1 virus produced in the +Dox treated cells. However, the lack of any significant change in the growth profile of HSV-GFP between +Dox and -Dox treated cells suggests that the level of growth observed is the maximum possible for this virus. It is likely that this is a result of the selection procedure used in this experiment in which the viruses are only given 1 hour to bind and enter a cell before all extracellular viruses are neutralized with the acidic glycine treatment.

**Experiment 3.4. Generation 2, a Second Round of Selection.**

The results from experiment 3.3 show that the high affinity HSV-CX3CL1 virus can be enriched from a multi-virus library when applied to cells expressing the CX3CR1 receptor. Significant enrichment was seen when the virus was present in as little as 1% of the starting population. Therefore, the goal of experiment 3.4 was to determine if enrichment can be compounded between multiple rounds of selection by applying the enriched populations of viruses harvested from cells in experiment 3.3 onto fresh cells for a second, 6-day generation of viral infection.

**Experiment 3.4. Experimental Design. Generation 2, a Second Round of Selection.**

Clarified lysates prepared from cells harvested after the 6-day generation of infection from experiment 3.3 were used to infect fresh cells. The cell-pellet clarified lysates collected from each

condition in experiment 3.3 were applied to fresh HeLa-CX3CR1 cells using the same infection procedure as before. Lysates collected from -Dox treated cells were used to infect -Dox treated cells and those from +Dox treated cells were used to infect +Dox treated cells. Cells were then harvested 6 days after infection and viral DNA was extracted and analyzed as before. The only procedural difference between experiment 3.3 and 3.4 is that only two replicates from each condition were passaged in this second generation of selection.

**Experiment 3.4. Results. Generation 2, a Second Round of Selection**

Cells harvested from generation 2 of competition contained significantly less viral DNA than cells from generation 1. Both +Dox and -Dox treated generation 2 cells contained significantly less HSV-GFP viral DNA (P=.0174, +Dox P=.02 -Dox) and HSV-CX3CL1 viral DNA (P<.01 for +Dox/-Dox) when means were compared collapsed across all virus mixtures tested (Fig. 16 A & C vs Fig. 15 A & C). In addition, +Dox and -Dox generation 2 cells infected with inoculums from generation 1 cells infected with HSV-CX3CL1 (alone) also contained significantly less HSV-CX3CL1 viral DNA than seen in generation 1 (P<.01) (Fig. 16 E & F vs Fig 15. E & F). Comparisons within generation 2 samples showed that +Dox cells infected with inoculums from generation 1 +Dox cells infected with 0:1 virus mixture (HSV-CX3CL1 alone) contained significantly more HSV-CX3CL1 viral DNA than -Dox cells (Fig. 16 E & F). Generation 2 +Dox cells infected with inoculums from generation 1 +Dox cells infected with the 1:1 and $1:10^{-1}$ virus mixtures contained significantly higher percentages of HSV-CX3CL1 viral DNA (P<.01) than the parallel generation 2 -Dox cells. Lastly, generation 2 +Dox cells did not contain significantly higher levels of HSV-CX3CL1 viral DNA compared to generation 2 -Dox cells (P=.44). Conversely, generation 2 +Dox cells did contain significantly higher overall levels of HSV-GFP viral DNA compared to generation 2 -Dox cells

Fig. 16

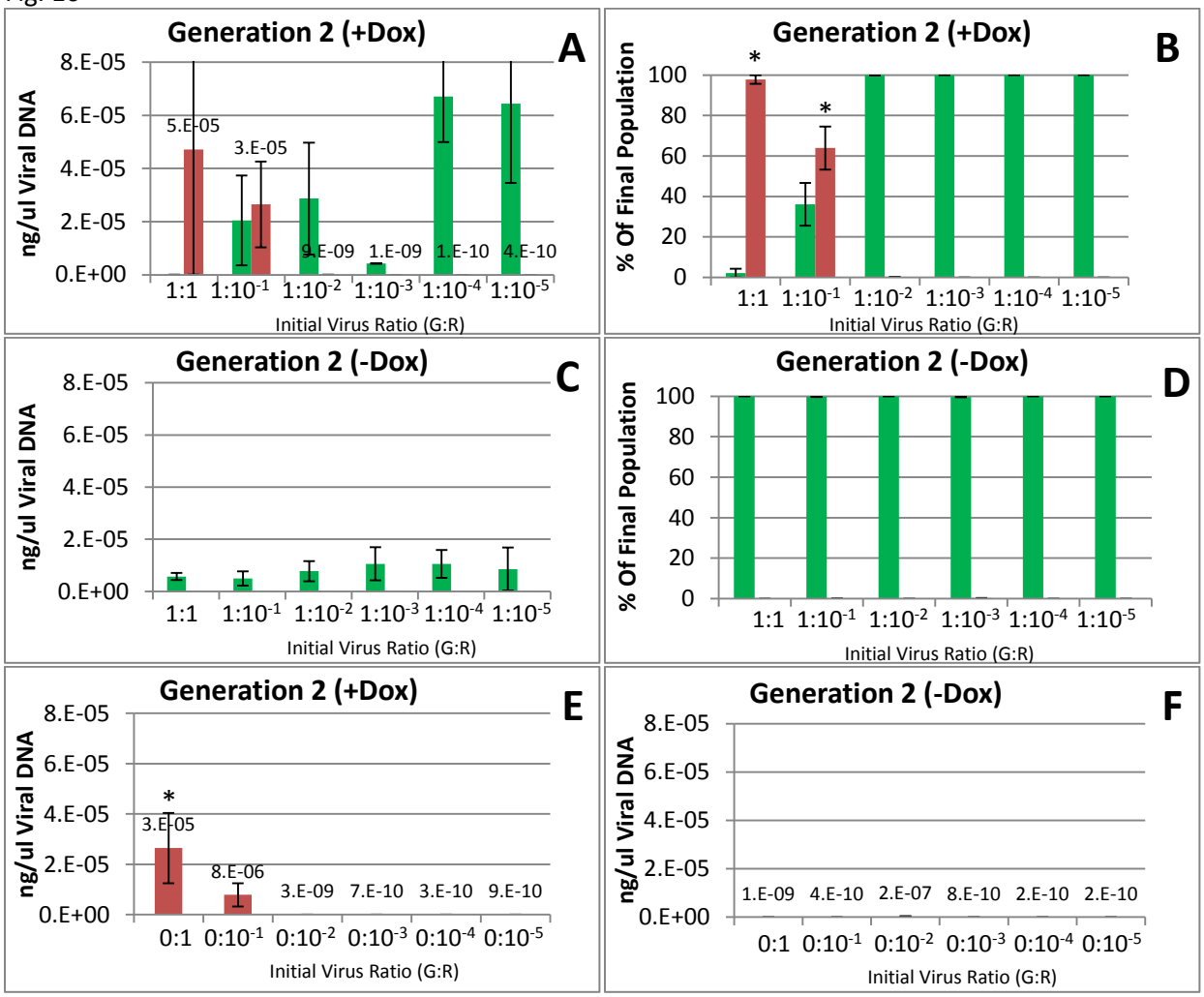


Fig. 16. Experiment 3.4. Quantitative PCR analysis of viral DNA isolated from HeLa-CX3CR1 cells infected with virus populations isolated from the first generation of competition performed in experiment 3.3. The ratios of input virus that went into generation 1, HSV-GFP:HSV-CX3CL1 (G:R), are indicated across horizontal axis of each graph. Each sample from generation 1 was independently passaged onto fresh cells with the same +/-Dox treatment for generation 2. Cells were treated (+Dox A, B, E) or not treated (-Dox C,D, F) with doxycycline to induce the expression of the CX3CR1 receptor 24 hrs prior to infection. Cells were harvested 6 days after infection. Primers specific to each virus were used for detection, viral DNA detected with primers specific to HSV-CX3CL1 is shown in red (values shown) and HSV-GFP in green. The percentage of each virus in the final population (B & D) was calculated from the concentration of each viral DNA detected (A & C). E and F shown the amount of HSV-CX3CL1 viral DNA detected in +Dox and -Dox treated cells infected with the same amount of HSV-CX3CL1 contained in the mixed virus infections but without any competing HSV-GFP virus present. * indicates a significantly higher value (ng/ul viral DNA or percentage) than the same virus mixture on -Dox treated cells within generation 2. Bars represent SEM.

(P=.03). The latter was only observed as a collapsed group effect and no significant differences between individual conditions were seen.

**Experiment 3.4. Conclusions. Generation 2, a Second Round of Selection**

The results from experiment 3.4 show that cells infected with inoculums from generation 1 of selection in a second round of viral competition, generation 2, contain significantly less overall levels of DNA from both viruses than seen in generation 1. This suggests losses of both viruses between the first and the second round of infection. This loss appears to have reversed some of the HSV-CX3CL1 enrichment seen in generation 1. Inoculums from generation 1 +Dox cells containing the lowest still-significant amount of HSV-CX3C1, $1{:}10^{-2}$, failed to produce any significant amount of HSV-CX3CL1 in generation 2. It would appear that the loss of virus between these two successive rounds of selection was too great to allow for viable infections from anything other than the most concentrated amounts of virus. These results suggest that the current selection parameters are too harsh to successfully enrich for a high-affinity virus that is present in low or even medium amounts. The loss of virus appears to be independent of competition as lower levels of HSV-GFP DNA were observed in generation 2 -Dox cells and lower levels of HSV-CX3C1 DNA were observed in generation 2 +Dox cells infected with inoculums containing HSV-CX3CL1 alone. This suggests that selection parameters can be loosened while still maintaining enrichment for the high affinity virus. Interestingly, significantly higher overall levels of HSV-GFP DNA were found in generation 2 +Dox cells compared to generation 2 -Dox cells. This phenomenon was not observed in generation 1 and is likely the result of viral "pseudotyping," a phenomenon that will be addressed in detail below.

**Experiment 3.5.Testing for Enrichment Using Relaxed Selection Parameters.**

The results from the previous experiments showed that, while current selection parameters allowed for enrichment of the high affinity HSV-CX3CL1 virus in a mixed population infection, these

parameters were too harsh to allow enrichment from anything other than a large starting amount of HSV-CX3CL1 virus. Therefore, the purpose of experiment 3.5 was to test for enrichment of HSV-CX3CL1 virus using relaxed selection parameters. In order to reduce the stringency of the selection procedure, the wash and glycine neutralization step used in experiments 3.3 and 3.4 was removed. As this would reduce selective pressure against low-affinity binding, the spinning procedure was also altered. The spinning-infection procedure was used as it has been reported to stabilize virus-cell interactions. Therefore, since the selective pressure against low-affinity binding had been reduced, the spinning procedure was also reduced. It was hypothesized that spinning in the absence of any wash step would be likely to favor the high concentrations of the competing low affinity virus more significantly than it would the small number of high affinity viruses.

**Experiment 3.5. Experimental Design. Testing for Enrichment Using Relaxed Selection Parameters.**

Mixtures of the high affinity HSV-CX3CL1 virus and the lower affinity HSV-GFP virus were used as before. 24 hours prior to infection, HeLa-CX3CR1 cells were plated at a density of 20% in +/-Dox containing media. To streamline optimization of the procedure and reduce sample size, only four virus mixtures (total MOI=10) were used. HSV-CX3CL1 was mixed with HSV-GFP at ratios of 1:1, $1:10^{-1}$, $1:10^{-2}$,$1:10^{-3}$ (PFUs of HSV-GFP : PFUs of HSV-CX3CL1). Cells were infected and then spun for 30, 60 or 90 minutes at 4$^{o}$C at 3000xg or not at all. Non-spun cells were placed in a 4$^{o}$C refrigerator for 60 minutes immediately after virus was applied in order to control for the effect of chilling the cells. All cells were then placed back into a 37$^{o}$C tissue culture incubator without any washing. Cells and media were harvested six days after infection. Pilot testing had shown that the viral DNA concentration in clarified lysates prepared from infected cells was nearly identical to concentrations in pelleted cells (Data not shown). Using clarified lysate samples for DNA analysis instead of pelleted cells would reduce the amount of sample consumed by the analysis procedure as well as allow for direct analysis of the

inoculum used to infect cells in subsequent generations of selection. Therefore, for this and all subsequent experiments, qPCR analysis was performed on viral DNA extracted from 200ul of clarified lysate using the DNeasy Blood and Tissue Kit (Qiagen) as previously described. Data was analyzed as described in experiment 3.3.

**Experiment 3.5. Results. Testing for Enrichment Using Relaxed Selection Parameters.**

In experiment 3.5, an overall trend was observed where levels of HSV-CX3CL1 enrichment were directly related to the length of time the cells were spun following the application of virus (Fig. 17). The greatest levels of Dox-dependent HSV-CX3CL1 enrichment were seen in cells that were spun for 90 minutes (Fig. 17 H). However, this was only trending enrichment and no significant differences were seen between any of the conditions tested due to a high degree of variation between replicates (P=.15, 90'+Dox vs 90'-Dox). There was, however, a very significant effect of spin duration on the total concentration of viral DNA detected. The amount of viral DNA detected was inversely proportional to the amount of time cells were spun (Fig. 18). This was true for both viruses and for both +Dox and -Dox cells. Non-spun +/-Dox treated cells had significantly higher amounts of viral DNA than all other conditions tested (P<.01). This significant decrease in the overall concentration of viral DNA was seen when comparisons were made between identical virus mixtures, collapsed means were compared between Dox-treatment comparisons, and even when DNA amounts from all treatments and viruses were collapsed and compared between the 4 spinning conditions. In the most extreme comparison, non-spun +Dox treated cells contained 100-fold more DNA from both viruses compared to +Dox cells spun for 90 minutes (Fig. 18 B vs H). When comparing between + and -Dox treated cells within the same spinning treatment , only non-spun +Dox cells contained significantly more HSV-CX3CL1 viral DNA compared to their corresponding -Dox treated cells.

Fig. 17

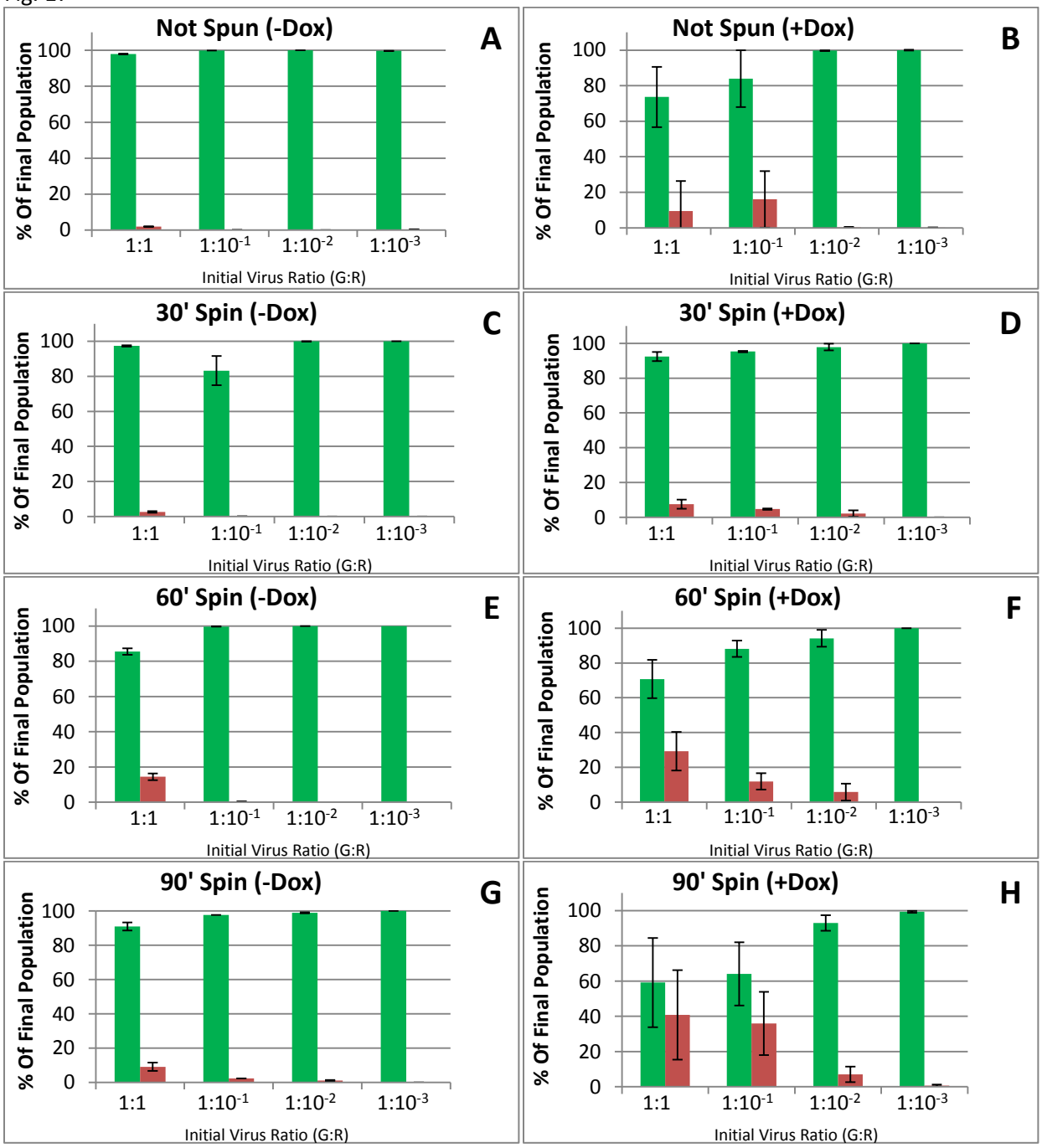


Fig. 17. Experiment 3.5. Quantitative PCR analysis of viral DNA isolated from HeLa-CX3CR1 cells infected with 4 different mixtures of low-affinity HSV-GFP virus and high-affinity HSV-CX3CL1 virus (G:R) at a total MOI of 10. Immediately following infection, cells were spun for 30, 60, 90 minutes, or not at all. Cells were not washed after spinning. Cells were treated (+Dox B, D, F, H) or not treated (-Dox A, C, E, G) with doxycycline to induce the expression of the CX3CR1 receptor 24 hrs prior to infection. Cells were harvested 6 days after infection. Primers specific to the DNA from each virus were used for detection. Percentages were computed from total amounts of viral DNA detected (Fig 18). Primers specific to HSV-CX3CL1 DNA are shown in red and primers for HSV-GFP DNA in green. Bars represent SEM.

Fig. 18

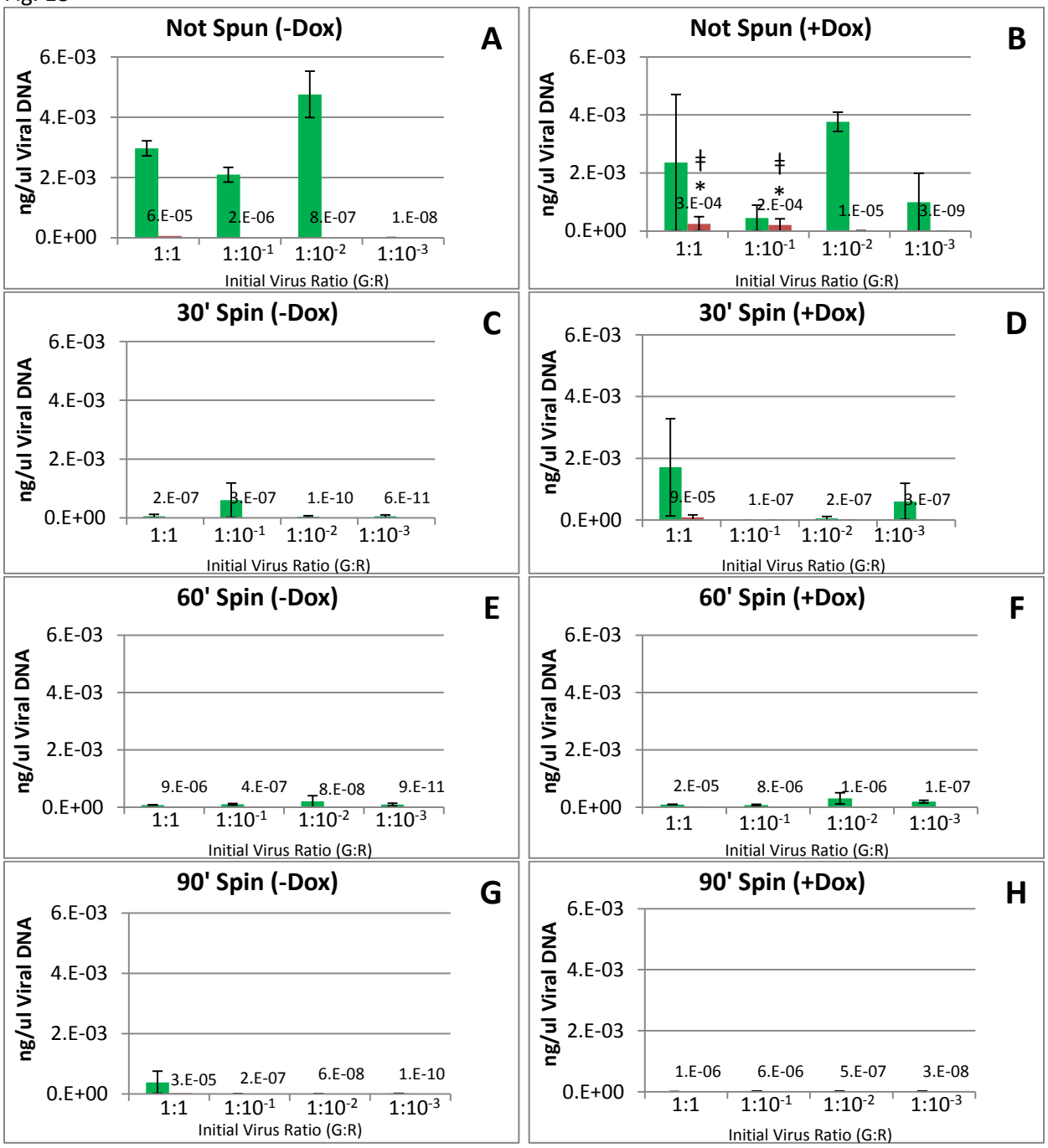


Fig. 18. Experiment 3.5. Quantitative PCR analysis of viral DNA isolated from HeLa-CX3CR1 cells infected with 4 different mixtures of low-affinity HSV-GFP virus and high-affinity HSV-CX3CL1 virus (G:R) at a total MOI of 10. Immediately following infection, cells were spun for 30, 60, 90 minutes, or not at all. Cells were not washed after spinning. Cells were treated (+Dox B, D, F, H) or not treated (-Dox A, C, E, G) with doxycycline to induce the expression of the CX3CR1 receptor 24 hrs prior to infection. Cells were harvested 6 days after infection. Primers specific to the DNA from each virus were used for detection. Primers specific to HSV-CX3CL1 DNA are shown in red (values shown) and primers for HSV-GFP DNA in green. * indicates significantly more HSV-CX3CL1 DNA compared -Dox cells (P<.01) and ǂ indicates significantly more HSV-CX3CL1 DNA compared to all other conditions (P<.01). Bars represent SEM.

**3.5 Conclusions.**

Results from experiment 3.5 showed that enrichment for HSV-CX3CL1 from a multiple-virus library is still possible without the selective wash procedure but is severely reduced. Only non-significant trends of increased percentages of HSV-CX3CL1 on +Dox cells compared to -Dox cells were observed in all conditions tested. A high degree of variability between replicates likely contributed to the lack of statistical significance. While there was a significantly higher amount of HSV-CX3CL1 viral DNA in non-spun +Dox cells compared to non-spun -Dox cells, this did not translate into significant increases in the percentage of HSV-CX3CL1 DNA present due to a high degree of variation in HSV-GFP DNA. It is worth noting that even the trending enrichment seen in this experiment was markedly less than the levels of enrichment seen in experiment 3.3 where the selective wash step was used. In experiment 3.3, when the mixture containing the 1:1 ratio of the two viruses was applied to +Dox cell, the final population was seen to contain more than 90% HSV-CX3CL1 DNA. This same mixture applied to +Dox cells in experiment 3.5 actually produced a final virus population that contained slightly less than 50% HSV-CX3CL1 DNA. This "de-enrichment" occurred across all parameters tested and was also observed in cells infected with the $1:10^{-1}$ mixture as these samples contained less than 10% HSV-CX3CL1 in the final population. It is possible this phenomenon can be explained by increased rates of HSV-GFP virus growth in the absence of the selective wash procedure. On average, 10-fold more HSV-GFP viral DNA was observed in experiment 3.5 compared to cells infected with the same amount of virus in experiment 3.3. This increase in HSV-GFP growth is likely the result of reduced selective pressure against the virus with lower binding affinity by the removal of the wash procedure. Without the washing of unbound viruses, the large amount of HSV-GFP virus (MOI=10) can, overtime, likely occupy the majority of cells in the dish. While the high-affinity HSV-CX3CL1 virus appears to bind and infect cells more quickly than HSV-GFP, this advantage only pertains to cell binding and entry. Upon entering a cell, the HSV-CX3CL1 virus will not be any faster at completing its replication cycle than HSV-GFP.

Therefore, even if a significantly greater percentage of HSV-CX3CL1 viruses bind and enter cells before HSV-GFP viruses, the HSV-GFP viruses will still have 10-12 hours (average HSV-1 replication cycle in culture) to bind and infect a cell before any progeny HSV-CX3CL1 virions emerge. The large amount of HSV-GFP in the virus mixtures (MOI=10) may actually be able to occupy all remaining cells in the dish by the time HSV-CX3CL1 progeny emerge. This would dramatically reduce the amount of possible enrichment within a round of infection.

Experiment 3.5 also showed that spinning appears to have an overall negative effect on the amount of both viruses that are produced. Non-spun cells produced significantly higher amounts, nearly 100-fold, of both viruses compared to all spun conditions. This suggests this reduction is independent of binding affinity and probably the result of the spinning procedure having an adverse effect on cell health in a manner that reduces viral production. It is likely this was a major contributor to the loss of virus between generation 1 and generation 2 in experiments 3.3 and 3.4. This procedure will therefore be removed from subsequent experiments. Overall, the results of experiment 3.5 show that the selection procedure requires further modifications in order to achieve significant enrichment of a small number of HSV-CX3CL1 viruses.

**Experiment 3.6. Addressing Issues of Binding Avidity.**

The results from experiments 3.3-3.5 show that the selection procedures tested thus far were unable to support significant levels of enrichment from a small number of high-affinity HSV-CX3CL1 viruses. Experiments 3.3 and 3.4 showed that while enrichment was achieved, massive losses in overall virus concentration inhibited the ability to compound enrichment between successive generations of selection. Experiment 3.5 showed the spinning procedure may have contributed largely to these losses. However, experiment 3.5 also showed that in the absence of any kind of selection, the HSV-CX3CL1 virus could simply not compete with HSV-GFP when outnumbered as little as 10 to 1. One possible solution

to these observed issues could be to combine iterative rounds of stringent selection followed by non-stringent amplification generations. These strategies were only marginally effective (data not shown). It was therefore hypothesized that the nature of the HSV-GFP binding interactions with the cells may cause these competitions to not be a true test of binding affinity alone. The HSV-GFP virus binds to cells via the use of glycoprotein D (reviewed in chapter 1). Glycoprotein D binds to its cell-surface targets with approximately 10,000-fold lower binding affinity than that of CX3CL1 for CX3CR1 (~$1x10^{-6}$M Kd vs ~$1x10^{-10}$M Kd respectively). However, it has been observed that gD can bind to multiple different cell-surface targets. Of these, both Nectin-1 and 3-O sulfated heparan sulfate proteoglycans (3-O-HSPG) are known to be present on HeLa cells (O'Donnell et al., 2010). This would potentially give the HSV-GFP virus many possible binding targets and allow binding avidity to overcome the disadvantage of having lower binding affinity. Furthermore 3-O HSPGs, reportedly highly expressed on the surface of HeLa cells, can vary in length from short to very long strings of over 150 disaccharide units. As it is known that a single 3-O HSPG moiety can contain multiple gD binding sites, these proteoglycans could effectively serve as "molecular Velcro" for gD binding (O'Donnell et al., 2010). Both HSV-GFP and HSV-CX3CL1 viruses contain gD and therefore, can both bind to these cell-surface targets. However, when greatly outnumbered by HSV-GFP, it is likely that a small amount of HSV-CX3CL1 simply cannot compete. Any advantage conveyed by the higher binding affinity of CX3CL1 is not enough to overcome the high binding avidity of gD in the absence of stringent binding selection.

In order to reduce the high binding avidity of gD, soluble heparin was added to cells prior to infection. Soluble heparin has been reported to efficiently inhibit binding interactions between viral glycoproteins and cell-surface HSPGs (reviewed in chapter 1). The negatively charged heparin molecule competitively binds to stretches of positively charged amino acids within the HSPG binding domains of HSV-1 viral glycoproteins. The addition of soluble heparin would therefore eliminate the ability of gD to bind to HSPG and restrict gD binding to only cell-surface Nectin-1 molecules, thereby reducing HSV-GFP

binding avidity. It was therefore hypothesized that the addition of heparin would allow for the viral competitions to be a more true comparison of binding affinity.

**Experiment 3.6 Experimental Design. Addressing Issues of Binding Avidity.**

Mixtures of HSV-CX3CL1 and HSV-GFP were applied to HeLa-CX3CR1 cells as in experiment 3.5. In order to streamline optimization and reduce sample size a limited number of -Dox control cells were used. HeLa-CX3CR1 cells -Dox were infected with virus mixtures containing 1:1, $1:10^{-1}$, $1:10^{-2}$,$1:10^{-3}$ ratios and +Dox treated cells were infected with virus mixtures containing 1:1, $1:10^{-1}$, $1:10^{-2}$, $1:10^{-3}$, $1:10^{-4}$, $1:10^{-5}$,$1:10^{-6}$ (PFUs of HSV-GFP to PFUs of HSV-CX3CL1) at a total MOI of 10. In order to determine the effect of the presence of a competing virus, +Dox treated cells were also infected with the same amount of HSV-CX3CL1 present in the competition mixtures but in the absence of HSV-GFP (0:1, $0:10^{-1}$, $0:10^{-2}$, $0:10^{-3}$, $0:10^{-4}$, $0:10^{-5}$,$0:10^{-6}$). Replicate 10cm dishes were infected with each combination of conditions. All cells were treated with a sterile solution of Heparin Sodium Salt (Sigma) 2hrs prior to infection at a final media concentration of 1ug/ml. For infection, virus mixtures were applied to cells which were rocked gently and then placed back into a tissue culture incubator. Cells were harvested 6 days after infection and a clarified lysate was prepared as described above. Viral DNA was isolated using a Nucleospin Blood DNA Extraction Kit (Clontech) following the manufacturer's protocol with the exception of also adding 10ug of carrier DNA prior to DNA precipitation. This kit allows for the removal of the heparin from the DNA samples which would otherwise inhibit the PCR reaction. Quantitative PCR measurements and statistical analysis were performed as before.

**Experiment 3.6 Results. Addressing Issues of Binding Avidity.**

Significantly higher levels of HSV-CX3CL were seen in +Dox treated cells compared to -Dox treated cells. Significantly higher concentrations and percentages of HSV-CX3CL1 were seen on +Dox cells infected with the 1:1, $1:10^{-1}$, $1:10^{-2}$,$1:10^{-3}$ mixtures of HSV-GFP:HSV-CX3CL1 ($P<.01$) (Fig. 19 A vs B, C vs D). Furthermore, the percentage of HSV-CX3C1 DNA in cells infected with the $1:10^{-4}$ mixture also

Fig. 19

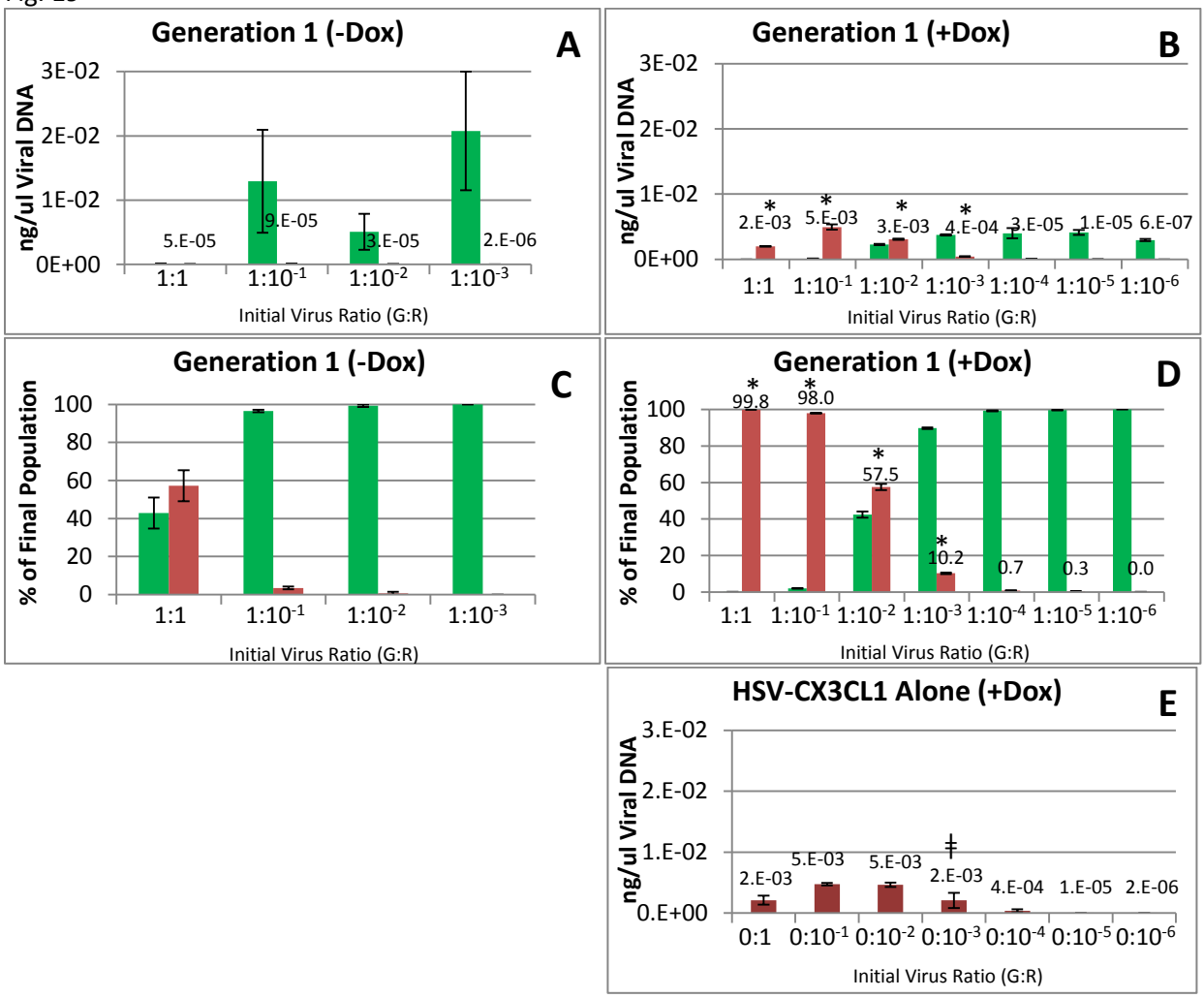


Fig 19. Experiment 3.6. Quantitative PCR analysis of viral DNA isolated from clarified lysates of HeLa-CX3CR1 cells infected with 7 different mixtures of HSV-GFP and HSV-CX3CL1 (G:R) total MOI=10. Cells were treated (+Dox B, D, E, G) or not (-Dox A,C) with doxycycline to induce the expression of the CX3CR1 receptor. Cells were treated with 1ug/ml soluble heparin 2 hrs prior to infection. Cells were not washed nor spun. Viral DNA was isolated from clarified lysates from cells harvested 6 days after infection. Primers specific to HSV-CX3CL1 DNA are shown in red (values shown) and primers for HSV-GFP DNA in green. Quantitative PCR analysis was used to determine the concentration of viral DNA in each sample (A, B,E) and from these percentages of each virus in the total population were calculated (D,C). * indicates significantly more HSV-CX3CL1 DNA or higher percentage of HSV-CX3CL1 than -Dox (P<.01). ‡ indicates significantly more HSV-CX3CL1 DNA from cells infected with HSV-CX3CL1 alone compared to the same amount in the presence of HSV-GFP (P<.01).

appeared to be greatly increased compared to the starting percentage of the virus. In this mixture, the HSV-CX3CL1 virus was .01% of the initial starting virus population. After the 6 day infection this percentage appeared to be increased nearly 100-fold to 0.7%. However, as no corresponding -Dox control was infected with this mixture it is unclear if this represents significant enrichment. In comparisons collapsed across the first four virus mixtures, -Dox treated cells contained significantly higher amounts of HSV-GFP viral DNA compared to +Dox treated cells(Fig. 19 A vs B) ($P<.05$). Lastly, significantly higher ($P<.01$) amounts of HSV-CX3CL1 viral DNA were measured in +Dox cells infected with the HSV-CX3CL1 virus alone than seen in +Dox cells infected with the same amount of HSV-CX3CL1 virus but in the presence of the HSV-GFP virus (Fig. 19 E vs B).

**Experiment 3.6 Conclusions. Addressing Issues of Binding Avidity.**

The results from experiment 3.6 show that the addition of 1ug/ml soluble heparin significantly increased the enrichment of HSV-CX3CL1 in multi-virus infections. The total amount and percentage of HSV-CX3CL1 DNA measured in +Dox treated cells after one 6 day generation of infection were dramatically higher than those seen in experiment 3.5. This enrichment appears to be dependent on CX3CL1 binding to CX3CR1, as no enrichment is seen in -Dox cells not expressing the CX3CR1 receptor. Significantly higher amounts of Dox-dependent enrichment were seen in experiment 3.6 than seen in any previous experiment. Furthermore, the results from experiment 3.6 also show that the addition of soluble heparin did not completely inhibit the ability of the HSV-GFP virus to infect cells. The significantly higher concentrations of HSV-GFP viral DNA in -Dox cells compared to +Dox cells show that, in the absence of the high-affinity binding-advantage of HSV-CX3CL1, the HSV-GFP virus continues to sustain significant growth. Further evidence of viral competition can be seen by the increased amounts of HSV-CX3CL1 virus on +Dox cells infected with the $0:10^{-3}$ virus mixture compared to +Dox cells infected with the same amount of HSV-CX3CL1 but in the presence of HSV-GFP $1:10^{-3}$ (Fig. 19 E v B). Collectively the results from experiment 3.6 show that the addition of soluble heparin reduced the binding avidity

advantage that was previously being used by HSV-GFP. This effectively has made the viral competition a more true test of binding affinity and accordingly the selective advantage of the higher-affinity HSV-CX3CL1 virus is apparent

**Experiment 3.7. Expanding Enrichment in a Second Generation of Virus Competition.**

The results from experiment 3.6 showed higher levels of HSV-CX3CL1 enrichment than achieved in any pervious mixed virus population competition experiment thus far. 100-fold enrichment was seen when the HSV-CX3CL1 virus was present at as little as 0.1% in the initial virus population. Therefore, a second and third generation of virus competition was performed in experiment 3.7 in order to further enrich for HSV-CX3CL1 through successive rounds of compounding selection. If the rates of HSV-CX3CL1 enrichment remain consistent with those seen in generation 1, the virus population harvested from generation 1 cells infected with the $1{:}10^{-3}$ mixture of HSV-GFP:HSV-CX3CL1 should contain over 50% HSV-CX3CL1 virus after generation 2. Furthermore, enrichment might also be seen in lower dilutions of HSV-CX3CL1 where levels of virus were simply below the detection sensitivity of the viral DNA qPCR analysis of generation 1.

**Experiment 3.7. Experimental Design. Expanding Enrichment in a Second Generation of Virus Competition.**

Virus-containing clarified lysates, harvested from cells infected with the first generation of viral competition (experiment 3.6), were passaged onto fresh cells for a second and subsequently third generation of virus competition. Infections were performed exactly as described in experiment 3.6. 1ml of clarified lysate from each condition was used to infect fresh HeLa-CX3CR1 cells. For the purposes of streamlining the optimization process and reducing sample size, -Dox treated cells were not used. It was decided that previous experiments had sufficiently established the accelerated rate of growth of HSV-CX3CL1 was dependent on the presence of CX3CR1 induced by the addition of Dox. Therefore, only

lysates from generation 1 +Dox treated cells were used. For generation 2, duplicate dishes of +Dox treated cells were infected with 1ml of lysate from cells infected with each of the seven virus dilutions described in experiment 3.6. These 14 dishes were then harvested 6 days after infection, a clarified lysate was prepared and 14 additional dishes were infected with 1ml of lysate from each for a third generation of competition. Clarified lysates from the second and third generation were analyzed as described in the previous experiments.

**Experiment 3.7 Results. Expanding Enrichment in a Second Generation of Virus Competition.**

No significant levels of HSV-CX3CL1 enrichment were seen in generation 2 or generation 3 of viral competition (Fig. 20). No increases in the percentage of HSV-CX3CL1 were observed. In fact, non-significant decreases in the percentage of HSV-CX3CL1 were seen between generation 1 and generation 3 (Fig. 20 F vs B). There were no significant changes in the overall concentration of either viral DNA between any of the three generations.

**Experiment 3.7 Conclusions. Expanding Enrichment in a Second Generation of Virus Competition.**

The results from experiment 3.7 showed no further enrichment of HSV-CX3CL1 past that obtained in the first generation of viral competition. As no alterations were made to the selection procedure, these results were unexpected and not in line with those observed in experiment 3.6. It was therefore determined that these results must be caused by a phenomenon involving the interaction between the two viruses once mixed together during the process of infection. Prior to generation 1, these two viruses had not come into contact as they were prepared by expansion of purified clonal virus stocks. It was hypothesized that swapping of viral coats, or "pseudotyping," had occurred (Fig. 21). As previously stated, cells are typically refractory to "super-infection," infection by more than one viruses. Shortly after infection (<1hr, reviewed in chapter 1) viral proteins that are contained within the tegument of the infecting virus act on cellular machinery to inhibit the cell-surface expression of gD

Fig. 20

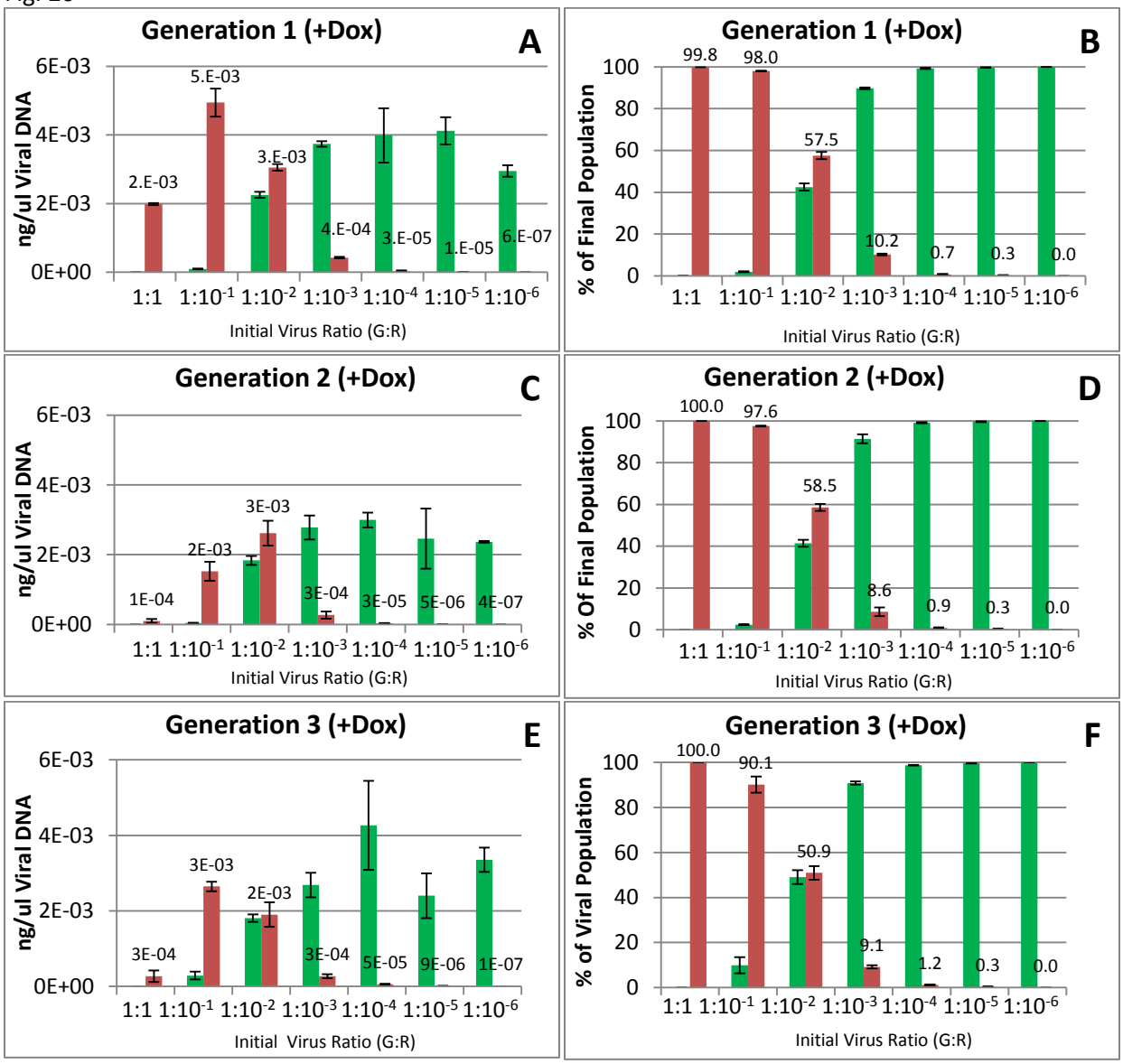


Fig 20. Experiment 3.7. Quantitative PCR analysis of viral DNA isolated from clarified lysates of HeLa-CX3CR1 cells infected with 7 different mixtures of HSV-GFP and HSV-CX3CL1 (G:R) total MOI=10. All cells were treated with doxycycline to induce the expression of the CX3CR1 receptor 24hr prior to infection. Cells were treated with 1ug/ml soluble heparin 2 hrs prior to infection. Cells were not washed nor spun. Viral DNA was isolated from clarified lysates from cells 6 days after infection. 1ml of clarified lysate from each sample was used to infect fresh cells for a subsequent generation. Primers specific to HSV-CX3CL1 DNA are shown in red (values shown) and primers for HSV-GFP DNA in green. Quantitative PCR analysis was used to determine the concentration of viral DNA in each sample (A, C, E) and from these percentages of each virus in the total population were calculated (B, D, F). Bars represent SEM.

Fig. 21.

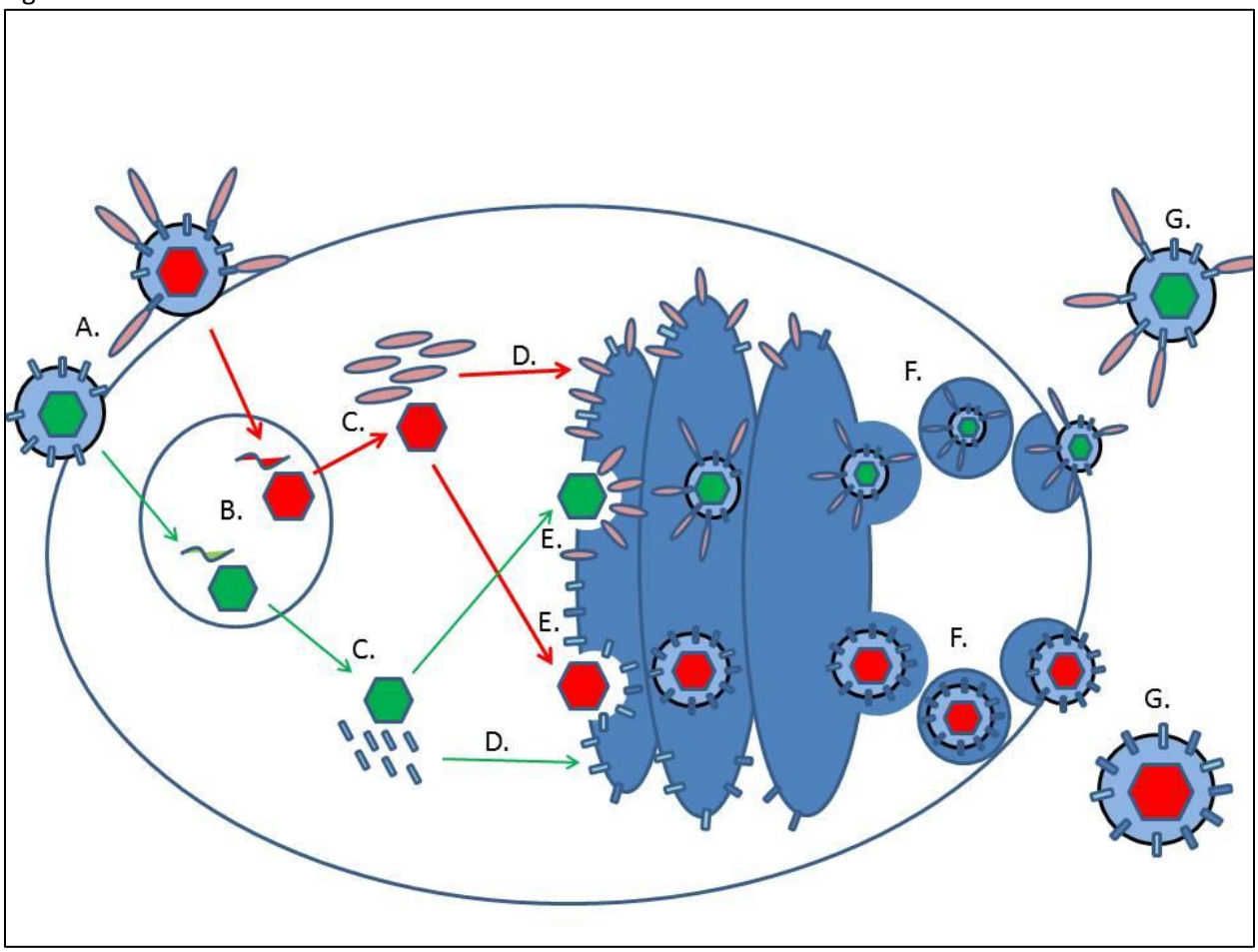


Fig. 21. A schematic representation of viral pseudotyping. **A.** Two genetically different viruses simultaneously bind to and infect a cell. **B.** Both viruses penetrate the cell and the viral chromosomes are delivered to the nucleus where viral genes are expressed and new capsids are assembled. **C.** Replicated viral chromosomes are packaged into new capsids and capsids exit the nucleus. For simplicity, only one progeny capsid from each virus is shown. **D.** During the expression of viral genes, viral glycoproteins are made and inserted into the Golgi membrane. **E.** During the process of viral envelopment, the progeny capsids bud into the Glogi membrane subsequently obtaining their final viral envelope which is studded with glycoproteins. During this process, a capsid could bud into an area of Golgi membrane that is studded with glycoproteins which its genome does not encode. **F.** Enveloped viruses egress via the secretory pathway in Golgi-derived vesicles that are delivered to the cell surface. **G.** Progeny viruses emerge bearing a viral envelope containing glycoproteins encoded by the other virus.

binding targets which are required for HSV-1 cell penetration. However, if two viruses contact a cell simultaneously, or within the window that the cell is susceptible to super-infection, both viruses can enter the cell and initiate viral replication in parallel with one another. The likelihood of such an occurrence increases at high MOI infections. Due to the nature by which the HSV-1 virus acquires its final glycoprotein-containing envelope, by budding into the golgi membrane, a virus capsid could be enveloped by a region of golgi that is studded with glycoproteins encoded by the other virus (Fig. 21 E). The resulting virus would therefore display glycoproteins that are not encoded within its own genome. This phenomenon has been reportedly observed for many viruses, including HSV-1 (Spear et al., 2003). It is likely that during the typical growth of HSV-1 viruses in culture this phenomenon occurs frequently as high MOIs are often used. However, the vast majority of viruses grown in culture are individual virus clones not mixed population infections. Pseudotyped virus progeny from a cell super-infected with identical virus clones would be functionally identical to the parental viruses and therefore would not be of consequence. However, if pseudotyping occurs between HSV-CX3CL1 and HSV-GFP, the final outcome would be quite different. Capsids containing genomes encoding for the CX3CL1-gC fusion that are enveloped by a membrane containing only the glycoproteins encoded by HSV-GFP would be genetically HSV-CX3CL1 but phenotypically HSV-GFP (Fig. 21 G, bottom). This progeny virus would therefore no longer have the growth advantage implied by its genomic content. Conversely, a capsid containing the HSV-GFP genome could "cheat" by obtaining a viral envelope that contains the high-affinity CX3CL1-gC, which its genome does not encode (Fig. 21 G, top). For both viruses, the phenotypic effect of pseudotyping would only last through one round of cell-binding and entry as the viral envelope will be removed upon infection. Provided super-infection does not re-occur, the resulting progeny virions of this subsequent infection will contain only the viral glycoproteins encoded within their genome.

This pseudotyping phenomenon could explain why the virus populations in experiment 3.7 appeared to reach a steady-state equilibrium where enrichment had stopped. Due to the high initial MOI of 10, it is likely that all cells in the dish were infected after an initial single wave of virus binding and penetration. The high concentration of HSV-GFP would increase the likelihood that a cell infected with HSV-CX3CL1 would also be infected with HSV-GFP. As the resulting pseudotyped progeny would have no additional cells to infect and remove their pseudotyped membranes, the pseudotyped binding behavior would be carried into the subsequent generation where HSV-CX3CL1 would not have a growth advantage and enrichment would not occur. HSV-GFP viruses displaying CX3CL1-gC would bind and enter cells at an accelerated rate in +Dox treated cells. However, as these viruses do not possess the gene to express additional copies of the high-affinity protein, it would not be present on progeny HSV-GFP virions and the growth advantage would not be sustained. At sufficiently high MOI, this process would likely continue to cycle, causing a net effect of no significant enrichment and no selection. A solution to this problem will be addressed in experiment 3.8.

**Experiment 3.8. Avoiding Viral Pseudotyping with Low MOI Virus Competitions.**

Experiment 3.8 was designed in order to determine if the high initial MOI used in experiment 3.7 was the cause of the lack of successive enrichment that was observed. In order to reduce the likelihood of super-infection and pseudotyping, as discussed above, the total MOI of the mixed virus infections was reduced 100-fold from 10 to 0.1.

**Experiment 3.8. Avoiding Viral Pseudotyping with Low MOI Virus Competitions.**

Cells were infected using procedures identical to those in experiment 3.7 except that the total amount of virus in each virus mixture was reduced to an MOI of 0.1. For the 7 virus mixtures that were tested, this corresponded to 250,000, 50,000, 5,000, 500, 50, 5, and 0.5 PFUs of HSV-CX3CL1 in each. $5x10^6$ HeLa-CX3CR1 cells, were infected and then harvested 6 days later and clarified lysates were

prepared. 1ml of lysate was used to infect fresh cells for subsequent generations of virus competition with the exception of generation 4. Only 100ul (10X dilution from 1ml standard passage amount) of lysate from generation 3 was used to infect cells for generation 4. This "cutback" procedure was performed out of concern that, as the virus population was propagated between successive generations, increasing rates of HSV-CX3CL1 growth would raise the virus concentration of virus to the point of, once again, causing super-infection and pseudotyping.

**Experiment 3.8 Results. Avoiding Viral Pseudotyping with Low MOI Virus Competitions.**

Higher levels of HSV-CX3CL1 enrichment than ever previously obtained were observed in experiment 3.8. Significantly higher ($P<.05$) percentages of HSV-CX3CL1 were seen in cells infected with mixtures of viruses containing ratios of $1:10^{-2}$, $1:10^{-3}$, $1:10^{-4}$ HSV-GFP to HSV-CX3CL1 compared to the same generations in experiment 3.7 (Fig. 22 vs Fig. 20). Furthermore, significantly higher percentages of HSV-CX3CL1 were seen in cells in generation 2 infected with the $1:10^{-5}$ mixture of viruses (Fig. 22 D) compared to generation 2 cells infected with the same mixture in experiment 3.7 (Fig. 20 D). However, this enrichment was not sustained onto generation 3 (Fig. 22 F). Significantly higher amounts of total HSV-CX3CL1 viral DNA concentration were seen in cells infected with the two most concentrated mixtures of HSV-CX3CL1 in experiment 3.8 compared to amounts seen experiment 3.7 (Fig. 22 vs Fig. 20 A,C,E).

**Experiment 3.8 Conclusions. Avoiding Viral Pseudotyping with Low MOI Virus Competitions.**

Reducing the total MOI used to infect cells in experiment 3.8 dramatically increased the level of HSV-CX3CL1 enrichment over that seen in experiment 3.7. Using this new low-MOI infection procedure, higher levels of HSV-CX3CL1 enrichment were obtained than ever seen before. The greatest enrichment observed was that in four generations of viral competition, a virus population that initially contained 0.01% HSV-CX3CL1 ($1:10^{-4}$) was enriched to over 80% HSV-CX3CL1. These results suggest that using the current viral competition procedure, a library containing 10,000 different viruses can be screened to

Fig. 22

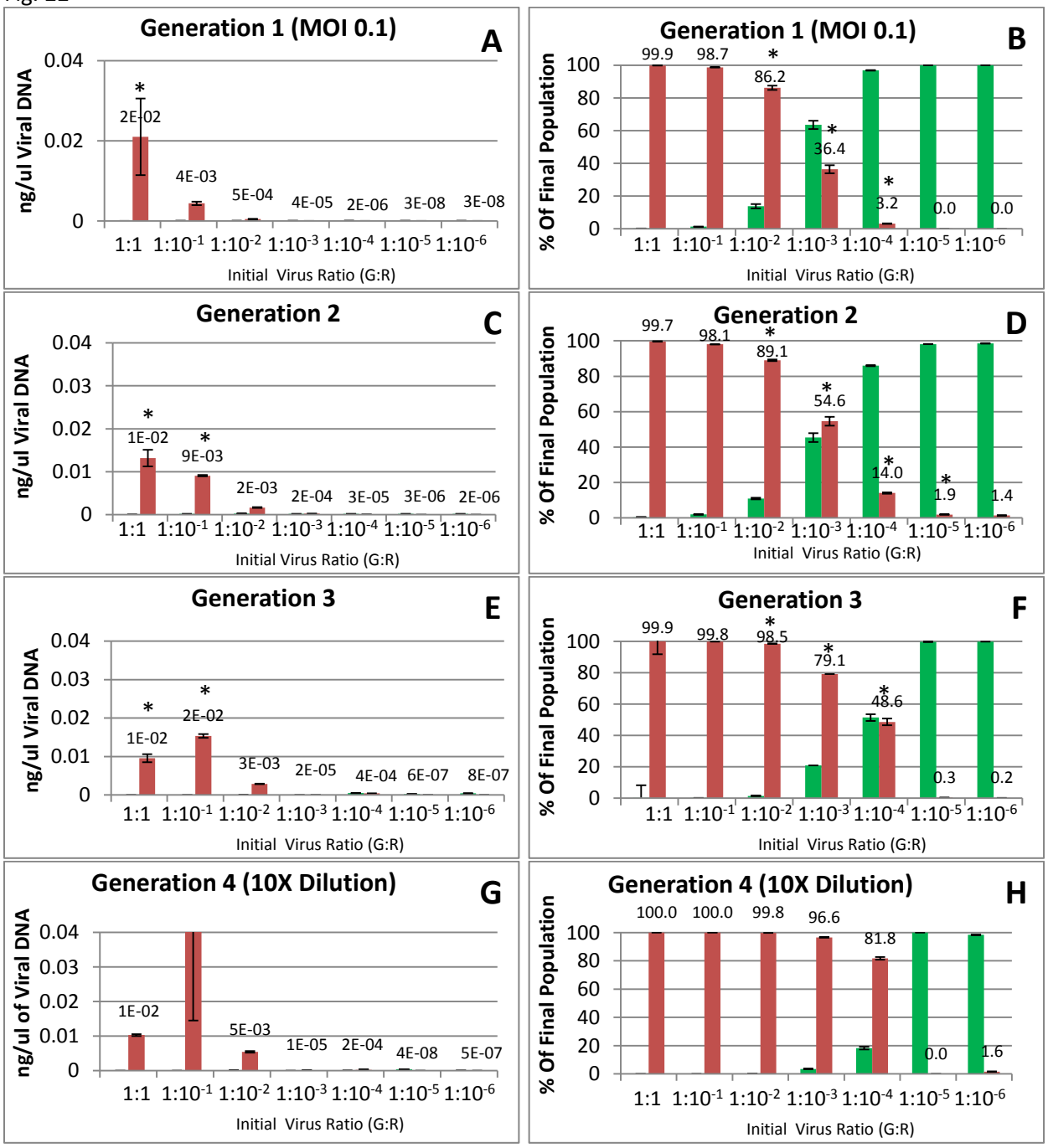


Fig 22. Experiment 3.8. Quantitative PCR analysis of viral DNA from HeLa-CX3CR1 cells infected with 7 different mixtures of HSV-GFP and HSV-CX3CL1 (G:R) at a MOI=0.1. All cells were treated with doxycycline to induce CX3CR1 expression. Cells were treated with 1ug/ml soluble heparin 2 hr prior to infection. Viral DNA was isolated from clarified lysates 6 days after infection. 1ml of clarified lysate was used to infect subsequent generations, except generation 4 where 100ul from generation 3 was used. Primers specific to HSV-CX3CL1 DNA are shown in red (values shown) and primers for HSV-GFP DNA in green. Quantitative PCR analysis was used to determine the concentration of viral DNA in each sample (A,C,E,G) from these percentages of each virus in the population were calculated (B,D,F,H). * indicates significantly higher than the same condition and generation in experiment 3.7. Bars represent SEM.

enrich for a single member displaying a protein with higher affinity to a cell surface target than other library members. Significantly higher percentages of HSV-CX3CL1 were also briefly seen in generation 2 cells from experiment 3.8 infected with the $1:10^{-5}$ initial virus mixture compared to generation 2 cells infected with the same initial mixture in experiment 3.7. However, this enrichment was not sustained and disappeared in generation 3 of experiment 3.8. This suggests that further modifications to the viral competition system could support enrichment of even smaller starting amounts of HSV-CX3CL1.

**Experiment 3.9. Rolling Dilutions Between Generations.**

In generation 2 of experiment 3.8, cells infected with lysates from generation 1 cells infected with a virus mixture initially containing 0.001% HSV-CX3CL1 produced a virus population that contained 1.9% HSV-CX3CL1. This apparent 1000-fold enrichment suggested that the virus competition system could reach even greater levels of final enrichment than observed generation 4 of experiment 3.8. It appears likely that viral pseudotyping was indeed a major factor that inhibited enrichment of HSV-CX3CL1 viruses as the 100-fold reduction in the total MOI (10 to 0.1) greatly enhanced enrichment. It was hypothesized that pseudotyping would have a greater effect of inhibiting HSV-CX3CL1 enrichment in virus populations that contained very small starting amounts of HSV-CX3CL1. As the total number of initial HSV-CX3CL1 virus decreases, and pseudotyping occurs, the likelihood that all of HSV-CX3CL1 viruses present in the population will be pseudotyped and effectively stripped of their selective advantage, is increased. Therefore, for populations containing very small starting amounts of a high-affinity virus, it is necessary to very carefully control the total concentration of the virus population. For this reason a new system of successive “cutbacks” between generations was developed.

**Experiment 3.9. Experimental Design. Rolling Dilutions Between Generations.**

Standardization of the HSV-GFP and HSV-CX3CL1 specific qPCR primers with plaque titered viral stocks revealed that a measurement of $1x10^{-5}$ ng/ul of viral DNA corresponded with a viral titer of

~$5x10^5$ pfu/ml. Therefore, for experiment 3.9, a system of virus "cutbacks" was established where any virus population at this concentration was diluted so that the MOI in the successive generation would not greatly exceed 0.1. As these virus populations are constantly dynamic and can apparently enter phases of dramatically accelerated virus growth, this represents somewhat of a moving target. For samples containing greater than 50% HSV-CX3CL1, even 100-fold dilutions did not often significantly reduce HSV-CX3CL1 growth in the following generation. However, as these samples had reached maximal required enrichment (>50%) this was inconsequential. Additionally, a parameter was established where, if a 10-fold cutback did not prevent an increase in HSV-CX3CL1 viral DNA concentration in a successive generation, it was interpreted to mean that a highly accelerated phase of HSV-CX3CL1 growth had been achieved and a 100-fold cutback was used to infect the subsequent generation. Following these parameters in experiment 3.9, new generation 2 cells were infected with 100ul of lysate from generation 1 cells (10X dilution from the standard 1ml passage volume). A 10-fold dilution was again used for all samples between generation 2 and 3, and finally 100-fold dilutions were made between generations 3-4 and 4-5. All other infection parameters used were identical to those in experiment 3.8.

Samples of clarified lysates from each generation infected with the $1:10^{-6}$ initial virus mixture were plaque purified in order to isolate individual virus clones using the Nobel-agar plaque purification protocol as described in chapter 2. Ten plaques from each generation were randomly picked and the resulting viruses were individually expanded on fresh cells. Virus-encoded fluorescence was analyzed using an inverted MM AF Epifluoresecent Light microscope (Leica). Cells were observed at 50X magnification for GFP fluorescence using a GFP 488nm excitation filter cube and for mCherry using a Texas-Red 580nm excitation filter cube. None of the viruses isolated expressed both fluorescent markers and all were found to contain high amounts of fluorescence. Viral DNA was isolated from four of the plaque isolates from generation 1 and four from generation 5. PCR amplification was performed

using primers specific to the RMCE cassette region of the viral chromosome as described in chapter 2. These PCR products were then sequenced in order to confirm the presence of the unique HSV-GFP or HSV-CX3CL1 RMCE cassette as described in chapter 2.

**Experiment 3.9. Results. Rolling Dilutions Between Generations.**

Significantly higher levels of HSV-CX3CL1 enrichment were observed in generation 2 cells in experiment 3.9 compared to experiment generation 2 cells in experiment 3.8 (Fig 23. B vs Fig. 22 D). Significantly higher levels of HSV-CX3CL1 enrichment were also seen in generations 3 and 4 of experiment 3.9 compared experiment 3.8 (Fig. 23 D and F). By the $5^{th}$ generation of viral competition, even the virus mixture containing the lowest percentage of HSV-CX3CL1 had produced a final virus population that was enriched to almost 100%. Examination of plaque isolates from each of the five generations infected with the initial virus mixture of $1{:}10^{-6}$, ten-per generation, show that the qPCR detection method closely parallels the apparent virus composition from each population (Fig 24). DNA sequencing analysis of four plaques from generations 1 and 5 show that all plaques contained viruses with the expected GFP or CX3CL1-gC/mCherry cassette.

**Experiment 3.9 Conclusions. Rolling Dilutions Between Generations.**

The results from experiment 3.9 showed that the implementation of the rolling cutback procedure to prevent super-infection and pseudotyping, allowed for the successful enrichment of the high-affinity HSV-CX3CL1 virus when diluted with the HSV-GFP virus as much as $1x10^{-6}$. Importantly it should be noted that two additional replicate dishes (total of 4) were infected with this mixture of virus because the initial MOI of 0.1 corresponded to a total of 500,000 viruses in the infection. This then correlated with 0.5 HSV-CX3CL1 viruses present in the initial $1x10^{-6}$ virus population. It was therefore expected that the presence of a single HSV-CX3CL1 PFU in the initial population would be stochastic. Accordingly, only three of the four replicate dishes contained any significant amount of HSV-CX3CL1 viral DNA. All three of these dishes reached generation 5 enrichment of ~100%. The fourth dish was omitted

Fig. 23

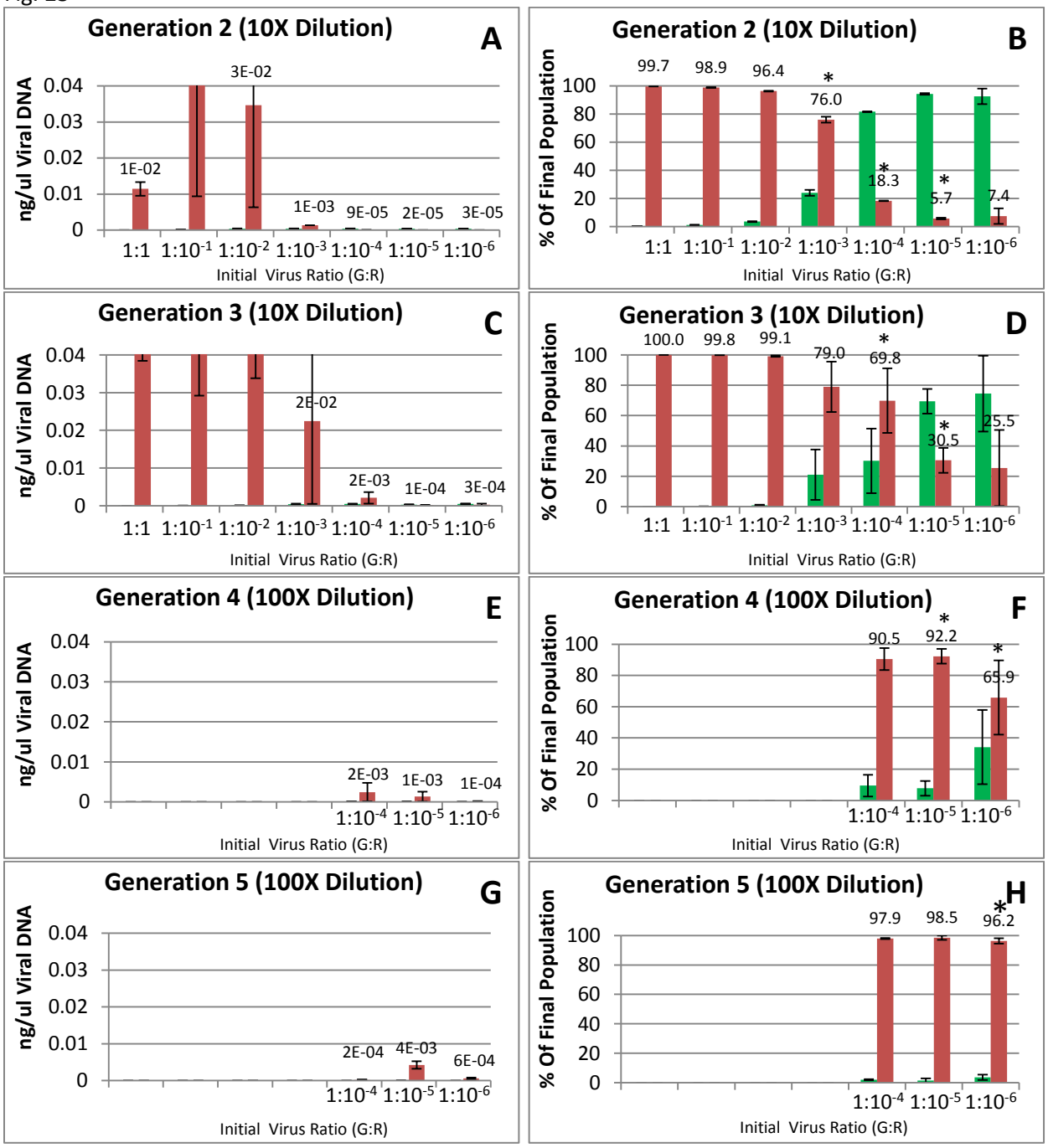


Fig. 23. Experiment 3.9. Quantitative PCR analysis of viral DNA from HeLa-CX3CR1 cells infected with 7 different mixtures of HSV-GFP and HSV-CX3CL1 (G:R) total MOI=0.1. Cells were treated with doxycycline to induce CX3CR1 expression 24 hrs prior and with 1ug/ml soluble heparin 2 hrs prior to infection. Cells were harvested 6 days after infection. The amount of clarified lysate from the previous generation used to infect a generation is indicated (1ml base unit). Primers specific to HSV-CX3CL1 DNA are shown in red (values shown) and primers for HSV-GFP DNA in green. qPCR analysis was used to determine the concentration of viral DNA in each sample (A,C,E,G) and from these percentages of each virus in the total population were calculated (B,D,F,H). * indicates significantly higher (P<.05) percentage of HSV-CX3CL1 compared to the same condition in the previous generation. Bars represent SEM.

Fig. 24

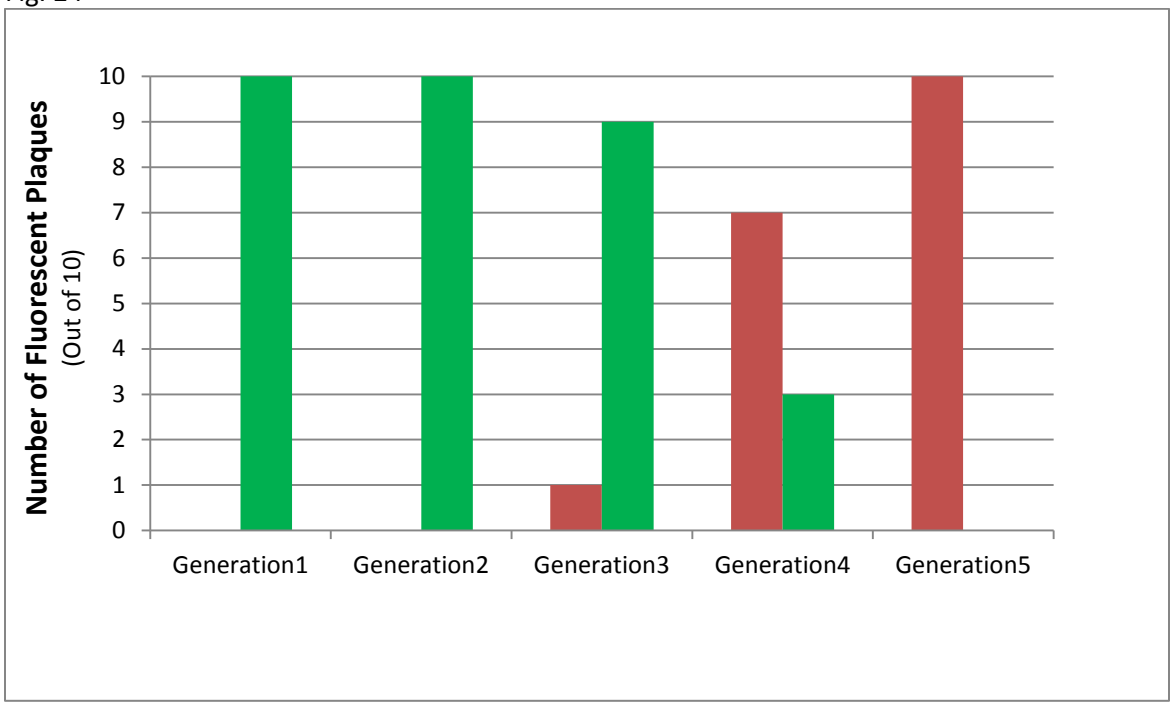


Fig. 24. Experiment 3.9. Fluorescence analysis of plaque purified viruses isolated from 5 successive rounds of selection. Limiting dilutions of clarified lysates were used to generate discrete virus plaques on cell monolayers overlaid with hardened-agar media. Ten plaques were picked from each of the five generations of HeLa-CX3CR1 cells infected with the virus mixture containing an initial ratio of $1:10^{-6}$ HSV-GFP:HSV-CX3CL1 in experiment 3.9. Plaques were individually expanded onto liquid-culture dishes and virus-encoded GFP (shown in green) or mCherry (shown in red) fluorescence was observed using an epifluorescent microscope. All plaques picked caused significant CPE and fluorescence when expanded onto cells. None of the plaque isolated samples contained both fluorescent proteins.

from statistical analysis as it was determined to not be reflective of the enrichment ability of this system since it was likely that not a single HSV-CX3CL1 PFU was ever present to be enriched. Lastly, fluorescence and DNA sequence analysis confirmed that the qPCR results are indeed reflective of the actual virus population and plaque purified red and green fluorescent viruses contained the HSV-CX3CL1 and HSV-GFP viral chromosomes respectively.

**Chapter 3. Overall Conclusions.**

The development of a novel system using viral competition for the affinity selection of proteins was described in chapter 3 of this thesis. This procedure appears capable of higher levels of enrichment for a virus displaying a high-affinity protein than ever before seen in any other known report of a mammalian-virus based protein selection system. Furthermore, this procedure appears to capable of levels of enrichment that are comparable to those seen in successful reports of the selection of novel high affinity proteins using currently established display techniques such as phage, yeast and bacculovirus display. To finally establish the functional utility of this system for a "real-world" protein affinity selection application, the procedure developed in chapter 2 was combined with the procedure developed in chapter 3. The use of this virus-display system to screen a large plasmid DNA-based protein library is described in chapter 4.

## Chapter 4. Functional Testing of the HSV-1 selection system.

**Experiment 4.1. Enrichment of Viruses with Genes from a Plasmid DNA Library.**

Chapter 3 of this thesis described the development of a virus competition system that successfully enriched for a single high affinity virus when outnumbered 1:1x$10^6$ by lower affinity viruses. These are the highest known levels of enrichment for any reported mammalian virus display protein

affinity selection system. However, while these results suggest this system can be used to screen large libraries of proteins, the ability of this system to screen a large DNA library has not yet been demonstrated. As reviewed in chapter 1, similar mammalian virus systems have been reported that to have the ability to enrich for viruses displaying high-affinity proteins. However, compared to these reported systems, this HSV-1 system is capable of greater levels of enrichment from a smaller starting amount of a high-affinity virus.

None of these reports have described the successful enrichment of viruses displaying proteins encoded by genes that were derived from a DNA-library. These reports, similar to chapter 3 of this thesis, only describe enrichment using mixtures of separately-prepared, purified virus clones. In order for any protein-display selection system to be useful, it must be able to utilize a DNA library as the initial source for protein-encoding genes. If a system is only capable of screening individually-prepared virus clones, then the potential library size that can be screened is quite small. Therefore, a practical protein-display system must possess the capability to efficiently insert genes from a DNA library into viruses, which subsequently display the protein products. Chapter 2 of this thesis describes the development of a system to allow a library of plasmid-based genes to be inserted into the genomes of actively replicating HSV-1 viruses. This system resulted in the creation of a virus library with an apparent diversity of $10^5 – 10^6$ unique viruses. In the experiment described below, this system was combined with the selection system described in chapter 3 to screen a plasmid DNA library containing genes encoding high and low affinity proteins.

**Experiment 4.1. Experimental Design. Enrichment of Viruses with Genes from a Plasmid DNA Library.**

The chemokine CX3CL1 binds to the receptor CX3CR1 with high binding-affinity, ~$1x10^{-10}$M Kd, as described above. Mutagenesis of CX3CL1 has revealed a stretch of amino acids contained within the chemokine domain in the N-terminus that is heavily involved in receptor binding. Several reports

describe alterations to the first N-terminal lysine residue which cause dramatic reductions in CX3CL1 binding affinity to CX3CR1 (Harrison et al., 2001; Mizoue et al., 2001). This lysine residue is the 7$^{th}$ residue found on the mature protein after the signal peptide has been removed and the 31$^{st}$ codon found within the CX3CL1 gene. This amino acid is commonly referred to as K7 in literature and will be referred to as such in this thesis. A point mutation where K7 was changed to glutamic acid (E), K7E, was reported to cause a 500-fold reduction in binding affinity, ~5x10$^{-7}$M Kd (Mizoue et al., 2001). This mutation did not cause a reduction in the expression of this protein in mammalian cells. In experiment 4.1, CX3CL1-K7E was used as a proof-of-principle lower-affinity gene. In this experiment, a plasmid "library" containing a mixture of CX3CL1 and CX3CL1-K7E shuttle plasmids was created. In this library, shuttle plasmids containing the CX3CL1 gene were diluted with shuttle plasmids containing the CX3CL1-K7E gene at a ratio of 1:10$^{-5}$(CX3CL1-K7E : CX3CL1). This plasmid library was then inserted into a library of viruses using the final RMCE procedure described in chapter 2. This library of viruses was then subjected to the final virus competition procedure described in chapter 3. At the end of selection, virus plaques were picked and sequenced in order to determine if viruses containing the CX3CL1 gene were enriched over viruses containing the CX3CL1-K7E gene.

*Construction of the K31E Point mutant*

The plasmid FKN-Shuttle contains the gene for the CX3CL1-gC fusion protein, as well as the CMV-mCherry fluorescent marker, all contained within two lox sites (as described in chapter 2, experiment 2.7 methods part 2). As described above, this shuttle plasmid supports the insertion of the entire lox cassette into the recombination locus contained within the HSV-GFP genome, which contains a pair of corresponding lox sites. Upon RMCE, a virus chromosome is created that encodes for a virus that displays the CX3CL1-gC fusion protein. In order to create the plasmid "K7E-Shuttle," the PCR primers CX3CL1-K7E-Inv-Sense 5'-TGCAACATCACGTGCCAC-3'and CX3CL1-K7E-Inv-Anti 5'-TTCCGTCATGCCGAGGTGC-3' were used in an inverse PCR reaction with the FKN-Shuttle plasmid as the

DNA template, using the iProof DNA polymerase kit (BioRad) following the manufacturer's protocol. The resulting PCR product was gel purified, phosphates were added and the ends were ligated together as described in chapter 2. The resulting plasmid was identical to the FKN-Shuttle plasmid with the exception that codon 7 within the CX3CL1 ORF was changed from AAA (encodes K) to GAA (encodes E). A bacterial DH5α clone was generated, screened, and plasmid DNA was prepared as described above.

It was determined that viruses containing the K31E-Shuttle and FKN-Shuttle cassettes were too similar to be distinguished by qPCR primers. Therefore, an additional modification to the plasmid FKN-Shuttle was performed to allow these two viruses to be easily distinguished from one another. A 591 b.p. region of the mCherry gene (bp 2804-3375) within the FKN-Shuttle was removed using an inverse-pcr reaction. Forward primer shut-mCher-KO-INV-sense1 5'-atgattaattaaATCGTGGAACAGTACGAACG-3' and reverse primer Shut-mCher-KO-INV-Anti1 5'-gtcattaattaaCTCCATGTGCACCTTGAAGC-3' were used in an inverse PCR reaction as above. The resulting plasmid was name FKN-Shuttle-MCKO. A bacterial DH5α clone was generated, screened, and plasmid DNA was prepared as described above. This deletion abolished mCherry fluorescence causing viruses containing the FKN-Shuttle cassette to be distinguishable from HSV-GFP and HSV-K7E viruses by expressing neither red, nor green fluorescence.

*Quantitative PCR*

All quantitative PCR was performed as described in chapter 2. For the detection of non-recombined, parental HSV-GFP virus, the forward primer GFP ORF1 Sense 5'-CTGGAGTACAACTACAACAGC-3' and the reverse primer GFP ORF1 Anti 5'-GCGAGCTGCACGCTGC-3' were used. For detection of all recombinant RMCE-produced viruses, the forward primer RT RMCE 5' Sense2 5'-GGGAACGCTAGCCGATCC-3' and the reverse primer RT RMCE 5' Anti2 5'-GCTGTGAGGGAGCCATGG-3' were used. These primers amplify a region of DNA that is present in all viruses containing a RMCE cassette. This region is unique from the HSV-GFP chromosome as well as the shuttle plasmids. These

primers do not distinguish between HSV-CX3CL1 and HSV-K7E. All primers were extensively screened for target specificity and efficiency.

Viral *DNA Extraction*

Viral DNA was extracted from 200ul of clarified lysates using the NucleoSpin Blood DNA extraction columns (Clontech) as described in chapter 3.

*Viral Plaque Isolation, Fluorescence Analysis and Viral DNA Sequencing*

Individual virus clones were isolated from plaques from the initial RMCE reaction as well as from generation 1 +Dox and generation 3 +Dox treated cells. The plaquing and picking procedure were performed as described in detail in chapter 2. Briefly, 4cm tissue culture plates containing confluent 293 cells were infected with 5 10-fold serial dilutions of clarified lysate (100ul per dish). Two hours after infection the media was aspirated and cells were overlaid with a mixture of molten Nobel agar and media. This solution was approximately 42$^{o}$C when applied to the cells and quickly hardens as it cools and remains solid at 37$^{o}$C. The hardened agar overlay prevents diffusion of virus particles and allows for individual clonal virus plaques to develop on cells infected with dilute amounts of virus (MOI greatly less than 1). Two days later, a second overlay containing 0.1% neutral red vital stain was applied. Visible, physically separate plaques, containing individual virus clones, were manually picked using sterile glass pipettes which were inserted through the agar to contact the virus-containing cell plaque below. The plug of agar and cells was placed into Eppendorf 1.5ml tubes containing 100ul of Tris-buffered media. Tubes were freeze-thawed three times in liquid nitrogen to lyse cells and release intracellular virus. The virus-containing media was then applied to 293T cells at 10% density in 4cm tissue culture dishes to allow growth of the virus clone contained within the plaque. Virus plaques were isolated from the RMCE reaction, generation 1 +Dox and generation 3 +Dox populations (12 each).

All of the 4cm dishes infected with virus clones isolated using the above procedure showed significant CPE 4 days after infection. The cells were monitored for fluorescence using an epifluorescent

microscope as described in chapter 3. All dishes showed either green, red, or non-fluorescent (clear) CPE. No dishes contained more than one type of fluorescence.

After fluorescence analysis, the 4cm dishes were harvested and a clarified lysate was prepared. Viral DNA was extracted for DNA sequencing as described in chapter 3. DNA from 4 clones that expressed red fluorescence and 4 that expressed non-fluorescence were sequenced. For sequencing, a region of the viral chromosome was amplified using 1ul of purified viral DNA as template and the PCR primers #2-PgC1-SeqSense 5'-TCACTACCGAGGGCGCTT-'3 and FKN-500-Anti 5'-CTGCTGGTGGCTCTTGG-3' using iProof DNA polymerase (BioRad) kit following the manufacturer's protocol. The PCR reaction was then cleaned using a Zyppy DNA Clean & Concentrator-5 Kit (Zymo Research) following the manufacturer's protocol. PCR products were sequenced using the sequencing primer CX3CL1-K7A-ORF1-Sense 5'-AGGCGGCCATGGCTCC-3' by ACGT DNA Sequencing Services.

*Data Analysis of qPCR*

The qPCR-based system for the quantification of viral titers was used as described in chapter 2. Briefly, viral DNA was extracted from serial dilutions of plaque tittered purified virus stocks. This DNA was then analyzed via qPCR using virus-specific primers. The CT value from each dilution was then plotted against the titer (pfu/ml) of the sample. From this, regression equations were generated that were used to make titer predictions from CT values obtained from samples. For statistical analysis, triplicate viral DNA measurements from each dish were compared between +Dox and -Dox treated cells collapsed across all generations using a one way ANOVA. If a main effect of means was observed between +Dox and -Dox samples, ($P<.05$), then individual comparisons were made between +Dox and -Dox treated cells within the same generation using Turkey's HSD post-hoc analysis and, where applicable, one way ANOVA excluding non-relevant comparisons.

*Creation of the Virus Library*

The optimized live-virus RMCE procedure, as described in chapter 2, was used to create a library of viruses displaying plasmid-derived gene products. Briefly, ~20ug of plasmid, consisting of 20ug of K7E-Shuttle and 0.2ng of CX3CL1-Shuttle, was used to transfect 293T cells via the BES transfection procedure as described in chapter 2. 24hrs prior to transfection, 293T cells were seeded onto a 10cm tissue culture plate at a density of 10% and placed into a 37$^{o}$C tissue culture incubator at 3% $CO_2$. At the time of transfection cells were at 40% density. 24hrs after transfection, media was aspirated, cells were washed once using 5ml of PBS/EDTA, once with 5ml PBS, and then 10ml of fresh media was added. 2hrs after washing, cells were infected (MOI=1) with a .22um filtered clarified-lysate containing HSV-GFP recipient virus. 6 days after infection, cells showed significant CPE where nearly all cells had detached. The cells and media were harvested and a clarified lysate was prepared as described above. A portion of this clarified lysate was used to infect HeLa-CX3CR1 cells for a first generation of competitive infection.

*Competitive Infections and Addressing the Concern for RMCE-Pseudotyping*

The competitive infection procedure to select for viruses displaying high affinity proteins was used as described in chapter 2. Cells were plated in 10cm tissue culture dishes at 20% density 24hrs prior to infection and were treated (+Dox) or not treated (-Dox) with Dox. 2hr prior to infection, cells were treated with 1ug/ml soluble heparin. Clarified lysate from the RMCE reaction was used to infect the cells (50% density at the time of infection) . Virus titer measurements were made using the qPCR method described above and were used to calculate the appropriate amount of clarified lysate to apply to cells for each generation of competition for a MOI of 0.1. This corresponded to dilution cutbacks of 0X,10X and 10X (1ml base unit) for generations 1, 2 and 3 respectively. It should be noted that generation 1 of competition was performed using HeLa-CX3CR1 cells plated in large T225 tissue culture flasks instead of the 10cm dishes which were used for all subsequent generations. At the time of infection the cells were 50% confluent inside the flasks and this corresponded to ~20x10$^{6}$ total cells in 30ml of media. Therefore, an infection using 1ml of clarified lysate from the RMCE reaction (~4x10$^{6}$

pfu/ml) corresponded to an MOI of ~0.2. One flask of +Dox and one of -Dox treated cells was infected for generation 1.

These larger flasks were used due to the concern of possible pseudotyping during the RMCE reaction. It was hypothesized that "RMCE-pseudotyping" could occur due to the nature of the RMCE reaction. It is likely that each cell could be transfected with multiple plasmids and therefore contain both the FKN-Shuttle and K7E-Shuttle (Fig. 25). If multiple recipient HSV-GFP chromosomes are present, either from super-infection or from viral replication, then multiple shuttle cassettes could be inserted and their gC-fusion proteins would be expressed. This would effectively produce the same result as a super-infection with two different viruses. As discussed in chapter 3, progeny virions could be produced that have viral envelopes containing glycoproteins which their genomes do not encode. If this process occurs, it is possible that the entire RMCE population is initially pseudotyped. Therefore, a low MOI infection immediately following the RMCE reaction is necessary to strip-away this pseudotyping. As stated above, at a low MOI the likelihood of super-infection is low and therefore progeny virions that only display glycoproteins encoded by the genome of their progenitor virus will be produced. However, it is possible that a virus containing a rare high-affinity gene, present in a small percentage of the RMCE population, could be lost due to the large dilutions required to achieve an MOI of 0.1. Chapter 3 showed that it was possible to enrich for a high-affinity virus even when only a single PFU was present. However, during these experiments, the initial virus populations were mixtures of individually plaque-purified virus clones that had no chance of chance of being pseudotyped going into the initial round of viral competition. Therefore, the rare high-affinity virus could immediately benefit from the displayed high-affinity protein and begin enrichment. If a high affinity virus is present in similar low amounts but is pseudotpyed and displays non-high affinity glycoproteins, then it would have to bind and infect a cell via the non-high affinity glycoproteins first before it can produce progeny that display the high-affinity glycoprotein encoded by its genome. Therefore, the use of the large T225 flasks

Fig. 25

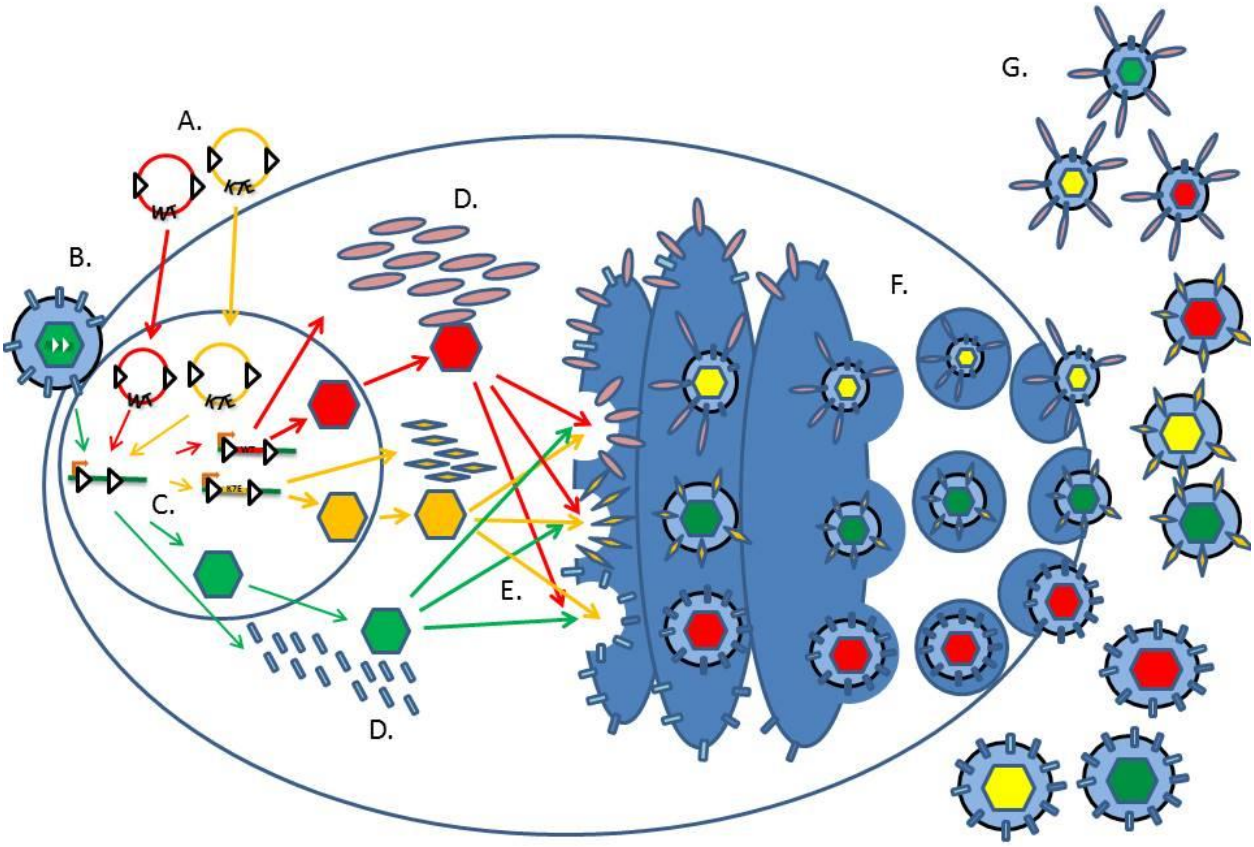


Fig. 25. A Diagram of RMCE-Pseudotyping. **A.** During the RMCE transfection, a cell can be transfected with both wt-CX3CL1 (red) and K7E-CX3CL1 (yellow) shuttle plasmids. **B.** This cell is then infected with one, or multiple, HSV-GFP recipient viruses. **C.** The viral chromosome and the shuttle plasmids are delivered to the nucleus, if multiple viral chromosomes are present then each plasmid can exchange with a chromosome and insert its library gene. **D.** Once inserted into a chromosome, these library genes are expressed and protein products produced. Progeny virus capsids are produced and can be packaged with, if present, the wt-CX3CL1 chromosome (red) the K7E-CX3CL1 chromosome (yellow) and the un-recombined parental HSV-GFP chromosome (green). **E.** These capsids can bud into an area of Golgi that contains glyocoproteins expressed by any of the three viral chromosomes. **F.** Enveloped viruses egress via secretory vesicles. **G.** Progeny virions emerge with a Golgi-derived envelope that contains any one of the three different types of viral glycoproteins. Envelopes containing multiple different types of glycoproteins are also possible.

allowed for a low MOI (0.2) to be obtained while still passaging a large amount, ~$4x10^6$ PFUs, of virus. To achieve the same MOI on smaller 10cm dishes 5-10-fold less virus would need to be used which would decrease the chance of passaging a rare high-affinity library member that successfully becomes un-pseudotyped and then becomes enriched. Pilot testing using other parameters involving 10cm and T225 generation 1 dishes at various MOIs, +/-Dox and +/- heparin treatments were not successful (data not shown).

**Experiment 4.1. Results. Enrichment of Viruses with Genes from a Plasmid DNA Library.**

The RMCE reaction produced a virus population that contained 27% recombinant viruses at a concentration of $1.2X10^6$ PFU/ml (Fig. 26 A & B). The percentages of recombinant virus in the total virus population from +Dox treated cells were 75%, 87% and 98% in generations 1,2 and 3 respectively (Fig.26 B). No significant increase in this percentage was observed on -Dox treated cells. The concentration of recombinant viruses in +Dox treated cells was significantly higher than in -Dox treated cells across all three generations (Fig. 26 A)($P<.05$). After 3 generations of selection, the virus population from +Dox treated cells had reached nearly 100% enrichment (Fig. 26 B). This corresponded to a total concentration of $5.7x10^5$ PFU/ml of recombinant virus (Fig. 26 A).

As the qPCR primers used to detect recombinant viruses in the population could not distinguish between HSV-CX3CL1 and HSV-K7E viral DNA, fluorescent analysis of plaque-purified virus clones was performed. 12 plaques containing individual virus clones were randomly picked from each sample. Virus plaques from the RMCE reaction, generation 1 +Dox and generation 3 +Dox treated cells all produced significant CPE when passaged onto 293 cells (Fig. 27). Fluorescence microscopy analysis showed that 11 and 1 plaques from the RMCE lysate contained green and red fluorescent virus respectively (Fig. 27 B). Plaques from the generation 1 +Dox population showed that 10 and 2 plaques contained red and green fluorescent virus respectively (Fig. 27 B). Plaques from the generation 3 +Dox

Fig. 26

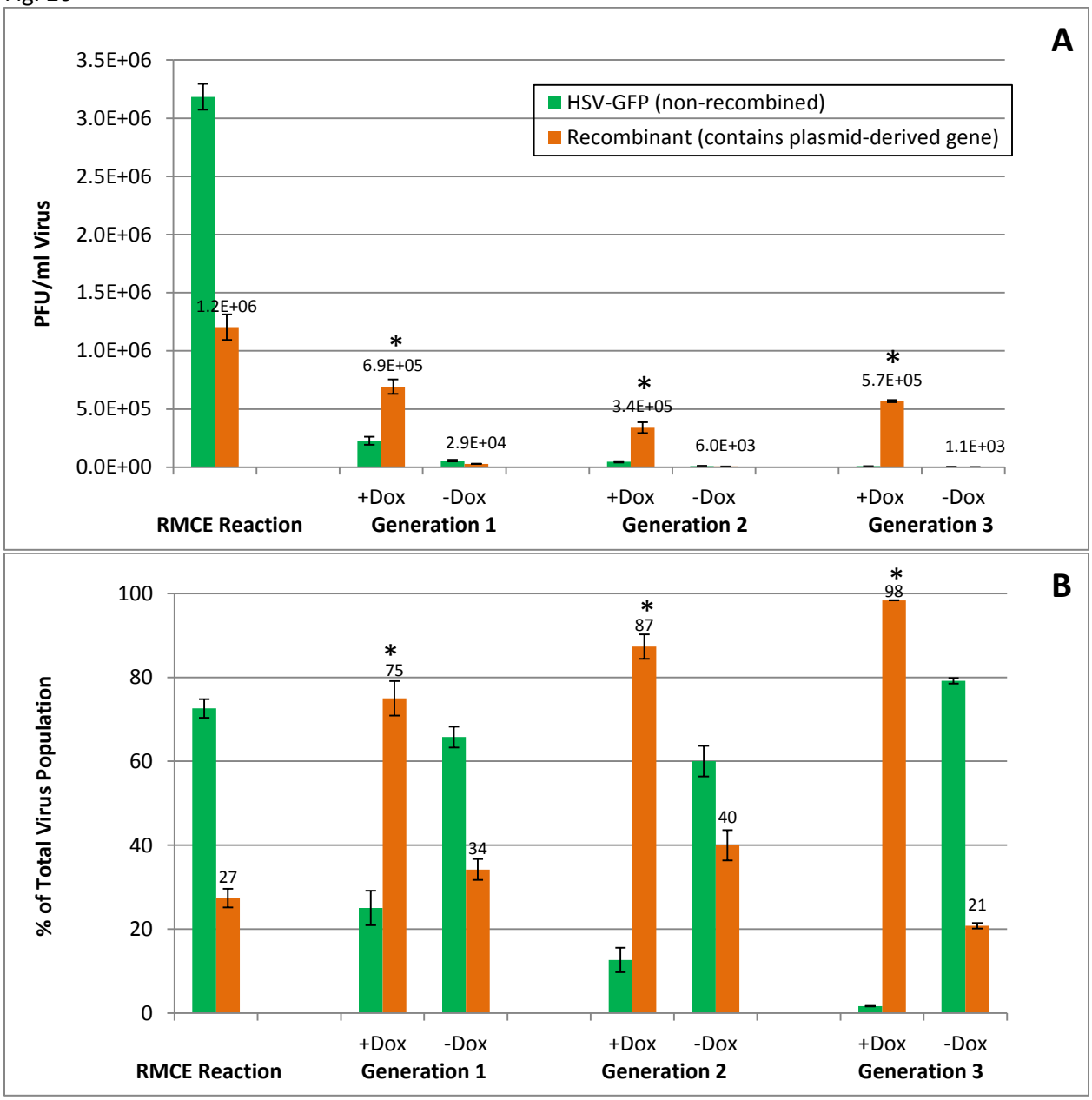


Fig. 26. Experiment 4.1. qPCR analysis of viral DNA in clarified lysates from 293T cells and HeLa-CX3CR1 cells. For the RMCE reaction, 293T cells were transfected with a mixture containing a 1:$10^{-5}$ ratio of CX3CL1-K7E : CX3CL1 shuttle plasmids and then infected with the recipient HSV-GFP virus. 5 days later the resulting virus population was passaged onto HeLa-CX3CR1 cells that were treated +/-Dox 24hrs prior to infection. Cells and media were harvested 6 days after infection and a clarified lysate was passaged onto fresh cells with the same Dox treatment. The initial MOI for each generation was kept at <0.1. Primers specific to the HSV-GFP viral chromosome (green) and recombinant viruses that contained a plasmid-derived RMCE cassette (orange, values shown) were used. **A.** Total concentration of viral DNA, * indicates significantly more (P<.05) recombinant virus than –Dox. **B.** Percentages of each type of virus in the total population derived from the total concentrations in A. * indicates significantly higher (P<.05) percentage of recombinant virus than the RMCE reaction and –Dox. Bars indicate SEM.

Fig. 27

A

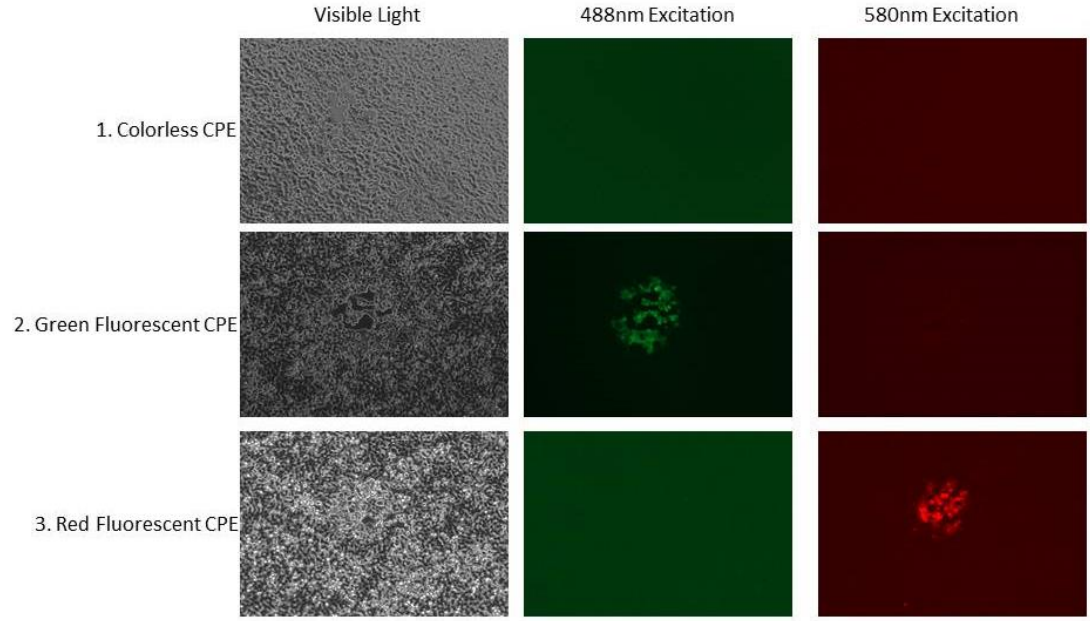


B

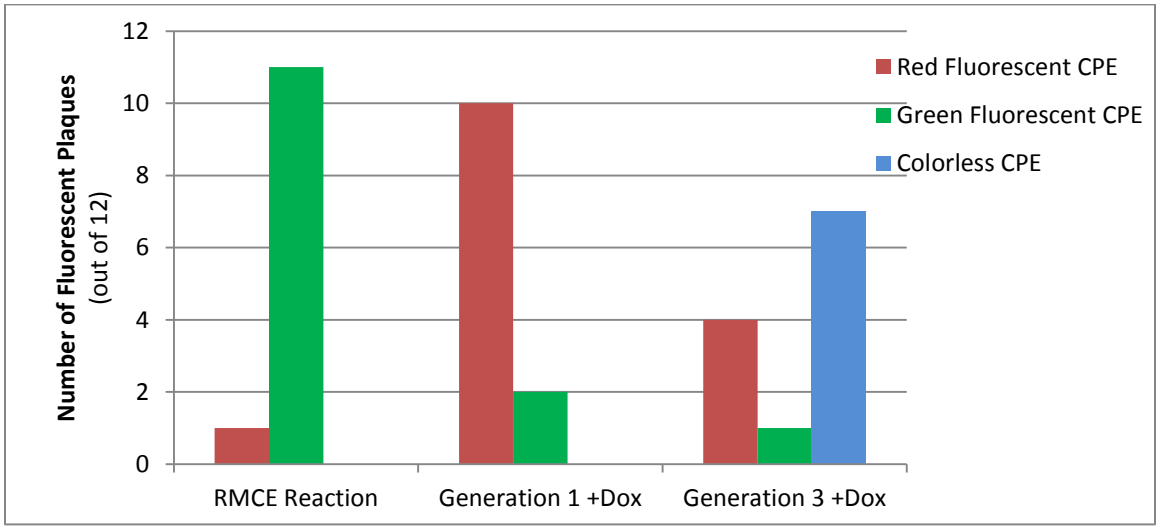


Fig. 27. Experiment 4.1. Fluorescence microscopy analysis of plaque purified virus clones. **A.** Examples of green (1), red (2) and colorless (3) CPE on HEK293 cells infected with plaque purified virus clones isolated from generation 1 and 3 of selection in experiment 4.1. For 1-3 the same field is shown with visible light, and using epifluorescent 488nm and 580nm excitation filters. **B.** Quantification of the observed fluorescence of 293 cells infected with plaque purified virus clones from the RMCE reaction and generation 3 +/- Dox treated cells. 12 plaques from each were picked and individually expanded on separate 4cm dishes. All 36 dishes showed significant CPE 5 days after infection with plaque clones. No dishes contained more than one type of CPE.

population showed that 7, 4 and 1 plaques contained colorless (non-fluorescent), red and green fluorescent viruses respectively (Fig. 27 B).

DNA sequence analysis of plaque-purified virus clones from generation 3 showed that all viruses which produced colorless (non-fluorescent CPE) contained the wt CX3CL1 codon (Fig. 28 A & B). Furthermore, DNA sequence analysis showed that all viruses that produced red fluorescent CPE contained the K7E point mutation (Fig. 28 C).

**Experiment 4.1. Conclusions. Enrichment of Viruses with Genes from a Plasmid DNA Library.**

The results from experiment 4.1 show that the viral competition system was successful in selecting for a gene encoding for a high-affinity protein derived from a plasmid DNA library. These results show that the system, in its current form, can successfully screen a DNA library containing at least $10^5$ unique genes and enrich for a virus containing the high-affinity gene in three rounds of selection. While qPCR analysis showed the percentage of recombinant viruses in the population nearly doubled in generation 1, compared to the RMCE reaction (Fig. 26 B), fluorescent analysis of individual plaque purified virus clones suggest that the majority of this population was likely the HSV-K7E virus (Fig. 27 B). Since none of the 12 randomly chosen generation 1 plaques contained a colorless virus (HSV-CX3CL1), it is likely that less than 10% of this population contained the high-affinity HSV-C3CL1 virus. This is consistent with the rate of enrichment seen when the high affinity HSV-CX3CL1 virus was present at a similar starting percentage in experiment 3.9. Furthermore, this enrichment for HSV-K7E over HSV-GFP is not unexpected as the binding affinity of HSV-K7E for CX3CR1 ($5x10^{-7}$M Kd) is higher than the binding affinity of gD, used by HSV-GFP for cell-binding, for Nectin 1 ($1x10^{-6}$M Kd). After a third generation of selection, HSV-CX3CL1 had become the majority of the recombinant virus population. Lastly this enrichment appears specific to CX3CR1 binding as no significant enrichment was seen on -Dox treated cells in any of the three generations.

Fig. 28

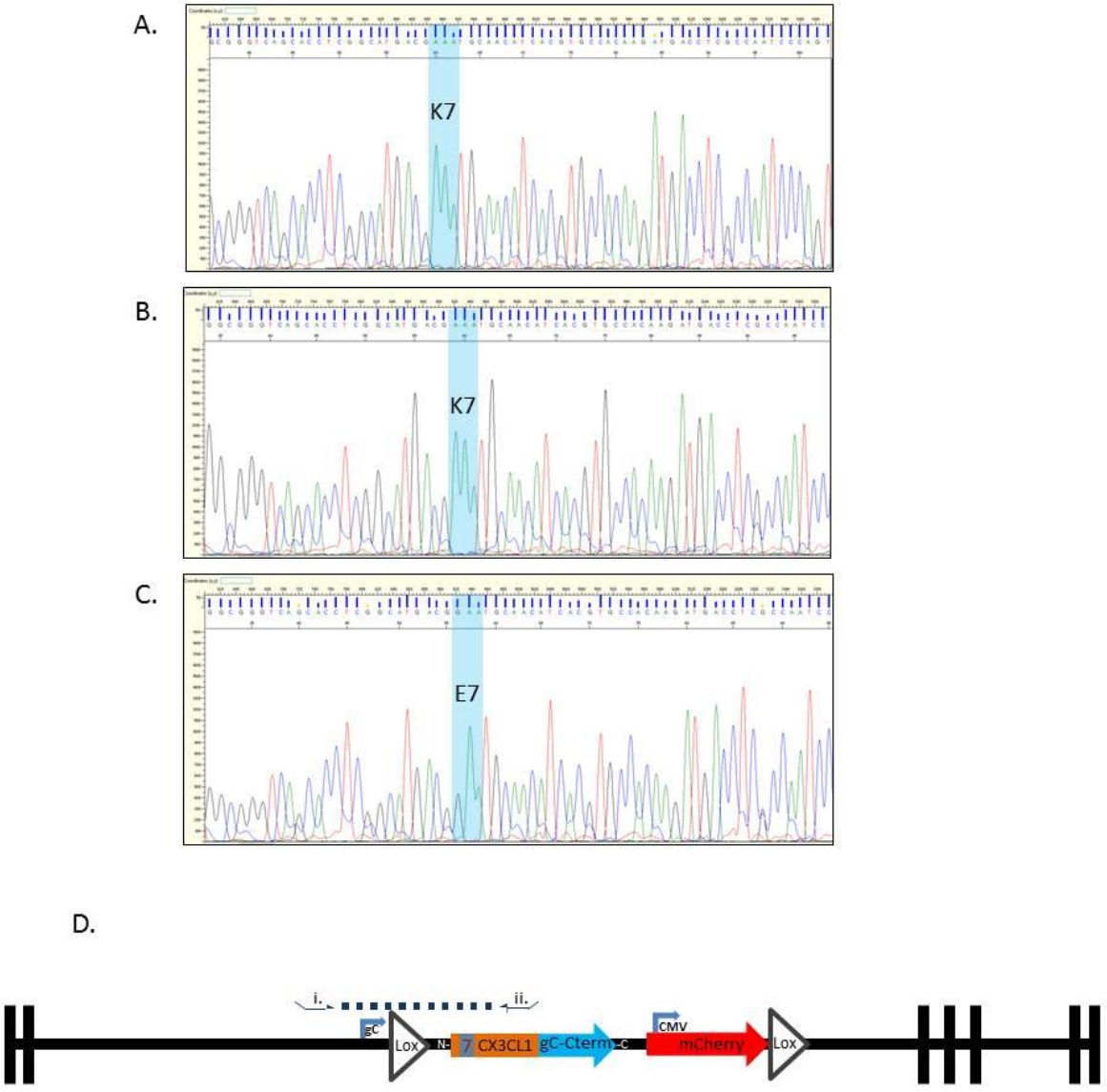


Fig. 28. Experiment 4.1 DNA sequencing analysis of a region of the CX3CL1 gene within plaque purified virus clones from generation 3 of selection. **A,B.** Examples of DNA sequence chromatogram from viral DNA isolated from plaque purified viruses that produced clear (non-fluorescent) CPE. The codon for the amino acid at position 7 within the CX3CL1 gene is highlighted and shows the sequence for the wt K7 codon. **C.** An example DNA sequence chromatogram from viral DNA isolated from plaque purified viruses that produced red fluorescent CPE. The codon for the amino acid at position 7 within the CX3CL1 gene is highlighted and shows the sequence for the mutant low-affinity E7 codon. **D.** A diagram of the PCR product that was produced from each plaque purified virus and sequenced. For this, a primer that anneals to a portion of the HSV viral chromosome (i) and a primer that anneals to a site within the CX3CL1 ORF (ii) were used.

Several conclusions can be made from the results obtained from experiment 4.1. The first of which is that the wt-CX3CL1 gene was successfully inserted into a virus during the live-virus RMCE reaction despite being only 0.001% of all shuttle plasmids in the transfection. The second is that the virus competition procedure successfully enriched for the HSV-CX3CL1 virus from the RMCE-produced virus library. The third conclusion is that the system has the ability to distinguish between low, medium and high affinity proteins. This is seen in the enrichment of HSV-K7E over HSV-GFP between the RMCE population and generation 1 and in the enrichment for HSV-CX3CL1 over HSV-K7E after generation 3. In this comparison, HSV-GFP, HSV-K7E and HSV-CX3C1 represent low, medium and high affinity viruses respectively. The fourth conclusion is that this selection system could be successfully used to identify novel, or otherwise unknown, high-affinity proteins from a DNA library. This conclusion is based on the observation that the high-affinity HSV-CX3CL1 virus was present in more than 50% of the randomly selected virus plaques from the generation 3 virus population. If this would have been a library containing unknown members, this over-representation would indicate that this library member had significantly higher binding affinity than others. The final conclusion that can be made is that the presence of some non-recombined HSV-GFP is actually a benefit to the system. This virus serves as an indicator of enrichment and effectively sets the bar for binding affinity. If the recombinant population did not contain a virus with higher binding affinity than HSV-GFP, then no enrichment for the recombinant population would be seen with qPCR analysis using the HSV-GFP and HSV-Recombinant primers. The percentage of HSV-GFP in the population after each generation was in fact what guided the number of generations used in experiment 4.1. After generation 3, 98% of the virus population contained a plasmid-derived RMCE cassette. It was for this reason that it was decided to plaque isolate virus clones at that point. This alleviates the necessity to create new qPCR primers for every different library that is screened and allows for monitoring of enrichment when the DNA sequence of library members is unknown.

This is the only known report of a mammalian virus display system successfully selecting for high affinity proteins from a DNA library and not mixtures of virus clones.

**Experiment 4.2. Selection of Novel CX3CL1 Mutants from a Degenerate Library.**

The results from experiment 4.1 showed that the HSV-1 viral display system can successfully enrich for a virus containing a gene encoding the high-affinity CX3CL1 protein derived from a plasmid library. These results demonstrate that this system is capable of inserting genes from a DNA library into a library of at least $1x10^5$ unique viruses. To further test the capabilities of this selection system, a more diverse library of CX3CL1 mutants were created and screened.

As previously stated, the N-terminus of CX3CL1 has been shown to be critical for binding to the CX3CR1 receptor. The point mutation, K7E, reportedly reduces CX3CL1 receptor binding affinity 500-fold. The less dramatic alteration of K7 to A reportedly resulted in 100-fold reduction in receptor binding affinity (Mizoue et al., 2001). Additionally, residues C8 and C11 have been shown to form disulfide bonds that are responsible for producing a distinct secondary structure that makes CX3CL1 unique among the other chemokine subfamilies (Davis et al., 2004). Each chemokine subfamily has a highly conserved and structurally distinct pattern of N-terminal cysteine residues. The spacing and number of intervening amino acids between these cysteine residues is indicated in the name given to each chemokine subfamily: CC, CXC, CX3C and XC. Residues C8 and C11 are highly conserved in CX3CL1 proteins across species. These cysteines form disulfide bonds with additional cysteine residues located near the core of the protein which anchor the N-terminus and creates the unique CX3CL1 “X3 bulge” (Fig. 29 A)(Davis et al., 2004). This structural motif is unique to CX3CL1 and is believed to be important for CX3CR1 binding. An N-inked glycosylation site (N X T) is found to naturally occur in the X3 bulge of human and rat CX3CL1, which contain the amino acids N, I and T. Conflicting report have shown this glycosylation site to be both filled (Harrison et al., 2001)and not filled (Streit et al., 2005). This

Fig. 29

A

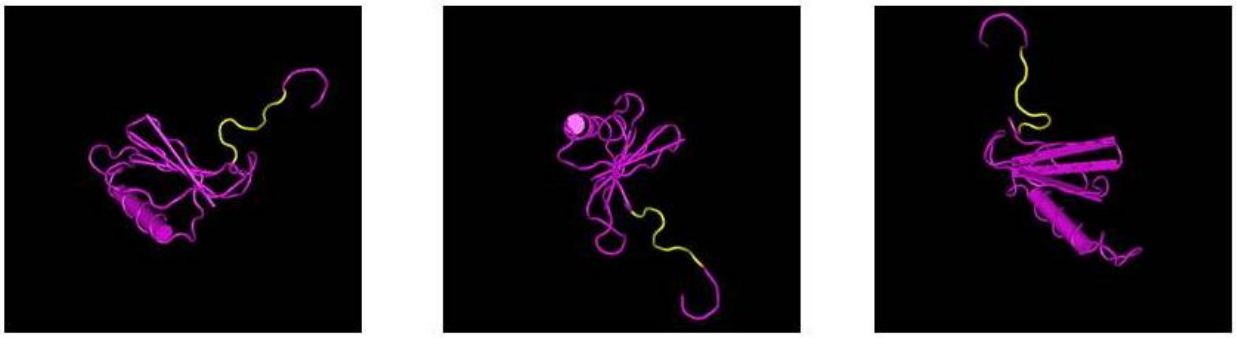

B

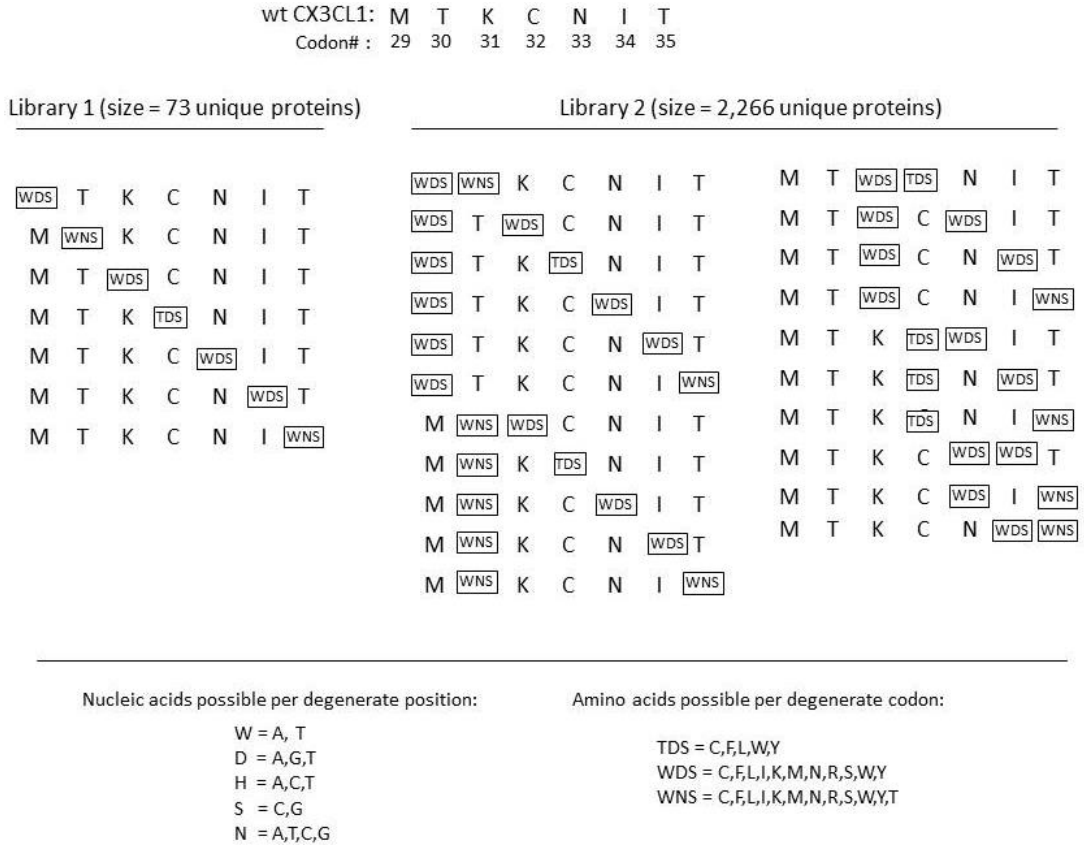


Fig. 29. Experiment 4.2. **A.** Three different views of the ribbon structure of CX3CL1 with amino acids 29-35 highlighted in yellow. The distinct X3 bulge can be clearly seen in this region. **B.** An illustration of the level of degeneracy used in experiment 4.2 to create a mutant library of site-saturated CX3CL1 mutants with a bias towards large aromatic amino acids. The codons have been numbered counting from the first codon in the CX3CL1 gene, therefore codon 31 encodes for amino acid K7 in the mature protein. The codons encoding the seven amino acids from 29-35 in the CX3CL1 N-terminus were mutated with the minimal amount of degeneracy that allowed for the occurrence of the wt amino acid as well as amino acids F, W and Y. Using this mutagenesis scheme, for library 1, each codon within the seven amino acid stretch was individually mutated. For library 2, every possible pair of two codons was mutated.

glycosylation site does not occur in murine CX3CL1 which contains the X3 residues E, I and M (Harrison et al., 2001). Replacement of the X3 bulge with the amino acids AAA was reported to cause a modest decrease in CX3CL1 binding to transfected cells and microglia (Davis et al., 2004; Harrison et al., 2001). These results suggest the involvement of N-linked glycosylation in CX3CL1 binding is unclear. Complete removal of the X3 bulge by the deletion of the intervening amino acids was reported to create a protein with no detectible affinity for CX3CR1 suggesting that the X3 bulge, regardless of glycosylation, is important for CX3CR1 binding (Davis et al., 2004). Lastly, the insertion of the residues N, I and T within the CC motif found in the N-terminus of the viral chemokine mimic vMIP-II was shown to increase the apparent binding affinity of vMIP-II for CX3CR1 6-fold and created a chimeric protein that had only 4-fold lower CX3CR1 binding affinity than wt CX3CL1 (Davis et al., 2004). Due to the apparently profound importance of this small stretch of N-terminal amino acids for CX3CR1 binding, it was targeted for site-saturation mutagenesis to generate a library of CX3CL1 mutants. This library was then screened in order to test the ability of this viral display system to screen a diverse library of mutant proteins and potentially identify novel, high-affinity proteins.

**Experiment 4.2. Experimental Design. Selection of Novel CX3CL1 Mutants from a Degenerate Library.**

In a collaboration with SomaLogic Inc (Boulder, CO), a library of mutant CX3CL1 genes was designed and synthesized. In order to increase the possibility of isolating novel high affinity CX3CL1 mutants, a strategy involving mutagenesis with restricted nucleic acid degeneracy was employed. The large aromatic amino acids F, W, and Y have been found to occur at a disproportionately high rate within the antigen binding regions of many different antibodies (Ramaraj et al., 2012). It is believed that the large aromatic side chains of these amino acids have a higher frequency of interactions with binding targets than those of other amino acids. Tyrosine amino acids have been reported to have a particularly

high incidence of molecular interactions with binding targets (Fellouse et al., 2005). There have been reports of “tyrosine saturation mutagensis” within antibody paratopes which successfully produced novel high-affinity antibodies (Fellouse et al., 2005). These reports suggest that binding interactions could potentially be increased within protein-binding domains utilizing a limited amino acid repertoire. Therefore, in order to skew mutagenesis in favor of production of mutants with the amino acids F, W and Y in the CX3CL1 receptor-binding domain, a library of partially-degenerate CX3CL1 genes was created. It was hypothesized that this strategy could increase the likelihood of creating mutants with increased binding affinity by promoting the occurrence of molecular interactions between residues in the CX3CL1 binding domain and the CX3CR1 receptor.

*Construction of the CX3CL1 Mutant Library*

DNA fragments were synthesized which corresponded with codons 29-35 (amino acids 5-11 of the mature protein) of the CX3CL1 gene. In separate synthesis reactions, performed by SomaLogic Inc, a library of DNA oligonucleotides were produced where the DNA sequence within a single or a pair of codons was made degenerate while all other codons contained the wt CX3CL1 sequence (Fig. 29 B). The level of nucleic acid degeneracy allowed at these codons during synthesis was designed to produce the least possible number of different amino acids that still included the wt amino acid as well as the amino acids F, W and Y. Two separate libraries were made (Fig 29 B). For library 1, DNA oligonucleotides were synthesized that contained a single degenerate codon at every position within the 7 codon stretch (Fig. 29B) . For library 2, every possible combination of two codons was made degenerate. The resulting libraries were predicted to contain 73 and 2,266 possible unique protein sequences respectively. This rather reserved mutagenesis strategy was used as it was hypothesized that complete random mutagenesis of this heavily conserved region would result in the production of a large number of mutants that were devoid of any CX3CR1 binding ability and occupy library space.

For each library, sense and antisense oligonucleotides were separately synthesized for each mutant codon position, this corresponded with 7 sense and 7 antisense oligonucleotides for library 1 and 21 sense and 21 antisense oligonucleotides for library 2 (Fig. 29 B). To create dsDNA fragments that could be inserted into the CX3CL1 ORF, each pair of sense and antisense fragments (with the same mutant codon position) were annealed together in separate annealing reactions. For this, 20ul of the sense and antisense oligonucleotides were mixed together in an Eppendorf tube at a final DNA concentration of 100uM. This mixture was then heated to $75^{o}$ for 15 minutes in order to remove any self-dimers or secondary structures within the oligonucleotides and increase the annealing efficiency of the sense and antisense strands. The tubes were then allowed to slowly cool to room temperature over the span of ~15 minute to allow annealing. The newly produced dsDNA fragments for each library (7 for library 1 and 21 for library 2) were then pooled together.

The ssDNA oligonucleotides were all designed to contain a small stretch of DNA sequence that is complementary to the ssDNA overhangs produced by the restriction endonuclease Bae1 (Fig. 30 3 & 4). Once annealed together, the dsDNA oligonucleotides would contain ssDNA overhangs complementary to these (Fig. 30 4). The recognition sequence for the Bae1 restriction endonuclease was inserted into the CX3CL1 ORF within the plasmid FKN-Shuttle via an inverse PCR reaction using the primers FKN-Bae1-Sense 5'-GCGTACCCTTGTTGTGCCACAAGATGACCTCG-3' and FKN-Bae1-Anti 5'-AAGTAGTTCGACATGCCGAGGTGCTGACC-3' using the iProof DNA Polymerase Kit (BioRad) following the manufacturer's instructions. The PCR product was gel purified, phosphates were added to the ends, ligated together, transformed into DH5α *E. coli*, and plasmid DNA was prepared as previously described. The resulting plasmid containing the CX3CL1-Bae1 gene was named "Shuttle-Bae1." The Bae1 restriction endonuclease system was used because it cuts DNA, regardless of sequence, at a specific distance upstream and downstream of a conserved recognition sequence (Fig.30 2). This allowed the Bae1 site to be easily inserted at the desired location within the CX3CL1 ORF at codons 29-35. This

Fig. 30

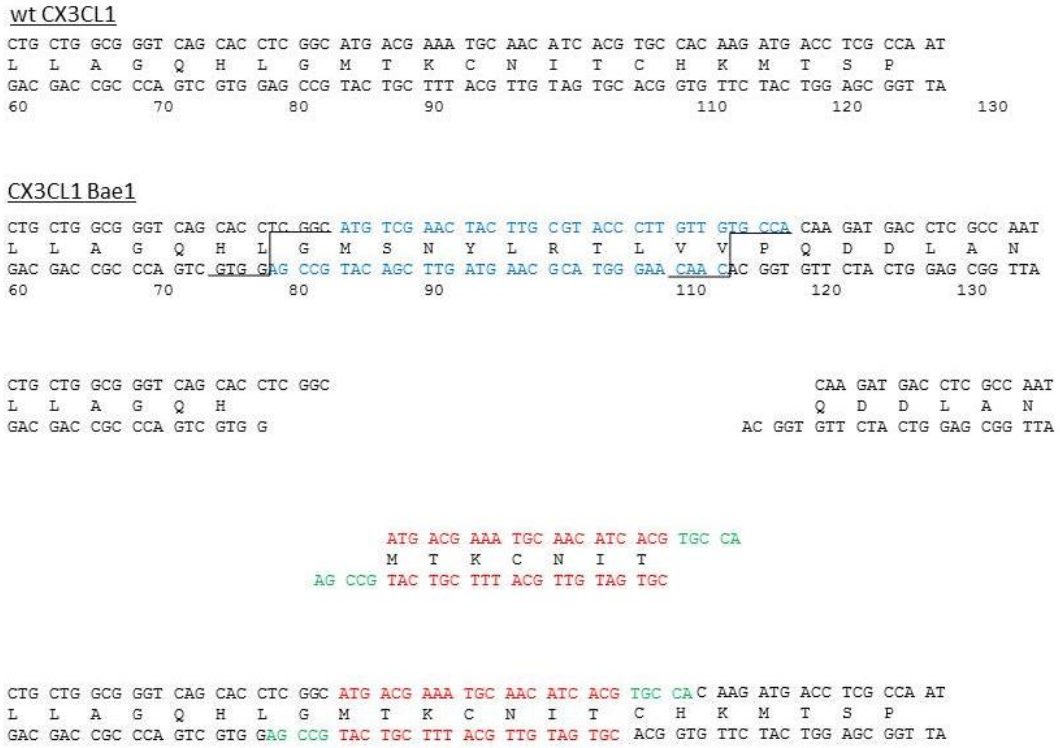


Fig. 30. Experiment 4.2. A diagram of the process used to insert dsDNA oligonucleotides containing degenerate codon sequences into the open reading frame of the CX3CL1. **1.** The sense and antisense sequence and the translated amino acids found in a portion of the N-terminus of the CX3CL1 gene. Nucleotide numbering begins at nucleotide 1 in the start codon of the CX3CL1 gene (not shown). The 7 codons that were targeted during mutagenesis encode for M T K C N I T in the wt CX3CL1 gene. **2.** The sense and antisense sequence and the translated amino acids found in the same N-terminal region of the CX3CL1-Bae1 gene inside Shuttle-Bae1. DNA sequence including the Bae1 recognition sequence $AC(N_4)GTAYC$ was inserted as described in experiment 4.2. This insertion results in a frame-shift that causes a premature stop codon at nucleotide position 231 (not shown). The region of DNA that is excised by the Bae1 endonuclease is shown in blue. **3.** The ssDNA overhangs that result after Bae1 digestion of the Shuttle-Bae1 plasmid. **4.** An example of two single-stranded synthetic sense and antisense oligonucleotides that were annealed together to form a dsDNA fragment. The 7 codons that were included in the degenerate mutagenesis scheme are shown in red. For simplicity the wt CX3CL1 sequence is shown in this example. During annealing it is possible that two oligonucleotides with different degenerate codon sequences could come together at some frequency. Pilot testing showed that such a mis-match did not affect annealing or ligation efficiency and was resolved during DNA replication. The nucleotides that were engineered into the synthetic oligonucleotides to create 3' ssDNA overhangs are shown in green. These overhanging nucleotide sequences were kept constant and not subjected to degeneracy during synthesis. **5.** The resulting product from a ligation between the synthetic dsDNA fragment and the ssDNA overhangs in Bae1 digested Shuttle-Bae1 plasmid. Note the original CX3CL1 reading frame is restored.

strategy was used because this insertion causes a nonsense frame-shift mutation within the CX3CL1 ORF so, during viral-library construction, any uncut Shuttle-Bae1 plasmids would not encode the CX3CL1 fusion protein and therefore would be removed quickly during the selection process (Fig 30 2). Furthermore, Bae1 digested Shuttle-Bae1 plasmids do not have compatible overhangs and therefore cannot self-ligate (Fig. 30 3). This is important because a successful RMCE reaction requires a circular plasmid, therefore any linear cut Shuttle-Bae1 plasmids would not be a viable substrate and would not be inserted into a viral chromosome. Lastly, upon the successful ligation of a dsDNA oligonucleotide library fragment, the Shuttle-Bae1 plasmids both re-circularized and the original CX3CL1 reading frame is restored (Fig. 30 5).

*Transformation-Free Ligation Reactions*

The dsDNA oligonucelotides were ligated into Bae1 digested Shuttle-Bae1. For each library, 30ug of Shuttle-Bae1 was digested with the Bae1 endonuclease (NEB) in separate 50ul digestion reactions each containing 2ug of plasmid DNA following the manufacturer's instructions. The digested plasmids were then individually gel-purified in separate lanes of a 1% TAE-Agarose gel. DNA was extracted from the gel using the Zyppy Gel-DNA Extraction Kit (Zymo Research) following the manufacturer's instructions. The purified plasmid backbone was then used in a 25ul ligation reaction (2ug per reaction) with 1ul of 100uM pooled dsDNA oligonucleotide library fragments using T4 DNA Ligase (NEB) following the manufacturer's instructions. In total, 30 ligation reactions were performed, 15 using library 1 oligonucleotides and 15 using library 2 oligonucleotides. After over-night ligation at 16$^{o}$C, the ligation reactions for each library were pooled together and DNA was extracted and sterilized via ethanol precipitation as previously described. Plasmid DNA was pelleted by centrifugation at 15,000xg for 10mins, ethanol was removed and the DNA was resuspended in 50ul of sterile water.

These transformation-free ligation reactions were used because it was not necessary to make bacterial clones. Rather, the ligated plasmids could be directly transfected into mammalian cells which

could then repair any mis-matched degenerate codons or nicked DNA during plasmid replication utilizing the sv40 replication origin. Furthermore, it was hypothesized that this could circumvent the potential problem of reduced library diversity due to low bacterial transformation efficiency and avoid the need for ultra-competent bacterial cells.

*Production and Screening of the HSV CX3CL1 Mutant Libraries*

For the creation of a library of viruses displaying the HSV-CX3CL1 mutant proteins, the Live-Virus RMCE protocol was used as described in experiment 4.1. This virus library was then screened using the competitive infection selection procedure in HeLa-CX3CR1 cells (+/-Dox) as described in experiment 4.1. Viral titers were measured using qPCR primers specific to the non-recombined HSV-GFP parent virus and the RMCE cassette-containing recombinant population. The same MOI cutback procedure as well as the use of large T255 flasks for generation 1 were used as described in experiment 4.1. 5 generations of selection were used at which point the recombinant populations had reached ~90% for both libraries

*Sequence Analysis of Plaque Purified Virus Clones*

Virus clones were obtained from clarified lysates from the RMCE virus population, as well as Generations 1,2,3 and 5 from both +Dox treated and -Dox cells using the plaque purification protocol as described in experiment 4.1. Regions of the viral chromosome containing the CX3CL1 gene were amplified via PCR as described in experiment 4.1 using primers specific to RMCE-cassette containing viruses (Illustrated in Fig. 28 B). DNA sequencing of the resulting PCR products was performed as described in experiment 4.1. Due to the large number of plaques that were picked (in order to increase sampling size) a procedure was developed where the PCR reaction was performed directly using virus containing media as template and not purified viral DNA. Plaques were picked, placed in tubes containing 100ul of media and freeze-thawed 3-times to release intracellular virus. 1ul of this virus-containing media was then used in a 50ul PCR reaction using the iProof DNA Polymerase Kit (BioRad) following manufacturer's instruction. Reactions were performed as described in experiment 4.1 with

the exception that 35 cycles were used in the PCR reaction in order to increase amplification of the dilute viral DNA template. The PCR reactions were then screened on an agarose gel to confirm the presence of a PCR product which was then sequenced. On average, <50% of the plaques picked using this procedure produced a usable PCR product. It was determined that a failure to produce a PCR product could be caused by failure to successfully lift sufficient virus-containing cells during plaque picking, as well as by the isolation of a virus plaque containing non-recombined HSV-GFP. The primers used for amplification were specific to recombined viruses and therefore would not produce a product from the HSV-GFP template. Virus plaques which produced usable DNA sequence are identified in Fig. 33.

*Growth Profiles of Plaque Purified Virus Clones*

Viruses from plaques that successfully produced a DNA sequence were expanded on fresh cells as described in experiment 4.1. From these, clarified lysates were prepared and viral titers were measured using qPCR as described above. Viral growth analysis was then performed where the purified virus clones were used to infect +Dox and -Dox treated HeLa-CX3CR1 cells at MOIs of 0.1 and 0.01. Cells were treated (or not) with Dox 24hrs prior to infection and with soluble heparin 2hrs prior to infection as described above. Clarified lysates were harvested 3 days after infection and viral titers were measured using qPCR. All conditions were performed on duplicate 4cm dishes. This growth profile analysis was used as a quick surrogate for affinity testing in order to determine if any viruses displaying novel, mutant CX3CL1 proteins showed a Dox-dependent growth profile that was similar to or faster than that of HSV-CX3CL1. As it was shown in chapter 2, viruses displaying proteins with high-binding affinity to cell-surface targets had faster rates of growth than viruses displaying lower affinity proteins.

*Quantitative PCR and Statistical Analysis.*

Quantitative PCR was performed using the primers and procedures described in experiment 4.1. Statistical analysis of the qPCR determined virus titers was compared between Dox treatments within the same generation using a one way ANOVA and post-hoc testing as described above.

**Experiment 4.2. Results 1. Selection of Novel CX3CL1 Mutants from a Degenerate Library.**

The results from experiment 4.2 showed that the RMCE reactions using plasmid shuttles containing the mutant CX3CL1 library produced a virus population that contained ~16% recombinant viruses (Fig. 31 B & 32 B). This corresponded with a total concentration of more than $1x10^5$ recombinant viruses per ml of lysate (Fig. 31 A & 32 A). The results showed that virus populations produced from exchange reactions with Library 1 and Library 2 shuttle plasmids both reached ~90% enrichment for recombinant viruses (containing library genes) after 5 generations of competitive infections (Fig. 31 B and Fig. 32 B). For both libraries, the virus populations from +Dox treated cells at generations 2, 3, 4 and 5 had significantly higher ($P<.05$) percentages of recombinant virus compared to the virus population from -Dox treated cells for the same generation. Furthermore, both libraries showed the same pattern of large reductions in the total virus concentration after 1 or 2 generations followed by a gradual increase in the concentration of recombinant viruses by generations 4 and 5.

**Experiment 4.2. Interim Conclusions. Selection of Novel CX3CL1 Mutants from a Degenerate Library.**

The results from experiment 4.2 showed that the RMCE reactions with both plasmid libraries were successful in making virus populations containing over $1x10^5$ recombinant viruses. This is well above the expected diversity of both libraries and suggests complete library coverage. The RMCE reaction was slightly less efficient than in experiment 4.1. This could be the result of transfecting plasmids directly from the ligation reactions rather than supercoiled plasmids which may be a better substrate for transfection. Enrichment for recombinant viruses reached almost 100% by Generation 5. This indicated the likely presence of a high-affinity virus or viruses within these populations. The trend

Fig. 31

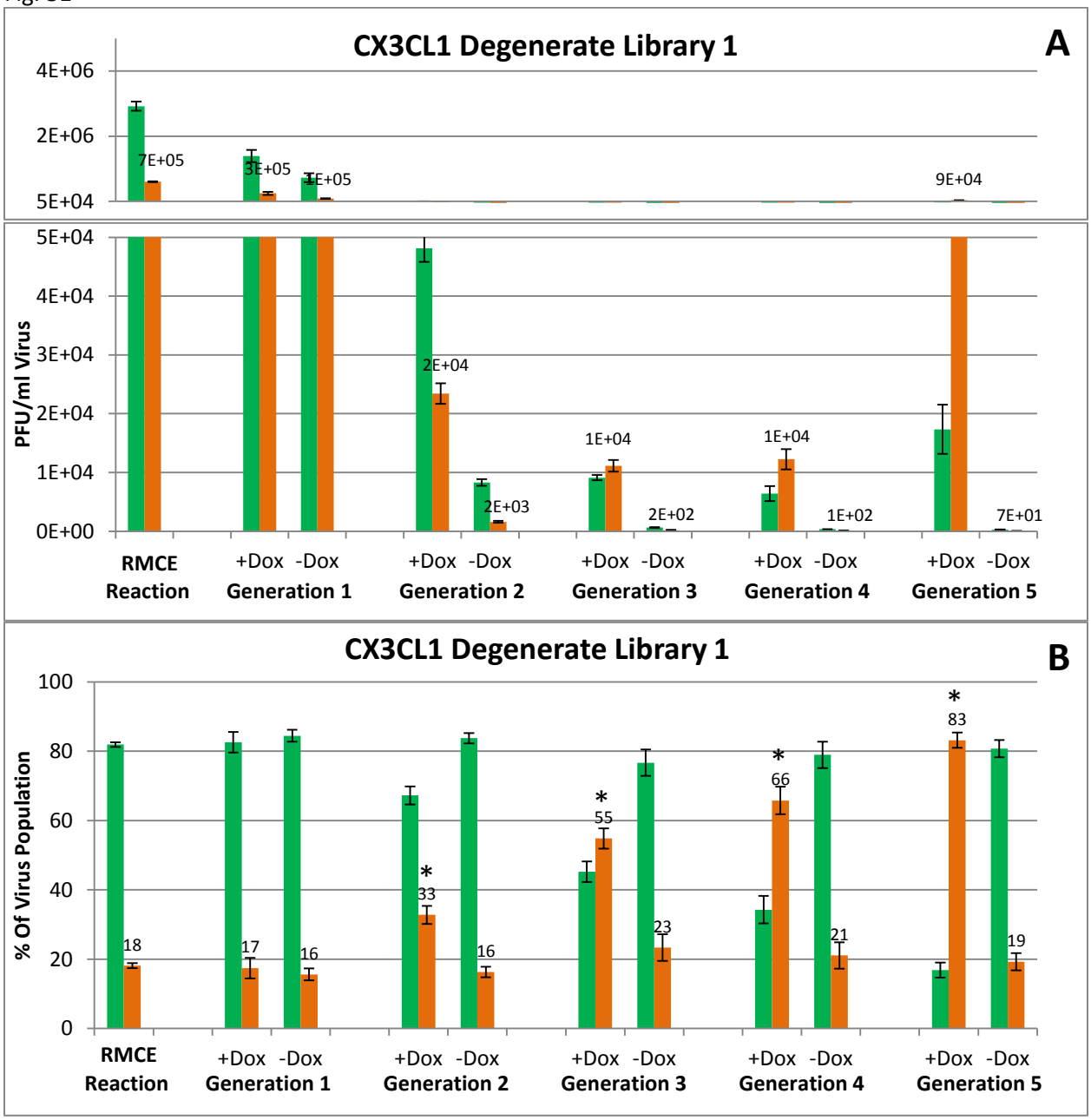


Fig. 31. Experiment 4.2. Quantitative PCR analysis of clarified lysates from cells infected with viruses containing genes from the degenerate CX3CL1 Library 1. Viruses from the RMCE reaction were used to infect HeLa-CX3CR1 cells that were treated with Dox (+Dox) or not (-Dox) 24hrs prior to infection. After 6 days, viruses were again harvested and used to infect fresh cells with the same Dox treatment in a subsequent generation of infection. **A.** qPCR measurement using primers standardized to plaque titered samples were used to measure the concentration of each virus in the lysate. Measurements using primers specific to the non-recombined HSV-GFP are shown in green and from primers specific to viruses containing a RMCE-cassette with a library gene are shown in orange. **B.** The percent of non-recombined HSV-GFP and recombinant viruses in the total virus population computed from the measurements in A. * indicates significantly higher percentage of recombinant virus compared to –Dox treated cells for the same generation. Bars indicate SEM.

Fig. 32

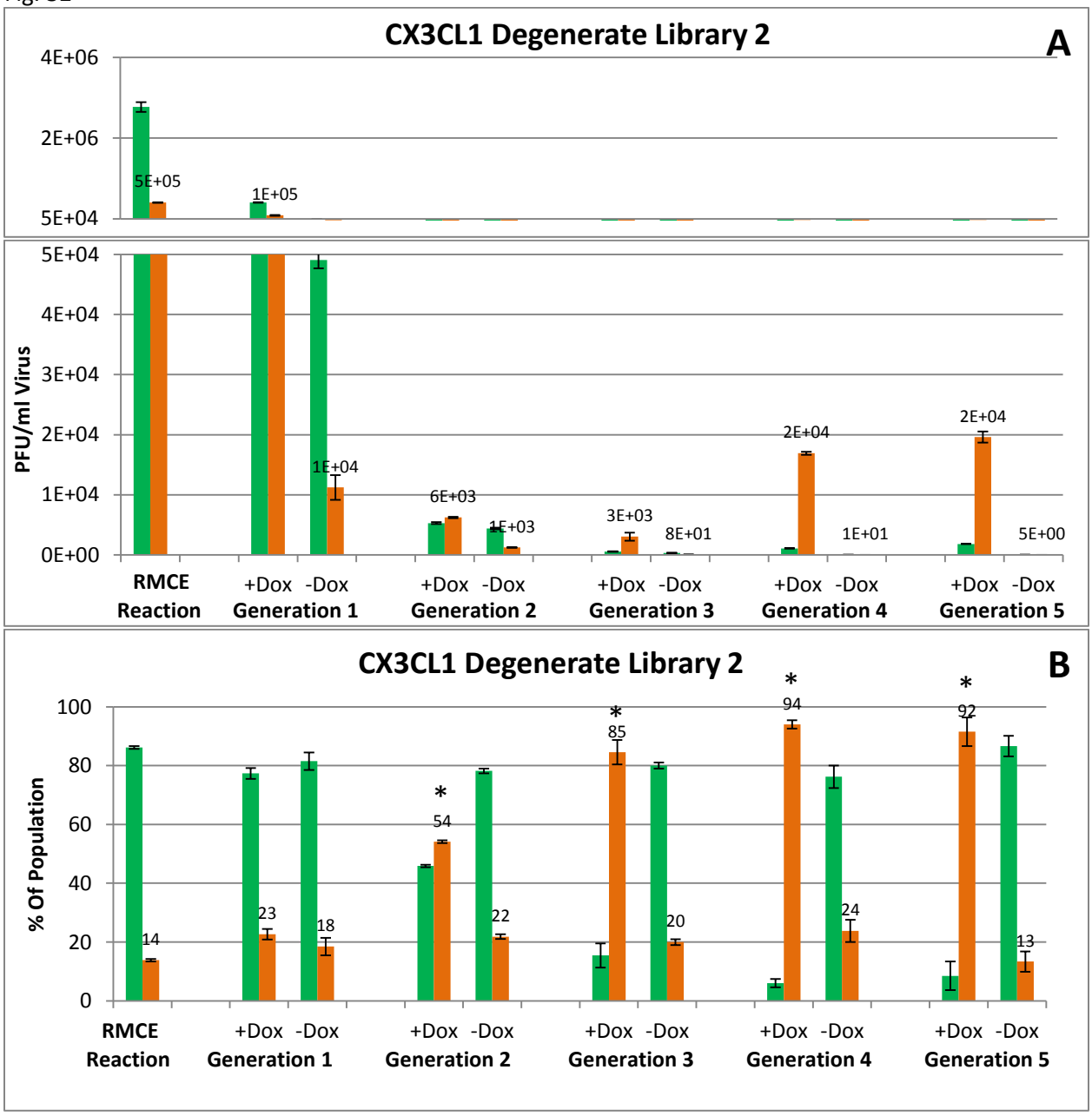


Fig. 32. Experiment 4.2. Quantitative PCR analysis of clarified lysates from cells infected with viruses containing genes from the degenerate CX3CL1 Library 2. Viruses from the RMCE reaction were used to infect HeLa-CX3CR1 cells that were treated with Dox (or not -Dox) 24hrs prior to infection. After 6 days, viruses were again harvested and used to infect fresh cells with the same Dox treatment in a subsequent generation of infection. **A.** qPCR measurement using primers standardized to plaque titered samples were used to measure the concentration of each virus in the lysate. Measurements using primers specific to the non-recombined HSV-GFP are shown in green and from primers specific to viruses containing a RMCE-cassette with a library gene are shown in orange. **B.** The percent of non-recombined HSV-GFP and recombinant viruses in the total virus population computed from the measurements in A. * indicates significantly higher (P<.05) percentage of recombinant virus compared to –Dox treated cells for the same generation. Bars indicate SEM.

observed in both library populations where the concentration of virus decreased rapidly after the first two generations was interpreted to be the result of the loss of low-affinity HSV-GFP viruses and viruses containing library genes that did not encode high-affinity proteins. These viruses were likely rapidly lost during the dilutions of the lysates used for infections of subsequent generations performed in order to keep the MOI under 0.1. The trend of increasing amounts of recombinant virus after generations 4 and 5 was hypothesized to be the result a rare high-affinity virus (or viruses) beginning to reach noticeable levels of increased virus growth.

Virus plaques were picked across successive generations of infection on +Dox and -Dox treated cells and the DNA sequence of the CX3CL1 gene within these virus clones was determined (Fig. 33). As described in the detailed methods, not all plaques that were picked resulted in a PCR product that could be sequenced. Unique virus mutants were named as indicated, and the number of plaques that contained that identical sequence within that generation is indicated (Fig. 33). For both libraries, a trend was observed where the majority of clones isolated directly from the RMCE reaction contained the empty FKN-Bae1 gene. This suggests that the Bae1 digestion was not entirely efficient and the plasmid library contained large amount of plasmids that were not successfully cut and could therefore still undergo RMCE without gaining a degenerate dsDNA fragment. However, as the FKN-Bae1 gene does not encode a functional protein, it is not surprising that these viruses are only seen prior to selection or in -Dox treated cells. Very few clones were obtained from -Dox treated cells which was likely the result of the large decreases in total virus concentration seen in these cells at later generations due to dilutions between generations and a lack of rapidly growing viruses.

Across the subsequent generations of selection on +Dox cells, novel CX3CL1 mutants were identified (Fig. 33). Several of these mutants were seen to occur multiple times within the same generation and across successive generations suggesting a significant amount of enrichment. The amino acid sequence of these mutants is shown in Fig. 34A (DNA and amino acid sequences are shown in

Fig. 33

| **Library 1** | | | **Total Plaques Picked** | **PCR Products Recovered** |
|---|---|---|---|---|
| **RMCE Reaction** | Bae1 (3) | | 10 | 3 |
| | | | | |
| **Generation 1 +Dox** | mt: 3-1 | | 10 | 1 |
| **Generation 1 -Dox** | Bae1 (2) | | 10 | 2 |
| | | | | |
| **Generation 2 +Dox** | mt: Del4 | mt: 3-1 | 10 | 2 |
| **Generation 2 -Dox** | | | 10 | 0 |
| | | | | |
| **Generation 3 +Dox** | mt: Del1 (3) | mt:6-5 | 10 | 4 |
| **Generation 3 -Dox** | | | 10 | 0 |
| | | | | |
| **Generation 5 +Dox** | mt: Del1 (3) | mt:6-5 | 10 | 4 |
| **Generation 5 -Dox** | | | 10 | 0 |
| | | | | |
| | | | | |
| **Library 2** | | | **Total Plaques Picked** | **PCR Products Recovered** |
| **RMCE Reaction** | Bae1 (4) | | 10 | 4 |
| | | | | |
| **Generation 1 +Dox** | mt: Del3 | mt: 3-7 | 10 | 2 |
| **Generation 1 -Dox** | Bae1 (3) | | 10 | 3 |
| | | | | |
| **Generation 2 +Dox** | mt: 7-3 | mt: 3-7 | 10 | 2 |
| **Generation 2 -Dox** | Bae1 (2) | | 10 | 2 |
| | | | | |
| **Generation 3 +Dox** | mt: Del2 | mt: 7-3 | 10 | 2 |
| **Generation 3 -Dox** | | | 10 | 0 |
| | | | | |
| **Generation 5 +Dox** | mt: 7-3 (4) | | 10 | 4 |
| **Generation 5 -Dox** | | | 10 | 0 |

Fig. 33. Experiment 4.2. A table of mutants recovered during different generations of selection from library 1 and library 2 in experiment 4.2. Each mutant is listed next to the generation and Dox treatment from which it was recovered. The number of times that a mutant was recovered during a generation is listed in parenthesis. Viruses containing the empty Bae1 shuttle plasmid are listed as "Bae1." Virus mutants that resulted from the correct insertion of degenerate oligonucleotides into the Bae1 site are labeled with the prefix "mt" and a unique hyphenated number. Mutants that occurred as a result of a deletion or rearrangement of the empty Bae1 shuttle plasmid are labeled with the prefix "mt" and then "Del" and a unique number. Ten plaques were picked from each generation and Dox treatment however not all plaques produced a viable PCR product that could be sequenced. In many instances the same mutant were seen to persist across multiple generations of selection. Mutant mt:3-7 contains a DNA sequence identical to wt CX3CL1 and mt:3-1 encodes the same amino acids as wt CX3CL1 with a single codon usage change (as shown in appendix 1).

Fig. 34

A

```
mt:3-7- MAPSQLAWLLRLAAFFHLCTLLAGQHLGMTKCNITCHKMTSPIPVTLLIHYQLNQES
mt:3-1- MAPSQLAWLLRLAAFFHLCTLLAGQHLGMTKCNITCHKMTSPIPVTLLIHYQLNQES
mt:7-3- MAPSQLAWLLRLARSFICVLCWRVS---MTCCNITCHKMTSPIPVTLLIHYQLNQES
mt:6-5- MAPSQLAWLLRLAAFFHLCTLLAGQHLGMTKCNKTCHKMTSPIPVTLLIHYQLNQES
mt:Del4-MAPSQLAWLLRLAAFFHLCTLLAGQHL--TKCNMTCHKMTSPIPVTLLIHYQLNQES
mt:Del3-MAPSQLAWLLRHGRVLSSVYSAS---------------MTSPIPVTLLIHYQLNQES
mt:Del2-MAPSQLAKLCSALARSFSVYSAGGSA------------MTSPIPLTLLIHYQLNQES
mt:Del1-MAPSQLAWLLRLAAFF-LCVLCWRVST----------KMTSPIPVTLLIHYQLNQES
 Wt-    MAPSQLAWLLRLAAFFHLCTLLAGQHLGMTKCNITCHKMTSPIPVTLLIHYQLNQES
 Bae1-  MAPSQLAWLLRLAAFFHLCTLLAGQHLGMSNYLRTLVVPQDDLANPSDLAHPLSTEPG
        VLRQARHHPGDETAQTLLC*
```

B

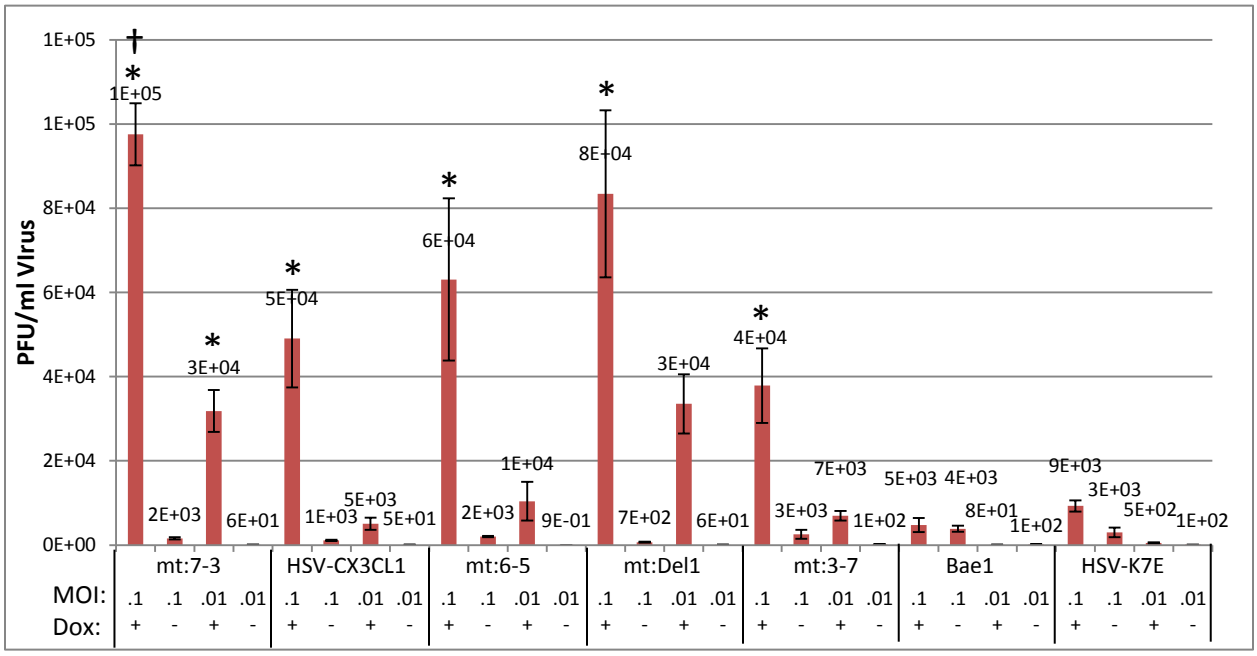


Fig. 34. Experiment 4.2. **A.** The amino acid sequences for the CX3CL1 N-terminus found in 8 unique viruses that were plaque isolated from library members in experiment 4.2. The origin of each member is listed in Fig. 32. The sequences for the wt-CX3CL1 protein as well as the empty Bae1 shuttle are also listed. Amino acids that differ from the wt sequence are highlighted in red, the amino acids that differ in the empty Bae1 shuttle as a result of the insertion of the Bae1 restriction site are highlighted in blue. The insertion of the Bae1 site causes a frame-shift resulting in a premature stop codon (shown). **B.** qPCR analysis of the viral growth profiles of selected mutants from experiment 4.2. Plaque purified clones were used to infect HeLa-CX3CR1 cells +/- Dox treatment at initial MOIs of 0.1 and 0.01. Cells and media were harvested 3 days after infection and a clarified lysate was prepared from which viral DNA was extracted and analyzed using qPCR primers specific to a region within the RMCE cassette common to all the viruses that is outside the mutated region. These primers are standardized to plaque tittered viral stocks to allow virus concentration predictions based on the amount of viral DNA detected. Replicates of two 4cm dishes of cells were used for each condition. *Indicates significantly higher ($P<.05$) amount of virus than in the -Dox treated cells infected with both MOIs of the same virus. † Indicates significantly higher ($P<.05$) amount of virus than in +Dox treated cells infected with HSV-CX3CL1 at the same dose. Bars represent SEM.

alignment with the wt-CX3CL1 and FKN-Bae1 gene in appendix 1). Interestingly, several of these clones appear to contain mutant CX3CL1 genes that were not the result of the insertion of a degenerate dsDNA oligonucleotide fragment. Rather, it appears that these clones are the result of deletions in the region of CX3CL1-Bae1 gene that contained the Bae1 fragment. All of the observed deletions resulted in the restoration of the reading frame encoding the CX3CL1 fusion protein. It is likely that these deletions occurred as the result of DNA repair to Bae1 digested Shuttle-Bae1 plasmids that had not been successfully ligated with a dsDNA fragment. This repair could have occurred as a result of non-homologous end-joining within the mammalian cells which is known to often resolve after branch-migration of the recombined DNA, resulting in deletions. This type of DNA repair would have likely not been observed if the ligated plasmids had been transformed into bacterial cells prior to the transfection. Amazingly, these types of deletion mutants were only seen from infections of +Dox treated cells implying that their production is more likely indicative of selective pressure than a high frequency of occurrence. Additional evidence of this selective pressure can be seen in the unique DNA sequences of these deletion mutations (appendix 1). In addition to a deletion in the region of the CX3CL1 gene that corresponds to the loss of Bae1 fragment (codons 29-35) each deletion mutant also has small nucleotide deletions in the upstream coding regions, without which the correct CX3CL1 reading frame would not be restored. Each deletion mutant uses different, unique deletions by which to restore the CX3CL1 reading frame and allow the production of the mutant CX3CL1-gC fusion protein. All of the deletion mutants recovered contained a gene that maintained the appropriate reading frame. It appears that the selective pressure within these viral competitions is so high that such rare events are promoted and enriched.

In addition to the observed deletion mutants, several clones were recovered that contain mutant CX3CL1 genes that appear to be the result of the correct insertion of the degenerate dsDNA oligo fragments. The mutants mt:3-7 and mt:3-1 both encode the wt-CX3CL1 amino acid sequence.

Mutant 3-1 contains a single nucleotide substitution that did not alter the amino acid sequence. Mutant 6-5 contains a single point mutation where amino acid 10 was changed from an Isoleucine to a lysine residue. As it is known that the loss of positively charged residues within this region of the CX3CL1 N-terminus can cause reductions in binding affinity (i.e. K7E) it is tempting to speculate that this mutation may further stabilize CX3CL1 binding by adding an additional positively charged residue. Among the recovered mutants that were not the result of a large deletion, an interesting observation is that none contain alterations that would result in a loss of the attachment site for N-linked glycosylation: NXT (where X is any amino acid). It remains unclear if glycosylation at this site is important for CX3CL1 binding. Non-glycosylated CX3CL1 protein produced in bacteria appears to have the same binding affinity as CX3CL1 produced in mammalian cells (Harrison et al., 2001). However it is possible that this glycosylation moiety could indirectly enhance CX3CL1 binding in a manner that is not apparent using standard affinity testing procedures. For example, it is possible that this glycosylation motif protects the N-terminus from degradation by enzymes present in serum and cultured cells.

The mutants Del4 and mt:7-3, appear to be the result of both an insertion of a degenerate dsDNA oligonucleotide as well as a deletion mutation. This was possibly caused by an imperfect or incomplete ligation of an oligonucleotide into the Bae1 site which was then resolved by DNA repair within the transfected cells. Mutant mt:7-3 contains the sequence for MTCCNITC at codons 29-36 as well as an upstream deletion that created an additional stretch of 10 mutant amino acids. This mutant has a noticeable increase in the number of cysteine residues in the CX3CL1 N-terminus compared to the wild type sequence. It is well documented that N-terminal cysteine residues form disulfide bonds that are crucial for the structure and function of chemokines (discussed above). It is therefore possible that this mutant possess a new N-terminal structure conferred by additional or different disulfide bonds. Like the mutants mt:3-7, mt:3-1, mt:6-5, and Del4, mt:7-3 also retained the N-linked glycosylation site.

A final observation is that all but one of the recovered deletion mutants resulted in frame-shift mutations creating novel N-terminal sequences that contain at least one F, W, or Y residue. However, no additional F, W or Y residues are seen in any of the recovered mutants that incorporated a degenerate oligonucleotide fragment. It is possible that additional large, aromatic amino acids cannot be incorporated into codons 29-36 or do not increase binding affinity, but they are beneficial to binding when added further upstream in the N-terminus. However, it is unknown if these residues are even present on the mature proteins encoded by these deletion mutants as the first 24 amino acids of wt CX3CL1 are removed during protein maturation and cleavage of the signal peptide.

**Experiment 4.2. Results 2. Selection of Novel CX3CL1 Mutants from a Degenerate Library.**

An analysis of growth profiles of plaque purified viruses containing the genes encoding mt:7-3, mt:6-5, mt:Del1, and mt:3-7 show that all four clones have a robust Dox-dependent rate of growth similar to HSV-CX3CL1 (Fig. 34 B). At a MOI of 0.1, all four mutants grew significantly ($P<.05$) faster on +Dox treated cells compared to the same MOI applied to -Dox treated cells. Due to a large amount of variation in cells infected at an MOI of 0.01, this same trend was only significant for mt:7-3 compared to -Dox cells at this lower MOI. No significant differences in viral growth were seen between +Dox and -Dox treated cells that were infected with HSV-Bae1 or HSV-K7E. A small, non-significant, increase in the growth of K7E was seen on +Dox treated cells. Lastly, a significantly higher ($P<.05$) concentration of virus was seen in +Dox treated cells infected with mt:7-3 at an MOI of 0.1 compared to +Dox treated cells infected with HSV-CX3CL1 at the same MOI.

**Experiment 4.2. Conclusions. Selection of Novel CX3CL1 Mutants from a Degenerate Library.**

The growth profiles of several of the plaque-purified novel mutants identified during experiment 4.2 were compared to the profiles of viruses displaying wt CX3CL1 and CX3CL-Bae1 which does not encode a functional protein. These growth profiles were used as an easy first step in determining if the mutant proteins recovered during selection have similar or increased binding affinity compared to wt

CX3CL1. However, it should be noted that there are many other factors that can contribute to an accelerated rate of virus production that are independent of binding affinity. Furthermore, as previous results have shown, the rate of virus growth differs greatly across the course of viral infection in cultured cells. This could translate into differences in virus production that do not directly translate into differences in binding affinity of the same magnitude. Notwithstanding these caveats, the results shown in Fig. 34 B suggest that the novel CX3CL1 protein mutants encoded by enriched library members have very similar binding affinity for CX3CR1 compared to wt CX3CL1. The increased rates of growth of these virus clones appear to be dependent to CX3CR1 binding as indicated by the large differences in between +Dox and -Dox treated cells. This is further confirmed by a lack of any significant difference in growth, regardless of Dox treatment, of the virus clone containing the CX3CL1-Bae1 gene, which does not encode a functional protein. No significant differences in growth were seen between the viruses encoding mt:6-5, and mt: Del1 and viruses encoding wt CX3CL1. Furthermore, it is possible that mt:7-3 encodes for a protein that has even higher affinity for CX3CR1 than wt CX3CL1, as mt:7-3 grew significantly faster during growth profile analysis (Fig. 34). The fact that mt:7-3 was seen in later generations of selection while mt:3-7, which contains a perfectly wt gene, was not seen at these times further suggests that mt:7-3 was able to out-compete mt:3-7 (Fig. 33). However this could also be an artifact of the small sample size of the plaque picking procedure . Deep sequence analysis of the genomes of the entire virus population will provide a clearer picture of the relative amount of each virus. Such analysis over successive rounds of selection will also provide insight into how the virus population changes and which library members are out-competing others.

The results from experiment 4.2 suggest that this novel, virus-based protein affinity selection system may have successfully identified novel high affinity CX3CL1 mutants. Furthermore, while the intended starting diversity of each library was relatively low, it is possible that this was greatly increased by the unique recombination events caused by DNA repair of shuttle plasmids within the transfected

cells. This suggests exciting possibilities for the creation of additional library diversity in future applications of this system through mutagenesis that would not be possible using bacterial library clones. Furthermore, the results suggest that selective pressure during viral competitions is quite strong and can enrich for very rare DNA recombination events that result in proteins with increased binding capabilities.

**Experiment 4.3. Using The Novel Virus Display System to Screen an Antibody Library.**

One of the most common applications of currently established display techniques is the screening of antibody libraries to identify novel, high-affinity antibodies. High-affinity antibodies have been shown to be very successful therapeutics and many are currently approved for the treatment of a wide range of medical conditions. However, complications can arise when expressing non-human expression systems. As reviewed extensively in chapter 1, many antibodies are not appropriately expressed in bacterial cells. For this reason, screening of antibody libraries using yeast display has become increasingly common. In fact, the screening of antibody libraries using yeast display has shown that many high-affinity antibodies are potentially missed by phage display due to poor levels of expression of some particular antibodies in bacteria. An excellent example of this was reported by Burton et. al in 2007 (Burton, 2007). Here, a B-cell derived single chain antibody (scFv) library was screened to identify antibodies with high binding affinity to the HIV coat protein GP160 (the GP120 and GP41 complex). This library, referred to as the FDA2 library, was derived from the B-cells contained within the bone marrow of an HIV positive but asymptomatic individual. Phage display screening of this library against GP160 revealed several high-affinity HIV-neutralizing antibodies. One of these antibodies has been extensively studied and is referred to as clone Z-13 (Zwick et al., 2001). Clone Z-13 was reported to bind to a portion of the HIV coat protein GP160 with low nanomolar affinity. When the FDA2 library was further screened using yeast display, additional high affinity αGP160 antibodies were

discovered that were missed by phage display because they were poorly expressed in bacterial cells (Bowley et al., 2007). It is possible that additional high-affinity HIV antibodies remain undetected by both systems as they require expression in human cells for full functionality.

The FDA2 library provides an excellent opportunity to use this novel viral display system to screen a library that has been shown to contain proteins that are sensitive to expression in non-human cells. Furthermore, the high affinity antibodies that have already been identified from this library present a type of positive control for potential characteristics that may be found on novel, high-affinity proteins. This will allow for better characterization of this novel HSV display system during this preliminary testing.

**Experiment 4.3. Experimental Design. Using The Novel Virus Display System to Screen an Antibody Library.**

*Creation of the FDA2 Shuttle Plasmid Library*

The FDA2 scFv kappa library contained within the phage display vector PComb3 was generously provided by Dr. Dennis Burton (Scripps Research Institute). In this plasmid, the scFv genes are contained between two unique Sfi1 restriction endonuclease sites. These Sfi1 sites are commonly used for the cloning of library fragments. For this reason they were included during the construction of the RMCE shuttle plasmid Shuttle3.1-Sfi1 (described in chapter 2). The scFv fragment was removed by digestion of PComb3 with Sfi1 restriction endonuclease (NEB) following the manufacturer's protocol and gel purified as previously described. The scFV Sfi1 fragment was ligated into the Sfi1 sites in Shuttle3.1-Sfi. The resulting plasmid, Shuttle–FDA2, contains a gene that encodes for a ScFv-gC-C-terminus fusion protein that, when inserted into a viral chromosome, will be expressed and displayed on the surface of an HSV virion. The Shuttle-FDA2 library was prepared using the same large-scale ligation procedure as described in experiment 4.2. This large scale ligation was used as it would allow for production of

Shuttle-FDA2 plasmid that could be transfected directly into 293T cells, for the RMCE reaction, without the potential bottleneck of transformation into bacteria. The reported diversity of the FDA2 library is ~$1x10^7$ (Burton, 2007). Pilot testing showed that this level of transformation efficiency was difficult to achieve even using commercially available ultra-competent bacterial cells. Therefore, it was determined that avoiding the need for a bacterial transformation would increase the likelihood of more complete library coverage. The preparation of Shuttle-FDA2 plasmid for the transformation-free transfection procedure was performed as described in experiment 4.2. A sample of the Shuttle-FDA2 ligation was used to transform DH5α *e. coli,* plasmid DNA was extracted from a bacterial clone and the sequence for the scFv-gC fusion protein was confirmed by DNA sequencing as previously described.

*Live-Virus RMCE Production and Competitive Infections of the HSV-Displayed*

A library of viruses displaying the scFv-gC fusion proteins was prepared using the Live-virus RMCE protocol as described in experiment 4.1. The resulting virus library was used to infect +Dox and -Dox treated HeLa-GP160 cells using the same competitive infection procedure as described in experiment 4.1.

*Construction and Screening of the HeLa-GP160 cell line*

HeLa cells stably expressing the membrane-bound GP160 protein were created using the same procedure used to produce the HeLa-CX3CR1 cell line described in detail in chapter 2. For this, the gene encoding a protease cleavage-resistant, membrane-bound form of GP160 was amplified from plasmid pCDNA-HIV-1JRFL-Env(-)-deltaCT which was generously provided by Dr. Joseph Sodroski (Harvard University). The gene was amplified using primers GP160-Sense-Ecor1 5'-TTAAGTCGACTCCAAGAGAAGGCCAGAAACC-3' and GP160-Anti-NotI 5'-TTAAGGATCCTTAGTGGTGGTGGTGGTGGTG-3'. These primers amplify the entire GP160 open reading frame as well as add the recognition sequences for EcoR1 and Not1 restriction endonucleases. This PCR product, and Plasmid pSIN.Bi-F3-Ig-F, were digested with EcoR1 and Not1 restriction endonucleases, gel

purified, ligated together, transformed into DH5α bacterial cells and plasmid DNA was isolated as previously described. Plasmid pSIN.Bi-F3-Ig-F contains FRT recombination sites which correspond with the recombination sites within the genome of HeLa-TK-FRT cells described in detail in chapter 2. The resulting plasmid, pINA-GP160 was confirmed by DNA sequencing and used to transfect into HeLa-TK-FRT cells in order to produce a cell line that stably expresses GP160 under a Dox inducible promoter. GP160-expressing HeLa cell line was created and verified using the same procedure for the production of HeLa-CX3CR1 cells as described in detail in chapter 2. The resulting cell line, HeLa-GP160 showed robust Dox-inducible mRNA expression of GP160 transcript as described in chapter 2 using the qPCR primers RT-GP160-Sense-1 5'-ACTGAGCACTTCAACATGTGG-3' and RT-GP160-Anti-1 5'-AGTTCAGGGTCACACACAGG-3'.

*Sequence Analysis of Plaque Purified Virus Clones*

Virus clones were obtained from clarified lysates from cells from the RMCE reaction, as well as Generations 1,2,3 and 4 +Dox and -Dox treated cells using the plaque purification protocol as described in experiment 4.2. For this, regions of the viral chromosome were amplified via PCR as using primers specific to recombinant, RMCE-cassette containing viruses #2-Seq-PgC1 5'-TCACTACCGAGGGCGCTT-3' and Sfi-ORF-Anti-1 5'-GCGGTGATGTTCGTCAGG-3'. DNA sequencing of the resulting PCR products was performed as described in experiment 4.2.

*Growth Profiles of Plaque Purified Virus Clones*

Viruses from plaques that successfully produced DNA sequences were expanded on fresh cells as described in experiment 4.2. From these, clarified lysates were prepared and viral titers were measured via the qPCR titering procedure. Viral growth analysis was then performed where the purified virus clones were used to infect +Dox and -Dox treated HeLa-GP160 cells at MOIs of 0.1 and 0.01 as described in experiment 4.2. As before, this growth profile analysis was used as a quick surrogate for affinity testing in order to determine if any viruses showed a Dox-dependent increase in growth that

would suggest increased cell-attachment caused by a binding interaction specific to GP160. Unlike in experiment 4.2, a positive control high-affinity scFv-displaying virus was not available. However, the growth profiles of virus clones isolated during selection were compared to the growth profiles of viruses that contained scFv genes with pre-mature stop codons to verify that increased rates of viral growth were specific to viruses that encoded functional scFv proteins.

*Quantitative PCR and Statistical Analysis*

Quantitative PCR was performed using the primers and procedures described in experiment 4.2. Statistical analysis of the qPCR determined virus titers was compared between Dox treatments within the same generation using a one way ANOVA and post-hoc testing as described in experiment 4.1.

**Experiment 4.3. Results-1. Using The Novel Virus Display System to Screen an Antibody Library.**

The results from experiment 4.3 show that the Live-virus RMCE reaction produced a virus population that contained 8% recombinant viruses at concentration of $2x10^5$ PFU/ml (Fig. 35 A & B). Trending, non-significant enrichment of the recombinant virus population was seen in generations 1 and 2 in +Dox treated cells. Virus populations containing significantly higher percentages ($P<.05$) of recombinant virus were seen in generation 3 and 4 +Dox treated cells compared to -Dox treated cells in the same generations (Fig. 35 B). Enrichment of the recombinant population reached 73% after the fourth generation of selection. Similar to experiment 4.2, a large decrease in the total concentration of virus was seen after generation 1. Significantly higher ($P<.05$) concentrations of HSV-GFP and recombinant virus were detected in +Dox cells compared to -Dox cells in the same generation for generations 1, 2, and 3 (Fig. 35A). Only levels of recombinant virus were significantly higher ($P<.05$) in +Dox cells compared to -Dox cells in generation 4.

Fig. 35

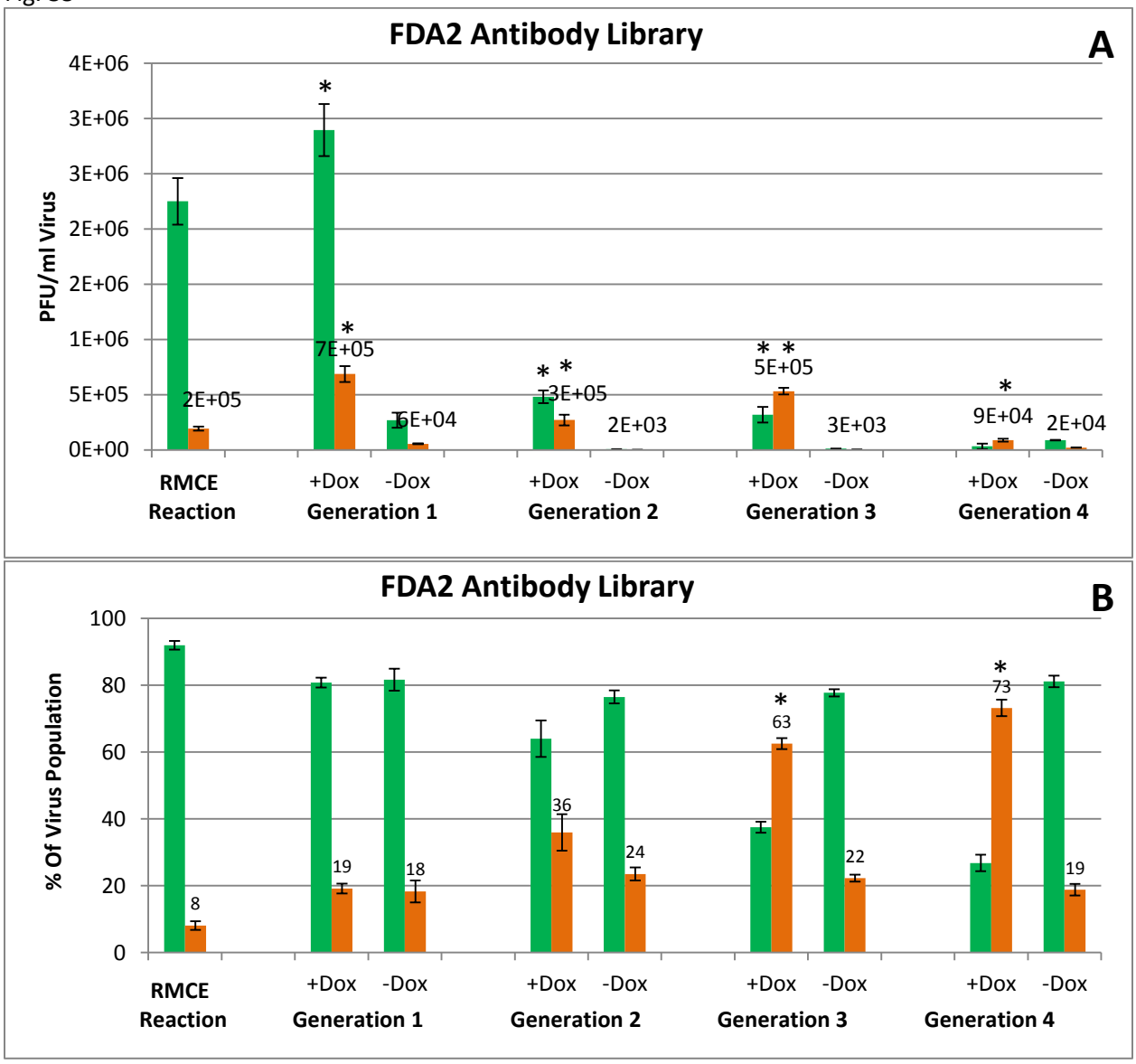


Fig. 35. Experiment 4.3. Quantitative PCR analysis of clarified lysates from cells infected with viruses containing genes from the FDA2 scFv library. Viruses from the RMCE reaction were used to infect HeLa-GP160 cells that were treated with Dox (+Dox) or not (-Dox) 24hrs prior to infection. After 6 days, viruses were again harvested and used to infect fresh cells with the same Dox treatment in a subsequent generation of infection. **A.** qPCR measurement using primers standardized to plaque titered samples were used to measure the concentration of each virus in the lysate. Measurements using primers specific to the non-recombined HSV-GFP are shown in green and from primers specific to viruses containing a RMCE-cassette with a library gene are shown in orange. **B.** The percent of non-recombined HSV-GFP and recombinant viruses in the total virus population computed from the measurements in A. * indicates significantly higher percentage or concentration of recombinant virus compared to –Dox treated cells for the same generation. Bars indicate SEM.

**Experiment 4.3. Interim Conclusions. Using The Novel Virus Display System to Screen an Antibody Library.**

The results from experiment 4.3 show that a population of viruses was created containing 8% recombinant viruses which contained genes from the Shuttle-FDA2 plasmid DNA library. This percentage and the total concentration of virus was lower than that seen in experiment 4.1 and suggests that, as in experiment 4.2, the use of the transformation-free transfections may have reduced the efficiency of the Live-virus RMCE procedure. Since the reported diversity of the FDA2 library is $1x10^7$ members, the $1x10^5$ recombinant viruses produced suggests less than complete library coverage. However, considering that a maximum MOI of 0.1 can be used in generation 1, the entire FDA2 library could not be screened without significantly scaling up the size of the tissue culture procedures.

The results from experiment 4.3 show that successive enrichment of the recombinant virus population occurred across 4 generations of selection. This suggests the presence of a virus (or viruses) displaying a scFv with high binding affinity to cell-surface GP160. This enrichment was not seen in -Dox cells showing it was specific to GP160 binding. Interestingly, significant higher concentrations of recombinant viruses in addition to non-recombined HSV-GFP were seen in +Dox treated cells compared to -Dox treated cell in the same generation. This is likely the result of pseudotyping in which HSV-GFP viruses obtained viral envelopes containing high-affinity scFvs. This phenomenon occurred despite the use of continual MOI cutbacks between successive generations to maintain a starting MOI that was less than 0.1. It is possible that a greater occurrence of pseudotyping was seen in this experiment due to the nature of the library being displayed. Unlike the CX3CL1-CX3CR1 ligand-receptor interaction, the scFv binding interaction is solely a binding interaction with no potential for complications such as ligand-induced receptor conformational changes which could possibly interfere with subsequent viral processes required for virus penetration. Furthermore, it is possible that the FDA2 library may already be partially enriched for with antibodies that have some appreciable affinity for GP160 since it was

isolated from an HIV-infected individual. Lastly, it is possible that an antibody library may contain some proteins that have appreciable binding affinity for other cell-surface molecules. The latter is a less likely explanation due to the apparent GP160/Dox-dependent nature of the observed increase in viral growth. Any one, or a combination of these factors, could result in a recombinant virus population that contains a relatively high percentage of viruses that display a protein that allows efficient virus binding and entry. This could potentially result in a very rapid rate of growth that would increase the occurrence of super-infection and pseudotyping despite the initially low MOI. This explanation is further supported by the observation of faster rates of CPE occurrence than seen in any previous experiments. Furthermore, selection of this library required greater dilutions between successive generations to produce populations without extremely high apparent levels of pseudotyping (data not shown). It would appear that over generations 2, 3 and 4 this phenomenon subsides and the rate of pseudotyping decreases.

Another observation of note was the increased percentage of the recombinant virus population in -Dox cells after generation 1 compared to the RMCE reaction (Fig. 35 B). This could be the result of the antibody library containing proteins with appreciable binding affinity for non-GP160 cell surface targets as mentioned above. To address this, prior to generation 2 of competition, viruses from generation 1 were applied to -Dox treated cells for 15 minutes in a pre-adsorption step to remove viruses that had high-affinity binding to these non-GP160 cell surface targets. This was performed in a low volume so as to increase the potential rate of contact between viruses and cells. The virus containing media was then removed from these cells and applied to cells with the appropriate Dox treatment. No significant enrichment of the recombinant population was observed on -Dox cells in subsequent generations.

**Experiment 4.3. Results-2. Using The Novel Virus Display System to Screen an Antibody Library.**

Plaque recovery of virus clones containing scFv genes over successive generations of selection yielded the recovery of 17 unique clones (Fig. 36). Several of these were recovered multiple times suggesting significant enrichment (Fig. 36 A). Sequence analysis of scFv genes within the recovered clones showed that 90% of all clones recovered from +Dox treated cells did not contain a premature stop codon while only 17% of those recovered from -Dox treated did not (Fig. 36 B). Additional analysis showed that +Dox recovered clones had a trending, non-significant, increase in the average number of hypervariable, complementarity determining region (CDR) loops similar to loops reported for scFvs previously recovered from the FDA2 library compared to -Dox recovered clones (Fig. 37 B, alignment shown in appendix 2). Additionally, scFv sequences in clones recovered from +Dox treated cells had a significantly higher average percent identity to the sequence of the previously identified high affinity scFv Clone Z-13 compared to clones recovered from -Dox treated cells. Lastly, the clones 1-4, 4-11, and 4-12, isolated from generation 4 of competition in +Dox treated cells all showed significantly higher rates of viral growth in +Dox treated HeLa-GP160 cells compared to the -Dox treated cells (Fig 38). The clone 5-21, which was isolated from generation 3 of competition in -Dox treated cells and contains a premature stop codon within the scFv sequence did not show any significant differences in viral growth on +Dox compared to -Dox cells (Fig. 38).

**Experiment 4.3. Conclusions. Using The Novel Virus Display System to Screen an Antibody Library.**

The results from experiment 4.3 show that none of the scFv sequences found in virus clones isolated after 4 generations of selection are identical to those of previously reported high-affinity scFvs recovered from library FDA2. However, the results do show that clones recovered from competitive infections on +Dox treated cells contain CDR loops with a greater percent identity to the sequences of

Fig. 36

A

| FDA2 Library | | | | | | | | Total Plaques Picked | PCR Products Recovered |
|---|---|---|---|---|---|---|---|---|---|
| RMCE Reaction | 3-4 | | | | | | | 10 | 1 |
| | | | | | | | | | |
| Gen1 +Dox | 7-5 | | | | | | | 10 | 1 |
| Gen1 -Dox | | | | | | | | 10 | 0 |
| | | | | | | | | | |
| Gen2 +Dox | 3-1 | 1-4 | | | | | | 10 | 2 |
| Gen2 -Dox | 5-14 | 5-13 | | | | | | 10 | 2 |
| | | | | | | | | | |
| Gen3 +Dox | 4-3(2) | 4-12 | 1-4 | | | | | 10 | 3 |
| Gen3 -Dox | 5-1 | 5-7 | 5-21 | | | | | 10 | 3 |
| | | | | | | | | | |
| Gen4 +Dox | 13-1 | 13-6 | 13-7 | 13-9 | 4-12 | 1-4 | 4-11 | 10 | 7 |
| Gen4 -Dox | | | | | | | | 10 | 0 |

B

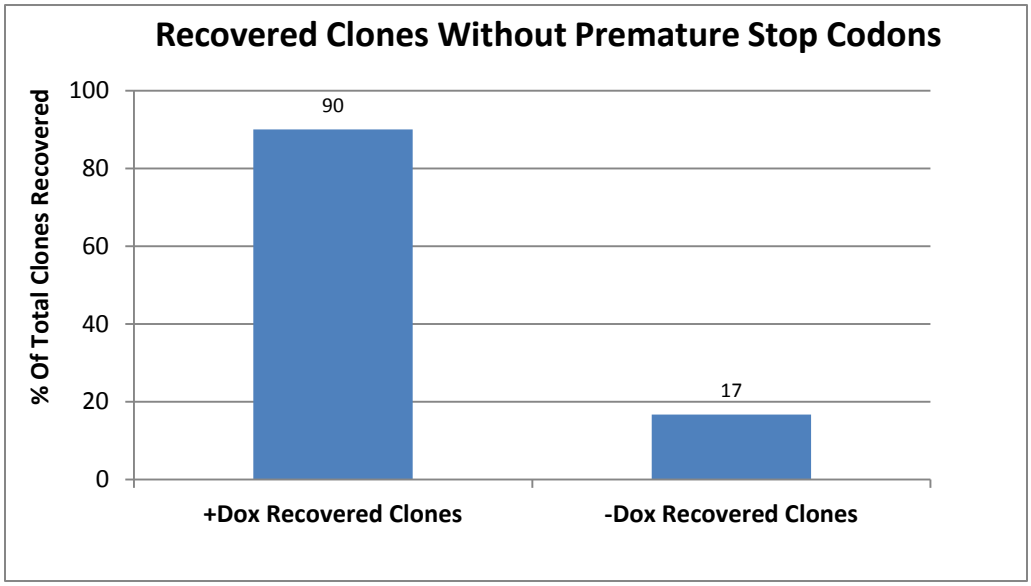


Fig. 36. Experiment 4.3. **A.** The identification plaque purified virus clones containing unique scFv genes isolated from virus populations from different generations of viral competition. 10 virus plaques were picked from the RMCE reaction and each generation of +Dox and -Dox treated cells and PCR was performed to amplify the scFv containing region of the viral genome. Inefficiencies in the plaque picking procedure as well as the inability of HSV-GFP to produce a PCR product are likely explanations for only a small number of plaques that yielded a usable PCR product for sequencing. The amino acid sequences of each clone are listed in appendix 2. **B.** An analysis of the total percentage of all +Dox and -Dox recovered scFv sequences that did not contain a premature stop codon.

Fig. 37
A

**Clone Z-13 (previously reported)**
TQSPATLSLSPGERATLSCRASQSVGRNLGWYQQKPGQAPRLLIYDASNRATGIPARFSGSGSGTDFTLTISSLEPEDFAVY
YCQQRSDWPRTFGQGTKVEIKR

% Identical:

82% **Clone 1-4 (Generation 2, 3 & 4 +Dox)**
TQSRGTLSLSPGERATLSCRTSESLNSNYLAWYQQKPGQAPRLLIYGGSTRAAGIPDRFRGSGSGTDFTLTISRLEPEDFAV
YYCQQFGTSPPITFGQGTRLEIKR

83% **Clone 4-12 (Generation 3 & 4 +Dox)**
TQSPGTLSLSPGERATLSRRASQSVIGSYLAWYQQKPSQAPRLLIYGASSRASGVPDRFSGRGSGTDFTLTISRLEPED
FAVYFCQQYGGSPQVFTFGPGTKVEIKR

87% **Clone 4-11 (Generation 4 +Dox)**
TQSPATLSVSPGERATLSCRASQSVRSDLAWYQQKPGQAPRLLIYDASTRATGIPARFRGSGSGTEFTLTISSLQPEDSAVYYCQQYK
NWPPWTFGQGTKVDIKR

68% **Clone 5-21 (Generation 3 –Dox)**
LSASVGDRVTITCRASEPISTYLNWYQQKPGKAPKVLIYAASSLQSGVPPRFSGSGSGTDFTLTIGSLQPEDFATYYCQQANSPRVTFGGGTK
VEIKR

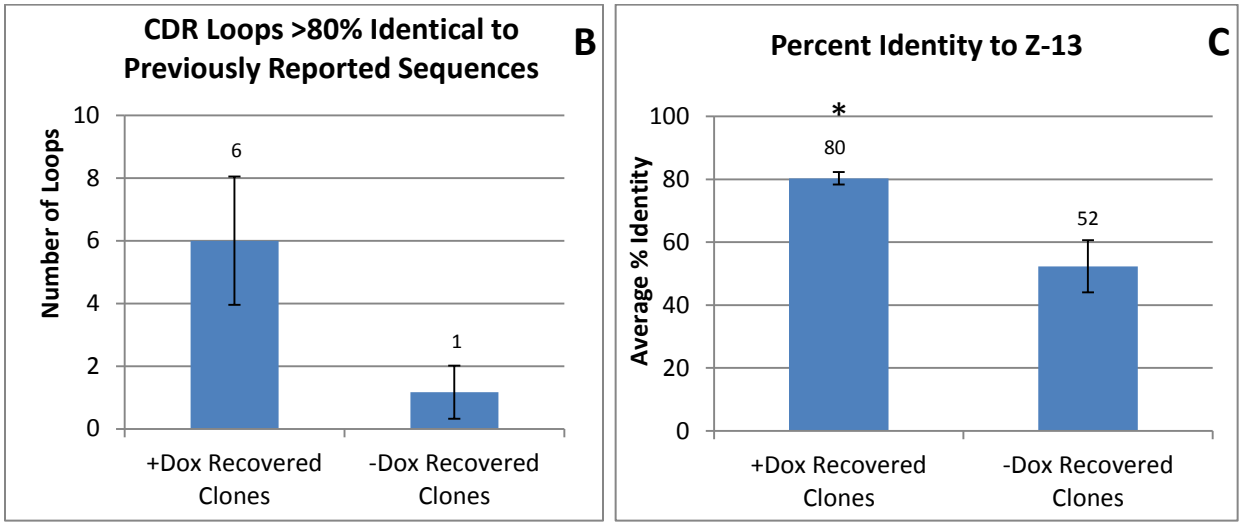


Fig. 37. Experiment 4.3. **A.** The amino acid sequence of the light chain of the high affinity αGP160 scFv clone "Z-13" previously isolated from the FDA2 library as reported by (Parren, 2001). Shown below are the light chain scFv amino acid sequences from four unique virus clones isolated from different generations of competition and their percent sequence identity to clone Z-13. The three clones isolated from +Dox treated cells with the highest percent identity to Z-13 are shown and the clone with the highest percent identity from -Dox treated cells is shown. **B.** The average number of CDR loops (From 6 total) found in clones from +Dox and -Dox treated cells with greater than 80% sequence identity to loops found in high affinity scFvs recovered from the FDA2 library as reported by (Burton, 2007) (P=.09). **C.** The average percent identity to the Z-13 light chain sequence of light chain sequences from unique clones recovered from +Dox treated cells and -Dox treated cells (P<.01).

Fig. 38

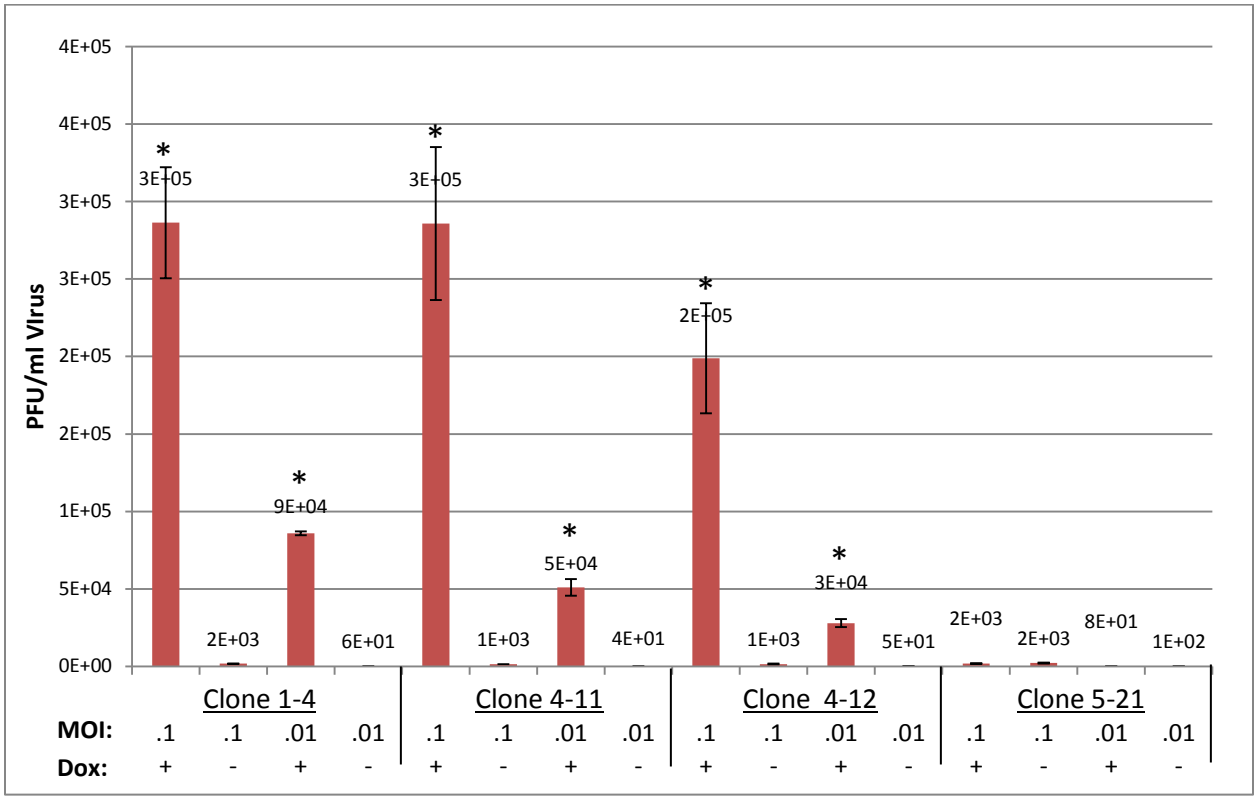


Fig. 38. Experiment 4.3. qPCR analysis of the viral growth profiles of selected scFv-expressing clones from experiment 4.3. Plaque purified clones were used to infect HeLa-GP160 cells +/- Dox treatment at initial MOIs of 0.1 and 0.01. Cells and media were harvested 3 days after infection and a clarified lysate was prepared from which viral DNA was extracted and analyzed using qPCR primers specific to a region within the RMCE cassette common to all the viruses. These primers are standardized to plaque titered viral stocks to allow virus concentration predictions based on the amount of viral DNA detected. Replicates of two 4cm dishes of cells were used for each condition. Clones 1-4, 4-11, and 4-12 were isolated from +Dox treated cells during library selection, Clone 4-21 was isolated from –Dox treated cells during library selection and contains a premature stop codon. * indicates significantly higher (P<.01) amount of virus than in the -Dox treated cells as well as +Dox treated cells infected with Clone 5-21. Bars represent SEM.

previously reported high affinity scFvs compared to clones recovered from -Dox treated cells. As these CDR loops are the hypervariable antibody regions largely responsible for antigen binding, this suggests that this virus-display system was successful in enriching for clones with similar structures and likely binding abilities. Furthermore, the observation that a greater percentage of scFv sequences in clones recovered from +Dox treated cells did not contain premature stop codons compared to -Dox recovered clones further suggests that this system successfully selected for the functional expression of scFvs with binding to GP160. The occurrence of premature stop codons within antibody open reading frames has been reported to naturally occur during somatic hypermuation within B cell populations and is increased in antibody libraries that have been converted into scFv plasmids cloned into bacteria (Daugherty et al., 1999; González-Fernández and Milstein, 1993).

Growth profile analysis of virus clones that were recovered multiple times during selection showed robust increases in the growth of these viruses on +Dox treated cells compared to -Dox treated cells. While not a direct measure of binding affinity, this strongly suggests a significant binding interaction between these virus clones and cell-surface GP160.

Lastly, while several virus clones were recovered multiple times during plaque selection, this occurred less frequently than observed in experiment 4.2. This could be the result insufficient sampling size or a higher prevalence of different clones with high binding affinity than in the mutant library screened in experiment 4.3. Additional deep sequence analysis of the entire virus population over successive generations would provide much more information about the changes in population diversity over successive rounds of selection. This analysis would help further identify sequence characteristics of virus clones that become enriched.

The results from experiment 4.3 show that the novel virus display system was successful in enriching for a population of viruses that contain scFvs with amino acid sequences that are highly similar to the sequences of previously reported scFvs with high binding affinity to GP160. Further

characterization of these scFvs may reveal that they have comparable or even higher binding affinity to GP160 than previously identified scFvs. Furthermore, these antibodies may possess features such as novel glycosylation or sulfation patterns that would have been missed by phage and yeast selection and impart increased HIV neutralizing capabilities.

**Final Conclusions**

The results summarized in this thesis describe the development of a novel, human-virus based display platform that shows great promise as potential new tool for the discovery of novel high affinity proteins. The initial testing of this mammalian-cell based system has already shown the occurrence of unpredicted and exciting possibilities with regards to mutagenesis and directed evolution. The nature of these occurrences is undoubtedly related to the amazing complexity of mammalian cells. It is this same complexity that has likely contributed to the requirement of a large number of specific procedural parameters and high-degree of optimization before the establishment of the final system as described in the last chapter of this thesis. As a result of this extensive enhancement and procedural improvement, this system has been shown to yield reproducible and exciting results. It is my hope that this technology will serve as effective tool in the discovery of new therapeutics for the treatment of human diseases.

Bibliography

Albert, H., Dale, E.C., Lee, E., and Ow, D.W. (1995). Site-specific integration of DNA into wild-type and mutant lox sites placed in the plant genome. Plant J. Cell Mol. Biol. *7*, 649–659.

Alonso-Camino, V., Sánchez-Martín, D., Compte, M., Sanz, L., and Alvarez-Vallina, L. (2009). Lymphocyte display: a novel antibody selection platform based on T cell activation. PloS One *4*, e7174.

Arii, J., Goto, H., Suenaga, T., Oyama, M., Kozuka-Hata, H., Imai, T., Minowa, A., Akashi, H., Arase, H., Kawaoka, Y., et al. (2010). Non-muscle myosin IIA is a functional entry receptor for herpes simplex virus-1. Nature *467*, 859–862.

Batterson, W., and Roizman, B. (1983). Characterization of the herpes simplex virion-associated factor responsible for the induction of alpha genes. J. Virol. *46*, 371–377.

Beck, A., Cochet, O., and Wurch, T. (2010). GlycoFi's technology to control the glycosylation of recombinant therapeutic proteins. Expert Opin. Drug Discov. *5*, 95–111.

Bender, F.C., Whitbeck, J.C., Lou, H., Cohen, G.H., and Eisenberg, R.J. (2005). Herpes simplex virus glycoprotein B binds to cell surfaces independently of heparan sulfate and blocks virus entry. J. Virol. *79*, 11588–11597.

Boder, E.T., and Wittrup, K.D. (1997). Yeast surface display for screening combinatorial polypeptide libraries. Nat. Biotechnol. *15*, 553–557.

Boehmer, P.E., and Nimonkar, A.V. (2003). Herpes virus replication. IUBMB Life *55*, 13–22.

Bonomi, M., Busnelli, M., Persani, L., Vassart, G., and Costagliola, S. (2006). Structural differences in the hinge region of the glycoprotein hormone receptors: evidence from the sulfated tyrosine residues. Mol. Endocrinol. Baltim. Md *20*, 3351–3363.

Boublik, Y., Di Bonito, P., and Jones, I.M. (1995). Eukaryotic virus display: engineering the major surface glycoprotein of the Autographa californica nuclear polyhedrosis virus (AcNPV) for the presentation of foreign proteins on the virus surface. Biotechnol. Nat. Publ. Co. *13*, 1079–1084.

Bowley, D.R., Labrijn, A.F., Zwick, M.B., and Burton, D.R. (2007). Antigen selection from an HIV-1 immune antibody library displayed on yeast yields many novel antibodies compared to selection from the same library displayed on phage. Protein Eng. Des. Sel. PEDS *20*, 81–90.

Breloy, I., Pacharra, S., Ottis, P., Bonar, D., Grahn, A., and Hanisch, F.-G. (2012). O-linked N,N'-diacetyllactosamine (LacdiNAc)-modified glycans in extracellular matrix glycoproteins are specifically phosphorylated at subterminal N-acetylglucosamine. J. Biol. Chem. *287*, 18275–18286.

Bustos, M.M., Luckow, V.A., Griffing, L.R., Summers, M.D., and Hall, T.C. (1988). Expression, glycosylation and secretion of phaseolin in a baculovirus system. Plant Mol. Biol. *10*, 475–488.

Calistri, A., Sette, P., Salata, C., Cancellotti, E., Forghieri, C., Comin, A., Göttlinger, H., Campadelli-Fiume, G., Palù, G., and Parolin, C. (2007). Intracellular trafficking and maturation of herpes simplex virus type 1 gB and virus egress require functional biogenesis of multivesicular bodies. J. Virol. *81*, 11468–11478.

Campbell, C.T., and Yarema, K.J. (2005). Large-scale approaches for glycobiology. Genome Biol. *6*, 236.

Cao, H., Zhang, G., Wang, X., Kong, L., and Geller, A.I. (2008). Enhanced nigrostriatal neuron-specific, long-term expression by using neural-specific promoters in combination with targeted gene transfer by modified helper virus-free HSV-1 vector particles. BMC Neurosci. *9*, 37.

Carter, P.J. (2011). Introduction to current and future protein therapeutics: a protein engineering perspective. Exp. Cell Res. *317*, 1261–1269.

Chen, C., and Okayama, H. (1987). High-efficiency transformation of mammalian cells by plasmid DNA. Mol. Cell. Biol. *7*, 2745–2752.

Claesson-Welsh, L., and Spear, P.G. (1987). Amino-terminal sequence, synthesis, and membrane insertion of glycoprotein B of herpes simplex virus type 1. J. Virol. *61*, 1–7.

Cocchi, F., Fusco, D., Menotti, L., Gianni, T., Eisenberg, R.J., Cohen, G.H., and Campadelli-Fiume, G. (2004). The soluble ectodomain of herpes simplex virus gD contains a membrane-proximal pro-fusion domain and suffices to mediate virus entry. Proc. Natl. Acad. Sci. U. S. A. *101*, 7445–7450.

Coia, G., Pontes-Braz, L., Nuttall, S.D., Hudson, P.J., and Irving, R.A. (2001). Panning and selection of proteins using ribosome display. J. Immunol. Methods *254*, 191–197.

Conner, J., Braidwood, L., and Brown, S.M. (2008). A strategy for systemic delivery of the oncolytic herpes virus HSV1716: redirected tropism by antibody-binding sites incorporated on the virion surface as a glycoprotein D fusion protein. Gene Ther. *15*, 1579–1592.

Connolly, S.A., Jackson, J.O., Jardetzky, T.S., and Longnecker, R. (2011). Fusing structure and function: a structural view of the herpesvirus entry machinery. Nat. Rev. Microbiol. *9*, 369–381.

Costagliola, S., Panneels, V., Bonomi, M., Koch, J., Many, M.C., Smits, G., and Vassart, G. (2002). Tyrosine sulfation is required for agonist recognition by glycoprotein hormone receptors. EMBO J. *21*, 504–513.

Darling, R.J., Kuchibhotla, U., Glaesner, W., Micanovic, R., Witcher, D.R., and Beals, J.M. (2002). Glycosylation of erythropoietin affects receptor binding kinetics: role of electrostatic interactions. Biochemistry (Mosc.) *41*, 14524–14531.

Daugherty, P.S., Olsen, M.J., Iverson, B.L., and Georgiou, G. (1999). Development of an optimized expression system for the screening of antibody libraries displayed on the Escherichia coli surface. Protein Eng. *12*, 613–621.

Davies, J., Jiang, L., Pan, L.Z., LaBarre, M.J., Anderson, D., and Reff, M. (2001). Expression of GnTIII in a recombinant anti-CD20 CHO production cell line: Expression of antibodies with altered glycoforms leads to an increase in ADCC through higher affinity for FC gamma RIII. Biotechnol. Bioeng. *74*, 288–294.

Davis, C.N., Zujovic, V., and Harrison, J.K. (2004). Viral macrophage inflammatory protein-II and fractalkine (CX3CL1) chimeras identify molecular determinants of affinity, efficacy, and selectivity at CX3CR1. Mol. Pharmacol. *66*, 1431–1439.

Dee, K.U., Shuler, M.L., and Wood, H.A. (1997). Inducing single-cell suspension of BTI-TN5B1-4 insect cells: I. The use of sulfated polyanions to prevent cell aggregation and enhance recombinant protein production. Biotechnol. Bioeng. *54*, 191–205.

Delorme, E., Lorenzini, T., Giffin, J., Martin, F., Jacobsen, F., Boone, T., and Elliott, S. (1992). Role of glycosylation on the secretion and biological activity of erythropoietin. Biochemistry (Mosc.) *31*, 9871–9876.

Diefenbach, R.J., Miranda-Saksena, M., Douglas, M.W., and Cunningham, A.L. (2008). Transport and egress of herpes simplex virus in neurons. Rev. Med. Virol. *18*, 35–51.

Dobrikova, E., Shveygert, M., Walters, R., and Gromeier, M. (2010). Herpes simplex virus proteins ICP27 and UL47 associate with polyadenylate-binding protein and control its subcellular distribution. J. Virol. *84*, 270–279.

Dollery, S.J., Wright, C.C., Johnson, D.C., and Nicola, A.V. (2011). Low-pH-dependent changes in the conformation and oligomeric state of the prefusion form of herpes simplex virus glycoprotein B are separable from fusion activity. J. Virol. *85*, 9964–9973.

Durocher, Y., Perret, S., and Kamen, A. (2002). High-level and high-throughput recombinant protein production by transient transfection of suspension-growing human 293-EBNA1 cells. Nucleic Acids Res. *30*, E9.

Egrie, J.C., and Browne, J.K. (2001). Development and characterization of novel erythropoiesis stimulating protein (NESP). Nephrol. Dial. Transplant. Off. Publ. Eur. Dial. Transpl. Assoc. - Eur. Ren. Assoc. *16 Suppl 3*, 3–13.

Egrie, J.C., Dwyer, E., Browne, J.K., Hitz, A., and Lykos, M.A. (2003). Darbepoetin alfa has a longer circulating half-life and greater in vivo potency than recombinant human erythropoietin. Exp. Hematol. *31*, 290–299.

Elliott, S., Egrie, J., Browne, J., Lorenzini, T., Busse, L., Rogers, N., and Ponting, I. (2004a). Control of rHuEPO biological activity: the role of carbohydrate. Exp. Hematol. *32*, 1146–1155.

Elliott, S., Chang, D., Delorme, E., Eris, T., and Lorenzini, T. (2004b). Structural requirements for additional N-linked carbohydrate on recombinant human erythropoietin. J. Biol. Chem. *279*, 16854–16862.

Encarnação, M., Kollmann, K., Trusch, M., Braulke, T., and Pohl, S. (2011). Post-translational modifications of the gamma-subunit affect intracellular trafficking and complex assembly of GlcNAc-1-phosphotransferase. J. Biol. Chem. *286*, 5311–5318.

Ernst, W., Grabherr, R., Wegner, D., Borth, N., Grassauer, A., and Katinger, H. (1998). Baculovirus surface display: construction and screening of a eukaryotic epitope library. Nucleic Acids Res. *26*, 1718–1723.

Fan, J.Q., Quesenberry, M.S., Takegawa, K., Iwahara, S., Kondo, A., Kato, I., and Lee, Y.C. (1995). Synthesis of neoglycoconjugates by transglycosylation with Arthrobacter protophormiae endo-beta-N-acetylglucosaminidase. Demonstration of a macro-cluster effect for mannose-binding proteins. J. Biol. Chem. *270*, 17730–17735.

Farzan, M., Mirzabekov, T., Kolchinsky, P., Wyatt, R., Cayabyab, M., Gerard, N.P., Gerard, C., Sodroski, J., and Choe, H. (1999). Tyrosine sulfation of the amino terminus of CCR5 facilitates HIV-1 entry. Cell *96*, 667–676.

Fellouse, F.A., Li, B., Compaan, D.M., Peden, A.A., Hymowitz, S.G., and Sidhu, S.S. (2005). Molecular recognition by a binary code. J. Mol. Biol. *348*, 1153–1162.

Ferris, S.P., Kodali, V.K., and Kaufman, R.J. (2014). Glycoprotein folding and quality-control mechanisms in protein-folding diseases. Dis. Model. Mech. *7*, 331–341.

Freeze, H.H., Chong, J.X., Bamshad, M.J., and Ng, B.G. (2014). Solving glycosylation disorders: fundamental approaches reveal complicated pathways. Am. J. Hum. Genet. *94*, 161–175.

Gac, N.T.L., Villani, G., Hoffmann, J.-S., and Boehmer, P.E. (1996). The UL8 Subunit of the Herpes Simplex Virus Type-1 DNA Helicase-Primase Optimizes Utilization of DNA Templates Covered by the Homologous Single-strand DNA-binding Protein ICP8. J. Biol. Chem. *271*, 21645–21651.

Gage, P.J., Sauer, B., Levine, M., and Glorioso, J.C. (1992). A cell-free recombination system for site-specific integration of multigenic shuttle plasmids into the herpes simplex virus type 1 genome. J. Virol. *66*, 5509–5515.

Gai, S.A., and Wittrup, K.D. (2007). Yeast surface display for protein engineering and characterization. Curr. Opin. Struct. Biol. *17*, 467–473.

Galdiero, M., Whiteley, A., Bruun, B., Bell, S., Minson, T., and Browne, H. (1997). Site-directed and linker insertion mutagenesis of herpes simplex virus type 1 glycoprotein H. J. Virol. *71*, 2163–2170.

Gemmill, T.R., and Trimble, R.B. (1999). Schizosaccharomyces pombe produces novel Gal0-2Man1-3 O-linked oligosaccharides. Glycobiology *9*, 507–515.

Gerngross, T.U. (2004). Advances in the production of human therapeutic proteins in yeasts and filamentous fungi. Nat. Biotechnol. *22*, 1409–1414.

Gianni, T., Martelli, P.L., Casadio, R., and Campadelli-Fiume, G. (2005). The ectodomain of herpes simplex virus glycoprotein H contains a membrane alpha-helix with attributes of an internal fusion peptide, positionally conserved in the herpesviridae family. J. Virol. *79*, 2931–2940.

Gianni, T., Cerretani, A., Dubois, R., Salvioli, S., Blystone, S.S., Rey, F., and Campadelli-Fiume, G. (2010). Herpes simplex virus glycoproteins H/L bind to cells independently of {alpha}V{beta}3 integrin and inhibit virus entry, and their constitutive expression restricts infection. J. Virol. *84*, 4013–4025.

Goder, V., and Melero, A. (2011). Protein O-mannosyltransferases participate in ER protein quality control. J. Cell Sci. *124*, 144–153.

González-Fernández, A., and Milstein, C. (1993). Analysis of somatic hypermutation in mouse Peyer's patches using immunoglobulin kappa light-chain transgenes. Proc. Natl. Acad. Sci. U. S. A. *90*, 9862–9866.

Graham, F.L., and van der Eb, A.J. (1973). A new technique for the assay of infectivity of human adenovirus 5 DNA. Virology *52*, 456–467.

Grandi, P., Wang, S., Schuback, D., Krasnykh, V., Spear, M., Curiel, D.T., Manservigi, R., and Breakefield, X.O. (2004). HSV-1 virions engineered for specific binding to cell surface receptors. Mol. Ther. J. Am. Soc. Gene Ther. *9*, 419–427.

Grapes, M., and O'Hare, P. (2000). Differences in determinants required for complex formation and transactivation in related VP16 proteins. J. Virol. *74*, 10112–10121.

Grünewald, K., Desai, P., Winkler, D.C., Heymann, J.B., Belnap, D.M., Baumeister, W., and Steven, A.C. (2003). Three-dimensional structure of herpes simplex virus from cryo-electron tomography. Science *302*, 1396–1398.

Handler, C.G., Eisenberg, R.J., and Cohen, G.H. (1996). Oligomeric structure of glycoproteins in herpes simplex virus type 1. J. Virol. *70*, 6067–6070.

Hang, H.C., and Bertozzi, C.R. (2005). The chemistry and biology of mucin-type O-linked glycosylation. Bioorg. Med. Chem. *13*, 5021–5034.

Harrison, R.L., and Jarvis, D.L. (2006). Protein N-glycosylation in the baculovirus-insect cell expression system and engineering of insect cells to produce "mammalianized" recombinant glycoproteins. Adv. Virus Res. *68*, 159–191.

Harrison, J.K., Fong, A.M., Swain, P.A., Chen, S., Yu, Y.R., Salafranca, M.N., Greenleaf, W.B., Imai, T., and Patel, D.D. (2001). Mutational analysis of the fractalkine chemokine domain. Basic amino acid residues differentially contribute to CX3CR1 binding, signaling, and cell adhesion. J. Biol. Chem. *276*, 21632–21641.

Hartley, J.L., Temple, G.F., and Brasch, M.A. (2000). DNA cloning using in vitro site-specific recombination. Genome Res. *10*, 1788–1795.

Hayward, G.S., Jacob, R.J., Wadsworth, S.C., and Roizman, B. (1975). Anatomy of herpes simplex virus DNA: evidence for four populations of molecules that differ in the relative orientations of their long and short components. Proc. Natl. Acad. Sci. U. S. A. *72*, 4243–4247.

Heldwein, E.E., Lou, H., Bender, F.C., Cohen, G.H., Eisenberg, R.J., and Harrison, S.C. (2006). Crystal structure of glycoprotein B from herpes simplex virus 1. Science *313*, 217–220.

Helenius, A., and Aebi, M. (2004). Roles of N-linked glycans in the endoplasmic reticulum. Annu. Rev. Biochem. *73*, 1019–1049.

Herold, B.C., WuDunn, D., Soltys, N., and Spear, P.G. (1991). Glycoprotein C of herpes simplex virus type 1 plays a principal role in the adsorption of virus to cells and in infectivity. J. Virol. *65*, 1090–1098.

Higuchi, K., Araki, T., Matsuzaki, O., Sato, A., Kanno, K., Kitaguchi, N., and Ito, H. (1997). Cell display library for gene cloning of variable regions of human antibodies to hepatitis B surface antigen. J. Immunol. Methods *202*, 193–204.

Ho, M., Nagata, S., and Pastan, I. (2006). Isolation of anti-CD22 Fv with high affinity by Fv display on human cells. Proc. Natl. Acad. Sci. U. S. A. *103*, 9637–9642.

Hoess, R.H., Wierzbicki, A., and Abremski, K. (1986). The role of the loxP spacer region in P1 site-specific recombination. Nucleic Acids Res. *14*, 2287–2300.

Hutchinson, L., Browne, H., Wargent, V., Davis-Poynter, N., Primorac, S., Goldsmith, K., Minson, A.C., and Johnson, D.C. (1992). A novel herpes simplex virus glycoprotein, gL, forms a complex with glycoprotein H (gH) and affects normal folding and surface expression of gH. J. Virol. *66*, 2240–2250.

Irving, M.B., Pan, O., and Scott, J.K. (2001). Random-peptide libraries and antigen-fragment libraries for epitope mapping and the development of vaccines and diagnostics. Curr. Opin. Chem. Biol. *5*, 314–324.

Jefferis, R. (2009). Glycosylation as a strategy to improve antibody-based therapeutics. Nat. Rev. Drug Discov. *8*, 226–234.

Jespers, L.S., Roberts, A., Mahler, S.M., Winter, G., and Hoogenboom, H.R. (1994). Guiding the selection of human antibodies from phage display repertoires to a single epitope of an antigen. Biotechnol. Nat. Publ. Co. *12*, 899–903.

Johnson, D.C., Burke, R.L., and Gregory, T. (1990). Soluble forms of herpes simplex virus glycoprotein D bind to a limited number of cell surface receptors and inhibit virus entry into cells. J. Virol. *64*, 2569–2576.

Kamionka, M. (2011). Engineering of therapeutic proteins production in Escherichia coli. Curr. Pharm. Biotechnol. *12*, 268–274.

Kanno, T., Yaguchi, T., Nagata, T., Mukasa, T., and Nishizaki, T. (2010). Regulation of AMPA receptor trafficking by O-glycosylation. Neurochem. Res. *35*, 782–788.

Karasneh, G.A., and Shukla, D. (2011). Herpes simplex virus infects most cell types in vitro: clues to its success. Virol. J. *8*, 481.

Kitts, P.A., and Possee, R.D. (1993). A method for producing recombinant baculovirus expression vectors at high frequency. BioTechniques *14*, 810–817.

Kouvatsis, V., Argnani, R., Tsitoura, E., Arsenakis, M., Georgopoulou, U., Mavromara, P., and Manservigi, R. (2007). Characterization of herpes simplex virus type 1 recombinants that express and incorporate high levels of HCV E2-gC chimeric proteins. Virus Res. *123*, 40–49.

Kriplani, U., and Kay, B.K. (2005). Selecting peptides for use in nanoscale materials using phage-displayed combinatorial peptide libraries. Curr. Opin. Biotechnol. *16*, 470–475.

Landon, L.A., Zou, J., and Deutscher, S.L. (2004). Is phage display technology on target for developing peptide-based cancer drugs? Curr. Drug Discov. Technol. *1*, 113–132.

Langer, S.J., Ghafoori, A.P., Byrd, M., and Leinwand, L. (2002). A genetic screen identifies novel non-compatible loxP sites. Nucleic Acids Res. *30*, 3067–3077.

Laquerre, S., Anderson, D.B., Stolz, D.B., and Glorioso, J.C. (1998a). Recombinant herpes simplex virus type 1 engineered for targeted binding to erythropoietin receptor-bearing cells. J. Virol. *72*, 9683–9697.

Laquerre, S., Argnani, R., Anderson, D.B., Zucchini, S., Manservigi, R., and Glorioso, J.C. (1998b). Heparan sulfate proteoglycan binding by herpes simplex virus type 1 glycoproteins B and C, which differ in their contributions to virus attachment, penetration, and cell-to-cell spread. J. Virol. *72*, 6119–6130.

Leader, B., Baca, Q.J., and Golan, D.E. (2008). Protein therapeutics: a summary and pharmacological classification. Nat. Rev. Drug Discov. *7*, 21–39.

Levin, A.M., and Weiss, G.A. (2006). Optimizing the affinity and specificity of proteins with molecular display. Mol. Biosyst. *2*, 49–57.

Lin, Y., Tsumuraya, T., Wakabayashi, T., Shiraga, S., Fujii, I., Kondo, A., and Ueda, M. (2003). Display of a functional hetero-oligomeric catalytic antibody on the yeast cell surface. Appl. Microbiol. Biotechnol. *62*, 226–232.

Lis, H., and Sharon, N. (1993). Protein glycosylation. Structural and functional aspects. Eur. J. Biochem. FEBS *218*, 1–27.

Loret, S., Guay, G., and Lippé, R. (2008). Comprehensive characterization of extracellular herpes simplex virus type 1 virions. J. Virol. *82*, 8605–8618.

Lupold, S.E., Kudrolli, T.A., Chowdhury, W.H., Wu, P., and Rodriguez, R. (2007). A novel method for generating and screening peptides and libraries displayed on adenovirus fiber. Nucleic Acids Res. *35*, e138.

Lymberopoulos, M.H., and Pearson, A. (2010). Relocalization of upstream binding factor to viral replication compartments is UL24 independent and follows the onset of herpes simplex virus 1 DNA synthesis. J. Virol. *84*, 4810–4815.

Marinaro, J.A., Neumann, G.M., Russo, V.C., Leeding, K.S., and Bach, L.A. (2000). O-glycosylation of insulin-like growth factor (IGF) binding protein-6 maintains high IGF-II binding affinity by decreasing binding to glycosaminoglycans and susceptibility to proteolysis. Eur. J. Biochem. FEBS *267*, 5378–5386.

Mattanovich, D., Branduardi, P., Dato, L., Gasser, B., Sauer, M., and Porro, D. (2012). Recombinant Protein Production in Yeasts. In Recombinant Gene Expression, A. Lorence, ed. (Humana Press), pp. 329–358.

McCafferty, J., Griffiths, A.D., Winter, G., and Chiswell, D.J. (1990). Phage antibodies: filamentous phage displaying antibody variable domains. Nature *348*, 552–554.

McGeoch, D.J., Dalrymple, M.A., Dolan, A., McNab, D., Perry, L.J., Taylor, P., and Challberg, M.D. (1988). Structures of herpes simplex virus type 1 genes required for replication of virus DNA. J. Virol. *62*, 444–453.

Milne, R.S.B., Nicola, A.V., Whitbeck, J.C., Eisenberg, R.J., and Cohen, G.H. (2005). Glycoprotein D receptor-dependent, low-pH-independent endocytic entry of herpes simplex virus type 1. J. Virol. *79*, 6655–6663.

Miranda-Saksena, M., Boadle, R.A., Aggarwal, A., Tijono, B., Rixon, F.J., Diefenbach, R.J., and Cunningham, A.L. (2009). Herpes simplex virus utilizes the large secretory vesicle pathway for anterograde transport of tegument and envelope proteins and for viral exocytosis from growth cones of human fetal axons. J. Virol. *83*, 3187–3199.

Mizoue, L.S., Sullivan, S.K., King, D.S., Kledal, T.N., Schwartz, T.W., Bacon, K.B., and Handel, T.M. (2001). Molecular determinants of receptor binding and signaling by the CX3C chemokine fractalkine. J. Biol. Chem. *276*, 33906–33914.

Monier, K., Armas, J.C., Etteldorf, S., Ghazal, P., and Sullivan, K.F. (2000). Annexation of the interchromosomal space during viral infection. Nat. Cell Biol. *2*, 661–665.

Moore, K.L. (2003). The biology and enzymology of protein tyrosine O-sulfation. J. Biol. Chem. *278*, 24243–24246.

Moremen, K.W., Tiemeyer, M., and Nairn, A.V. (2012). Vertebrate protein glycosylation: diversity, synthesis and function. Nat. Rev. Mol. Cell Biol. *13*, 448–462.

Murase, K., Morrison, K.L., Tam, P.Y., Stafford, R.L., Jurnak, F., and Weiss, G.A. (2003). EF-Tu binding peptides identified, dissected, and affinity optimized by phage display. Chem. Biol. *10*, 161–168.

Nezlin, R., and Ghetie, V. (2004). Interactions of immunoglobulins outside the antigen-combining site. Adv. Immunol. *82*, 155–215.

O'Donnell, C.D., Kovacs, M., Akhtar, J., Valyi-Nagy, T., and Shukla, D. (2010). Expanding the role of 3-O sulfated heparan sulfate in herpes simplex virus type-1 entry. Virology *397*, 389–398.

O'Neil, K.T., and Hoess, R.H. (1995). Phage display: protein engineering by directed evolution. Curr. Opin. Struct. Biol. *5*, 443–449.

Ojala, P.M., Sodeik, B., Ebersold, M.W., Kutay, U., and Helenius, A. (2000). Herpes simplex virus type 1 entry into host cells: reconstitution of capsid binding and uncoating at the nuclear pore complex in vitro. Mol. Cell. Biol. *20*, 4922–4931.

Oker-Blom, C., Airenne, K.J., and Grabherr, R. (2003). Baculovirus display strategies: Emerging tools for eukaryotic libraries and gene delivery. Brief. Funct. Genomic. Proteomic. *2*, 244–253.

Osbourn, J.K., Derbyshire, E.J., Vaughan, T.J., Field, A.W., and Johnson, K.S. (1998). Pathfinder selection: in situ isolation of novel antibodies. Immunotechnology Int. J. Immunol. Eng. *3*, 293–302.

Parry, C., Bell, S., Minson, T., and Browne, H. (2005). Herpes simplex virus type 1 glycoprotein H binds to alphavbeta3 integrins. J. Gen. Virol. *86*, 7–10.

Patel, T.P., Parekh, R.B., Moellering, B.J., and Prior, C.P. (1992). Different culture methods lead to differences in glycosylation of a murine IgG monoclonal antibody. Biochem. J. *285 ( Pt 3)*, 839–845.

Peng, T., Ponce de Leon, M., Novotny, M.J., Jiang, H., Lambris, J.D., Dubin, G., Spear, P.G., Cohen, G.H., and Eisenberg, R.J. (1998). Structural and antigenic analysis of a truncated form of the herpes simplex virus glycoprotein gH-gL complex. J. Virol. *72*, 6092–6103.

Perlman, S., van den Hazel, B., Christiansen, J., Gram-Nielsen, S., Jeppesen, C.B., Andersen, K.V., Halkier, T., Okkels, S., and Schambye, H.T. (2003). Glycosylation of an N-terminal extension prolongs the half-life and increases the in vivo activity of follicle stimulating hormone. J. Clin. Endocrinol. Metab. *88*, 3227–3235.

Pertel, P.E., Fridberg, A., Parish, M.L., and Spear, P.G. (2001). Cell fusion induced by herpes simplex virus glycoproteins gB, gD, and gH-gL requires a gD receptor but not necessarily heparan sulfate. Virology *279*, 313–324.

Plückthun, A. (1991). Antibody engineering. Curr. Opin. Biotechnol. *2*, 238–246.

Plückthun, A., and Pfitzinger, I. (1991). Comparison of the Fv fragments of different phosphorylcholine binding antibodies expressed in Escherichia coli. Ann. N. Y. Acad. Sci. *646*, 115–124.

Ramaraj, T., Angel, T., Dratz, E.A., Jesaitis, A.J., and Mumey, B. (2012). Antigen-antibody interface properties: composition, residue interactions, and features of 53 non-redundant structures. Biochim. Biophys. Acta *1824*, 520–532.

Rao, B.M., Girvin, A.T., Ciardelli, T., Lauffenburger, D.A., and Wittrup, K.D. (2003). Interleukin-2 mutants with enhanced alpha-receptor subunit binding affinity. Protein Eng. *16*, 1081–1087.

Raska, M., Takahashi, K., Czernekova, L., Zachova, K., Hall, S., Moldoveanu, Z., Elliott, M.C., Wilson, L., Brown, R., Jancova, D., et al. (2010). Glycosylation patterns of HIV-1 gp120 depend on the type of expressing cells and affect antibody recognition. J. Biol. Chem. *285*, 20860–20869.

Renschler, M.F., Bhatt, R.R., Dower, W.J., and Levy, R. (1994). Synthetic peptide ligands of the antigen binding receptor induce programmed cell death in a human B-cell lymphoma. Proc. Natl. Acad. Sci. U. S. A. *91*, 3623–3627.

Reske, A., Pollara, G., Krummenacher, C., Chain, B.M., and Katz, D.R. (2007). Understanding HSV-1 entry glycoproteins. Rev. Med. Virol. *17*, 205–215.

Runkel, L., Meier, W., Pepinsky, R.B., Karpusas, M., Whitty, A., Kimball, K., Brickelmaier, M., Muldowney, C., Jones, W., and Goelz, S.E. (1998). Structural and functional differences between glycosylated and non-glycosylated forms of human interferon-beta (IFN-beta). Pharm. Res. *15*, 641–649.

Rux, A.H., Lou, H., Lambris, J.D., Friedman, H.M., Eisenberg, R.J., and Cohen, G.H. (2002). Kinetic analysis of glycoprotein C of herpes simplex virus types 1 and 2 binding to heparin, heparan sulfate, and complement component C3b. Virology *294*, 324–332.

Satoh, T., and Arase, H. (2008). HSV-1 infection through inhibitory receptor, PILRalpha. Uirusu *58*, 27–36.

Scanlan, P.M., Tiwari, V., Bommireddy, S., and Shukla, D. (2003). Cellular expression of gH confers resistance to herpes simplex virus type-1 entry. Virology *312*, 14–24.

Schaffitzel, C., Hanes, J., Jermutus, L., and Plückthun, A. (1999). Ribosome display: an in vitro method for selection and evolution of antibodies from libraries. J. Immunol. Methods *231*, 119–135.

Schmidt, P.M., Sparrow, L.G., Attwood, R.M., Xiao, X., Adams, T.E., and McKimm-Breschkin, J.L. (2012). Taking down the FLAG! How insect cell expression challenges an established tag-system. PloS One *7*, e37779.

Schröder, C.H., and Urbaczka, G. (1978). Excess of interfering over infectious particles in herpes simplex virus passaged at high m.o.i. and their effect on single-cell survival. J. Gen. Virol. *41*, 493–501.

Sheren, J., Langer, S.J., and Leinwand, L.A. (2007). A randomized library approach to identifying functional lox site domains for the Cre recombinase. Nucleic Acids Res. *35*, 5464–5473.

Shusta, E.V., Kieke, M.C., Parke, E., Kranz, D.M., and Wittrup, K.D. (1999). Yeast polypeptide fusion surface display levels predict thermal stability and soluble secretion efficiency. J. Mol. Biol. *292*, 949–956.

Smith, G.P. (1985). Filamentous fusion phage: novel expression vectors that display cloned antigens on the virion surface. Science *228*, 1315–1317.

Sodeik, B., Ebersold, M.W., and Helenius, A. (1997). Microtubule-mediated transport of incoming herpes simplex virus 1 capsids to the nucleus. J. Cell Biol. *136*, 1007–1021.

Solá, R.J., and Griebenow, K. (2009). Effects of glycosylation on the stability of protein pharmaceuticals. J. Pharm. Sci. *98*, 1223–1245.

Solá, R.J., and Griebenow, K. (2010). Glycosylation of therapeutic proteins: an effective strategy to optimize efficacy. BioDrugs Clin. Immunother. Biopharm. Gene Ther. *24*, 9–21.

Song, R., Oren, D.A., Franco, D., Seaman, M.S., and Ho, D.D. (2013). Strategic addition of an N-linked glycan to a monoclonal antibody improves its HIV-1-neutralizing activity. Nat. Biotechnol. *31*, 1047–1052.

Spear, M.A., Schuback, D., Miyata, K., Grandi, P., Sun, F., Yoo, L., Nguyen, A., Brandt, C.R., and Breakefield, X.O. (2003). HSV-1 amplicon peptide display vector. J. Virol. Methods *107*, 71–79.

Van den Steen, P., Rudd, P.M., Dwek, R.A., and Opdenakker, G. (1998). Concepts and principles of O-linked glycosylation. Crit. Rev. Biochem. Mol. Biol. *33*, 151–208.

Stiles, K.M., and Krummenacher, C. (2010). Glycoprotein D actively induces rapid internalization of two nectin-1 isoforms during herpes simplex virus entry. Virology *399*, 109–119.

Stiles, K.M., Whitbeck, J.C., Lou, H., Cohen, G.H., Eisenberg, R.J., and Krummenacher, C. (2010). Herpes simplex virus glycoprotein D interferes with binding of herpesvirus entry mediator to its ligands through downregulation and direct competition. J. Virol. *84*, 11646–11660.

Stone, S.R., and Hofsteenge, J. (1986). Kinetics of the inhibition of thrombin by hirudin. Biochemistry (Mosc.) *25*, 4622–4628.

Streit, W.J., Davis, C.N., and Harrison, J.K. (2005). Role of fractalkine (CX3CL1) in regulating neuron-microglia interactions: development of viral-based CX3CR1 antagonists. Curr. Alzheimer Res. *2*, 187–189.

Subramanian, R.P., and Geraghty, R.J. (2007). Herpes simplex virus type 1 mediates fusion through a hemifusion intermediate by sequential activity of glycoproteins D, H, L, and B. Proc. Natl. Acad. Sci. U. S. A. *104*, 2903–2908.

Tal-Singer, R., Peng, C., Ponce De Leon, M., Abrams, W.R., Banfield, B.W., Tufaro, F., Cohen, G.H., and Eisenberg, R.J. (1995). Interaction of herpes simplex virus glycoprotein gC with mammalian cell surface molecules. J. Virol. *69*, 4471–4483.

Taube, R., Zhu, Q., Xu, C., Diaz-Griffero, F., Sui, J., Kamau, E., Dwyer, M., Aird, D., and Marasco, W.A. (2008). Lentivirus display: stable expression of human antibodies on the surface of human cells and virus particles. PloS One *3*, e3181.

Tian, E., and Ten Hagen, K.G. (2009). Recent insights into the biological roles of mucin-type O-glycosylation. Glycoconj. J. *26*, 325–334.

Tognon, M., Cattozzo, E.M., Bianchi, S., and Romanelli, M.G. (1996). Enhancement of HSV-DNA infectivity, in Vero and RS cells, by a modified calcium-phosphate transfection technique. Virus Genes *12*, 193–197.

Ulrich, H.D., Patten, P.A., Yang, P.L., Romesberg, F.E., and Schultz, P.G. (1995). Expression studies of catalytic antibodies. Proc. Natl. Acad. Sci. U. S. A. *92*, 11907–11911.

Unligil, U.M., Zhou, S., Yuwaraj, S., Sarkar, M., Schachter, H., and Rini, J.M. (2000). X-ray crystal structure of rabbit N-acetylglucosaminyltransferase I: catalytic mechanism and a new protein superfamily. EMBO J. *19*, 5269–5280.

Urban, J.H., Schneider, R.M., Compte, M., Finger, C., Cichutek, K., Alvarez-Vallina, L., and Buchholz, C.J. (2005). Selection of functional human antibodies from retroviral display libraries. Nucleic Acids Res. *33*, e35.

Varki, A. (1993). Biological roles of oligosaccharides: all of the theories are correct. Glycobiology *3*, 97–130.

Varki, A., Freeze, H.H., and Gagneux, P. (2009). Evolution of Glycan Diversity. In Essentials of Glycobiology, A. Varki, R.D. Cummings, J.D. Esko, H.H. Freeze, P. Stanley, C.R. Bertozzi, G.W. Hart, and M.E. Etzler, eds. (Cold Spring Harbor (NY): Cold Spring Harbor Laboratory Press),.

Wang, X.X., and Shusta, E.V. (2005). The use of scFv-displaying yeast in mammalian cell surface selections. J. Immunol. Methods *304*, 30–42.

Wang, X., Kong, L., Zhang, G., Sun, M., and Geller, A.I. (2005). Targeted gene transfer to nigrostriatal neurons in the rat brain by helper virus-free HSV-1 vector particles that contain either a chimeric HSV-1 glycoprotein C-GDNF or a gC-BDNF protein. Brain Res. Mol. Brain Res. *139*, 88–102.

Wawrzynczak, E.J., Cumber, A.J., Parnell, G.D., Jones, P.T., and Winter, G. (1992). Blood clearance in the rat of a recombinant mouse monoclonal antibody lacking the N-linked oligosaccharide side chains of the CH2 domains. Mol. Immunol. *29*, 213–220.

Werstuck, G., Bilan, P., and Capone, J.P. (1990). Enhanced infectivity of herpes simplex virus type 1 viral DNA in a cell line expressing the trans-inducing factor Vmw65. J. Virol. *64*, 984–991.

Whitbeck, J.C., Peng, C., Lou, H., Xu, R., Willis, S.H., Ponce de Leon, M., Peng, T., Nicola, A.V., Montgomery, R.I., Warner, M.S., et al. (1997). Glycoprotein D of herpes simplex virus (HSV) binds directly to HVEM, a member of the tumor necrosis factor receptor superfamily and a mediator of HSV entry. J. Virol. *71*, 6083–6093.

Wilson, D.S., Keefe, A.D., and Szostak, J.W. (2001). The use of mRNA display to select high-affinity protein-binding peptides. Proc. Natl. Acad. Sci. U. S. A. *98*, 3750–3755.

Wittels, M., and Spear, P.G. (1991). Penetration of cells by herpes simplex virus does not require a low pH-dependent endocytic pathway. Virus Res. *18*, 271–290.

Wright, A., and Morrison, S.L. (1998). Effect of C2-associated carbohydrate structure on Ig effector function: studies with chimeric mouse-human IgG1 antibodies in glycosylation mutants of Chinese hamster ovary cells. J. Immunol. Baltim. Md 1950 *160*, 3393–3402.

Wright, A., Tao, M.H., Kabat, E.A., and Morrison, S.L. (1991). Antibody variable region glycosylation: position effects on antigen binding and carbohydrate structure. EMBO J. *10*, 2717–2723.

Wright, R.M., Gram, H., Vattay, A., Byme, S., Lake, P., and Dottavio, D. (1995). Binding epitope of somatostatin defined by phage-displayed peptide libraries. Biotechnol. Nat. Publ. Co. *13*, 165–169.

Zago, A., and Spear, P.G. (2003). Differences in the N termini of herpes simplex virus type 1 and 2 gDs that influence functional interactions with the human entry receptor Nectin-2 and an entry receptor expressed in Chinese hamster ovary cells. J. Virol. *77*, 9695–9699.

Zhou, C., Jacobsen, F.W., Cai, L., Chen, Q., and Shen, W.D. (2010). Development of a novel mammalian cell surface antibody display platform. mAbs *2*, 508–518.

Ziltener, H.J., Clark-Lewis, I., Jones, A.T., and Dy, M. (1994). Carbohydrate does not modulate the in vivo effects of injected interleukin-3. Exp. Hematol. *22*, 1070–1075.

Zwick, M.B., Labrijn, A.F., Wang, M., Spenlehauer, C., Saphire, E.O., Binley, J.M., Moore, J.P., Stiegler, G., Katinger, H., Burton, D.R., et al. (2001). Broadly neutralizing antibodies targeted to the membrane-proximal external region of human immunodeficiency virus type 1 glycoprotein gp41. J. Virol. *75*, 10892–10905.

Appendix 1.

Appendix 1 contains the DNA and amino acid sequences of novel CX3CL1 mutants that were isolated during experiment 4.2. The name of each mutant is listed, followed by the alignment of the DNA sequence for that mutant against the FKN-Bae1 gene. Only the portion of the gene containing the site of mutagenesis is shown. Insertions and deletions are indicated by a "-" symbol. An alignment between the protein sequence for the mutant against the wt-CX3CL1 protein and the CX3CL1-Bae1 protein is shown. Novel sequences are shown in red. For reference, the CX3CL1-Bae1 gene aligned next to the CX3CL1 gene is shown at the beginning of appendix 1.

Bae1

```
Wt-  ATGGCTCCCTCACAGCTCGCGTGGCTGCTGCGCCTGGCCGCGTTCTTTCATCTGTGTACT  60
     ||||||||||||||||||||||||||||||||||||||||||||||||||||||||||||
Bae1-atggctccctcacagctcgcgtggctgctgcgcctggccgcgttctttcatctgtgtact  60

CTGCTGGCGGGTCAGCACCTCGGCATGACGAA--A--TGCAA-CATCAC--GTGCCACAA
|||||||||||||||||||||||||||||||  |  |||   |       |||||||||
ctgctggcgggtcagcacctcggcatgacgaactacttgcgtacccttgttgtgccacaa

GATGACCTCGCCAATCCCAGTGACCTTGCTCATCCACTATCAACTGAACCAGGAGTCCTG  173
||||||||||||||||||||||||||||||||||||||||||||||||||||||||||||
gatgacctcgccaatcccagtgaccttgctcatccactatcaactgaaccaggagtcctg  180

Wt-  MAPSQLAWLLRLAAFFHLCTLLAGQHLGMTKCNITCHKMTSPIPVTLLIHYQLNQES
Bae1-MAPSQLAWLLRLAAFFHLCTLLAGQHLGMSNYLRTLVVPQDDLANPSDLAHPLSTE
      PGVLRQARHHPGDETAQTLLC*
```

Del 1

```
Bae1-ATGGCTCCCTCACAGCTCGCGTGGCTGCTGCGCCTGGCCGCGTTCTTTCATCTGTGTACT  60
     ||||||||||||||||||||||||||||||||||||||||||||||| ||||||||||
Del1-atggctccctcacagctcgcgtggctgctgcgcctggccgcgttctttc-tctgtgtact  59

CTGCTGGCGGGTCAGCACCTCGGCATGACGAACTACTTGCGTACCCTTGTTGTGCCACAA  120
||||||||||||||||||                                        ||
ctgctggcgggtcagcacc----------------------------------------aa  80

GATGACCTCGCCAATCCCAGTGACCTTGCTCATCCACTATCAACTGAACCAGGAGTCCTG  180
||||||||||||||||||||||||||||||||||||||||||||||||||||||||||||
gatgacctcgccaatcccagtgaccttgctcatccactatcaactgaaccaggagtcctg  140

Bae1-MAPSQLAWLLRLAAFFHLCTLLAGQHLGMSNYLRTLVVPQDDLANPSDLAHPLSTE
Del1-MAPSQLAWLLRLAAFF-LCVLCWRVST----------KMTSPIPVTLLIHYQLNQES
Wt-  MAPSQLAWLLRLAAFFHLCTLLAGQHLGMTKCNITCHKMTSPIPVTLLIHYQLNQES
```

Appendix 1 (cont.)

Del 2

```
Bae1-ATGGCTCCCTCACAGCTCGCG-TGGC--TGCTGCGCCTGGCCGCGTTCTTTCATCTGTGT  57
     ||||||||||||||||||||    ||  || |  ||   | ||||||||||| |||||||
Del2-atggctccctcacagctcgcgaa-gctatgttctgcgctggcgcgttctttc-tctgtgt  58

ACTCTGCTGGCGGGTCAGCACCTCGGCATGACGAACTACTTGCGTACCCTTGTTGTGCCA  117
||||||||||||||||||||
actctgctggcgggtcagca----------------------------------------  78

CAAGATGACCTCGCCAATCCCAGTGACCTTGCTCATCCACTATCAACTGAACCAGGAGTC  177
    |||||||||||||||| |||||||||||||||||||||||||||||||||||||||
----atgacctcgccaatcccattgaccttgctcatccactatcaactgaaccaggagtc  134


Bae1-MAPSQLAWLLRLAAFFHLCTLLAGQHLGMSNYLRTLVVPQDDLANPSDLAHPLSTE
Del2-MAPSQLAKLCSALARSFSVYSAGGSA------------MTSPIPLTLLIHYQLNQES
Wt-  MAPSQLAWLLRLAAFFHLCTLLAGQHLGMTKCNITCHKMTSPIPVTLLIHYQLNQES
```

Del 3

```
Bae1-ATGGCTCCCTCACAGCTCGCGTGGCTGCTGCGCC-TGGCCGCGTTCTTTCATCTGTGTAC 60
     |||||||||||||||||||||||||||||||| |||||||||||||||||||||||||
Del3-atggctccctcacagctcgcgtggctgctgcgccatggccgcgttctttcatctgtgtac 61

TCTGCTGGCGGGTCAGCACCTCGGCATGACGAACTACTTGCGTACCCTTGTTGTGCCACA
|||||        |||
tctgc--------cagt-------------------------------------------

AGATGACCTCGCCAATCCCAGTGACCTTGCTCATCCACTATCAACTGAACCAGGAGTCCT
  ||||||||||||||||||||||||||||||||||||||||||||||||||||||||||
--atgacctcgccaatcccagtgaccttgctcatccactatcaactgaaccaggagtcct


Bae1-MAPSQLAWLLRLAAFFHLCTLLAGQHLGMSNYLRTLVVPQDDLANPSDLAHPLSTE
Del3-MAPSQLAWLLRHGRVLSSVYSAS---------------MTSPIPVTLLIHYQLNQES
Wt-  MAPSQLAWLLRLAAFFHLCTLLAGQHLGMTKCNITCHKMTSPIPVTLLIHYQLNQES
```

Appendix 1 (Cont.)

Del 4

```
Bae1-ATGGCTCCCTCACAGCTCGCGTGGCTGCTGCGCCTGGCCGCGTTCTTTCATCTGTGTACT  60
     ||||||||||||||||||||||||||||||||||||||||||||||||||||||||||||
Del4-atggctccctcacagctcgcgtggctgctgcgcctggccgcgttctttcatctgtgtact  60

CTGCTGGCGGGTCAGCACCTCGGCATGACGAACTACTTGCGT-ACCCTTGTTGTGCCACA  119
||||||||||||||||||||      ||||||  | |     | ||       ||||||||
ctgctggcgggtcagcacct------gacgaaatgcaaca-tgac-------gtgccaca  106

AGATGACCTCGCCAATCCCAGTGACCTTGCTCATCCACTATCAACTGAACCAGGAGTCCT  179
||||||||||||||||||||||||||||||||||||||||||||||||||||||||||||
agatgacctcgccaatcccagtgaccttgctcatccactatcaactgaaccaggagtcct  166


Bae1-MAPSQLAWLLRLAAFFHLCTLLAGQHLGMSNYLRTLVVPQDDLANPSDLAHPLSTE
Del4-MAPSQLAWLLRLAAFFHLCTLLAGQHL--TKCNMTCHKMTSPIPVTLLIHYQLNQES
Wt-  MAPSQLAWLLRLAAFFHLCTLLAGQHLGMTKCNITCHKMTSPIPVTLLIHYQLNQES
```

6-5 (library)

```
Wt- ATGGCTCCCTCACAGCTCGCGTGGCTGCTGCGCCTGGCCGCGTTCTTTCATCTGTGTACT  60
    ||||||||||||||||||||||||||||||||||||||||||||||||||||||||||||
6-5-atggctccctcacagctcgcgtggctgctgcgcctggccgcgttctttcatctgtgtact  60

CTGCTGGCGGGTCAGCACCTCGGCATGACGAAATGCAACATCACGTGCCACAAGATGAC  119
|||||||||||||||||||||||||||||||||||  |  ||||||||||||||||
ctgctggcgggtcagcacctcggcatgacgaaatgcaataagacgtgccacaagatgac  119

CTCGCCAATCCCAGTGACCTTGCTCATCCACTATCAACTGAACCAGGAGTCCTGCGGCAA  179
|||||||||||||||||||||||||||||||||||||||||||||||||||||||||||
Ctcgccaatcccagtgaccttgctcatccactatcaactgaaccaggagtcctgcggcaa


Bae1-MAPSQLAWLLRLAAFFHLCTLLAGQHLGMSNYLRTLVVPQDDLANPSDLAHPLSTE
6-5- MAPSQLAWLLRLAAFFHLCTLLAGQHLGMTKCNKTCHKMTSPIPVTLLIHYQLNQES
Wt-  MAPSQLAWLLRLAAFFHLCTLLAGQHLGMTKCNITCHKMTSPIPVTLLIHYQLNQES
```

Appendix 1 (Cont.)

7-3

```
Bae1-ATGGCTCCCTCACAGCTCGCGTGGCTGCTGCGCCTGGCCGCGTTCTTTCATCTGTGTACT  60
     |||||||||||||||||||||||||||||||||||| ||||||||||||||||||||
7-3- atggctccctcacagctcgcgtggctgctgcgcctggc-gcgttctttcatctgtgtact  59

CTGCTGGCGGGTCAGCACCTCGGCATGACGAACTACTTGCGT-ACCCTTGTTGTGCCACA  119
||||||||||||||||        |||||  || |     | ||       ||||||||
ctgctggcgggtcagca--------tgacgtgctgcaaca-tcac-------gtgccaca  103

AGATGACCTCGCCAATCCCAGTGACCTTGCTCATCCACTATCAACTGAACCAGGAGTCCT
||||||||||||||||||||||||||||||||||||||||||||||||||||||||||||
Agatgacctcgccaatcccagtgaccttgctcatccactatcaactgaaccaggagtcct


Bae1-MAPSQLAWLLRLAAFFHLCTLLAGQHLGMSNYLRTLVVPQDDLANPSDLAHPLSTE
7-3- MAPSQLAWLLRLARSFICVLCWRVS---MTCCNITCHKMTSPIPVTLLIHYQLNQES
Wt-  MAPSQLAWLLRLAAFFHLCTLLAGQHLGMTKCNITCHKMTSPIPVTLLIHYQLNQES
```

3-1 (wt)

```
Wt- ATGGCTCCCTCACAGCTCGCGTGGCTGCTGCGCCTGGCCGCGTTCTTTCATCTGTGTACT  60
    ||||||||||||||||||||||||||||||||||||||||||||||||||||||||||||
3-1-atggctccctcacagctcgcgtggctgctgcgcctggccgcgttctttcatctgtgtact  60

CTGCTGGCGGGTCAGCACCTCGGCATGACGAAATGCAACATCACGTGCCACAAGATGACC  120
|||||||||||||||||||||||||||| ||||||||||||||||||||||||||||||
ctgctggcgggtcagcacctcggcatgaccaaatgcaacatcacgtgccacaagatgacc  120

TCGCCAATCCCAGTGACCTTGCTCATCCACTATCAACTGAACCAGGAGTCCTGCGGCAAG  180
||||||||||||||||||||||||||||||||||||||||||||||||||||||||||||
tcgccaatcccagtgaccttgctcatccactatcaactgaaccaggagtcctgcggcaag  180


Bae1-MAPSQLAWLLRLAAFFHLCTLLAGQHLGMSNYLRTLVVPQDDLANPSDLAHPLSTE
3-1- MAPSQLAWLLRLAAFFHLCTLLAGQHLGMTKCNITCHKMTSPIPVTLLIHYQLNQES
Wt-  MAPSQLAWLLRLAAFFHLCTLLAGQHLGMTKCNITCHKMTSPIPVTLLIHYQLNQES
```

Appendix 1 (Cont.)

3-7 (wt)

```
Wt- ATGGCTCCCTCACAGCTCGCGTGGCTGCTGCGCCTGGCCGCGTTCTTTCATCTGTGTACT  60
    ||||||||||||||||||||||||||||||||||||||||||||||||||||||||||||
3-7-atggctccctcacagctcgcgtggctgctgcgcctggccgcgttctttcatctgtgtact  60

CTGCTGGCGGGTCAGCACCTCGGCATGACGAAATGCAACATCACGTGCCACAAGATGACC  120
||||||||||||||||||||||||||||||||||||||||||||||||||||||||||||
ctgctggcgggtcagcacctcggcatgacgaaatgcaacatcacgtgccacaagatgacc  120

TCGCCAATCCCAGTGACCTTGCTCATCCACTATCAACTGAACCAGGAGTCCTGCGGCAAG  180
||||||||||||||||||||||||||||||||||||||||||||||||||||||||||||
tcgccaatcccagtgaccttgctcatccactatcaactgaaccaggagtcctgcggcaag  180


Bae1-MAPSQLAWLLRLAAFFHLCTLLAGQHLGMSNYLRTLVVPQDDLANPSDLAHPLSTE
3-7- MAPSQLAWLLRLAAFFHLCTLLAGQHLGMTKCNITCHKMTSPIPVTLLIHYQLNQES
Wt-  MAPSQLAWLLRLAAFFHLCTLLAGQHLGMTKCNITCHKMTSPIPVTLLIHYQLNQES
```

Appendix 2.

Appendix 2 contains the amino acid sequences from plaque purified virus clones which contain the genes encoding αGP120 scFvs derived from the FDA2 kappa scFv library. The FDA2 library contains antibodies that were converted from a B cell (kappa) antibody library from HIV positive patient FDA2 into a library of scFv fragments. This library was originally described by (Cecilia, 1998). Appendix two contains the sequences for antibodies that were recovered from selective (+Dox) and non-selective (-Dox) viral competitions in experiment 4.3. The name of each library clone is listed at the top of each entry next to the > symbol. The amino acid sequence for the light chain of the library member is then shown underneath. This light chain sequence is then compared to the published light chain sequence of the high affinity scFv clone "Z-13" previously recovered from the FDA2 (kappa) library (Parren, 2001). The percent identity of the library member to Z-13 is listed and then the alignment with the Z-13 sequence is shown. Following that the full scFv sequence containing both the heavy and light chain sequences (if recovered from sequencing) for the library member is shown. The comparison of three light chain loops (CDR L 1-3) and the three heavy chain loops (CDR H 1-3) for that library member are compared to the published loop sequences from additional high affinity antibodies that were recovered by phage and yeast display of the FDA2 library as described by (Burton, 2007). Only the comparisons with the highest percent identical are shown. The name and loop of the previously described antibody clone is listed followed by a fraction and percent identity to the library member recovered during experiment 4.3. The alignment is then shown. The sequence of the previously published antibody clone is shown on top of the alignment, matching amino acids are listed in the middle, and the sequence of the library member recovered during experiment 4.3 is listed on the bottom. Where applicable, charge-conserving substitutions are indicated with a "+" and an additional score including these as a match is also shown.

The published heavy and light chain loops of 18 novel high affinity αGP120 scFvs previously isolated from the FDA2 library as described by (Bowley, 2007).

| clone name | CDR L1 | CDR L2 | CDR L3 | CDR H1 | CDR H2 | CDR H3 |
|---|---|---|---|---|---|---|
| *D02-1* | SGDKLGDKYVC | EDSKRPS | QAWDSSTVV | GGYLTGDTFSSFGIH | GITPFFGTANYAQKFQ | ERGELDYYDGSNFPKMMLFAI |
| C02-53 | WASQDISESLA | AASRLES | QQYFGNPLT | GGIFTTYAIS | GIIPMFGPAKYAQRFQ | GSPDWNEDAYDFFYMDV |
| *D02-7* | GGDDIRSYSVH | YADGDRPS | QVWESLIDHVV | GGIFTTYAIS | GIIPMFGPAKYAQRFQ | GSPDWNEDAYDFFYMDV |
| C02-19 | RASQAIGSSLA | HTSKLQS | QQYFGTPLT | GGTFNMYAFS | GTIPVFGTTNYAQKFQ | GDFYDFSSGEAGDFFYMDV |
| *D02-33* | GGNNIGSLSVH | DDSDRPS | QVWDSSNDPVV | GGVFSSVAIS | GIIPVFASTNYAQKFQ | GRYYDFESGEAGDYYYLDF |
| Sb1 | RTSESLNSNYLA | GGSTRAA | QRYGHSLT | RGTFDTYGIN | GIVPIFDTTNYAQKFQ | RNPNEYYDENADYSTVYHYMDV |
| X5 | RASQSVSSGSLA | GASTRAT | QQYGTSPYT | GGTFSMYGFN | GIIPIFGTSNYAQKFR | DFGPDWEDGDSYDGSGRGFFDF |
| *D02-24* | TGSSSDVGGSNSV | DVSNRPS | SSYRTFTTL | GDTFSNYAIS | GLIPVFGIAHYAQKFQ | LGGSGWSDYDY |
| C02-7 | RASQSVYGNYIA | GASSRAT | QQYGTSPLT | GDTFKMYGIN | GFIPLFGTTNYAQKFQ | SPVVEPAANEEEGESDYYYYMDV |
| C02-17 | RASQSVGSNLA | GVSTRAT | QQYNNWPPWT | GGTFSTYAIS | GLIPLFGTSNYAQKFQ | GAHVAAVIPDSQETDYYYYMDV |
| *D02-34* | GGNNIGSKSVH | DDSDRPS | QVWDSSSDHRVV | GGIFNVYAFN | GIIPVFGTTNYAQKFQ | GTYYDFSTGEAGDYFYMDV |
| 4KG.5 | KSSQSILDSSNNRN | WASTRES | QQYFSTPGIT | RDTFNNYVLN | GIGPIIETADYAEKFR | SPYSSLTDTYYYYMDL |
| *D02-6* | GGDNIADKNVQ | DDSDRPS | QVWDSSSALV | GFTLPNAWMT | QIKSKFDGGSADYAALVN | AKPSYYDMLSGRSRHYYYMDV |
| *D02-20* | AGSSSNIGAGFDV | GNTNRPS | QSYDSSLTGGV | GFAFNTYNMN | FISPTGDNIYYADSVK | ASFRLWFGELSGVFDY |
| *D02-3* | AGTSGDVGGYNY | DVSDRPS | CSYAGSSCV | GFTFSTHAMS | DIGIRGGSTYYADSVK | AGALLRGYFDS |
| C02-41 | RTGESLNSNYLA | GGSTRAA | QRYGHSLT | GFSFSQYGMH | VIWFDGSNEYYADSVR | EHPKDFFMSSGYSQV |
| C02-34 | KSSQSLLHSDGKTY | EVSYRFS | MQGLQTPQT | GFPFEDYAIS | VIRSQEYGGTTDFAASVK | MVVVIKEGRWFDP |
| C18-2 | RASQGISDSLA | AASSLQS | QQSNTFLGVT | GGSLSGYYWS | DINQSGGTNYNPSFK | RGIARSVIVLPRAGYMDV |

Appendix 2. (Cont.)

```
>4-11
TQSPATLSVSPGERATLSCRASQSVRSDLAWYQQKPGQAPRLLIYDASTRATGIPARFRGSGSGTEFTLTISSLQPEDSAVYYCQQ
YKNWPPWTFGQGTKVDIKRGGGGSGGGGSGGGGSRSS

z-13 87%

  4-11            TQSPATLSVSPGERATLSCRASQSVRSDLAWYQQKPGQAPRLLIYDASTRATGIPARFRG 60
  z-13            TQSPATLSLSPGERATLSCRASQSVGRNLGWYQQKPGQAPRLLIYDASNRATGIPARFSG 60
                  ********:****************  :*.*****************.********* *

  4-11            SGSGTEFTLTISSLQPEDSAVYYCQQYKNWPPWTFGQGTKVDIKRGGGGSGGGGSGGGGS 120
  z-13            SGSGTDFTLTISSLEPEDFAVYYCQQRSDWP-RTFGQGTKVEIKRGGGGSGGGGSGGGGS 119
                  *****:********:*** ******* .:**  ********:******************

  4-11            RSS 123
  z-13            RSS 122
                  ***

>4-11
TQSPATLSVSPGERATLSCRASQSVRSDLAWYQQKPGQAPRLLIYDASTRATGIPARFRGSGSGTEFTLTISSLQPEDSAVYYCQQ
YKNWPPWTFGQGTKVDIKRGGGGSGGGGSGGGGSRSSQVQLQESGPGLVRPSGTLSLTCAVSGASVSTPHWWIWVRQPPGQGLEWI
GEIYHSGAANYSPSLQSRVTMSVEKSQNQFSLNLRSVTAADTAVYYCARMDFDDSRGFDHWGQGTLVTVSSPRGPAGLEEV

X5 CDRL2 6/7 86%

         GASTRAT
          ASTRAT
         DASTRAT
C02-7 CDRL1 50% 6/12

         RASQSV
         RASQSV
         RASQSV
C02-17 CDRL1 82% 9/11 with positive 10/11 91%

         RASQSVRSDLA
         RASQSV S+LA
         RASQSVGSNLA
C02-17 CDRL3 90% 9/10

         QQYKNWPPWT
         QQY NWPPWT
         QQYNNWPPWT


>3-1 (Generation 2 +Dox)
TQSPSSLSASLGDRITITCRASQGISESLAWYQQTPGKAPKLLVSAASRLESGVPSRFSGGGSGPDFTLTINSLQPEDFAVYYCQQ
YFGTPLTFGGGTKVEIKRGGGGSGGGGSGGGGSRSS

z-13 70.5%

  3-1             TQSPSSLSASLGDRITITCRASQGISESLAWYQQTPGKAPKLLVSAASRLESGVPSRFSG 60
  Z-13            TQSPATLSLSPGERATLSCRASQSVGRNLGWYQQKPGQAPRLLIYDASNRATGIPARFSG 60
                  ****::** * *:* *::*****.:...*.****.**:**:**:  **.  :*:*:**** 

  3-1             GGSGPDFTLTINSLQPEDFAVYYCQQYFGTPLTFGGGTKVEIKRGGGGSGGGGSGGGGSR 120
  Z-13            SGSGTDFTLTISSLEPEDFAVYYCQQRSDWPRTFGQGTKVEIKRGGGGSGGGGSGGGGSR 120
                  .***.******.**:***********  . * *** ************************

  3-1             SS 122
  Z-13            SS 122
                  **
```

Appendix 2. (Cont.)

>3-1
KREIVLTQSPSSLSASLGDRITITCRASQGISESLAWYQQTPGKAPKLLVSAASRLESGVPSRFSGGGSGPDFTLTINSLQPEDFA
VYYCQQYFGTPLTFGGGTKVEIKRGGGGSGGGGSGGGGSRSSQVQLVQSGAEVKKPGSSVTVSCKVSGGTFSTHAISWVRQAPGKG
LEWMGGIIPIFASADYAQKFQDRVTISAYESTSTVYMELSSLRSDDTAVYYCARDAGPHYSNSDRGYMDVWGKGTTVTVSSTRGPA
GLEEV

D02-1 CDRH2 11/16 69% with positive 13/16 81%

GIIPIFASADYAQKFQ
GI P F +A+YAQKFQ
GITPFFGTANYAQKFQ

C02-53 CDRL1 82%

ASQGISESLA
ASQ ISESLA
ASQDISESLA

C02-53 CDRL2 7/7 100%

AASRLES
AASRLES
AASRLES

C02-53 CDRL3 8/10 80%

QQYFGTPLT
QQYFG PLT
QQYFGNPLT

C02-53 CDRH1 7/10 70% with positive 9/10 90%

GGTFSTHAIS
GG F+T+AIS
GGIFTTYAIS

C02-53 CDRH2 69% 11/16 with positive 13/16 81%

GIIPIFASADYAQKFQ
GIIP+F  A YAQ+FQ
GIIPMFGPAKYAQRFQ

D02-7 CDRH1 7/10 70% with positives 9/10 90%

GGTFSTHAIS
GG F+T+AIS
GGIFTTYAIS

D02-7 CDRH2 11/16 69% with positives 13/16 81%

GIIPIFASADYAQKFQ
GIIP+F  A YAQ+FQ
GIIPMFGPAKYAQRFQ

C02-19 CDRL3 100% 9/9

QQYFGTPLT
QQYFGTPLT
QQYFGTPLT

D02-33 CDRH1 7/10 70% with positives 8/10 80%

GGTFSTHAIS
GG FS+ AIS
GGVFSSVAIS

D02-33 CDRH2 81% 13/16 with positives 15/16 94%

GIIPIFASADYAQKFQ
GIIP+FAS +YAQKFQ
GIIPVFASTNYAQKFQ

Appendix 2. (Cont.)

Sb1 CDRH2 11/16 69% with positives 14/16 87%

GIIPIFASADYAQKFQ
GI+PIF + +YAQKFQ
GIVPIFDTTNYAQKFQ

X5 CDRH2 11/16 69% with positives 15/16 93%

GIIPIFASADYAQKFQ
GIIPIF +++YAQKF+
GIIPIFGTSNYAQKFR

D02-24 CDRH1 7/10 with positives 8/10 80%

GGTFSTHAIS
G TFS +AIS
GDTFSNYAIS

D02-24 CDRH2 11/16 69% with positives 13/16 81%

GIIPIFASADYAQKFQ
G+IP+F  A YAQKFQ
GLIPVFGIAHYAQKFQ

C02-7 CDRH2 10/16 63% with positives 13/16 81%

GIIPIFASADYAQKFQ
G IP+F + +YAQKFQ
GFIPLFGTTNYAQKFQ

C02-17 CDRH1 90% with positives 100%

GGTFSTHAIS
GGTFST+AIS
GGTFSTYAIS

C02-17 CDRH1 10/16 63% with positives 15/16 93%

GIIPIFASADYAQKFQ
G+IP+F +++YAQKFQ
GLIPLFGTSNYAQKFQ

D02-34 CDRH2 11/16 69% with positives 14/16 87%

GIIPIFASADYAQKFQ
GIIP+F + +YAQKFQ
GIIPVFGTTNYAQKFQ

4KG5 CDRH1 10/16 63% with positives 13/16 81%

GIIPIFASADYAQKFQ
GI PI  +ADYA+KF+
GIGPIIETADYAEKFR

D02-3 CDRL1 8/10 80% with positives 9/10 90%

GGTFSTHAIS
G TFSTHA+S
GFTFSTHAMS

C18-2 CDRL1 91% with positives 100%

RASQGISESLA
RASQGIS+SLA
RASQGISDSLA

Appendix 2. (Cont.)

>1-4
TQSRGTLSLSPGERATLSCRTSESLNSNYLAWYQQKPGQAPRLLIYGGSTRAAGIPDRFRGSGSGTDFTLTISRLEPEDFAVYYCQ
QFGTSPPITFGQGTRLEIKRGGGGSGGGGSGGGGSRSS

z-13 82% (100/122)

```
 1-4             TQSRGTLSLSPGERATLSCRTSESLNSNYLAWYQQKPGQAPRLLIYGGSTRAAGIPDRFR 60
 Z-13            TQSPATLSLSPGERATLSCRASQSVGRN-LGWYQQKPGQAPRLLIYDASNRATGIPARFS 59
                 *** .***************:*:*:. * *.***************..*.**:*** **

 1-4             GSGSGTDFTLTISRLEPEDFAVYYCQQFGTSPPITFGQGTRLEIKRGGGGSGGGGSGGGG 120
 Z-13            GSGSGTDFTLTISSLEPEDFAVYYCQQR-SDWPRTFGQGTKVEIKRGGGGSGGGGSGGGG 118
                 ************* *************  :. * ******::******************

 1-4             SRSS 124
 Z-13            SRSS 122
                 ****
```

>1-4
TQSRGTLSLSPGERATLSCRTSESLNSNYLAWYQQKPGQAPRLLIYGGSTRAAGIPDRFRGSGSGTDFTLTISRLEPEDFAVYYCQ
QFGTSPPITFGQGTRLEIKRGGGGSGGGGSGGGGSRSSEVQLVETGGGLVQPGRSLRLACSASGFSFDDYAMHWMRQVPGKGLQWV
SGITWNSGRLAYADSVKGRFTISRDNAKNSLFLQMNSLTTDDTAFYYCTRAGQSSGLNWYFDLWGRGTLVTVSSPRGPAGLEEV

Sb1 CDRL1 100% 12/12

```
        RTSESLNSNYLA
        RTSESLNSNYLA
        RTSESLNSNYLA
```

Sb1 CDRL2 100% 7/7

```
        GGSTRAA
        GGSTRAA
        GGSTRAA
```

X5 CDRL3 6/9 67% with positives 7/9 78%

```
        QQFGTSP
        QQ+GTSP
        QQYGTSP
```

C02-7 CDRL3 6/9 67% with positives 7/9 78%

```
        QQFGTSP
        QQ+GTSP
        QQYGTSP
```

C02-41 CDRL1 92% 11/12

```
        RTSESLNSNYLA
        RT ESLNSNYLA
        RTGESLNSNYLA
```

C02-41 CDRL2 100%

```
        GGSTRAA
        GGSTRAA
        GGSTRAA
```

C02-41 CDRH1 7/10 70%

```
        GFSFDDYAMH
        GFSF  Y MH
        GFSFSQYGMH
```

C02-34 CDRH1 6/10 with positives 8/10 80%

```
        GFSFDDYAM
        GF F+DYA+
        GFPFEDYAI
```

Appendix 2. (Cont.)

```
>4-12
TQSPGTLSLSPGERATLSRRASQSVIGSYLAWYQQKPSQAPRLLIYGASSRASGVPDRFSGRGSGTDFTLTISRLEPEDFAVYFCQ
QYGGSPQVFTFGPGTKVEIKRGGGGSGGGGSGGGGSRSS

z-13 83%

  4-12            TQSPGTLSLSPGERATLSRRASQSVIGSYLAWYQQKPSQAPRLLIYGASSRASGVPDRFS 60
  z-13            TQSPATLSLSPGERATLSCRASQS-VGRNLGWYQQKPGQAPRLLIYDASNRATGIPARFS 59
                  ****.************* ***** :*  *.******.********.**.**:*:* ***

  4-12            GRGSGTDFTLTISRLEPEDFAVYFCQQYGGSPQVFTFGPGTKVEIKRGGGGSGGGGSGGG 120
  z-13            GSGSGTDFTLTISSLEPEDFAVYYCQQRSDWPR--TFGQGTKVEIKRGGGGSGGGGSGGG 117
                  * *********** *********:*** .. *:  *** ********************

  4-12            GSRSS 125
  z-13            GSRSS 122
                  *****
>4-12
TQSPGTLSLSPGERATLSRRASQSVIGSYLAWYQQKPSQAPRLLIYGASSRASGVPDRFSGRGSGTDFTLTISRLEPEDFAVYFCQ
QYGGSPQVFTFGPGTKVEIKRGGGGSGGGGSGGGGSRSSQVTLKESGGGLIQPGGSLRLSCAVSGFTFSNYAMSWVRQAPGKGLEW
VSAISASTYSTYYADSVKGRFTISRDNSKNTLYLQMNSLRAEDTAVYYCAKDSASPDSSTWYYFDHWGQGTLVTVSSPRGPAGLEE
V

D02-24 CDRH1 80% 8/10 with positives 9/10 90%

        GFTFSNYAMS
        G TFSNYA+S
        GDTFSNYAIS
C02-7 CDRL1 9/12 75% with positives 11/12 91%

        RASQSVIGSYLA
        RASQSV G+Y+A
        RASQSVYGNYIA
C02-7 CDRL2 86% 6/7 with positives 7/7 100%

        GASSRAS
        GASSRA+
        GASSRAT
C02-17 CDRL1 83% 10/12

        RASQSVIGSYLA
        RASQSV GS LA
        RASQSV-GSNLA
D02-3 CDRH1 80% 8/10 with positives 9/10 90%

        GFTFSNYAMS
        GFTFS +AMS
        GFTFSTHAMS
C02-34 CDRH1 6/10 with positives 8/10 80%

        GFTFSNYAMS
        GF F +YA+S
        GFPFEDYAIS
```

Appendix 2. (Cont.)

```
>4-3
TQSPSSLSASVGDRVTITCRASQVINNRLAWFQQKPGKAPKSLIYDAFTLLSGVPSKFSGSGSGTDFTLTISSLEPEDFATYYCQH
YHAYPLTFGGGTKVEIKRGGGGSGGGGSGGGGSRSS
```

z-13 72%

```
 4-3             TQSPSSLSASVGDRVTITCRASQVINNRLAWFQQKPGKAPKSLIYDAFTLLSGVPSKFSG 60
 z-13            TQSPATLSLSPGERATLSCRASQSVGRNLGWYQQKPGQAPRLLIYDASNRATGIPARFSG 60
                 ****::** * *:*.*::***** :...*.*:*****:**: ***** .  :*:*::***

 4-3             SGSGTDFTLTISSLEPEDFATYYCQHYHAYPLTFGGGTKVEIKRGGGGSGGGGSGGGGSR 120
 z-13            SGSGTDFTLTISSLEPEDFAVYYCQQRSDWPRTFGQGTKVEIKRGGGGSGGGGSGGGGSR 120
                 ********************.****:   :* *** ************************

 4-3             SS 122
 z-13            SS 122
                 **
```

```
TQSPSSLSASVGDRVTITCRASQVINNRLAWFQQKPGKAPKSLIYDAFTLLSGVPSKFSGSGSGTDFTLTISSLEPEDFATYYCQH
YHAYPLTFGGGTKVEIKRGGGGSGGGGSGGGGSRSSQVQLQESGAGLLKPSETLSLTCAVHGGSFSGYYWSWIRQPPGKGLEWIGE
INHSGSANYNPSLKSRVTFSVDTSKNQFSLKLRSVTAADTAVYYCGRPKKNYDIWYFDLWGRGTPGPRLLHSWPGRPRGGP
```

C18-2 CDRH1 90% 9/10

```
        GGSFSGYYWS
        GGS SGYYWS
        GGSLSGYYWS
```

```
>4-2
TQSPSSLSASVGDRVTITCRASQVINNRLAWFQQKPGKAPKSLIYDAFTLLSGVPSKFSGSGSGTDFTLTISSLEPEDFATYYCQH
YHAYPLTFGGGTKVEIKRGGGGSGGGGSGGGGSRSS
```

z-13 72%

```
 4-2             TQSPSSLSASVGDRVTITCRASQVINNRLAWFQQKPGKAPKSLIYDAFTLLSGVPSKFSG 60
 z-13            TQSPATLSLSPGERATLSCRASQSVGRNLGWYQQKPGQAPRLLIYDASNRATGIPARFSG 60
                 ****::** * *:*.*::***** :...*.*:*****:**: ***** .  :*:*::***

 4-2             SGSGTDFTLTISSLEPEDFATYYCQHYHAYPLTFGGGTKVEIKRGGGGSGGGGSGGGGSR 120
 z-13            SGSGTDFTLTISSLEPEDFAVYYCQQRSDWPRTFGQGTKVEIKRGGGGSGGGGSGGGGSR 120
                 ********************.****:   :* *** ************************

 4-2             SS 122
 z-13            SS 122
                 **
```

```
TQSPSSLSASVGDRVTITCRASQVINNRLAWFQQKPGKAPKSLIYDAFTLLSGVPSKFSGSGSGTDFTLTISSLEPEDFATYYCQH
YHAYPLTFGGGTKVEIKRGGGGSGGGGSGGGGSRSSQVQLQESGAGLLKPSETLSLTCAVHGGSFSGYYWSWIRQPPGKGLEWIGE
INHSGSANYNPSLKSRVTFSVDTSKNQFSLKLRSVTAADTAVYYCGRPKKNYDIWYFDLWGRGTPGPRLLHSWPGRPRGGP
```

C18-2 CDRH1 90% 9/10

```
        GGSFSGYYWS
        GGS SGYYWS
        GGSLSGYYWS
```

Appendix 2. (Cont.)

```
>13-9
TQTPDSLAVSLGERATINCKSSQTVFYSSTNKNYLAWYQQKSGQPPRLLIYWASTREPGVPDRFSGSGSGTDFTLTISRLEPEDFA
VYYCQQYSGSPRTFGQGTKVEIKRGGGGSGGGGSGGGGSRSS

z-13 78%

 13-9            TQTPDSLAVSLGERATINCKSSQTVFYSSTNKNYLAWYQQKSGQPPRLLIYWASTREPGV 60
 z-13            TQSPATLSLSPGERATLSCRASQSVGRN------LGWYQQKPGQAPRLLIYDASNRATGI 54
                 **:* :*::* *****:.*::**:*  .      *.*****.**.****** **.* .*:

 13-9            PDRFSGSGSGTDFTLTISRLEPEDFAVYYCQQYSGSPRTFGQGTKVEIKRGGGGSGGGGS 120
 Clone           PARFSGSGSGTDFTLTISSLEPEDFAVYYCQQRSDWPRTFGQGTKVEIKRGGGGSGGGGS 114
                 * ********************* ************* *. ***********************

 13-9            GGGGSRSS 128
 Clone           GGGGSRSS 122
                 ********

TQTPDSLAVSLGERATINCKSSQTVFYSSTNKNYLAWYQQKSGQPPRLLIYWASTREPGVPDRFSGSGSGTDFTLTISRLEPEDFA
VYYCQQYSGSPRTFGQGTKVEIKRGGGGSGGGGSGGGGSRSSQVQLVESGPGLVKPADVLSLTCTVSGGSINAYYWSWLRQPAGKG
LEWIGRFHTSGVTTYNPTLKSRITVSVDTSKNLFSLKLRSVTVTDTAIYYCAKGPRASIDFNYVDQWGQGTLVTVSSTRGPAGLEE
V

4KG5 CDRL1 10/17 59% with positives 13/17 76%

        KSSQTVFYSSTNKNYL
        KSSQ++  SS N+NYL
        KSSQSILDSSNNRNYL
4KG5 CDRL2 6/7 86%

        WASTRE
        WASTRE
        WASTRE
C18-2 CDRH1 70% with positives 9/10 90%

        GGSINAYYWS
        GGS++ YYWS
        GGSLSGYYWS

>13-1
TQSPRTLSLSPGERATLSCRTSESLNSNYLAWYQQKPGQAPRLLIYGGSTRAAGIPDRFSGSGSGTDFTLTISRLEPEDVALYYCQ
RYGHSLTFGGGTKREIKRGGGGSGGGGSGGGGSRSS

z-13 82%

 13-1            TQSPRTLSLSPGERATLSCRTSESLNSNYLAWYQQKPGQAPRLLIYGGSTRAAGIPDRFS 60
 z-13            TQSPATLSLSPGERATLSCRASQSVGRN-LGWYQQKPGQAPRLLIYDASNRATGIPARFS 59
                 **** ***************:*:*:. * *.***************..*.**:*** ***

 13-1            GSGSGTDFTLTISRLEPEDVALYYCQ-RYGHSLTFGGGTKREIKRGGGGSGGGGSGGGGS 119
 z-13            GSGSGTDFTLTISSLEPEDFAVYYCQQRSDWPRTFGQGTKVEIKRGGGGSGGGGSGGGGS 119
                 ************* *****.*:**** * . . *** *** ******************

 13-1            RSS 122
 z-13            RSS 122
                 ***
TQSPRTLSLSPGERATLSCRTSESLNSNYLAWYQQKPGQAPRLLIYGGSTRAAGIPDRFSGSGSGTDFTLTISRLEPEDVALYYCQ
RYGHSLTFGGGTKREIKRGGGGSGGGGSGGGGSRSSEGQLGETGPRLVKPSGILSLTCDVSGGSFNNSHWRSWVRQPPGKGLEWIG
EIYHSGSTYYNASLRSRISMSVDESKNQFSLTLTSVTAADTAVYYCARVVPSWDVNGPFICGQWTMVTVSSTRV
```

Appendix 2. (Cont.)

Sb1 CDRL1 100% 12/12

RTSESLNSNYLA
RTSESLNSNYLA
RTSESLNSNYLA

Sb1 CDRL2 100%7/7

GGSTRAA
GGSTRAA
GGSTRAA

Sb1 CDRL3 100% 8/8

QRYGHSLT
QRYGHSLT
QRYGHSLT

C02-41 CDRL1 92% 11/12

RTSESLNSNYLA
RT ESLNSNYLA
RTGESLNSNYLA

C02-41 CDRL2 100% 7/7

GGSTRAA
GGSTRAA
GGSTRAA

C02-41 CDRL3 100% 8/8

QRYGHSLT
QRYGHSLT
QRYGHSLT

>7-5
TQSPSSVSASVGDRVTITCRASQGISSWLAWYQQKPGKAPKLLIYSASTLQPGVPSRFSGSGSGTDFTLTITSLQPEDFATYYCQQ
ANTFPLTFGPGTKVEIKRGGGGSGGGGSGGGGSRSS

z-13 73%

```
 7-5             TQSPSSVSASVGDRVTITCRASQGISSWLAWYQQKPGKAPKLLIYSASTLQPGVPSRFSG 60
 z-13            TQSPATLSLSPGERATLSCRASQSVGRNLGWYQQKPGQAPRLLIYDASNRATGIPARFSG 60
                 ****:::* * *:*.*::*****.:.  *.*******:**:****.**.  .*:*:****

 7-5             SGSGTDFTLTITSLQPEDFATYYCQQANTFPLTFGPGTKVEIKRGGGGSGGGGSGGGGSR 120
 z-13            SGSGTDFTLTISSLEPEDFAVYYCQQRSDWPRTFGQGTKVEIKRGGGGSGGGGSGGGGSR 120
                 ***********:**:*****.***** . :* *** **********************

 7-5             SS 122
 z-13            SS 122
                 **
```

TQSPSSVSASVGDRVTITCRASQGISSWLAWYQQKPGKAPKLLIYSASTLQPGVPSRFSGSGSGTDFTLTITSLQPEDFATYYCQQ
ANTFPLTFGPGTKVEIKRGGGGSGGGGSGGGGSRSSQVQLVQSGLR

C18-2 CDRL1 82% 9/11

RASQGISSWLA
RASQGIS  LA
RASQGISDSLA

Appendix 2. (Cont.)

```
>13-7
TQSPSSLSASVGDRVTITCRASRSISTFLNWYQQKPGQAPKLLIFGASNLQSGVPSRFSGGGSGTDFILTISGLQPEDFAAYYCQQ
GYSTPATFGGGTKVDIKRGGGGSGGGGSGGGGSRSS*
```

z-13 72%

```
 13-7            TQSPSSLSASVGDRVTITCRASRSISTFLNWYQQKPGQAPKLLIFGASNLQSGVPSRFSG 60
 z-13            TQSPATLSLSPGERATLSCRASQSVGRNLGWYQQKPGQAPRLLIYDASNRATGIPARFSG 60
                 ****::** * *:*.*::****:*:.  *.**********:***:.***  :*:*:**** 

 13-7            GGSGTDFILTISGLQPEDFAAYYCQQGYSTPATFGGGTKVDIKRGGGGSGGGGSGGGGSR 120
 z-13            SGSGTDFTLTISSLEPEDFAVYYCQQRSDWPRTFGQGTKVEIKRGGGGSGGGGSGGGGSR 120
                 .****** ****.*:*****.*****  . * *** ****:****************** 

 13-7            SS 122
 z-13            SS 122
                 **
```

```
TQSPSSLSASVGDRVTITCRASRSISTFLNWYQQKPGQAPKLLIFGASNLQSGVPSRFSGGGSGTDFILTISGLQPEDFAAYYCQQ
GYSTPATFGGGTKVDIKRGGGGSGGGGSGGGGSRSS*VQLVQSGGRLGQAWRVPETVLYSLWNQFQ*PLRELDPPGSREGAGMGLI
CEQ*WY*HVLRRRCGGPIHHLQGQRPGFSVFANQQPESRGHGCLFLRERSGVVRTLVTVSSPRGPAGLEEVLTHYFTAX
```

```
>5-14
TLSVSPGERVTLSCRASQTVTMEQLGWYQQKPGQAPRLLIYGASIRATGVPVRFTGSGSGTEFTLTITSLQPEDFAVYYCQQYSNW
PLTFGGGTKVDIKRGGGGSGGGGSGGGGSRSSQVTLKESGPALLQPTQTLTLTCAFSGFSLKSEGVSLAWIRQAPGRALEWLALIH
SNDVRRYSPLLQTRLTVSTGTSSNHVVLTLTDVDPEDTATYYCARRPPTLFGGGDYYFDLWGRGTLVTVSSPRGP
```

z-14 80%

```
 5-14            -----TLSVSPGERVTLSCRASQTVTMEQLGWYQQKPGQAPRLLIYGASIRATGVPVRFT 55
 Z-18            TQSPATLSLSPGERATLSCRASQSVG-RNLGWYQQKPGQAPRLLIYDASNRATGIPARFS 59
                      ***:*****.********:*  .:*****************.** ****:*.**: 

 5-14            GSGSGTEFTLTITSLQPEDFAVYYCQQYSNWPLTFGGGTKVDIKRGGGGSGGGGSGGGGS 115
 Z-18            GSGSGTDFTLTISSLEPEDFAVYYCQQRSDWPRTFGQGTKVEIKRGGGGSGGGGSGGGGS 119
                 ******:*****:**:*********** *:** *** ****:****************** 

 5-14            RSS 118
 Z-18            RSS 122
                 ***
```

X5 CDR L1 86% (6/7)

```
5-14     GASIRAT
         GAS RAT
X5-2     GASTRAT
```

C02-7 CDR L2 86% (6/7)

```
5-14     GASIRAT
         GAS RAT
C02-7    GASSRAT
```

C02-17 CDR L3 (6/10) 60% with positives (7/10) 70%

```
5-14     QQYSNWP
         QQY+NWP
C02-17   QQYNNWP
```

Appendix 2. (Cont.)

```
>3-4
TQSPSTLSASVGDRVTITCRASQGIGSWLAWYQLQAGKAPKLLIYGASSLQDGVPSRFSGSGSGTDFTLTISRLQPEDFASYFCQQ
ASRFPPTFGGGTKVDIKRGGGGSGVAVRVAVALDLPRSP*RSLGELWYGRGGP*DSHVQPLDSPLIIMAWPGSAKVQGRGWSGSLI
FFGMVIAQVMQTL*GADSPSPETTPRTPCTCK*TV*ESRTRPSITVREWTLHPSGLPVAGTLTTGGQGTLVTVSSPRGPAGLEEV

z-13 62%
  3-4             TQSPSTLSASVGDRVTITCRASQGIGSWLAWYQLQAGKAPKLLIYGASSLQDGVPSRFSG 60
  z-13            TQSPATLSLSPGERATLSCRASQSVGRNLGWYQQKPGQAPRLLIYDASNRATGIPARFSG 60
                  ****:*** * *:*.*::*****.:*  *.*** :.*:**:****.**.   *:*:****

  3-4             SGSGTDFTLTISRLQPEDFASYFCQQASRFPPTFGGGTKVDIKRGGGGSGVAVRVAVALD 120
  z-13            SGSGTDFTLTISSLEPEDFAVYYCQQRSDWPRTFGQGTKVEIKRGGGGSGGGGSGGGGSR 120
                  ************ *:***** *:*** * :* *** ****:********* .   . .

  3-4             LP 122
  z-13            SS 122
                   .
C02-19 CDRL1 82% 9/11

         RASQGIGSWLA
         RASQ IGS LA
         RASQAIGSSLA
C02-17 CDRL1 8/11 with positives 9/11 81%

         RASQGIGSWLA
         RASQ +GS LA
         RASQSVGSNLA

>5-21
LSASVGDRVTITCRASEPISTYLNWYQQKPGKAPKVLIYAASSLQSGVPPRFSGSGSGTDFTLTIGSLQPEDFATYYCQQANSPRV
TFGGGTKVEIKRGGGGSGGGGSGGGGSRSSQVQLQQWAQDC*SHRRPCPSPALSMVRPSMVITGVGSASPQVRGWSG*EKSIILEV
PSTIRPSRVESPCQETCPSSSSP*R*PL*PPPTRLFITAREAGKFHCRLGSCGSTPGAREPWSPFPHLVARPARGVCKSPPK

z-13 68%

  5-21            ------LSASVGDRVTITCRASEPISTYLNWYQQKPGKAPKVLIYAASSLQSGVPPRFSG 54
  z-13            TQSPATLSLSPGERATLSCRASQSVGRNLGWYQQKPGQAPRLLIYDASNRATGIPARFSG 60
                        ** * *:*.*::****:.:.  *.*******:**::*** **.  :*:*.****

  5-21            SGSGTDFTLTIGSLQPEDFATYYCQQANSPRVTFGGGTKVEIKRGGGGSGGGGSGGGGSR 114
  z-13            SGSGTDFTLTISSLEPEDFAVYYCQQRSDWPRTFGQGTKVEIKRGGGGSGGGGSGGGGSR 120
                  ***********.**:*****.*****  ..   *** **********************

  5-21            SS 116
  z-13            SS 122
                  **
C18-2 CDRL2 100% 7/7

         AASSLQS
         AASSLQS
         AASSLQS
```

Appendix 2. (Cont.)

```
>5-13
LSPGERATLSCRASQSVSSSYLAWYQQKPGQSPRLLIYGASSRATGIPDRFSGNGSGTDFTLTISGLQSEDFGFYYCQQYNDWPPY
TFGQGTKLEIKHGGGGSAVAVRVAVALDLPRCSGGVWGRRGPAWGVPETLLCSVWIHLQ*

z-13 66% (82/122)

  5-13            --------LSPGERATLSCRASQSVSSSYLAWYQQKPGQSPRLLIYGASSRATGIPDRFS 52
  z-13            TQSPATLSLSPGERATLSCRASQSVGRN-LGWYQQKPGQAPRLLIYDASNRATGIPARFS 59
                         *****************. . *.********:******.**.****** ***

  5-13            GNGSGTDFTLTISGLQSEDFGFYYCQQYNDWPPYTFGQGTKLEIKHGGGGSAVAVRVAVA 112
  z-13            GSGSGTDFTLTISSLEPEDFAVYYCQQRSDWP-RTFGQGTKVEIKRGGGGSGGGGSGGGG 118
                  *.***********.*:.***..***** .***  *******:***:*****. .   . .

  5-13            LDLP 116
  z-13            SRSS 122

X5 CDRL1 83% 10/12

         RASQSVSSSYLA
         RASQSVSS  LA
         RASQSVSSGSLA
X5 CDRL2 6/7 86% with positives 7/7 100%

         GASSRAT
         GAS+RAT
         GASTRAT
C02-7 CDRL1 8/12 with positives 10/12 83%

         RASQSVSSSYLA
         RASQSV  +Y+A
         RASQSVYGNYIA
C02-7 CDRL2 100% 7/7

         GASSRAT
         GASSRAT
         GASSRAT
C02-17 CDRL3 80% 8/10 with positives 10/10 100%

         QQYNDWPPYT
         QQYN+WPP+T
         QQYNNWPPWT
>5-7
ARNDTHAVSRHPVFVSRRKSHPLLQDQ*ES*QQLLSLVPAETWPGSQTPHLWWIHQGRWHPRQVQWQWVWDRLHSHHQQTGA*RCC
ALLLSAVWPLTHFRRRDQGEIKRGGGGSGGGGSGGGGSRSSQVTLKESGPTLVQPTQTLTLTCMFSGFSLDTDGVAVAWLRQAPGK
ALEWLALIHSNDVRRYSSSLEKRLTISRDTSKNHVVLVMTDLDHVDTATYYCAHRRYYLFGGGDNYFDIWGRGTLVPVSSTRGPAG
LEEVLTKFPRQ

z-13 30%

  5-7             ARNDTHAVSRHPVFVSRRKSHPLLQDQESQQLLSLVPAETWPGSQTPHLWWIHQGRWHPR 60
  z-13            ----TQSPATLSLSPGERATLSCRASQSVGRNLGWYQQK--PGQAPRLLIYDASNRATGI 54
                      *:: :  .:  ..* : .   .*.  : *.    :  **. .  * :  ..*

  5-7             QVQWQWV-----WDRLHSHHQQTGARCCALLLSAVWPLTHFRRRDQGEIKRGGGGSGGGG 115
  z-13            PARFSGSGSGTDFTLTISSLEPEDFAVYYCQQRSDWPRT-FGQGTKVEIKRGGGGSGGGG 113
                   .::.       :    *  :  .         : ** * * :  : *************

  5-7             SGGGGSRSS 124
  z-13            SGGGGSRSS 122
                  *********
No significant loop matches
```

Appendix 2. (Cont.)

```
>5-1
AHGS*RRYSLQARPRRPSAKRHSRSSRHPVFVSRGKSHPLLQGQSEC*QQLLSLVPAETWPVSQAPHLWCIQQGHWHPRQVQWQWV
WNRFHSHHQRPAV*RFRILLLSAI**LAPVHFWPGDQAGDQTWWRWLGGGGSGGGGSRSSQVQWWSLGEAWSSLGGP*DSPVQRLD
SPSVIMACTGSARLQARGWSGWHLSGMMEVKNTMQTP*RADSPSPETIPRTLCICK*PA*GLRTRLYITVRIR*RGSQSTGAREPW
SPSPQLVARPARGGLRNFPHNGITCCLFCLPAGGDGLADQGGWHHGKDLPFGIANSNSSN*QPTX

z-13 23%
 5-1            AHGSRRYSLQARPRRPSAKRHSRSS-RHPVFVSRGKSHPLLQGQSECQQLLSLVPAETWP 59
 z-13           TQSPATLSLSPGERATLSCRASQSVGRNLGWYQQKPGQAPRLLIYDASNRATGIPAR-FS 59
                ::..   **..  * . : * *:*  *:  : .:  .:.      :..:  : :**. :.

 5-1            VSQAPHLWCIQQGHWHPRQVQWQWVWNRFHSHHQRPAVRFRILLLSAILAPVHFWPGDQA 119
 z-13           GSGSGTDFTLTISSLEPEDFAVYYCQQRSD-------------------WPRTFGQGTKV 100
                 * :   : :  .  .*.:.   :  :* .                    *  *  * :.

 5-1            GDQTWWRWLGGGGSGGGGSRSS 141
 Clone          EIKRGGGGSGGGGSGGGGSRSS 122
                  :      ************


No significant loop matches
```